



UNIVERSITEIT VAN PRETORIA
UNIVERSITY OF PRETORIA
YUNIBESITHI YA PRETORIA

**PERFORMANCE EVALUATION OF INVERTED
PAVEMENTS: COMPARATIVE ANALYSIS OF SOUTH
AFRICAN AND BRAZILIAN EXPERIENCES**

DAMIRES CRISTOVÃO DE ALMEIDA

**A dissertation submitted in partial fulfilment of the requirements for the degree
MASTER OF ENGINEERING (TRANSPORTATION ENGINEERING)**

In the

**FACULTY OF ENGINEERING, BUILT ENVIRONMENT AND INFORMATION
TECHNOLOGY**

UNIVERSITY OF PRETORIA

January 2021

DISSERTATION SUMMARY

PERFORMANCE EVALUATION OF INVERTED PAVEMENTS: COMPARATIVE ANALYSIS OF SOUTH AFRICAN AND BRAZILIAN EXPERIENCES

DAMIRES CRISTOVÃO DE ALMEIDA

Supervisor: Prof Wynand JvdM Steyn

Department: Civil Engineering

University: University of Pretoria

Degree: Master of Engineering (Transportation Engineering)

The technical and economic feasibility of an inverted pavement has been proven abroad and in Brazil, but there are still doubts relating to the parameters that may affect the performance of this type of pavement, particularly in Brazil. There is a lack of studies that identify and characterize the variables that are directly related to the structural behaviour of the cement-treated layer and the contribution of each layer (thickness and elastic modulus) to inverted pavement performance as a whole. Furthermore, the main Brazilian specifications allow designers to make most decisions based on their experience, often generating doubts and uncertainties ranging from the design of the structure to the execution of quality control, directly reflecting on the pavement's service life.

Two test sections designed as inverted pavements, which were evaluated in Brazil, are assessed to identify and characterize the variables directly related to the structural behaviour of inverted pavements. In addition, a comparative analysis of the design, materials, construction, and quality control methods for Brazilian and South African inverted pavements is assessed. Both test sections were built based on the same design principles, but have been presented through different structural performances since their implementation in 2001.

Each test section was monitored with deflection measurements between 2003 and 2016. In 2017, two inspection pits were opened in each test section. Samples were collected from all layers, and sent to the laboratory. Additionally, the tests carried out in the laboratory and in-situ in both sections during their construction in 2001, requested in the quality control, were also analysed in this study. The test results from the quality control and the test results obtained exclusively for this study (alongside the available literature) were compared and analysed against each other.

Based on the analyses and discussions carried out throughout this research, it is possible to conclude that both the thickness and elastic modulus variables of the unbound base and the cement-treated layer played the most important roles in the behaviour of the inverted pavement, besides the support provided to the cement-treated layer by the underlying layer. Furthermore, the difference in the behaviour of both test sections can be linked to these three variables in addition to the constructive techniques adopted.

No direct correlations were found for obtaining resilient modulus through CBR, and obtaining CBR values through DCP tests may vary according to the type of soil. The back-calculated modulus are good and reliable indicators of resistance, however, it is essential to apply adjustment factors. Furthermore, it was possible to identify a linear function with $R^2 = 0.845$, where ITS varies as a function of USC, according to the tests result carried out in 2001. However, unfortunately, no satisfactory correlations were found between UCS and ITS, UCS and f_t , and ITS and f_t from the results obtained in 2017. It is possible that these results are due to the specimens being damaged.

DECLARATION

I, the undersigned hereby declare that:

- I understand what plagiarism is and I am aware of the University's policy in this regard;
- The work contained in this dissertation is my own original work;
- I did not refer to work of current or previous students, lecture notes, handbooks or any other study material without proper referencing;
- Where other people's work has been used this has been properly acknowledged and referenced;
- I have not allowed anyone to copy any part of my dissertation;
- I have not previously in its entirety or in part submitted this dissertation at any university for a degree.

DISCLAIMER:

The work presented in this dissertation is that of the student alone. Students were encouraged to take ownership of their projects and to develop and execute their experiments with limited guidance and assistance. The content of the research does not necessarily represent the views of the supervisor or any staff member of the University of Pretoria, Department of Civil Engineering. The supervisor did not read or edit the final report and is not responsible for any technical inaccuracies, statements or errors. The conclusions and recommendations given in the report are also not necessarily that of the supervisor, sponsors or companies involved in the research.

Signature of student:



Name of student: Damires Cristovão de Almeida

Student number: u19324333

Date: 19 November 2019

ACKNOWLEDGEMENTS

It has always been my dream to write a dissertation at the University of Pretoria. I am happy and grateful that this dream has come true!

Among so many thanks, which are not few, I begin by thanking God for allowing me to come to South Africa and for giving me the strength and motivation to write my dissertation in lockdown during the COVID-19 pandemic.

To Professors De Beer, Emile Horak, and James Maina for having inspired me, even without knowing me, to do my Master's degree at the University of Pretoria. Professors, your work crossed the Atlantic Ocean and changed my personal and professional life. Thank you very much for the production and contribution to the academic world. Special thanks to Prof. James Maina, which I had the honour of having as a professor of statistics. Thank you for being so helpful, quick, and practical.

I am grateful to Professor Alex Visser, coordinator of the post-graduate program of the Department of Civil Engineering at the University of Pretoria, for guiding and assisting throughout my Master's degree at the University of Pretoria.

To Ms. Stefanie Steenberg for always being kind, helpful and assisting with Masters-related admin.

I am grateful to Prof Wynand Steyn, Head of Department (HOD) of the Department of Civil Engineering, which I was fortunate and honoured to have as a supervisor and teacher of Pavement Design. Thank you for playing an integral part in my experience at the University of Pretoria. To you, Prof Steyn, my sincere thanks.

To Wilson França, superintendent of Technological Development at Engellog CCR. Thank you for having supported my idea and allowing the opening of inspection pits and sample collection on the Bandeirantes highway (SP-348), one of the main Brazilian highways.

To the Quality Team of Engellog and the Laboratory Team of AutoBan for having accompanied the opening of the inspection pits, carrying out the in situ tests, and collecting the samples for carrying out the tests in the Laboratory.

My sincere thanks to Valeria Faria and Miguel Klinsky, on behalf of the Centro de Pesquisa Rodoviárias (CPR), and Carlos on behalf of the Autoban Laboratory for carrying out the tests for this research.

I thank the Engineering Team of Dynatest Engenharia Ltda. and Technological Development at Engellog, where I have been working for the past 8 years. Thank you for all the shared knowledge and partnership.

To my friends and professional colleagues that I have made throughout my professional career. Paulo Ricardo, Guilherme Amarante, Giannina Massenli, Sandra Margarido, Douglas Negrão and André Vale, thank you very much. You are my reference point for resilience and intelligence within the technical environment. It was and always will be a pleasure to share ideas and knowledge with you.

To Paulo Ricardo, my mentor and great friend, my sincere thanks. Thank you for all the knowledge shared. You made me love road engineering since our first conversation. Thank you for believing in me since the beginning.

To Leandro Vieira, my friend, my brother and my professional colleague. Thank you for always support my decisions. To my longtime friends, Gabriele Ramalho, David Silva, Fátima Zapata, Mayra Bravo and .Daniele Fernandes, thank you for all your support.

To the friends I made in Pretoria and who made my journey lighter and more fun. Thanks especially to Potüya, Remi, Mable, Khololwethu, Benjamin, Frank, Isaac, Siyanda, and Donovan. I have learned so much from you!

To my siblings, Diorlando, Dioneide, Dilvânia and Diana Carla I would like to say thank you. Thank you for all your support and trust. You guys taught me a lot along this journey. I am, undoubtedly, a little bit of each one of you.

To my nephews and nieces (Saulo Emanuel, Ana Leticia, David Luís, Helena, Maria Emanuely and Heitor), the reason for my laughter and pride.

And lastly, because we leave the best for last. To my parents Dimas and Luzinete, I thank and dedicate this dissertation. You are and will always be the reason for my inspiration. Thank you for all your love, dedication, and trust. I love you!

TABLE OF CONTENTS

1. INTRODUCTION	1
1.1 Background	1
1.2 Objectives of the Study	2
1.3 Scope of the Study.....	3
1.4 Methodology	3
1.5 Organization of the Dissertation.....	5
2. LITERATURE REVIEW	7
2.1 National and international experience with inverted pavements.....	7
2.1.1 Brazilian experience	7
2.1.2 South African experience	10
2.1.3 United States experience	11
2.2 Design procedures for inverted pavement.....	12
2.2.1 Subgrade.....	13
2.2.2 Cement-treated Layer	17
2.2.3 Unbound Base Layer	20
2.2.4 Asphalt Concrete	23
2.3 Material properties for cement-treated layer	25
2.3.1 Type of Cement.....	26
2.3.2 Cement Content.....	29
2.3.3 Grain Size Distribution.....	30
2.3.4 Type of aggregate.....	33
2.3.5 Moisture Content.....	34
2.3.6 Compaction	35
2.3.7 Curing.....	36
2.4 Strength parameters of cement-treated layer.....	36
2.4.1 Elastic Response.....	37
2.4.2 Unconfined Compressive Strength and Indirect Tensile Strength	41
2.4.3 Relationship between UCS and tensile strength.....	42
2.5 Construction parameters of the cement-treated layer.....	43

2.5.1	Cement Content.....	43
2.5.2	Strength	43
2.5.3	Cement-treated layer thickness	44
2.5.4	Compaction Techniques	45
2.5.5	Moisture Content.....	46
2.5.6	Processing Time	47
2.5.7	Curing.....	48
2.5.8	Deflectometry Control.....	49
2.5.9	Laboratory and field tests for the acceptance control.....	50
2.6	Inverted pavement performance.....	50
2.6.1	Rutting.....	50
2.6.2	Deflection.....	51
2.6.3	Influence of the subgrade modulus	54
2.6.4	Influence of the cement-treated layer modulus	55
2.6.5	Influence of the cement-treated layer thickness	55
2.6.6	Influence of the unbound base modulus.....	55
2.6.7	Influence of unbound base thickness.....	56
2.6.8	Influence of the asphalt concrete modulus	56
2.6.9	Influence of asphalt concrete thickness.....	57
2.7	Summary	57
3.	EXPERIMENTAL WORK.....	59
3.1	Test sections selection.....	59
3.2	Field Measurements	62
3.2.1	Deflection measurement.....	62
3.2.2	Traffic Measurement	69
3.3	Materials characterization of the test sections.....	73
3.3.1	In-situ and laboratory trial planning.....	74
3.4	In-situ tests carried out in the test sections.....	77
3.4.1	Density	77

3.4.2	Soil Strength.....	79
3.5	Laboratory tests carried out in the unbound base.....	81
3.5.1	Gradation Test.....	81
3.6	Laboratory tests carried out in the cement-treated layer	82
3.6.1	Dynamic Modulus	82
3.6.2	Resilient Modulus	83
3.6.3	Flexural Modulus	84
3.6.4	Unconfined Compressive Strength.....	85
3.6.5	Indirect Tensile Strength	86
3.6.6	Flexural Tensile Strength	87
3.7	Laboratory tests carried out in the selected subgrade.....	87
3.7.1	California Bearing Ratio	88
3.7.2	Atterberg Limits	88
3.7.3	Resilient Modulus	89
3.7.4	Soil Classification	89
3.8	Tests carried out during quality control in 2001	91
3.8.1	Deflectometry control recommended in the Technical Design Report	91
3.8.2	Deflectometry performed in the Quality Control	92
3.8.3	Compaction	93
3.8.4	Cement Content.....	94
3.8.5	Unconfined Compressive Strength and Indirect Tensile Strength	95
3.8.6	Curing.....	95
4.	ANALYSIS OF THE PAVEMENT PERFORMANCE OF BOTH TEST SECTION	97
4.1	Analysis of back-calculation modulus	97
4.2	Analysis of deflection bowl parameters	102
4.3	Analysis of the cement-treated layer moduli as a function of traffic	104
4.4	Analysis of deflections obtained during quality control.....	106
4.5	Analysis of the influence of thickness and modulus in the performance of the inverted pavement	109
5.	ANALYSIS AND DISCUSSION OF TESTS CARRIED OUT IN-SITU AND LABORATORY IN QUALITY CONTROL.....	116

5.1	Compaction characteristics of both test section	116
5.1.1	Dry density obtained in the laboratory and the field	116
5.1.2	Moisture content in the compaction process	117
5.2	Comparative analysis of densities obtained in-situ in 2001 and 2017	118
5.3	Analysis of the strength parameters obtained for the cement-treated layer	119
5.3.1	Relationship between the strength parameter UCS and curing time	121
5.3.3	Analysis of the influence of curing of the cement-treated layers on the performance of test sections	122
6.	ANALYSIS AND DISCUSSIONS OF RESULTS CARRIED OUT IN LABORATORY IN 2017	124
6.1	Analysis of tests carried out on the subgrade and selected subgrade	124
6.1.1	Analysis of soil classification	124
6.1.2	Analysis of soil strength as a function of Soil classification	125
6.1.3	Resilient modulus as a function of CBR	126
6.1.4	Comparison of laboratory resilient moduli with back-calculated moduli	128
6.1.5	Dynamic Penetration Cone analysis	129
6.1.6	Comparison of $CBR_{\text{Laboratory}}$ with CBR_{DCP}	130
6.2	Analyses of the grain size distribution in the unbound base	131
6.3	Analysis of the strength parameters of the cement-treated layer	132
6.3.1	Elastic response analyses	132
6.3.2	Influence of the thickness and frequency in the Dynamic Modulus results	134
6.3.3	UCS and Tensile strength analyses	135
6.3.4	The relationship between UCS and tensile strength	137
7.	CONCLUSIONS AND RECOMMENDATIONS	138
7.1	Conclusions	138
7.2	Recommendations	142
8.	REFERENCES	143
	APPENDIX A	151
	APPENDIX B	166

LIST OF TABLES

Table 2-1: First section of inverted pavement in Brazil (Adapted from PINTO et al., 1988).....	8
Table 2-2: Second section of inverted pavement in Brazil (Adapted from Suzuki, 1992).....	9
Table 2-3: In-situ subgrade delineation for flexible pavements in South Africa (Adapted from SANRAL, 2014).....	15
Table 2-4: In-situ subgrade delineation for flexible pavements in Brazil (Adapted from PMSP/SIURB, 2004; DER/SP (2005a); DER/PR, 2006; DNIT, 2006a and DNIT, 2010).....	16
Table 2-5: Fatigue Models for subgrade and selected layer permanent deformation (Adapted from Suzuki, 1992 and DER/SP, 2006a)	17
Table 2-6: Modulus and Poisson's Ratio for the unbound base layer in an inverted pavement in Brazil	20
Table 2-7: Modulus and Poisson's Ratio for the unbound base layer in an inverted pavement in South Africa (Adapted from SANRAL, 2014)	21
Table 2-8: Suggested vertical modulus of top sublayer of normal standard base material (Austroads, 2017).....	21
Table 2-9: Grading of graded crushed stone used in South Africa and in Brazil (Adapted from TRH14, 1985; DERSA, 1997; DER/SP, 2005b and DNIT, 2009).....	22
Table 2-10: Modulus and Poisson's Ratio for the asphalt layer in Brazil.....	23
Table 2-11: Elastic moduli and Poisson's Ratio for asphalt materials used in SAMDM, 1996 (Adapted from SANRAL, 2014).....	24
Table 2-12: Minimum asphalt layer thicknesses adopted in Brazil (Adapted from DER/SP, 2006a and DNIT, 2006a)	24
Table 2-13: Fatigue models for asphalt concrete layer adopted in Brazil (Adapted from DER/SP, 2006a).....	25
Table 2-14: Recommendations of the most suitable type of cement for the cement-treated layer in Brazil and abroad	27
Table 2-15: Physical and mechanical requirements of the types of Portland cement available in Brazil (adapted from ABCP, 2002).....	28
Table 2-16: Cement strength classes in South Africa (Adapted from SANRAL, 2014).....	28
Table 2-17: Grading of aggregate of cement-treated layer in Brazil and in South Africa	31
Table 2-18: Influence of aggregate type on the 7 day UCS (adapted from Xuan, 2012).....	33
Table 2-19: Physical requirements for materials for aggregates used in stabilized base and subbase in Brazil and in in South Africa.....	34
Table 2-20: Modulus and Poisson's Ratio recommended for the cement-treated layer in inverted pavement in Brazil	38

Table 2-21: Modulus recommended for the cement-treated layer in inverted pavement in South Africa and Australia	38
Table 2-22: Prediction models of Tensile Strength of cement-treated layer (Adapted from Xuan, 2012)	43
Table 2-23: Strength parameter suggest in Brazil and in South Africa.....	44
Table 2-24: Minimum and maximum thicknesses layer adopted by Brazil, The United States and South Africa	44
Table 2-25: Compaction criterion in Brazil and in South Africa	45
Table 2-26: Moisture content requirements in Brazil and in South Africa	47
Table 2-28: Structural Interpretation of Rut Depths (SANRAL, 2014).....	51
Table 2-29: Deflection bowl parameters (Adapted from SANRAL, 2014 and Horak, 2008)	52
Table 3-1: Details of the location of the test sections	60
Table 3-2: Test sections I and II materials properties	61
Table 3-3: Pavement surface temperature measured in test sections T-I and T-II.....	67
Table 3-4: Test-Section I – Average annual daily traffic for the base year.....	69
Table 3-5: Test-Section II - Average annual daily traffic for the base year.....	69
Table 3-6: Most common Brazilian commercial vehicles spectrum: classes and silhouettes (Adapted from DNIT, 2006b)	70
Table 3-7: Permissible axle load limits changes	71
Table 3-8: Cumulative Equivalent Traffic in million ESALs	72
Table 3-9: Layer thickness identified in both test-sections	74
Table 3-10: Tests carried out in-situ and in laboratory	75
Table 3-11: Laboratory trial planning in Test Section – I.....	76
Table 3-12: Laboratory trial planning in Test Section – II.....	77
Table 3-13: Test results obtained in-situ by the Sand-Cone Method	78
Table 3-14: Dynamic moduli results obtained in both test sections.....	83
Table 3-15: Resilient moduli results obtained in both test sections	84
Table 3-16: Flexural Modulus results obtained in both test sections	85
Table 3-17: UCS results obtained in both test sections.....	86
Table 3-18: ITS results obtained in both test sections.....	86
Table 3-19: f_t results obtained in both test sections.....	87
Table 3-20: Bearing parameters obtained for the subgrade.....	88
Table 3-21: Atterberg Limits obtained for the selected subgrade	89
Table 3-22: Resilient Modulus for the selected subgrade	89
Table 3-23: Soil classification for the selected subgrade	91

Table 3-24: Deflections measured at the top of each layer	93
Table 3-25: Test results obtained in-situ by the sand-cone method during the quality control...	94
Table 3-26: UCS and ITS test results obtained during the quality control.....	95
Table 3-27: Deflectometry control date carried out in both test sections.....	96
Table 4-1: Structure and Poisson's Ratio adopted in the back-calculation process.....	98
Table 4-2: Structural gains obtained in the deflectometry measurement	106
Table 4-3: Structural gain obtained through the equivalent modulus	108
Table 4-4: Coefficient of variation obtained during deflectometry control	109
Table 4-5: Characteristics of the simulated structures	110
Table 5-1: Moisture content in the compaction Process	118
Table 5-2: Analysis of the release time of the layers	122
Table 6-1: Material application according to the classification	125
Table 6-2: Resilient modulus as a function of the CBR and MCT soil classification.....	127
Table 6-3: Strength of the selected subgrade and subgrade of both test sections obtained by DCP	130
Table 6-4: Comparison of $CBR_{\text{Laboratory}}$ with CBR_{DCP}	130

LIST OF FIGURES

Figure 2-1: Location of the first section of inverted pavement in Brazil	8
Figure 2-2: Location of the second section of inverted pavement in Brazil.....	8
Figure 2-3: Importing layers to obtain minimum subgrade strength (Adapted from SANRAL, 2014)	15
Figure 2-4: Grading envelopes for G1, G2, G3 G4 and B graded crushed stone materials (Adapted from TRH14, 1985 and DNIT, 2009).....	22
Figure 2-5: Influence factors on the mechanical properties of the cement-treated layer (Xuan, 2012)	26
Figure 2-6: Gradations of granular materials in relation to their use (Molenaar, 1998 mentioned in Xuan, 2012).....	32
Figure 2-7: Grading envelopes for cement-treated base in Brazil and in South Africa (Adapted from DER, 2005c; DNIT, 2017 and TRH14, 1985).....	32
Figure 2-8: Typical stress/strain relationship of cemented materials (TRH13, 1986)	39
Figure 2-9: Long-term changes in the elastic response of flexible pavements with lightly cemented layers (Adapted from SANRAL, 2014 and De Beer, 1985).....	40
Figure 2-10: Evaluation of the integrity of the cement-treated layer in inverted pavement in Brazil (Adapted from De Almeida, 2019a).....	41
Figure 2-11: a) UCS Test and b) ITS Test (ITS) (SANRAL, 2014)	41
Figure 2-12: Strength parameters of cement stabilised limestone compacted at 0 and 24 hours delay (Adapted from Yeo, 2011).....	48
Figure 2-13: Wide subgrade rutting (SANRAL, 2014).....	51
Figure 2-14: Elastic deflection and radius of curvature (SANRAL, 2014).....	52
Figure 2-15: Deflection Bowl (Horak, 2008).....	53
Figure 2-16: a) cemented layer over cemented layer b) cemented layer over subgrade and c) cemented layer over unbound base layer (Adapted from Balbo, 1993)	54
Figure 3-1: Flow diagram of the Experimental work.....	59
Figure 3-2: Test Sections' locations.....	60
Figure 3-3: a) Test section I (T-I) overview and b) Test section II (T-II) overview	60
Figure 3-4: Cross section of the Bandeirantes Highway (SP-348).....	61
Figure 3-5: FWD Equipment (SANRAL, 2014)	63
Figure 3-6: a) T-I - Deflection measurement carried out in 2003 b) T-II - Deflection measurement carried out in 2003.....	63
Figure 3-7: a) T-I - Deflection measurement carried out in 2005 b) T-II - Deflection measurement carried out in 2005.....	63

Figure 3-8: a) T-I - Deflection measurement carried out in 2007 b) T-II - Deflection measurement carried out in 2007.....	64
Figure 3-9: a) T-I - Deflection measurement carried out in 2009 b) T-II - Deflection measurement carried out in 2009.....	64
Figure 3-10: a) T-I - Deflection measurement carried out in 2012 b) T-II - Deflection measurement carried out in 2012.....	64
Figure 3-11: a) T-I - Deflection measurement carried out in 2014 b) T-II - Deflection measurement carried out in 2014.....	64
Figure 3-12: a) T- I - Deflection measurement carried out in 2016 b) T-II - Deflection measurement carried out in 2016	65
Figure 3-13: Test-Section I – Deflection bowls	66
Figure 3-14: Test-Section II – Deflection bowls.....	66
Figure 3-15: Precipitation in the month of the measurement (Adapted from CIIAGRO, 2020). 68	
Figure 3-16: Annual precipitation in Limeira (Adapted from CIIAGRO, 2020).....	68
Figure 3-17: Cumulative Equivalent Traffic in million ESALs for both test sections.....	72
Figure 3-18: a) IP-01 opened in Test Section I b) IP-02 opened in Test Section I c) IP-03 opened in Test Section II c) IP-04 opened in Test Section II	73
Figure 3-19: Cross section of the test sections T-I and T-II.....	74
Figure 3-20: Preparation of cylindrical specimens collected from both test sections	75
Figure 3-21: a) Prismatic specimen collected in IP-01 b) Prismatic specimen collected in IP-02 c) Prismatic specimen collected in IP-03 d) Prismatic specimen collected in IP-04.....	76
Figure 3-22: a) The sand-cone device b) and c) Determination of the density of the unbound base and selected subgrade in-situ by the Sand-Cone Method.....	78
Figure 3-23: Dynamic Cone Penetrometer (DCP) test.....	79
Figure 3-24: DCP field curves obtained in Test section I - IP-01	80
Figure 3-25: DCP field curves obtained in Test section I - IP-02	80
Figure 3-26: DCP field curves obtained in Test section II - IP-03.....	80
Figure 3-27: DCP field curves obtained in Test section II – IP-04	80
Figure 3-28: Particle size distribution curves obtained in T-I.....	81
Figure 3-29: Particle size distribution curves obtained in T-II.....	82
Figure 3-30: a) Selected subgrade samples collected from IP-02 b) Selected subgrade samples collected from IP-03 b) Selected subgrade samples collected from IP-04.....	88
Figure 3-31: Deflectometry control recommended during the construction of both test sections	92
Figure 3-32: Deflection measurement Locations	93

Figure 4-1: Back-calculated moduli of the infrastructure layers of both test sections	99
Figure 4-2: Back-calculated moduli of the cement-treated layers of both test sections	100
Figure 4-3: Back-calculated moduli of the unbound base layers of both test sections	101
Figure 4-4: Back-calculated moduli of the asphalt concrete layers of both test sections	102
Figure 4-5: a) T-I - LLI parameters and infrastructure moduli, and b) T-II - LLI parameters and infrastructure moduli	103
Figure 4-6: a) T-I - MLI parameters and cement-treated layer moduli, and b) T-II - MLI parameters and cement-treated layer moduli	103
Figure 4-7: a) T-I - BLI parameters and asphalt concrete and unbound base moduli and b) T-II - BLI parameters and asphalt concrete and unbound base moduli	104
Figure 4-8: Analysis of the integrity of the cement-treated layer as a function of traffic	105
Figure 4-9: Designed structure and executed structures	110
Figure 4-10: Parametric Numerical Study – Variation of D_0 and $\mu\epsilon_t$	112
Figure 4-11: Parametric Numerical Study – Variation of $\mu\epsilon$ and $\mu\epsilon_v$	112
Figure 4-12: a) Variation of ϵ_t as a function of time, b) Variation of ϵ as a function of time, and c) Variation of ϵ_v as a function of time	113
Figure 5-1: Test results obtained in-situ by the sand-cone method during the quality control .	116
Figure 5-2: a) Comparison of bulk and dry density of the selected subgrade b) Comparison of bulk and dry density of the unbound base	119
Figure 5-3: UCS as a function of cement content in both test sections	120
Figure 5-4: ITS as a function of cement content in both test sections	120
Figure 5-5: Analysis of the relationship between the strength parameter UCS and curing time	121
Figure 5-6: The relationship between UCS and ITS	122
Figure 6-1: Analysis of soil strength as a function of Soil classification	126
Figure 6-2: a) Laboratory resilient moduli and back-calculated moduli - Test section I and, b) Laboratory resilient moduli and back-calculated moduli - Test section II	128
Figure 6-3: Layer-strength diagram of both test sections	129
Figure 6-4: Grain size distribution of the unbound base executed in both test sections	131
Figure 6-5: Lab. and back-calculated moduli obtained for the cement-treated layer in T-I	133
Figure 6-6: Lab. and back-calculated moduli obtained for the cement-treated layer in T-II	134
Figure 6-7: a) Dynamic moduli results obtained in T-I and b) Dynamic moduli results obtained in T-II	135
Figure 6-8: a) UCS obtained in both test section, b) ITS obtained in both test section and c) f_t obtained in both test section	137

LIST OF SYMBOLS AND ABBREVIATIONS

$^{\circ}\text{C}$	Degrees Celsius
$^{\circ}\text{F}$	Degrees Fahrenheit
%	Per cent
ε_t	Horizontal tensile strains in the bottom of the asphalt concrete layer
ε	Horizontal tensile strains in the bottom of the cement-treated layer
σ_v	Vertical compressive stress on top of the cement-treated layer
ε_v	Vertical compressive strains at the surface of the subgrade
μ	Poisson's Ratio
AASHTO	American Association of State Highway and Transportation Officials
ABCP	Brazilian Association of Portland Cement
ABNT	Brazilian National Standards Organization
ARTESP	Sao Paulo State Transport Agency
ASTM	American Society for Testing and Material
BLI	Base Layer Index
Caltrans	California Department of Transportation
CBR	California Bearing Ratio
CCR	Highway Concession Company
CV	Coefficient of Variation
D_0	Maximum Deflection
DCP	Dynamic Cone Penetrometer
DER/PR	Parana State Department of Traffic
DER/SP	Sao Paulo State Department of Traffic
DERSA	Highway Development S/A
DN	DCP Number
DNIT	National Transport Infrastructure Department
DPCI	DCP index
DTS	Direct Tensile Strength
E	Modulus of elasticity
E_c	Cement-treated layer modulus
E_{Eq}	Equivalent modulus
Elsym	Elastic Layered System
E_s	Infra (Selected subgrade + subgrade) modulus

ESAL	Equivalent Single Axle Load
F	Stress Ratio or Safety Factor
F_E	Axle Factor
FHWA	Federal Highway Administration
F_{LEF}	Load Equivalency Factor
F_R	Regional Factor
f_t	Flexural Tensile Strength
F_V	Vehicle Factor
FWD	Falling Weight Deflectometer
H_c	Cement-treated layer thickness
HRB	Highway Research Board
H_u	Unbound base thickness
HVS	Heavy Vehicle Simulator
Hz	Hertz
ICS	Initial Consumption of Stabilizer
IP	Plasticity Index
IPR/DNER	National Department of Highways
ITS	Indirect Tensile Strength
km	Kilometres
kN	KiloNewtons
kPa	KiloPascals
LL	Liquid Limit
LLI	Lower Layer Index
LP	Plastic Limit
LVDTs	Linear Variable Differential Transformers
m	Metres
MCT	Miniature Compacted Tropical classification
MDD	Maximum Dry Density
MLI	Middle Layer Index
mm	Millimetres
MPa	MegaPascals
N	Equivalent Number of Standard Axles (80 kN)
PMSP/SIURB	Sao Paulo City Hall Standards
R^2	R-Squared
RMSE	Root Mean Square Error

RoC	Radius of Curvature
SADOT	South African Department of Transport
SAMDM	South African Mechanistic Design Method
SANRAL	South African National Roads Agency Limited
SR	Tensile Strain Relationship
TMH	Technical Methods for Highways
TRH	Technical Recommendations for Highways
UCS	Unconfident Comprehensive Strength
USACE	United States Army Corps of Engineers
V_P	Annual average daily traffic
μm	Micrometres

1. INTRODUCTION

1.1 Background

Inverted pavements were developed in South Africa as a cost-effective alternative to conventional rigid and flexible pavements. Improvements in aggregate base technology and exceptional field performance led to the establishment of inverted pavements as the primary design for high-traffic roads in South Africa (Freeme et al., 1980, mentioned in Papadopoulos and Santamarina, 2017).

According to Cortes (2010), an inverted pavement consists of a non-stabilized granular base between a rigid layer treated with cement and an asphalt layer. The term “inverted” is used because the pavement strength does not decrease with depth, leaving it unbalanced due to the rigid cement-treated layer found in the subbase (SANRAL, 2014).

In addition, according to Alessio (2016), the idea behind an inverted pavement is that the cement-treated layer provides a support for the unbound base, thus improving compaction and, consequently, its performance.

According to Suzuki (1992), in the late 1980s, Brazil had its first experience with inverted pavement on two sections of highway. The first one was built on the Governador Mário Covas highway (BR-101), outside city of Imbituba in the southern state of Santa Catarina. The second section was built during the 1990s on the Santos Dumont highway (SP-075), on the section between the cities of Sorocaba and Campinas, which was where Suzuki based his thesis and research.

Cortes (2010) concluded that inverted pavements present higher resistance to rutting and fatigue resistance when compared to common flexible pavement. Furthermore, its initial costs can result in a saving up to 40 %.

North Carolina State University researchers analysed the performance of 24 pavement sections, among them flexible and inverted structures, stating that inverted pavements presented the best results (Tutumluer and Barksdale, 1995). The French Design Guidelines also recommend inverted structures to avoid the propagation of crack reflection between cohesive layers (Corté and Goux, 1996).

In Brazil, some design methodologies endorse the employment of a cement-treated layer depending on the road traffic load. According to the São Paulo State Department of Traffic (DER/SP, 2006a) for equal or greater values than 50 million equivalent single axle loads (ESALs), the use of cement-treated layer as base or subbase layer is recommended. However, the São Paulo City Hall standards (PMSP/SIURB, 2004) sets this value at 10 million ESALs.

The technical and economic feasibilities of an inverted pavement have been proven (Suzuki 1992; Tutumluer and Barksdale, 1995; Corté and Goux, 1996; Cortes, 2010; Salviano and Motta, 2015 and Alessio, 2016) abroad and in Brazil, but there are still doubts related to the parameters that may affect the performance of this type of pavement in Brazil.

The DER/SP (2006a) and PMSP/SIURB (2004) do not distinguish between the performance of inverted pavement and conventional semi-rigid structure, both having the same design guidelines. The National Transport Infrastructure Department (DNIT, 2006a) indicates that, in the design of inverted pavements, the increase of the horizontal tensile strain in the bottom of the asphalt concrete layer (ϵ_t) should be considered as long as the progression of the subbase cracking decreases the effective modulus of the cement-treated layer.

According to Klinsky and Faria (2018), there are few specifications in Brazil that indicate the most adequate type of cement that should be used in the composition of the cement-treated layer, nor are there studies that have investigated its mechanical properties with different hydraulic binders.

The quantity of stabilizer is based on that required to achieve the specified standard for the pavement layer. Probably the most important component of the design is to ensure durability (SANRAL, 2014). According to Balbo (1993) there are still some unclear points regarding the manufacture of the cement-treated layer, since it is unknown the ideal cement content, the effects of the variation of cement content of the mixture and the adequate aggregate gradation.

1.2 Objectives of the Study

The aim of this study is to understand the mechanical behaviour of an inverted pavement, especially for the cement-treated used as a subbase layer. To this end, the study includes the following objectives:

- Identification and characterization of variables directly related to structural behaviour of inverted pavements;
- Comparative analysis of the design, materials, construction and quality control methods for Brazilian and South African inverted pavements, and
- Recommendation of procedures for the inverted pavement structures on basis of the Brazilian test sections.

1.3 Scope of the Study

To achieve the objectives of this study, a wide review of Brazilian and foreign literature had been evaluated, focusing mainly on the similarities and differences found between the methods, materials, and practices adopted during the various stages of the pavement such as: design, construction and quality control.

In addition, the structural performance of two test sections in Brazil designed as inverted pavements was evaluated. Both sections were built based on the same design principles, but have been presented through different structural performances since their implementation in 2001, and these differences have increased over time.

Each test section was monitored with deflection measurements between 2003 and 2016. Two inspection pits were opened in each test section. Samples were collected from all layers, and sent to the laboratory.

Additionally, the tests carried out in the laboratory and in-situ in both sections during their construction in 2001, requested in the quality control, were also analysed in this study. However, the construction of both test sections was done by different companies and consequently, quality control was performed by different companies as well.

The results of the tests of quality control and the results obtained exclusively for this study alongside the available literature, were compared and analysed against each other. These assisted in identifying the reasons associated with the difference in behaviour of the two test sections.

1.4 Methodology

The following methodology was applied to achieve the objectives set for this research study. This research is divided into two parts, presented below:

- a) **Theoretical Study:** This entails of a wide review of Brazilian and foreign literature. Under this topic, additional comparisons between practices used in Brazil and South Africa were made. These were focussed on the selection of the types of materials, methods of design, construction and quality control of all layers of the inverted pavement, especially for the cement-treated layer;
- b) **Experimental Study:** This entails field measurements and laboratory tests using representative samples collected from two test sections, as well as in-situ tests. The results obtained were compared between the test sections and with the results obtained in the quality

control test carried out during the test sections' construction in 2001. The stages of the study are:

- ⇒ Selection of two test sections, designed as inverted pavements. Each test section with a length of 320 m, named in this paper as Test Section I–TI (km 147+480 to km 147+800 North) and Test Section II –TII (km 142+480 to km 142+800 South). Both sections were built based on the same design principles, but they presented different structural performance since their implementation back in 2001, and these differences have only increased over time. During the selection of the tests, care was taken to reduce the effect of external variables. The test sections are located in a similar topographic region, this does not include curves or ramps, and the traffic of both test sections is the same order of magnitude;
- ⇒ Each test section was monitored every two years between 2003 and 2016, with deflections measurements. The results obtained were analysed in each year of measurement. Comparison of the results obtained took place in both test sections and with the available literature;
- ⇒ Two inspection pits were opened in the heavy traffic lane (lane 2) in each one of the test sections to verify the thicknesses of the layers, collection of samples from all layers followed and tests were carried out in the laboratory, as well as in-situ tests. At this stage, it was also possible to analyse anomalies through visual inspections;
- ⇒ In-situ tests were carried out in the unbound base and the stabilized subgrade. Using the Sand-Cone Method the bulk density, dry density, and moisture content were determined for the unbound base. For the selected subgrade, besides the tests previously mentioned, two tests were performed in each inspection pits with Dynamic Cone Penetrometer (DCP), and
- ⇒ In the laboratory the following tests were carried out: unbound base (Gradation test), cement-treated layer (dynamic modulus, resilient modulus, flexural modulus, Unconfined Compressive Strength (UCS), Indirect Tensile Strength (ITS) and flexural tensile strength) and for the selected subgrade (California Bearing Ratio (CBR), Atterberg limits, soil classification and resilient modulus).

The results of the tests obtained in this investigation phase and in the quality control were evaluated and compared with each other. Convergences and divergences between what was suggested in the project and what was actually done in the construction of the test sections were also analysed.

Finally, analyses were made based on the conclusions obtained in the theoretical and experimental studies, seeking to identify the possible causes associated with the difference in the performance of both test sections.

1.5 Organization of the Dissertation

The report consists of seven chapters, followed by a list of references and appendices. A brief overview of each chapter is given as follows:

- Chapter 1: Introduction - Gives an overview of the entire study. The background presents a brief discussion of the topic and highlights the significance of the research. Furthermore, the objectives of the research are introduced, followed by the scope, and the methodology applied to achieve the objectives set for this research.
- Chapter 2: Literature Review - Serves as a support to this research, providing the necessary knowledge to understand the behaviour of the inverted pavement, especially the cement-treated layer. This chapter provides an understanding of the properties of materials, methods, practices, and techniques employed from the design of the pavement structure to the construction and quality control of the cement-treated layer.
- Chapter 3: Experimental Work – Provides the experimental program followed to achieve the research objectives. The chapter contains details of the materials and approaches employed, tests conducted, instrumentation used, and in addition to data obtained in the field measurement, the results of the tests carried out in-situ and in the laboratory are used.
- Chapter 4: Pavement Performance - Provides the understanding of the interdependence of the variation of the thickness and modulus in the performance of inverted pavements through the analyses of deflections measured between 2003 and 2016, deflections obtained in 2001 during the quality control and the development of a parametric numerical study.
- Chapter 5 – Analysis of Quality Control Tests – This chapter presents an analysis and discussions of the test results carried in situ and the laboratory on the unbound base, cement-treated layer, selected subgrade and subgrade during the quality control of both test section.
- Chapter 6 – Analysis of the laboratories tests carried out in 2017 - This chapter presents the analyses and discussions of the test results carried out in the laboratory on the unbound base,

cement-treated layer and selected subgrade in 2017 in both test section. Besides the analyse of convergences and divergences of results obtained for both test sections, the test results were compared to test results obtained during quality control and what was suggested in the project of the pavement of both test sections.

- Chapter 7 – Conclusions and Recommendations - This chapter summarises the main conclusions reached throughout this study and includes recommendations for further research.
- Chapter 8 – References - provides a list of references used during the course of the research project.
- Appendix A – Correlation between Equivalent Modulus and Deflection – Contains the structures simulated using Elsym5 and the outcomes.
- Appendix B – Parametric Numerical Study - Contains the structures simulated in the parametric numerical study and the outcomes.

2. LITERATURE REVIEW

This chapter provides a review of the available literature. This literature review serves as a support to this study, providing the needed knowledge to its development. As an introduction to the chapter, an overview of the Brazilian, South African, and American experience of inverted pavements is presented. These three countries were chosen for different reasons:

- a) The test sections and scope of this work are located in Brazil;
- b) The inverted pavement was developed in South Africa, and since then it has been a reference in quality, techniques, and procedures for the rest of the world, and
- c) The United States of America has been studying inverted pavements on a large scale.

In general, the literature review seeks the knowledge necessary to understand the behaviour of the inverted pavement. To achieve this, the methods, practices, and techniques are covered. This section also provides an understanding of the properties of materials in different situations, whether in the analysis of correlations of these properties, in the individual analysis of the layer or in the analysis of the pavement as a whole, and the influence of each layer on the performance of the pavement.

2.1 National and international experience with inverted pavements

2.1.1 Brazilian experience

According to Pinto et al. (1988) Brazil had its first experience with inverted pavement in the late 1980s in a section built on the Governador Mário Covas highway (BR-101). The section is situated outside the city of Imbituba in the southern state of Santa Catarina (Figure 2-1). This section was under coordination of the Highway Research Institute and the old National Department of Highways (IPR/DNER). The stabilized layer was composed of a mixture of sand, fly ash, and lime. The thicknesses of the layers are shown in Table 2-1.



Figure 2-1: Location of the first section of inverted pavement in Brazil

Table 2-1: First section of inverted pavement in Brazil (Adapted from PINTO et al., 1988)

Layer	Thickness (mm)
Asphalt	
Asphalt Concrete	50
Base	
Unbound base	150
Subbase	
Stabilized layer	150
Subgrade	Semi-infinite

The second section, according to Suzuki (1992), was built during the 1990s on the Santos Dumont highway (SP-075), located between the cities of Sorocaba and Campinas in the State of Sao Paulo (Figure 2-2). The stabilized layer was composed of a mixture of crushed stone and approximately 3.5 % of cement. This section was part of the experimental study of Suzuki (1992). The thicknesses of the layers are shown in Table 2-2.

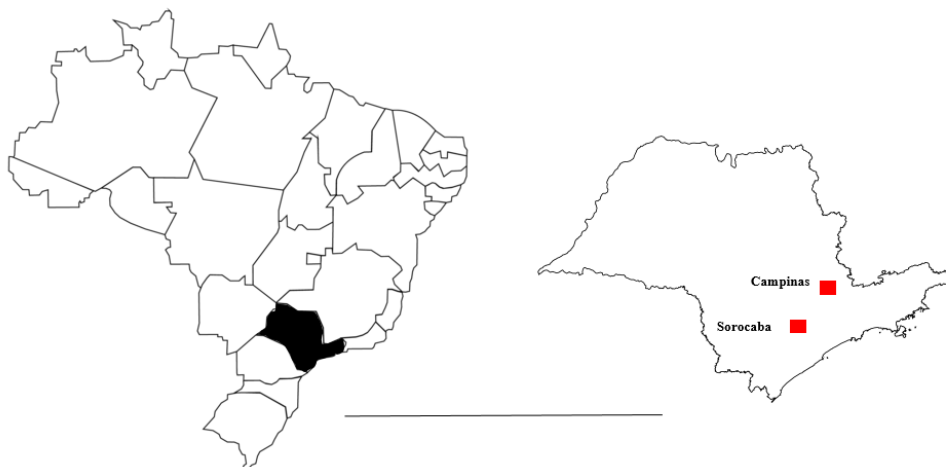


Figure 2-2: Location of the second section of inverted pavement in Brazil

Table 2-2: Second section of inverted pavement in Brazil (Adapted from Suzuki, 1992)

Layer	Thickness (mm)
Asphalt	100
Asphalt Concrete	
Base	100
Unbound base	
Subbase	170
Stabilized layer	
Subgrade	Semi-infinite

Suzuki (1992) monitored the section on an inverted pavement for six months. During this period, measurements were carried out to evaluate the functional and structural conditions of the pavement. The author concluded that the 6-month monitoring period was insufficient to prove the technical viability of the pavement. However, the first functional and structural evaluations carried out in the experimental section confirmed the expected performance.

Macêdo (1996) carried out tests in the laboratory and in the field in an experimental section located on Governador Carvalho Pinto highway (SP-070) built on an inverted pavement by Highway Development S/A (DERSA). For the cement-treated layer 200 mm thick and 3.5 % cement, modulus of 9 000 MPa was admitted. Macêdo (1996) concluded that the modulus obtained in the laboratory were greater than the modulus admitted in the project for all analysed layers. The deflections obtained in the field with Falling Weight Deflectometer (FWD) and Benkelman Beam were higher than the deflections admitted in the project.

Silva (2014) reported in his master's dissertation that the experimental section studied by Macêdo (1996) was still in good functional condition 18 years after its implementation. Salviano and Motta (2015) conducted a budgetary analysis of flexible, rigid, semi-rigid, and inverted pavements during the design of Lot 1 of the Metropolitan Arch in Rio de Janeiro and concluded that, the most adequate alternative for a designed service life of 30 years would be inverted pavement.

Alberto (2018) also conducted an economic analysis, comparing the initial costs of implementing flexible, semi-rigid, and inverted pavements. The author concluded that the inverted pavement was the most economical option, followed by the semi-rigid and flexible pavement.

Even though Brazil has had practical experiences with the inverted pavement since the 1990s, the adoption of this type of pavement is concentrated in the vast majority in the state of São Paulo. The Bandeirantes highway (SP-348), with an extension of 73 km (km 96 + 000 to km 172 + 000)

was built in 2001, by the AUTOBAN concessionaire, and since then it has been presenting an excellent performance.

The Mário Covas Ring Road - North section, also located in the state of São Paulo, is being built as an inverted pavement, under the responsibility of DERSA and the Construcap-Copasa Consortium. The project is 44 km long. The main objective of this project is to order road traffic to and from the city of São Paulo, estimated at 1.1 million vehicles per day, in addition to regulating the circulation of large road trucks in the city (Rodrigues, 2018).

It should be noted that over the years, the use of inverted pavements for road paving in Brazil has been observed, especially in the state of São Paulo. However, some of the main companies in the country have avoided this type of pavement. The use of the cement-treated layer Brazil has been used on a large scale, but as base layer. Unfortunately, there is a lack of publications that demonstrate and evaluate the mechanical performance of this type of pavement in Brazil.

2.1.2 South African experience

Inverted Pavement was developed in South Africa in the 1970s (De Beer, 1985; Lewis et al., 2012 and Etzi, 2015). According to Papadopoulos (2014) inverted pavement was developed in South Africa as a cost-effective alternative to concrete pavements. This kind of design faced early scrutiny as it was believed that they could not match the performance of full depth asphalt or concrete pavements.

Williams (1986) mentioned in Suzuki (1992) reports that the inverted pavement was formally tested in South Africa in 1969. The test section consisted of the following: 30 mm of asphalt concrete; 100 mm of crushed stone; 100 mm stone gravel treated with cement; 100 mm to 150 mm of stabilized gravel sub-base and 150 mm to 300 mm of selected subgrade.

To confirm the performance of the inverted pavement, South Africa conducted extensive full-scale accelerated pavement research using a Heavy Vehicle Simulator (HVS) (De Beer, 1985; Horne et al., 1997; Lewis et al., 2012; Alessio, 2016; Papadopoulos and Santamarina, 2017). Papadopoulos (2014) furthermore added that besides the reports publicly available on the several inverted pavements that have been tested using the HVS in South Africa, there are reports not publicly available.

According to Horne et al. (1997), South Africa is advanced in many highway technologies, but many of these design and construction techniques were largely unknown in the United States in

1997. Then, the Federal Highway Administration (FHWA) visited South Africa and conducted joint activities with the South African Department of Transport (SADOT). That exchange allowed the mutual sharing of ideas, practices, and experiences.

Inverted pavements are extensively used in South Africa to support heavy traffic loads (Horne et al. 1997; Lewis, 2012; Jooste and Sampson 2005 mentioned in Papadopoulos and Santamarina, 2017). Alessio (2016) in his thesis mentioned the N1 highway, located in the north of Pretoria. According to the author, the highway was still in good condition 26 years after its construction.

Earlier pavements in South Africa were built with granular bases, made of natural or stabilised gravel and various forms of macadam (Jooste and Sampson (2005) mentioned in Papadopoulos and Santamarina (2017)). Closure on this development and its capabilities was achieved during the South African HVS test program during the 1980s, resulting in the conclusive proof that a properly constructed G1 crushed stone layer as part of an inverted pavement structure can be used for pavements with a bearing capacity up to 50 million ESALs (Kleyn, 2012).

According to Rust et al. (1998) South Africa is one country, which designs and constructs their flexible pavements quite differently than most countries. About 70 % of its pavements are constructed with thin asphalt bound surfaces (40 mm or less) placed on top of high quality crushed stone bases. The South African flexible pavement design emphasizes the importance of a good foundation, they involve novel construction methods and careful material selection to achieve dense unbound aggregate layers that exhibit a remarkable ability to support the heaviest traffic loads under both dry and wet conditions (Horne et al., 1997).

2.1.3 United States experience

The inverted pavement started to be used in the United States, around 1954, in the state of New Mexico, when several old concrete pavements near Albuquerque had become so cracked and distorted that reconstruction was necessary. The old pavements were covered with 150 mm of granular material. Over the reshaped section, 60 mm of hot mixed asphalt were placed (Johnson, 1961).

Norling (1973) inspected 13 sections of inverted pavement, most of them 4 to 6 years old. The reflective cracks did not appear for 3 to 5 years. However when they eventually did appear, they were narrow and spaced farther apart than normal. The inverted pavements served satisfactorily, without maintenance problems, although a 10-year-old experimental section required overlaying.

Norling (1973), Maree et al. (1982), Metcalf et al. (1999), Rasoulilian et al. (2000), Lewis et al. (2012), Cortes (2010) and Cortes and Santamarina (2012) have shown that inverted pavements can outperform conventional flexible pavement structures performance. Inverted pavements have been identified as the most economical solution in several cost-comparison studies.

Cortes (2010) and Cortes and Santamarina (2012) presented a comprehensive experimental study on a full-scale inverted pavement test section built near LaGrange, Georgia. A detailed description of the mechanical behaviour of the test section before, during and after construction provides critically needed understanding of the internal behaviour and macro-scale performance of this pavement structure. Cortes and Santamarina (2012) also indicated that the use of inverted base pavements in the United States has been hindered by the lack of field experiments and related research required to investigate the mechanical response of this pavement structure under local conditions, construction practices, required quality control and performance.

Maree et al. (1982), Li et al. (1999), Terrell et al. (2003), Cortes et al. (2012), Cortes and Santamarina (2012) and Papadopoulos (2014) studied the response of the unbound granular base layer critical to the performance of the inverted pavement structure.

Papadopoulos and Santamarina (2015) conducted three-dimensional finite-element simulations to assess the mechanical performance of different inverted pavement structures, with emphasis placed on pavements that feature thin asphalt surface layers. Results indicated that the stress distribution within inverted base pavements is markedly different from that of conventional pavements due to the stiffness contrast between successive layers. Thin-asphalt layers deform more uniformly and experience lower tension than thick layers.

Frost (2017) studied long-term performance of granular bases including the effect of wet-dry cycles on inverted pavement performance. Hossain et al. (2017) evaluated the mechanical properties of cement-treated aggregate and recommended values for use in AASHTO Pavement ME Design software.

2.2 Design procedures for inverted pavement

Designing a pavement is a complex task. Many fatigue models check whether the pavement is suitable to accommodate the traffic predicted. However, it is not enough to just have access to several models and the latest generation software, it is necessary to have knowledge of what is being done, to know the advantages and limitations of each model. Fatigue models used in South Africa may for instance not be suitable in Brazil and vice versa.

Furthermore, it is important to have a comprehensive understanding of the design problem, the parameters governing the design and to obtain the necessary design inputs. Many fatigue models have the input Moduli and Poisson's Ratio of each layer, but how are these parameters defined without making mistakes? Understanding the properties of materials, how they behave under the influence of traffic and the environment is the first and most difficult task that must be completed before choosing the fatigue model. Incorrect assumptions during this investigation phase may lead to significant design risk.

Therefore, in this section, in addition to a bibliographic review of the fatigue models, a brief review is made of the elastic or resilient modulus suggested and adopted, either by standard agencies or available in the technical literature for each layer, with the exception of the cement-treated layer which will be discussed more comprehensively in Sections 2.3 and 2.4.

According to the literature review, it was noticed that the concept of pavement design is very similar between countries with a few changes on the materials and local conditions. During design, all layers need to be carefully evaluated, as the failure of one layer compromises the integrity of the others. The main parameters evaluated in a traditional pavement design method are:

- ⇒ Vertical compressive strains at the surface of the subgrade (ϵ_v);
- ⇒ Horizontal tensile strains in the bottom of the cement-treated layer (ϵ), and
- ⇒ Horizontal tensile strains in the bottom of the asphalt concrete layer (ϵ_t).

2.2.1 Subgrade

The aim of the design process is to protect, use and improve the bearing capacity of the in-situ subgrade material so that the pavement will be able to fulfil the service objective over the analysis period (TRH4, 1996).

The bearing capacity and quality of the subgrade roadbed fill is of prime importance in the selection of the appropriate pavement type and hence the overall life cycle strategy (TRH4, 1996). According to Cortes (2010) subgrade properties is a key input property in mechanistic empirical pavement design procedures. The support provided by the subgrade is generally regarded as one of the most important factors in determining pavement design thickness, composition and performance (Austroads, 2017).

Before applying the fatigue models, it is important to be aware of the subgrade's bearing capacity and whether external agents such as in-situ moisture can compromise the stability of the analysed material. For example, according to Frost (2017) in-situ moisture, density and porosity are some of the critical soil properties that affect resilience of a modulus and the quality of the subgrade material. For Weber (2013) the subgrade resilient modulus is not constant, as they suffer variations due to applied stresses and humidity variations and, therefore, the same value cannot be assumed for the modulus throughout the year.

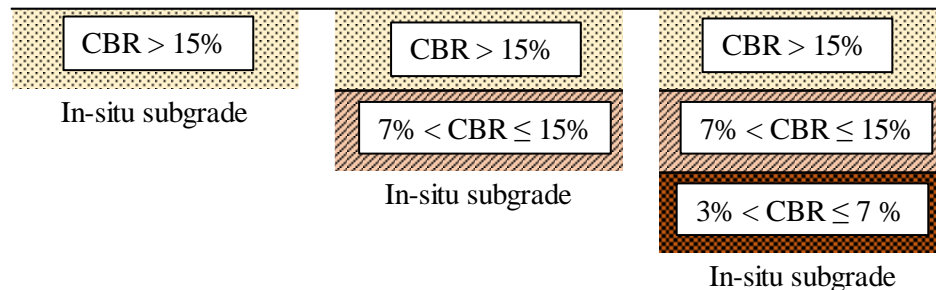
Tutumluer and Barksdale (1995) and Metcalf et al. (1999) indicated the inverted section is particularly attractive for use over a weak subgrade. However, there are many discussions about this subject around the world. According to Papadopoulos and Santamarina (2017) weak subgrades should be mechanically or chemically stabilised to prevent excessive bending in the cement treated base. Subgrade failure is decreased because cement-stabilized bases spread traffic loads over wide areas and can span weak subgrade locations (Adaska and Luhr, 2004).

Cortes (2010), for example, estimated the mean resilient modulus to be 250 MPa with a standard deviation of 100 MPa, based on an extensive field and laboratory study conducted at test sections in the inverted pavement. According to Frost (2017), in 2016 the Georgia Tech team conducted a study in the same test sections covered in Cortes (2010). In this study it was observed that the station with resilient modulus of the subgrade less than 100 MPa (classified as weak subgrade) presented high load cracking. The station with resilient modulus of subgrade higher than 250 MPa (classified as strong subgrade) showed relatively better performance.

According to SANRAL (2014) a minimum CBR of 15 % is generally required for flexible pavements with a minimum in-situ material density of 93 % of mod. AASHTO density. To determine the adequacy of the in-situ subgrade, it is divided into sections based on the CBR, using the ranges in Table 2-3. The 10th percentile CBR value is determined for each region and must exceed the minimum value in the range. The pavement foundation is built-up, as illustrated in Figure 2-3.

Table 2-3: In-situ subgrade delineation for flexible pavements in South Africa (Adapted from SANRAL, 2014)

CBR (%)s	Action
> 15	⇒ In-situ subgrade of a G7 standard and of sufficient strength to support structural layers. ⇒ Rip and recompact to 93 % of modified (mod.) AASHTO density.
7 to 15	⇒ In-situ subgrade of a G9 standard. ⇒ Rip and recompact in-situ material to 93 % of mod. AASHTO density. ⇒ Import a 150 mm thick layer of G7 standard material.
3 to 7	⇒ In-situ subgrade of a G10 standard. ⇒ Rip and recompact in-situ material to 93 % of mod. AASHTO density. ⇒ Import a 150 mm thick layer of G9 standard material. ⇒ Import a second 150 mm thick layer of G7 standard material.
< 3	⇒ Chemical/mechanical stabilization. ⇒ Or, remove and import new material. ⇒ Or, add additional cover to place poor quality in-situ material below material depth.

**Figure 2-3: Importing layers to obtain minimum subgrade strength (Adapted from SANRAL, 2014)**

In Brazil, 75 % of its area is covered by lateritic formations due to the tropical climate (Cordani et al., 2000). However, the main specifications and current guides in the country suggest that subgrade has CBR greater than or equal to 2 % (Table 2-4) when dimensioning new pavements (PMSP/SIURB, 2004; DER/SP, 2005a and DNIT, 2006a).

The Parana State Department of Traffic (DER/PR, 2005) and DNIT (2010) specifications do not define the minimum design CBR; this decision must be taken by the designer (Table 2-4). The main manuals and specifications in Brazil also do not make any association between the expected traffic and/or the service level of the project and the capacity of the subgrade.

Massenlli and Paiva (2019) and De Almeida et al. (2019a) through sensitivity analyses and mechanistic simulations, concluded that the subgrade is considered weak if the resilient modulus is less than 50 MPa. According to Austroads (2017) subgrades with CBR less than about 5 % may require treatment to avoid delays in construction and assist in compaction of subsequent layers. For Ferri (2013) subgrade with resilient modulus below 40 MPa means high risk of losses in the medium and long term.

Table 2-4: In-situ subgrade delineation for flexible pavements in Brazil (Adapted from PMSP/SIURB, 2004; DER/SP (2005a); DER/PR, 2006; DNIT, 2006a and DNIT, 2010)

Organization / Specification	Action
IP- 05/2004 - 2004 Sao Paulo City Hall standards	⇒ CBR > 2 % (new pavement design). ⇒ 100 % of normal density.
ET-DE-P00/001 - 2005 São Paulo State Department of Traffic - DER/SP	⇒ CBR ≥ 2 % (new pavement design). ⇒ Compaction energy is not defined. Can be eight 100 % normal or intermediate density.
ES-P 01/05 - 2005 Parana State Department of Traffic - DER/PR.	⇒ CBR defined by the designer. ⇒ Compaction energy is not defined. Can be eight 100 % normal or intermediate density.
Pavement Design - 2006 National Transport Infrastructure Department – DNIT	⇒ CBR ≥ 2% (new pavement design). ⇒ 100 % of normal density.
DNIT 137/2010 - ES - 2010 National Transport Infrastructure Department – DNIT	⇒ CBR defined by the designer. ⇒ 100 % of normal density.

Assuming that the subgrade is usually the least resistant material in the structure, it is through it that the process of structural compatibility verification begins. According to Tutumluer and Barksdale (1995), the inverted sections had lower vertical stresses on the subgrade and lower resilient surface deflections than the flexible conventional sections. Cortes (2010) also concluded the statement above. The influence of the subgrade on the inverted pavement response is discussed in Section 2.6.

According to the bibliographic research developed, it was possible to select a series of prediction models (Table 2-5) for specific deformations at the top of the subgrade. Note that the fatigue models are expressed by Equation 2.1.

$$N = a\left(\frac{1}{\varepsilon_v}\right)^b \quad (\text{Equation 2.1})$$

Where:

N: Standard axles to set level of permanent deformation

ε_v : Vertical compressive strain at top of layer

a and b: Experimental regression coefficients (see Table 2-5)

Table 2-5: Fatigue Models for subgrade and selected layer permanent deformation (Adapted from Suzuki, 1992 and DER/SP, 2006a)

Author/Organization	Year	Coefficients	
		a	b
Dorman & Metcalf	1965	0.00607E-07	4.762
CRR	1982	0.03050E-07	4.348
Shell			
50% reliability	1985	6.15000E-07	4.000
85% reliability	1985	1.94000E-07	4.000
95% reliability	1985	1.05000E-07	4.000
LCPC - Subgrade	1983	1.20000E-07	4.167
LCPC - Selected Layer	1983	0.02720E-07	4.098
Asphalt Institute	1984	0.01340E-07	4.484

In Brazil, for the mechanistic verification of the subgrade, DER/SP (2006a) recommends the use of a fatigue model proposed either by Dorman & Metcalf, Shell or the Asphalt Institute, however, the fatigue model proposed by Dorman & Metcalf is most commonly used among the designers.

In South Africa, the fatigue model (Equation 2.2.) for the selected and subgrade material also analyses the vertical compressive strain at top of layer. The fatigue model may be used in two different cases, considering 10 mm and 20 mm of rutting in the layer. However, according to SANRAL (2014), the fatigue model that considers 10 mm of rutting is commonly used, particularly for Category A and B roads.

$$N = 10^{(a-10\log\varepsilon_v)} \quad (\text{Equation 2.2})$$

Where:

N: Standard axles to set level of permanent deformation

ε_v : Vertical compressive strain at top of layer

a: Constant

2.2.2 Cement-treated Layer

Balbo (1993), when starting his research, believed that the failure of the cement-treated layer in Brazil was due to the lack of a design procedure in Brazil, pioneered a fatigue model for cement-treated layers in Brazil (Equation 2.3). However, during his research, the author realized that the lack of knowledge about the mechanical behaviour of the cement-treated layer aggravate the uncertainties and consequently cause failures in new projects.

According to Austroads (2017) the principal factors affecting the fatigue life of cemented materials include particle size distribution, particle shape, density, moisture content, mixing efficiency, and cracking pattern. Some of these factors are in turn dependent on binder type and content, etc. Therefore, due to the complexity of the variables involved in the success of the cement-treated layer and how its mechanical properties are influenced in different ways, Section 2.3 addresses the effects of varying the type and cement content, grain size and type of aggregate, as well as the effects of variations in moisture content, curing time and compaction. In Section 2.4, the strength parameters of the cement-treated layer are addressed.

$$\text{Log}_{10}N = 17.137 - 19.608SR \quad (\text{Equation 2.3})$$

Where:

N: Standard axles to set the fatigue life

SR: Relationship between the applied tensile strain (ϵ) and the tensile strain-at-break (ϵ_v) of the material

The Tensile Strain Relationship (SR) is another topic widely discussed among designers and scientists. For some researchers, the adoption of limiting strain criterion is essential for the success of the pavement structure. According to Balbo (2006), the relationship between tensile strain applied and tensile strain-at-break should be maintained at around 50 %. For modulus greater than 10 000 MPa, Murphy et al. (1980) recommends that the limiting strain to 65 % of the strain-at-break.

The fatigue model proposed by Balbo (1993) is widely used in Brazil for both inverted and semi-rigid pavement. However, the main current instructions and guides in Brazil are no up to date and therefore recommend the fatigue model (Equation 2.4) developed by De Beer and other researchers from South Africa in 1989 (DER/SP, 2006a and DNIT, 2006a).

$$N = 10^{7.19(1-\frac{SR}{8})} \quad (\text{Equation 2.4})$$

Where:

N: Standard axles to set the fatigue life

SR: Relationship between the applied tensile strain (ϵ) and the tensile strain at break (ϵ_v) of the material

In South Africa, cement-treated layers are analysed as bound layers for two fatigue models, effective fatigue and crushing. The critical parameters for cemented material are given by:

- (a) Maximum tensile strain (ϵ) at the bottom of the layer controlling the “effective fatigue life”;
- and
- (b) Vertical compressive stress (σ_v) on top of the cemented layer controlling crushing life.

According to SANRAL (2014) the term “effective fatigue” is used to suggest that the typical fatigue cracking. Once a cemented material has reached the end of its effective fatigue life, it enters into a new phase wherein it behaves as an equivalent granular layer. The effective fatigue model for cemented materials is shown in Equation 2.5.

$$N = SF * 10^{c \left(1 - \frac{\epsilon}{d \epsilon_b}\right)} \quad \text{(Equation 2.5)}$$

Where:

N: Effective fatigue life

ϵ : Horizontal tensile strain at bottom of layer (microstrain)

ϵ_b : Strain at break (microstrain)

c, d: Constants

SF: Shift Factor for crack propagation

Crushing life is analysed in two conditions, namely crush initiation with roughly 2 mm deformation on top of the layer and advanced crushing with 10 mm deformation and extensive breakdown of the cemented material (Theyse et al., 1996). According to SANRAL (2014), crushing is not considered a terminal condition and hence it is not used in the critical layer calculation. However, it is an important check, as any crushing has a significant impact on the surfacing. The damage model for crush initiation and advanced crushing is given in Equation 2.6.

$$N = 10^{a \left(1 - \frac{\sigma_v}{b USC}\right)} \quad \text{(Equation 2.6)}$$

Where:

N: Standard axles to crack initiation or advanced crushing

σ_v : Vertical compressive stress at top of layer

USC: Unconfined compressive strength (KPa)

a, b: Constants

In Australia, according to the Guide to Pavement Technology Part 2 (Austroads, 2017), the fatigue model depends on the flexural strength and modulus (Equation 2.7).

$$N_f = \left(\frac{K}{\mu\varepsilon}\right)^{12} \quad (\text{Equation 2.7})$$

Where:

N : Allowable number of repetitions of the load-induced tensile strain

$\mu\varepsilon$: Load-induced tensile strain at the base of the cemented material (microstrain)

K : Presumptive constant

2.2.3 Unbound Base Layer

The unbound aggregate base is the central component of the inverted pavement structure (TRH4, 1996 and Cortes and Santamarina, 2012). The knowledge about the mechanical properties of granular bases are key design inputs in both empirical pavement design methods as well as in mechanistic guidelines.

The modulus of unbound granular materials must be appropriate for the range of stresses under which they are likely to operate. The modulus and small-strain stiffness of granular materials depend on stress history, state of stress, density, gradation, and moisture content (Uzan, 1985 and Austroads, 2017).

In Brazil, DER/SP (2006a) recommends an interval of moduli for the unbound base layer. However, the institution does not discriminate where it is placed or make any relation between the grading and elastic modulus. In Table 2-6 the moduli and Poisson's Ratio recommended by DER/SP (2006a) are shown, as well as the moduli and Poisson's Ratio adopted for the unbound base layer in inverted pavements in some publications.

Table 2-6: Modulus and Poisson's Ratio for the unbound base layer in an inverted pavement in Brazil

Author/Organization	Modulus (MPa)	Poisson's Ratio
DER/SP (2006a)	150 to 300	0.35
Suzuki (1992)	450	0.40
Macêdo (1996)	200	-
Bernucci (2013) mentioned in Salvador and Motta (2015)	300	0.35
Alberto (2018)	300	0.40

According to SANRAL (2014), in South Africa, unbound granular layers are assumed to accumulate permanent deformation, from shear deformation, within the layer. The resilient properties for unbound granular base are given in Table 2-7. The suggested ranges are shown, along with the values in brackets used in the development the catalogues in TRH4 (1996).

Table 2-7: Modulus and Poisson's Ratio for the unbound base layer in an inverted pavement in South Africa (Adapted from SANRAL, 2014)

Material Code	Material Description	Modulus Over Cemented	Poisson's Ratio
G1	High quality crushed stone	250 to 1 000 (450)	0.35
G2	Crushed stone	200 to 800 (400)	0.35
G3	Crushed stone	200 to 800 (350)	0.35
G4	Natural gravel (base quality)	100 to 600 (300)	0.35
G5	Natural gravel	50 to 400 (250)	0.35
G6	Natural gravel (subbase quality)	50 to 200 (225)	0.35

In Australia, Austroads (2017) suggests a guide when assigning maximum values to base quality crushed rock materials under asphalt surfacings when other, more reliable information is unavailable (Table 2-8).

Table 2-8: Suggested vertical modulus of top sublayer of normal standard base material (Austroads, 2017)

Thickness of overlying bound material	Modulus of overlying bound material (MPa)				
	1 000	2 000	3 000	4 000	5 000
40 mm	350	350	350	350	350
75 mm	350	350	340	320	310
100 mm	350	310	290	270	250
125 mm	320	270	240	220	200
150 mm	280	230	190	160	150
175 mm	250	190	150	150	150
200 mm	220	150	150	150	150
225 mm	180	150	150	150	150
≥ 250 mm	150	150	150	150	150

Lekarp et al. (2000) reinforce the importance of the particle size and shape, maximum grain size, load duration, and load frequency in the resilient response of the granular base. In Brazil, the main standard organizations recommend normally four different types of grading of crushed stone classified from A to D (DERSA, 1997; DER/SP, 2005b; DNIT, 2009). DNIT (2006a) recommends the use of a grading crushed stone as a base layer between A to C, when the cumulative traffic is greater than 5 million ESALs. However, many designers have used and recommended the unbound base layer as a base in inverted pavement classified as B material. The B material recommended by each organization is quite similar, especially the maximum percentage passing in each sieve.

In South Africa, all the materials shown in Table 2-7 has been used as a base in inverted pavements, but the materials G1, G2, G3 and G4 has been used more often, according to design catalogue available in TRH4 (1996). Table 2-9 and Figure 2-4 the grading envelope often employed in Brazil and South Africa are shown. Note that to comparison purposes the grading proposed by DNIT (2009) was chosen since DNIT is a nationwide agency in Brazil.

Table 2-9: Grading of graded crushed stone used in South Africa and in Brazil (Adapted from TRH14, 1985; DERSA, 1997; DER/SP, 2005b and DNIT, 2009)

Sieve size (mm)	Brazil			South Africa		
	B (DERSA, 1997)	B (DER/SP, 2005)	B (DNIT, 2009)	G1, G2 and G3 (TRH14, 1985)	G4	
	Percentage Passing (%)					
53				100-100	100-100	100-100
50	100-100	100-100	100-100			
37.5				100-100	100-100	85-100
26.5				84-94	100-100	
25	75-90	82-90	75-90			
19				71-84	85-95	60-90
13.2				59-75	71-84	
9.5	40-75	60-75	40-75			
4.8	30-60	45-60	30-60	36-53	42-60	30-65
2	20-45	32-45	20-45	23-40	27-45	20-50
0.42	15-30	22-30	15-30	11-24	13-27	10-30
0.075	5-15	10-15	5-15	4-12	5-12	5-15

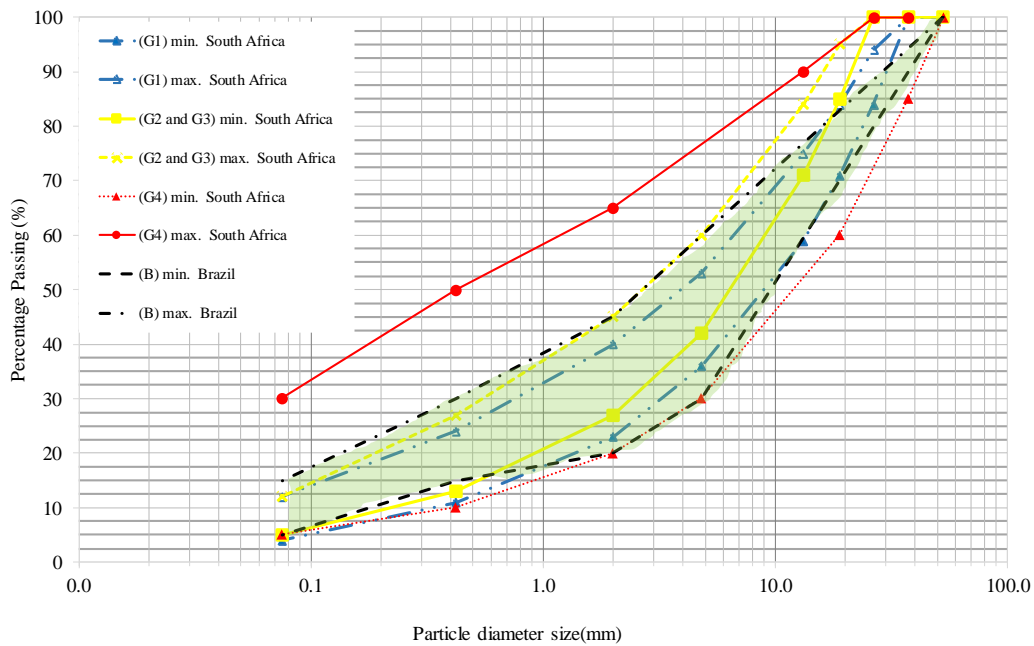


Figure 2-4: Grading envelopes for G1, G2, G3, G4 and B graded crushed stone materials (Adapted from TRH14, 1985 and DNIT, 2009)

The resilient or elastic modulus of the unbound layer in an inverted pavement also depends on its thickness and of the confinement created by the cement-treated layer and asphalt concrete. Modular variations in thickness of the unbound base layers are discussed in Section 2.6.

In Brazil, in the design of inverted pavements, the granular layer is not analysed by a fatigue model. In South Africa, granular layers are analysed by determining the shear stress state in the middle of the layer and comparing this to the shear strength, in terms of the cohesion and friction angle using the Mohr-Coulomb model. The fatigue model, given in Equation 2.8, calculates the structural capacity of the granular layer to a terminal condition of 20 mm of rutting in the layer.

$$N = 10^{(\alpha F + \beta)} \quad (\text{Equation 2.8})$$

Where:

N_f : Number of equivalent standard axles to safeguard against shear failure

α, β : Constants

F: Stress Ratio or Safety factor

2.2.4 Asphalt Concrete

According to Cortes (2010) the characterization of the asphalt layer is focused on the determination of elastic parameters, namely the elastic modulus and the Poisson's Ratio. For the design of new pavements, the (DER/SP, 2006a) recommends a range of different moduli for the asphalt layer. The variation of moduli is given in function the type of materials that includes the grading and the penetration grade bitumen. In Table 2-10 the moduli recommended by the (DER/SP, 2006a) and the moduli adopted for the asphalt layer in an inverted pavement in some publications are shown.

Table 2-10: Modulus and Poisson's Ratio for the asphalt layer in Brazil

Author/Organization	Elastic Modulus (MPa)	Poisson's Ratio
DER/SP (2006a)	2 000 to 4 000	0.30
Suzuki (1992)	8 000	0.30
Macêdo (1996)	3 500	-
Bernucci (2013) mentioned in Salvador and Motta (2015)	5 617 to 5 163	0.35
Alberto (2018)	3 500	0.35

According to SANRAL (2014), in South Africa, they generally use asphalt layers that are less than 50 mm thick, and failure of the asphalt layer is not necessarily a terminal condition for the

pavement. For Cortes (2010) the use of thin asphalt concrete layers can lead to the development of new failure mechanisms, such as shear fatigue along the periphery of the loaded area. Where the asphalt thickness is less than 150 mm, the granular base layer(s) provides a substantial proportion of the load carrying capacity and both deformation and fatigue distress mechanisms are possible. Therefore, the asphalt and granular base materials must be of appropriate quality to ensure the intended service life results (Austroads, 2017).

The moduli frequently adopted in new designs in South Africa for thin continuously and gap-graded asphalt surfacing layers are shown in Table 2-11. The influences of the thickness and modulus of the asphalt layer on the inverted pavement behaviour are discussed in Section 2.6.

Table 2-11: Elastic moduli and Poisson's Ratio for asphalt materials used in SAMDM, 1996 (Adapted from SANRAL, 2014)

Asphalt Materials	Depth (d) Below surface (mm)	Modulus (MPa)	Poisson's Ratio
Gap graded asphalt surfacing	≤ 50	3 000	0.44
	≤ 100	4 000	0.44
Continuously graded hot mix asphalt	$100 < d \leq 150$	5 000	0.44
	$150 < d \leq 200$	6 000	0.44
	$200 < d \leq 250$	7 000	0.44

In Brazil, when designing new pavements, minimum asphalt layer thicknesses are recommended. The minimum thickness variation is given according to the traffic accumulated during the project period. Table 2-12 shows the minimum thicknesses of asphalt coating recommended according to the experience of the DER/SP (2006a) and DNIT (2006a).

Table 2-12: Minimum asphalt layer thicknesses adopted in Brazil (Adapted from DER/SP, 2006a and DNIT, 2006a)

Cumulative equivalent traffic - ESALs	Asphalt surfacing Minimum thickness (mm) (DER/SP, 2006a)	Asphalt surfacing Minimum thickness (mm) (DNIT, 2006a)
< 1 million	Asphalt surfacing	Asphalt surfacing
1 million – 5 million	50 mm	50 mm
5 million – 10 million	75 mm	75 mm
10 million – 25 million	100 mm	100 mm
25 million – 50 million	125 mm	125 mm
> 50 million	150 mm	125 mm

After knowing the minimum thickness required for the asphalt layer, fatigue analysis begins. In Brazil, the fatigue analysis of the asphalt layer may be done through different models. DER/SP (2006a) recommends that the asphalt layer be analysed using Equation 2.9, whose coefficients may be changed according to the fatigue models presented in Table 2-13.

$$N = K\left(\frac{1}{\varepsilon_t}\right)^n \quad (\text{Equation 2.9})$$

Where:

N: Standard axles to set level of fatigue life

ε_t : Horizontal tensile strain at bottom of asphalt layer

K and n: Experimental regression coefficients

Table 2-13: Fatigue models for asphalt concrete layer adopted in Brazil (Adapted from DER/SP, 2006a)

Author/Organization	Year	Coefficients	
		a	b
FHWA	1976	1.092E-06	3.512
Asphalt Institute	1976	2.961E-05	3.291
Barker, Brabston & Chou	1977	9.700E-10	4.030
Pinto & Preussler – CAP 50-70	1980	2.850E-07	3.690

Many designers in Brazil prefer to use either fatigue model proposed by FHWA and the Asphalt Institute. The Asphalt Institute fatigue model presented by (DER/SP, 2006a) is an adjusted version, considering 13.5 % effective binder volume, 4 % air void content, and modulus of 3 000 MPa.

In South Africa, according to SANRAL (2014), the asphalt surfacing layers are only analysed for fatigue. The fatigue model (Equation 2.10) is applicable for thin (< 50 mm) surfacing layers and thick (> 75 mm) asphalt bases.

$$N_f = 10^{\alpha \left(1 - \frac{\log \varepsilon_t}{\beta}\right)} \quad (\text{Equation 2.10})$$

Where:

N_f : Fatigue life

α and β : Constants

ε_t : Horizontal tensile strain at bottom of asphalt layer

2.3 Material properties for cement-treated layer

The cement-treated layer is a mixture resulting from the mixing of crushed stone, cement, water, and eventually, additives, in proportions determined experimentally. After mixing, compacting, and curing, the mixture acquires specific physical properties to act as a base layer or sub-base of pavements.

Xuan (2012) shows in his thesis Figure 2-5, that the type of aggregate, its gradation and the degree of compaction mainly governs the aggregate structure. The bonding phase or matrix is controlled by the cement content, fines content, moisture content, curing time, curing condition, and so on.

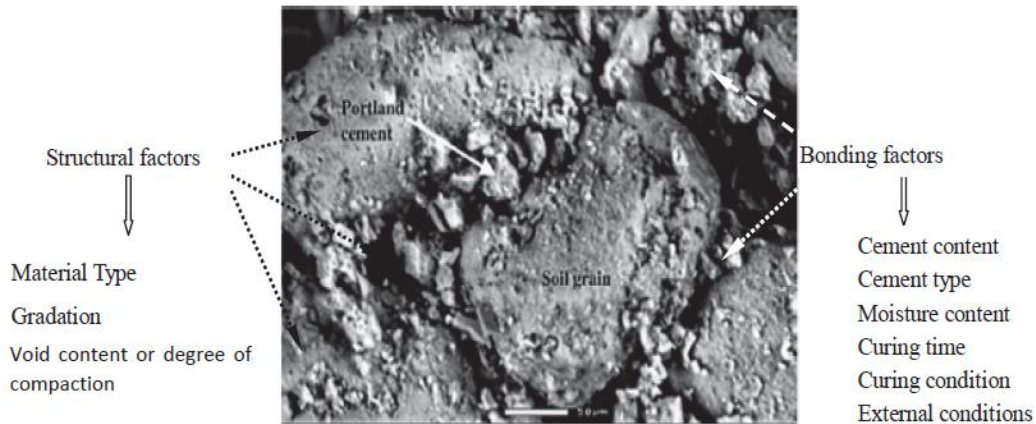


Figure 2-5: Influence factors on the mechanical properties of the cement-treated layer (Xuan, 2012)

2.3.1 Type of Cement

There are few specifications that indicate the most suitable type of cement that should be used in the composition of the cement-treated layer (Klinsky and Faria, 2018). According to Brazilian Association of Portland Cement (ABCP, 2002), there are several types of Portland cement that differ from each other, mainly due to their composition. SANRAL (2014) reinforce that different materials react differently with various stabilizers, it is important to ensure that the stabilizer selected is the best and most cost-effective for any specific material and that it will be readily and economically available at the specific construction site.

According to TRH13 (1986) cement consists essentially of finely ground calcium silicates and aluminates with small percentages of magnesium oxide, gypsum and uncombined calcium oxide. The availability of several types of Portland cement on the market provides the opportunity to select the most suitable one to meet specific criteria for strength, workability, and performance.

SANRAL (2014) indicates the types of cement currently used in South Africa, emphasizing that the production and properties of cement can change fairly rapidly over time. Another important point made is that not all of the types of cement recommended in the manual are produced in South Africa and many of those cements are very geographic-specific, which must be taken into account when planning any stabilization project.

In Brazil, the choice of Portland cement varies according to the availability of stabilizers at the time of construction, economics, and site conditions. In view of the variety of stabilizers available, care is taken to ensure that the resistance specifications recommended by national standards are met. However, it is important to note that in Brazil a type of cement intended for road construction has not yet been developed.

In Brazil and abroad there are a number of recommendations for the type of cement most suitable for the execution of the cement-treated layer. Table 2-14 summarises the recommendations of the most suitable type of cement for the cement-treated layer in Brazil and abroad.

Table 2-14: Recommendations of the most suitable type of cement for the cement-treated layer in Brazil and abroad

Organization	Country	Types of common cement
DNIT (2017)	Brazil	Ordinary Portland cement Portland pozzolana cement Portland blast furnace cement Compost Portland cement
DER/SP (2005c)	Brazil	Ordinary Portland cement Portland pozzolana cement Portland blastfurnace cement
SANRAL (2014)	South Africa	Portland cement Portland-slag cement Portland-silica fume cement Portland-pozzolana cement Portland-flyash cement Portland-burnt shale cement Portland-limestone cement Portland-composite cement Blast furnace cement Pozzolanic cement Composite cement
FHWA (1997)	United States	Ordinary Portland cement Blended Hydraulic Cement Expansive Hydraulic Cement Pozzolan use as a Mineral Admixture
Caltrans (2010)	United States	Ordinary Portland cement

In Brazil, ABCP (2002) recommends the physical and mechanical requirements of the types of Portland cement available in the country for different types of cement (Table 2-15). In South Africa, cement shall comply with the requirements of SANS 50197-1. The classification of the current cement types used in South Africa is summarised in Table 2-16.

Shall be note that the specification of the cement-treated layer (DNIT, 2017) is currently in process of approval by the responsible organs.

Table 2-15: Physical and mechanical requirements of the types of Portland cement available in Brazil (adapted from ABCP, 2002)

Type of cement	Class	Unconfined Compressive Strength (MPa)				
		1 day	3 days	7 days	28 days	91 days
CP I CP I-S	25		≥ 8	≥ 15	≥ 25	
	32		≥ 10	≥ 20	≥ 32	
	40		≥ 15	≥ 25	≥ 40	
CP II-E CP II-Z CP II-F	25		≥ 8	≥ 15	≥ 25	
	32		≥ 10	≥ 20	≥ 32	
	40		≥ 15	≥ 25	≥ 40	
CP III	25		≥ 8	≥ 15	≥ 25	≥ 32
	32		≥ 10	≥ 20	≥ 32	≥ 40
	40		≥ 12	≥ 23	≥ 40	≥ 48
CP IV	25		≥ 8	≥ 15	≥ 25	≥ 32
	32		≥ 10	≥ 20	≥ 32	≥ 40
CP V-ARI			≥ 24	≥ 34	-	-

Table 2-16: Cement strength classes in South Africa (Adapted from SANRAL, 2014)

Strength Class	Unconfined Compressive Strength (MPa)		
	Early Strength		Standard Strength
	2 days	7 days	28 days
32.5 N		≥ 16.0	
32.5 R	≥ 10.0		≥ 32.5 ≤ 52.5
42.5 N	≥ 10.0		≥ 42.5 ≤ 62.5
42.5 R	≥ 20.0		
52.5 N	≥ 20.0		≥ 52.5
52.5 R	≥ 30.0		

According to SANRAL (2014), cement types used for road stabilisation vary, but historically CEM II 32.5N types were mainly used. CEM V type cements have also been used successfully in road stabilisation projects. However, the availability of cement types depends heavily on the location of the project and the manufacturing capabilities of cement producers in the vicinity. The desired cement type for road stabilisation may, therefore, not be available. It is very important to go through a proper stabilisation design process to ensure that the correct cement type, in conjunction with the specific material, is used.

In South Africa, an investigation by Paige-Green and Netterberg (2004) was carried out on behalf of the cement producers through the Cement and Concrete Institute (C & CI). The study indicated that CEM II A and B cements using fly ash or granulated blast furnace cement as extenders, and CEM III A cements, appear to allow greater flexibility during construction than CEM I cements. The strength class of the cement should not generally exceed 32.5 MPa, although testing with class 42.5 MPa cement can be carried out for comparative purposes.

In Brazil, Klinsky and Faria (2018) evaluated the influence of the type of cement on the composition of the cement-treated layer. In the study, the type of aggregate (granite and basalt), type of cement (Portland-slag cement - CP-II E 32 and Portland-pozzolana cement - CP-III 32), cement content (2 %, 3 %, and 4 %), the time between mixing and compaction (0 hour, 2 hours and 4 hours) and curing time (7 and 28 days) was evaluated, totalling 72 experiments. The authors concluded that the parameters UCS, ITS, dynamic modulus, and resilient modulus indicate that cement type CP III 32 develops greater strength and stiffness after 28 days of curing when compared to CP II E 32.

2.3.2 Cement Content

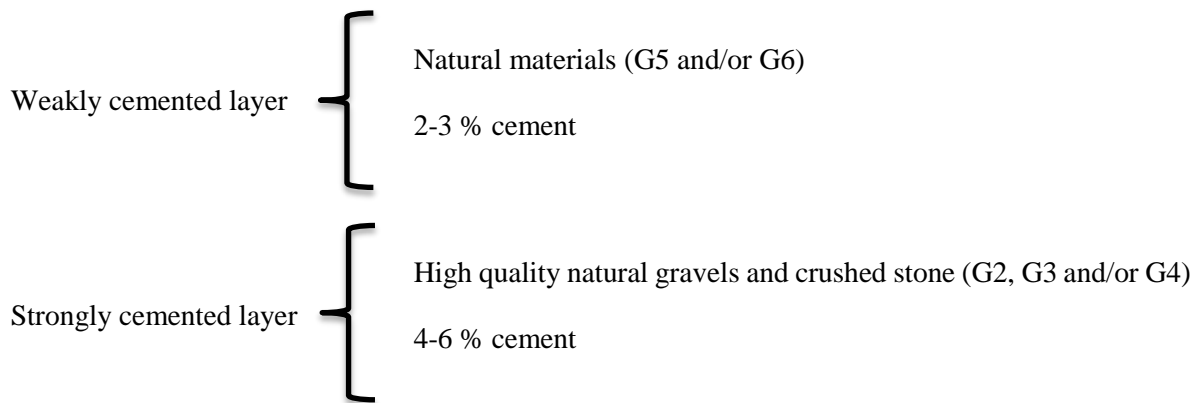
The cement content in the cement-treated base layer directly affects the strength and stiffness of the mixture as well as the parameters of UCS and ITS. In the elaboration of the mixture design, the ideal cement content to meet the resistance parameters indicated by the designer is sought, in addition to the composition of the material to adapt the grain size distribution.

Klinsky and Faria (2015) studied the influence of Portland cement content, compaction energy, and moisture on the mechanical behaviour of graded gravel treated with cement for two types of aggregates. The authors concluded that the cement content is the most influential factor when compared to the other factors studied. Hossain et al. (2017) also agree with this statement.

In Brazil, the specifications of cement-treated layers (DNIT, 2017 and DER/SP, 2005c) do not fix the cement content to the cement-treated layer. DER (2005c) suggests implicitly that the cement content vary between 3 % and 5 %, according to the payment item suggested by the organisation. Nowadays, designers have adopted a lower cement content, varying between 1.5% and 4%, due to the premature appearance of cracks.

According to Hossain et al. (2017) increases in cement content led to significant problems of shrinkage and cracking, and cement-treated layer design based on a fixed cement content would be difficult to use in mechanistic pavement analysis where a modulus value is required as input. A fixed amount of cement (say 4%) could generate a range of compressive strengths in the cement-treated layer, depending on the aggregate source. Balbo (1993) accentuates that the cement content is associated with the chosen grading distribution and that there is a trinomial that should not be separated: grading, cement content and resistance.

In South Africa, TRH13 (1986) and SANRAL (2014) do not refer to the cement content, but the minimum and maximum strengths for the cement-treated layer are set. TRH14 (1985) recommends that the strengths should be obtained with no more than 5 % by mass of stabiliser at the specified density and optimum moisture content. According to TRH13 (1986) there are four classes of cemented materials for crushed stone, crushed gravel and natural gravel, namely C1, C2, C3 and C4. C1 and C2 cement-treated layers are not commonly used anymore, as the high cement content results in significant cracking and consequent reflection cracking. Therefore, on higher trafficked roads, i.e., more than about 1 million ESALs, it is often necessary to provide a stabilised subbase, usually C3 or C4 quality SANRAL (2014). According to De Beer (1985), the cement-treated layer may be classified as weakly cemented layer and strongly cemented layer:



2.3.3 Grain Size Distribution

According to FHWA (1997) aggregates used in stabilised base and subbase mixtures play a major role in determining the quality and performance of stabilised base and subbase mixtures. Aggregate materials used in these types of mixtures must be properly graded and possess good to adequate particle shape, strength, and integrity. The key to strength development in stabilised base or subbase mixtures is in the matrix that binds the aggregate particles together.

In Brazil, DNIT (2017) recommends two different grading of aggregates for cemented material, classified as A and B material grading. DER/SP (2005c) recommends the A material grading for the mix of the cement-treated layer. The grading of aggregates recommend by these Departments are shown in Table 2-17.

In South Africa, as mentioned in Section 2.3.2, there are four classes of cemented materials for crushed stone. For cemented materials classified as C1 and C2, TRH14 (1985) suggest use of the grading of aggregates presented in Table 2-17. Cemented materials classified as C3 and C4 are selected natural materials equivalent to G5 and or G6 material. For these materials, the only grading requirement is the maximum stone size of 63 mm, or maximum of two-thirds of the compacted layer thickness, and grading modulus. Meanwhile, according to SANRAL (2014), it is becoming common practice to specify crushing and/or screening of G5 and G6 materials used in the construction of C3 and C4 stabilised layers. In these cases, some road authorities require the grading of these materials to comply with those of G4 quality materials.

Table 2-17: Grading of aggregate of cement-treated layer in Brazil and in South Africa

Sieve size (mm)	Brazil			South Africa	
	(DER/SP, 2005c)	(DNIT, 2017)		(THR14, 1985)	
	A	A	B	C1 G2	C1 and C2 G2/G3/G4
	Percentage Passing (%)				
53.0					
50.0					
37.5	100-100	100-100	100-100	100-100	100-100
28.0	-	-	-	84-94	100-100
25.0	90-100	90-100	-	-	-
19.0	75-95	75-95	60-95	71-84	85-95
13.2	-	-	-	59-75	71-84
9.5	45-64	45-64	40-75	-	-
4.8	30-45	30-45	25-60	36-53	42-60
2.0	18-33	18-33	15-45	23-40	27-45
0.42	7-17	7-17	8-25	11-24	13-27
0.18	1-11	1-11	-	-	-
0.075	0-8	0-8	2-10	4-12	5-12

Figure 2-6 shows some gradations in relation to the way the material is used in practice (Molenaar, 1998 mentioned in Xuan, 2012). Some remarks were made with respect to those gradations (Xuan, 2012):

- The grain-size distribution of the cemented layer should be continuous for obtaining a good mechanical stability;
- A certain amount of fines is always needed for mixture stability. Furthermore, the fines should have certain plasticity characteristics in order to act as a binder that keeps the coarse particles together; and
- By increasing the maximum grain size of particles, the load spreading capacity of cement-treated layer can increase.

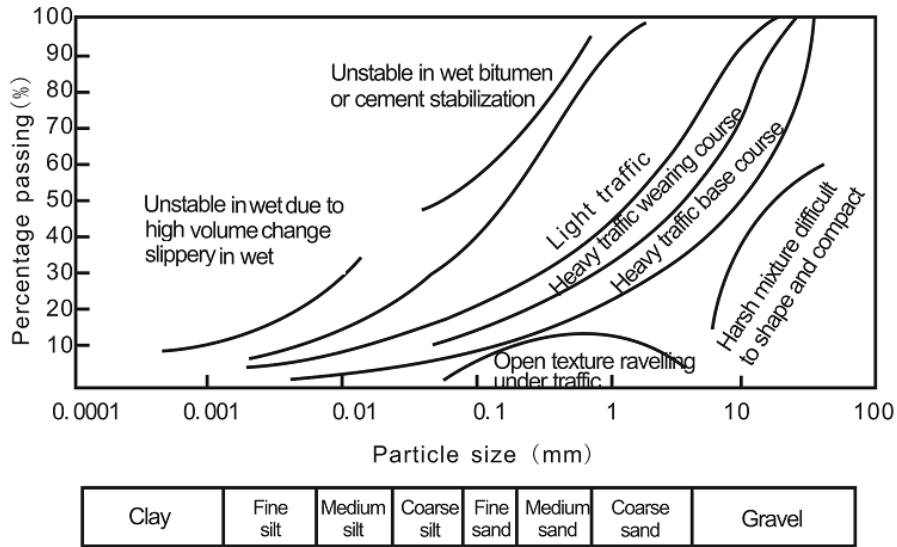


Figure 2-6: Gradations of granular materials in relation to their use (Molenaar, 1998 mentioned in Xuan, 2012)

To make it easy to analyse the grading of aggregate shown in Table 2-17 according to the remarks made by Xuan (2012), the grading envelop recommended in Brazil and in South Africa for cement-treated layers are show in Figure 2-7.

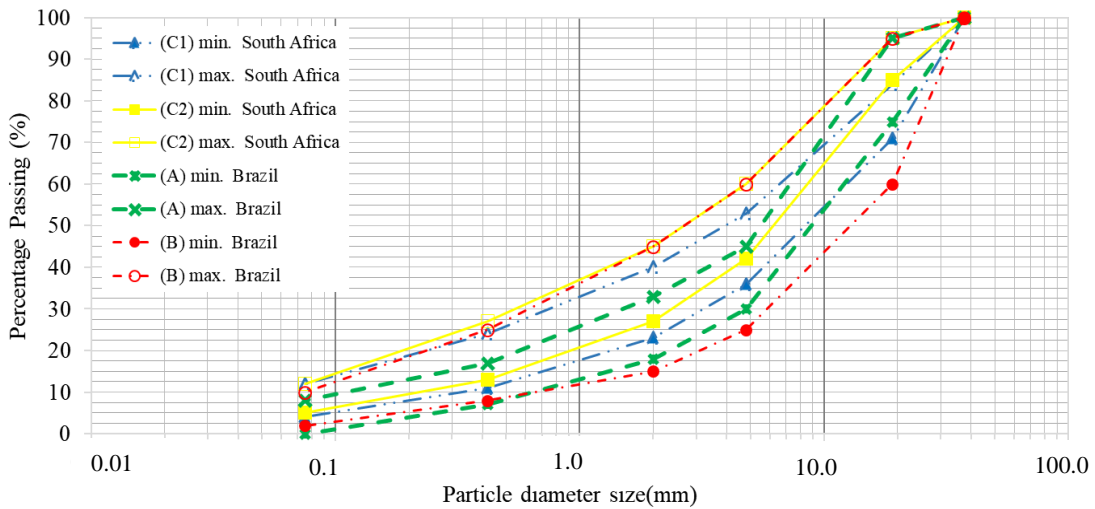


Figure 2-7: Grading envelopes for cement-treated base in Brazil and in South Africa (Adapted from DER, 2005c; DNIT, 2017 and TRH14, 1985)

Another fundamental property of the grading of the mix is the nominal maximum aggregate size. Through that, it is possible to indicate the minimum and maximum thicknesses, to ensure compatibility and to counter segregation during paving. The minimum and maximum thicknesses are covered in Section 2.5.

2.3.4 Type of aggregate

It is possible to treat almost all materials with cement to improve its properties. However, it is important to know whether the material is suitable for cement treatment and whether it meets the mechanic characteristics required. According to Xuan (2012) the physical properties of the granular aggregates are very important and will affect the mixture design of the cement-treated layer and its properties.

According to Klinsky and Faria (2018) basaltic aggregates have a higher maximum dry density and also demand a higher moisture content when compared to granitic aggregates. The authors also observed that the aggregates of basaltic origin produced a cement-treated layer with greater strength and stiffness than the cement-treated layer produced with granitic aggregates. Hossain et al. (2017) reinforce that one source of aggregate with a high resilient modulus achieved higher strength than another aggregate with a lower modulus for the same cement content. This difference is attributed to aggregate properties such as mineralogy, gradation, particle shape, texture, angularity, Atterberg limits, and percent passing the No. 0.075 mm sieve.

Davis et al. (2007) mentioned in Xuan (2012) also studied the physical properties of four types of aggregates (mica, diabase, limestone and granite). It is found that the aggregate size influences the linear relationship between the UCS and the cement content, and there is a significant difference in strength for the aggregates studied, as shown in Table 2-18.

Table 2-18: Influence of aggregate type on the 7 day UCS (adapted from Xuan, 2012)

Type of aggregate	UCS (MPa)
Mica	Min 0.9 - Max 2.4
Diabase	Min 2.0 - Max 4.8
Limestone	Min 1.3 - Max 4.0
Granite	Min 1.3 - Max 6.9

In Brazil, the recommendations made by DNIT (2017) and DER/SP (2005c) to choose the ideal aggregate are very similar (Table 2-19). The first recommendation made by them is that aggregates used must consist of resistant, clean, and durable fragments, free of excess lamellar or elongated particles, soft or easily disintegrated. Furthermore, the only difference between the departments is that the DER (2005c) recommends that the percentage of lamellar must be less than 10 %.

In South Africa, G5 and G6 natural gravels are subject to minimum grading modulus criteria, which also affects the maximum Plasticity Index. For G2, G3 and G4 further requirements are applied, as shown in Table 2-19.

Table 2-19: Physical requirements for materials for aggregates used in stabilized base and subbase in Brazil and in in South Africa

Organization	Country	Physical requirements for materials
DNIT (2017)	Brazil	⇒ Abrasion Resistance: Resistance to degradation of large-size coarse aggregate by abrasion and impact in the Los Angeles Machine. Max 50%
DER/SP (2005c)		⇒ Sand Equivalent: At least 55 % of the aggregate used be finer than 4.75 mm
		⇒ Index of the large-size aggregate: Min 0.5
		⇒ Soundness: Soundness of aggregates by use of sodium sulfate = Max 20%, Soundness of aggregates by use of magnesium sulfate= Max 30%,
SANRAL (2014)	South Africa	<p>Requirements applied to C1 (G2) and C2 (G2/G3/G4)</p> <p>⇒ Crushing strength: ACV (max) = 29% or 10% FACT (min) = 110 kN.</p> <p>⇒ Flakiness Index: Max 35%</p> <p>⇒ Sand Equivalent: Max 30% for any sand added to correct the grading</p> <p>Requirements applied to C3 (G5/G6) and C4 (G5/G6)</p> <p>a) Grading Modulus (min): 1.5 for G5 and 1.2 for G6</p>

2.3.5 Moisture Content

The moisture content is a variable that compromises the behaviour of the cement-treated layer. Thus, the evaluation of this parameter is essential in the characterization of the available materials to have a successful pavement design. According to Austroads (2017) an increase in moisture content beyond optimum results in a decrease in modulus.

Cement-treated layers are defined as mixtures in which a relatively small amount of cement is used as a binder of coarse granular particles, and which need a proper water content for both compaction and cement hydration (Xuan, 2012). According to TRH13 (1986) the degree of cracking is proportional to the amount of moisture lost on drying and thus the wetter the material on compaction, the greater the degree of cracking.

2.3.6 Compaction

The aggregates that present a good grading distribution facilitate the compaction and the reduction of voids, thus obtaining a cemented mixture with a good granular arrangement and superior mechanical stability. In general, as the compaction energy increases, the specific mass also increases, leading to higher UCS values (Klinsky and Faria, 2015).

According to SANRAL (2014), the purpose of compaction is to arrange the particles in such a way as to achieve the highest possible density of the layer with a minimum of voids, while using the least compaction energy. By achieving higher densities, the shear strength and elastic modulus are improved, leading to a lower tendency for additional traffic associated compaction and consequent rutting under traffic, while the deflection of the pavement under wheel loads is reduced.

Adequate compaction greatly improves the modulus and the performance of cemented materials. Increased resistance to compaction occurs as a result of the rapid formation of cementitious bonds that resist the applied compactive effort for rapid-setting binders such as general-purpose cement (Austroads, 2017).

In addition, according to Austroads (2017) the fatigue life of cemented materials varies with density to which the material is compacted. In practice, the mixture dry density of the cemented layer strongly depends on the degree of compaction. With the increase of the degree of compaction, the corresponding dry density and strength will increase, regardless of the material type. That is one of the reasons why the strength requirements for cement-treated base generally assume that a high degree of compaction is achieved. This is also based on the fact that although a low dry density may be compensated by increasing the cement content, it is generally more economical to achieve a high strength through a good compaction (Xaun, 2012).

Klinsky and Faria (2015) concluded that the cement-treated layers when compacted using the Modified Proctor Method, presented values of strength and stiffness higher than those moulded in the Intermediate Proctor Method. The authors found that when the cement-treated layer is compacted in the Modified Proctor Method the values of ITS are 55 % greater than the results obtained by Intermediate Proctor Method. According to Balbo (1993) it is convenient that the control is carried out based on the Modified Proctor Method. In the last years, the DNIT started to up to date its specifications, and then in DNIT (2017) the Modified Proctor must be adopted in determining the bulk density, maximum dry density, and optimum moisture content. Shall note

that the specification of the cement-treated layer (DNIT, 2017) is currently in process of approval by the responsible organs

2.3.7 Curing

According to Klinsky and Faria (2018), curing is another very important factor affecting the development of UCS in materials stabilized with cement. Curing is necessary to ensure that there is adequate water for hydration reactions to proceed and that drying shrinkage is limited while the hydration reactions are proceeding and the material is strengthening (Austroads, 2017).

SANRAL (2014) emphasise that curing is the most important aspect of stabilisation. The requirements should be strictly adhered to. The most important requirement is that the completed layer should never be allowed to dry out. This is because keeping the layer damp:

- Inhibits carbonation of the stabiliser;
- Provides enough moisture at the surface of the layer for cementation to take place, and
- Prevents the temperature of the surface increasing compared to the rest of the layer, which may induce thermal stresses and potentially inducing cracking.

Balbo (1993) evaluated the cure of the cement-treated layer after compaction in different times (7, 28, and 56 days). The results of these tests showed that increasing the cure time from 28 to 56 days did not significantly increase the resistance of the cement-treated layer. At 28 days of cure, approximately 97 % of the resistance recorded at 56 days of cure was obtained. Klinsky and Faria (2015) obtained at 7 days of cure, on average 50 % of the ITS value obtained at 28 days of cure.

2.4 Strength parameters of cement-treated layer

A pavement is a structure consisting of superimposed layers of processed materials above the subgrade, whose primary function is to distribute the applied vehicle loads to the subgrade. One of the most difficult tasks in pavement design is to find a modular balance between the layers, so that all the layers work together to dissipate the dynamic loads coming from the vehicles without any of the layers prematurely failing.

In inverted pavements, the cement-treated layer in many countries is the layer with the highest modular value, and consequently, it is the layer with the greatest possibility of fatigue. Therefore,

making correct predictions of the strength and stiffness of the cement-treated layer is essential and indispensable for its success.

The definition of cement-treated layer strength is undoubtedly the most complex parameter to be obtained from the cement-treated layer, as well as its strength and stiffness depends on numerous factors, as mentioned in Section 2.3. Thus, small errors or wrong assumptions in any of these factors or in the stages of the cement-treated layer construction may compromise the integrity of the pavement as a whole.

2.4.1 Elastic Response

According to De Beer and Maina (2008) engineers and technicians need a basic understanding of the fundamental definitions of elastic parameters for homogeneous isotropic, linear elastic materials in road pavement design and analysis for modern mechanistic analysis of road pavement. The elastic response of cemented materials are characterised by an elastic modulus and Poisson's Ratio (Austroads, 2017).

The resilient modulus and elastic modulus are parameters widely used for dimensioning and mechanistic verification of pavement structures. According to Klinsky and Faria (2018) the main difference between the elastic modulus and resilient modulus is that the first one is obtained in a static test, while the second one is obtained in repeated load tests. According to Motta and Ubaldo (2014), the elastic modulus and the resilient modulus are not of equal value, but both represent a stress-strain relationship of the material.

In addition to the aforementioned moduli, dynamic and flexural modulus are often used to measure the mechanical properties of the cement-treated layer. Dynamic moduli evaluates the stiffness of the cement-treated layer at different load frequencies. According to Xuan (2012) the knowledge on the dynamic response of cement-treated layer under repeated loading is important when designing pavements with a cement treated layer.

In Australia, according to Austroads (2017), due to similarities with the loading regime in-service, flexural modulus is the preferred design input. Furthermore, for pavement design purposes, the appropriate value of the modulus of cemented materials is an estimate of the in-situ flexural modulus after 90 days curing in the roadbed.

In addition to the definition of moduli for characterising the stiffness of the cement treated layer, the Poisson's Ratio is also an important parameter. According to De Beer and Maina (2008)

Poisson's Ratio is the ratio of the relative contraction strain or transverse strain (normal to the applied load) to the relative extension strain, or axial strain in the direction of the applied load).

Table 2-20 shows the range of moduli and Poisson's Ratio recommended by DER/SP (2006a) for cement-treated layer, and some moduli adopted or back-calculated in pavements researches in Brazil. Table 2-21 show the moduli recommended in South Africa (SANRAL, 2014 and De Beer, 1985) and Australia (Austroads, 2017).

Table 2-20: Modulus and Poisson's Ratio recommended for the cement-treated layer in inverted pavement in Brazil

Author/Organization	Modulus (MPa)	Poisson's Ratio
DER/SP (2006a)	7 000 – 18 000	0.15 – 0.30
Suzuki (1992)	15 000	0.20
Macêdo (1996)	9 000	-
Bernucci (2013) mentioned in Salvador and Motta (2015)	7 000	0.20
Alberto (2018)	7 500	0.20

Table 2-21: Modulus recommended for the cement-treated layer in inverted pavement in South Africa and Australia

Author/Organization	Modulus (MPa)
South Africa (SANRAL, 2014 and De Beer, 1985)	C1 = 3 000
	C2 = 2 500
	C3 = 2 000
	C4 = 1 500
Australia (Austroads, 2017)	Base quality granular material (4% - 5% cement) = 5 000
	Subbase quality crushed rock (3% - 4% cement) = 4 000
	Subbase quality natural gravel (4% - 5% cement) = 3 000

According to De Beer and Maina (2008) Young's Modulus, can be calculated by dividing the tensile stress by the tensile strain. Flexural and compressive tests have indicated that microcracking starts at about 35 % of the ultimate stress and at about 25 % of the flexural strain at break (TRH13, 1986). The slope of the initial straight-line portion represents the elastic modulus of the cemented material (Figure 2-8).

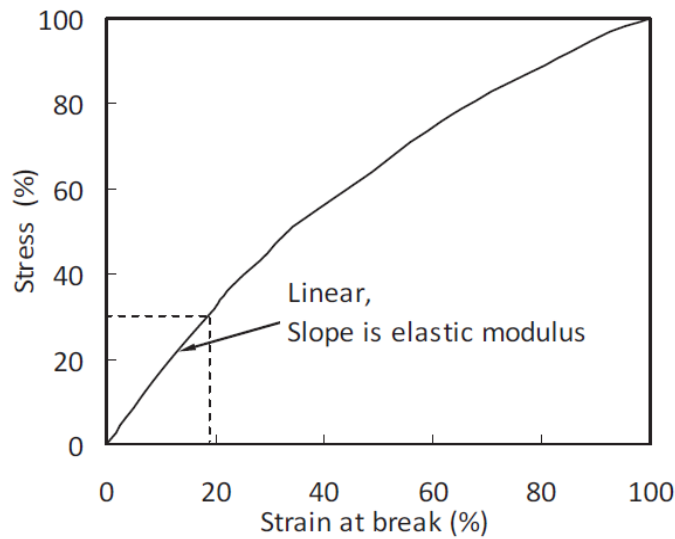


Figure 2-8: Typical stress/strain relationship of cemented materials (TRH13, 1986)

Moduli of cement-treated layer in-service vary markedly within a road project. According to Austroads (2017) following the initial fatigue cracking, further cracking and degradation of the cemented layer may occur, resulting in a reduction in the modulus to a value similar to that of the unbound granular material from which the cemented material was derived.

According to De Beer (1985) the change in the effective modulus in cement-treated layers (Figure 2-9) occurs with time (traffic) and may be characterised in three phases. Phase I begins with pre-cracked phase. In this phase, the effective modulus will be relatively high and the layer will behave much as a slab of concrete, i.e. "very stiff" state (De Beer, 1985). Phase II (post-cracked phase) is characterised in the beginning by the occurrence of discrete large blocks, but still retains the high modulus of the original cemented (stabilised) material. In this phase, the effective modulus can continue to drop to lower values in the order of 500 MPa, at which time the discrete blocks will be fairly small and could form a mosaic. For the author, almost 90 % of the weakly cemented layers occur in the post-cracked phase. Lastly, Phase III (equivalent granular phase), the behaviour at this stage is very similar (equivalent) to that of high quality granular material but the structure changes into a "flexible" state.

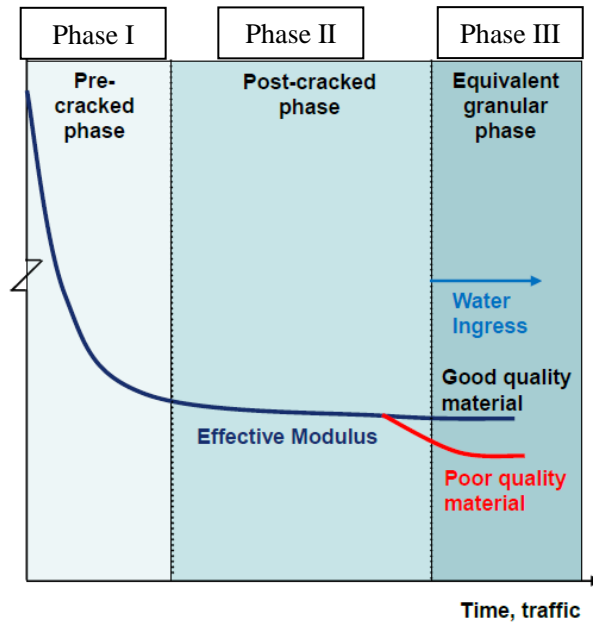


Figure 2-9: Long-term changes in the elastic response of flexible pavements with lightly cemented layers (Adapted from SANRAL, 2014 and De Beer, 1985)

According to SANRAL (2014) an equivalent granular state is when a lightly cement-treated layer has cracked or weakened to the extent that the effective modulus is similar to that of an unbound granular layer. The “cracked” state does not imply that the material has reached the consistency of a granular material, or that it has necessarily visibly cracked into smaller, granular like pieces. The cracks are generally micro-cracks that are not that visible, but result in a loss of stiffness.

In Brazil, DER/SP (2006b) suggests that the cracked condition of the cement-treated layer must be evaluated, and also recommends that allowed deflection is multiplied by a factor of 0.5 if the layer is intact, if the layer is partially intact this factor must be 0.7, and if the cement-treated layer has a granular behaviour, this factor must be 1. De Almeida et al. (2019a) indicated limits of modulus for the cement-treated layer (Figure 2-10) and associated these modular values to the multiplying factors indicated by DER/SP (2006b). The analysis was derived from the classification of the structural condition of the pavements carried out by Horak (2008).

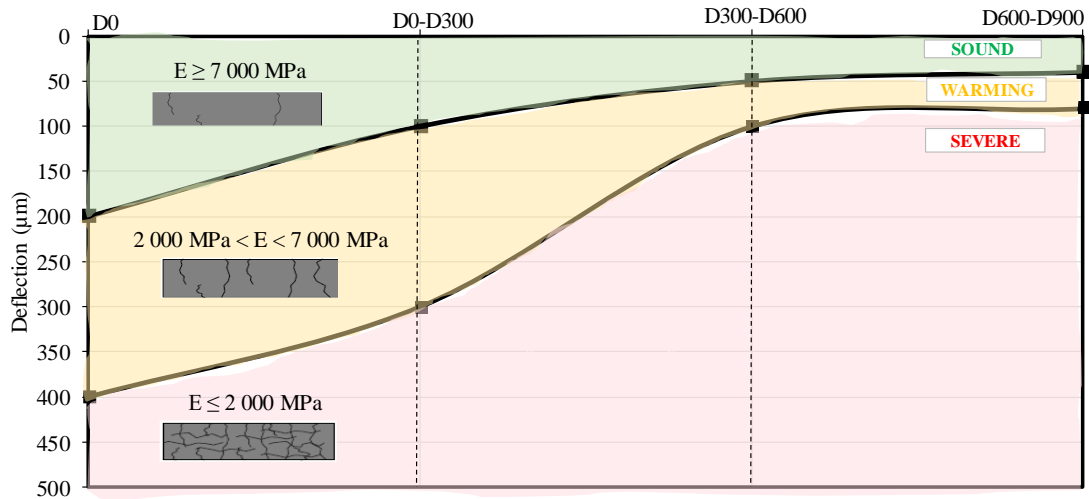


Figure 2-10: Evaluation of the integrity of the cement-treated layer in inverted pavement in Brazil (Adapted from De Almeida, 2019a)

2.4.2 Unconfined Compressive Strength and Indirect Tensile Strength

According to SANRAL (2014) UCS and ITS testing (Figure 2-11) is carried out as part of the mix design procedure to establish an appropriate stabilizing agent, as well as for quality control purposes during construction. Many researchers use those parameters, in particular UCS, in an attempt to establish the influence of several factors on the resistance of cement-treated layers, such as cement content, type of cement, type of aggregates and grading, degree of compaction, time and conditions healing (Klinsky and Faria, 2018).

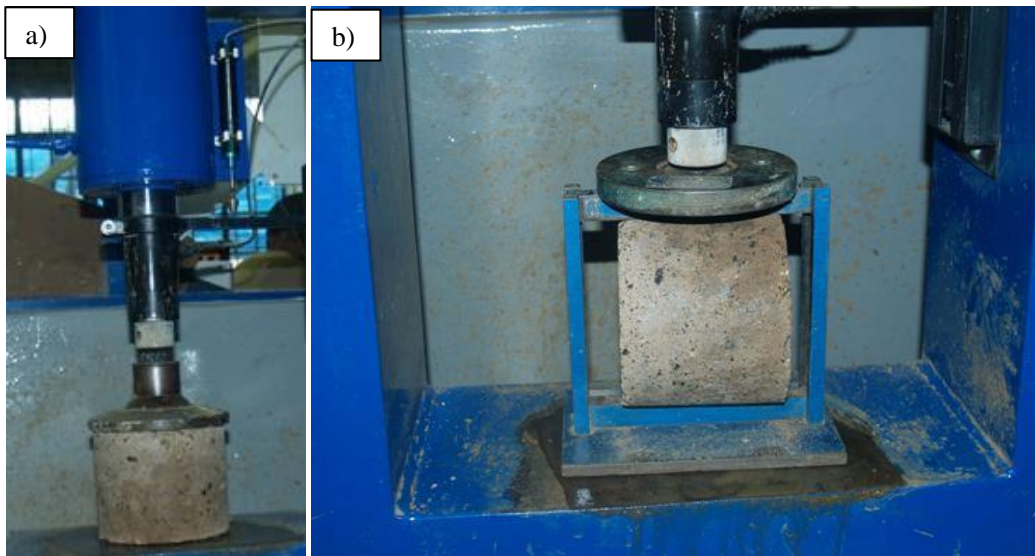


Figure 2-11: a) UCS Test and b) ITS Test (ITS) (SANRAL, 2014)

According to SANRAL (2014) the current specifications in South Africa can result in a conflict between the minimum ITS and the UCS range required. Then, where UCS and ITS results are in conflict, it is recommended to ensure that the ITS criteria is met, once the durability of the stabilized materials depends more on the ITS than the UCS. As it is more difficult to achieve the ITS than the UCS, the UCS results are typically higher than the specified upper limit. The minimum and maximum strengths for the cement-treated base layer widely suggested are shown in Section 2.5.2.

Besides the indirect tensile test, the direct test and the flexural test can be used to determine the tensile strength of the cement-treated layer. According to Xuan (2012), in general, flexural beam tests, direct tests and indirect tensile tests have been employed to evaluate the tensile strength of the cement-treated layer, and the values deduced from these tests differ from each other due to the different stress distribution.

2.4.3 Relationship between UCS and tensile strength

Several researchers have developed correlations to obtain the tensile strength value from UCS. Balbo (1993) concluded that ITS value varies between 16 % and 26 % of UCS value, and the direct tensile strength (DTS) is approximately 10 % of the UCS value. According to SANRAL (2014) experience has shown that, depending on stabiliser and soil type, the rough relationship between ITS and UCS can vary from 1:7 to 1:15.

According to Babic (1987) mentioned in Xuan (2012), with a degree of compaction of 98 %, 95 % and 90 % (Modified Proctor) the ITS is found to be 11.5 %, 13 % and 15 % of the UCS, respectively. According to TRH13 (1986) the ITS is about 1.5 times greater than the DTS, and ITS is approximately 13 % of the UCS value.

Some research has shown that the Flexural Tensile Strength (f_t) of the cement-treated layer is about 1/10 to 1/6 of the UCS (Kolias and Williams, 1984; NITRR, 1986 and Terrel et al., 1976 mentioned in Xuan, 2012). Xuan (2012) in his literature review found the prediction models of tensile strength (Table 2-22).

Table 2-22: Prediction models of Tensile Strength of cement-treated layer (Adapted from Xuan, 2012)

Prediction models of Tensile strength	Reference	Remarks
ITS = a.UCS + b ITS = a'.UCS	(Kolias and Williams, 1980)	Coefficients a, b and a' are influenced by mixture parameters.
$f_t = a.UCS$	(Kolias and Williams, 1984)	
DTS = 0.10 .UCS	(Balbo, 1993)	-

2.5 Construction parameters of the cement-treated layer

2.5.1 Cement Content

In Brazil, according to DER/SP (2005c) and DNIT (2017) the determination of the cement content for the cement-treated layer is obtained by the ratio between the mass difference of the mixture, with cement and without cement, by the mass of the mixture without cement, multiplied by 100. The percentage by mass of cement to be incorporated into the aggregates for constituting the mixture must be fixed in order to meet the USC and ITS at 28 days.

In South Africa, to determine the percentage of lime or cement necessary to satisfy the demand of clay minerals in soils and gravels the Initial Consumption of Stabilizer (ICS) has been applied. In the ICS test, according to SANRAL (2014), samples are prepared at varying stabilizer contents, usually, 0 %, 1 %, 2 %, 3 %, 4 %, and 10 %, and water is then added to form a paste. Furthermore, according to SANRAL (2014), if stabilization appears to be effective, feasible and economic, i.e., the ICS is not too high (not more than about 3.5 %) proceed with further tests to establish the best stabilizer type and content to achieve the desired strength.

In Section 2.3.2 are covered the influence of the cement content in the mixture of the cement-treated layer and in its behaviour over the years, as well as, cement content normally used in Brazil and in South Africa.

2.5.2 Strength

UCS and ITS testing are performed as part of the quality control purposes during construction. In Brazil, DER/SP (2006a) suggests the minimum and maximum strengths for the cement-treated layer (Table 2-23). The Brazilian specifications of cement-treated layers (DER/SP, 2005c and DNIT, 2017) do not fix the strengths for the cement-treated layer.

In South Africa, UCS is given at two densities (97 % and 100 % modified AASHTO density). According to SANRAL (2014) the test methods are different and the strength classes of cements are now based on the strength after 28 days and not 7 days as recommended in Technical Recommendations for Highways (TRH13, 1986). Table 2-23 synthesizes the information related to the cement content currently adopted in Brazil and in South Africa.

Table 2-23: Strength parameter suggest in Brazil and in South Africa

Organization	Country	N° of days	UCS (MPa)	ITS (MPa)
DER/SP(2006a)	Brazil	28	Min 4 - Max 6.2	Min 0.7 - Max 1
SANRAL (2014)	South Africa	28	C1- Min 6 - Max 12	C1- Not mentioned
		100%MDD	C2- Min 3 - Max 6	C2- Not mentioned
			C3- Min 1.5 - Max 3	C3- Min 0.25
			C4- Min 0.75 - Max 1.5	C4- Min 0.20
		28	C1- Min 4 - Max 6	
	97%MDD	C2- Min 2 - Max 4	Not applicable	
		C3- Min 1 - Max 2		
		C4- Min 0.5 - Max 1		

In Australia, according to Austroads (2017), for moderate-to-heavily trafficked roads, the minimum 28-day UCS is 2 MPa to ensure a cemented material with less variable fatigue properties. For some lightly trafficked roads, granular materials stabilised with cementitious binders to a UCS of 1 – 2 MPa have been used as there has been less concern about fatigue cracking causing detrimental effects on the life of thin bituminous surfacing.

2.5.3 Cement-treated layer thickness

The knowledge about the minimum and maximum thicknesses of the cement-treated layer is very important to ensure compatibility and to counter segregation during paving. Table 2-24 shows the minimum and maximum thicknesses layer adopted by Brazil, South Africa and United States.

Table 2-24: Minimum and maximum thicknesses layer adopted by Brazil, The United States and South Africa

Author/Organization	Country	Minimum and maximum thicknesses
DNIT (2017)	Brazil	120 mm – 180 mm
DER/SP (2005c)	Brazil	120 mm – 180 mm
TRH4 (1996)	South Africa	125 mm – 300 mm
Caltrans (2010)	United States	76.2 mm - 152.4 mm

In South Africa, according to design catalogue provided in TRH4 (1996), the minimum and the maximum of the cement-treated layer varied between 125 mm and 300 mm. However, nowadays, in practice, the minimum and maximum thicknesses vary between 125 mm and 200 mm.

According to DER/SP (2005c) and DNIT (2017), in the quality control, the difference between the thickness of the compacted layer and the thickness of the projected layer must not be greater than 10 % at any point of the cement-treated layer.

In South Africa, during quality control, the limit of acceptance varies according to the client and the current contract. However, in general, the difference between the thickness of the compacted layer and the thickness of the projected layer are the same as in Brazil, which must not be greater than 10 % at any point in the cement-treated layer. Unfortunately, no publication or guide that refers to that limit of acceptance was found.

2.5.4 Compaction Techniques

In Brazil, for many years the compaction energy has been adopted as a reference for the execution of the cement-treated layer is the Intermediate Proctor, according recommend in DER/SP (2005c). In the last years, the DNIT started to up to date its specifications, and then in DNIT (2017) the Modified Proctor must be adopted in determining the bulk density, maximum dry density, and optimum moisture content. Shall note that the specification of the cement-treated layer (DNIT, 2017) is currently in process of approval by the responsible organs. Table 2-25 are shown the compaction criterion currently applied in Brazil.

In South Africa, according to TRH13 (1986) the typical design strength given for the four classes of cemented materials (C1, C2, C3 and C4) is given at two densities (97 % and 100 % modified AASHTO density). The strength at 100 % modified AASHTO density is given since it is easy to compact samples to 100 % density, and the strength at 97 %, which can be determined from a strength/density relationship, is equivalent to the strength at the field density usually specified for a stabilised based. Table 2-25 shows the compaction criterion currently applied in South Africa.

Table 2-25: Compaction criterion in Brazil and in South Africa

Organization	Country	Compaction Criterion
DNIT (2017)	Brazil	⇒Degree of compaction Min = 100%; ⇒Modified Proctor density.
DER (2005c)		⇒Degree of compaction Min = 100%; ⇒Intermediate Proctor density.
SANRAL (2014)	South Africa	⇒Degree of compaction Min = 97%; ⇒Modified AASHTO density

In Brazil DNIT (2017) and DER/SP (2005c) recommend that the cement-treated layer be constructed and compacted in single layers. Balbo (1993) does not recommend the execution of two overlapping cement-treated layers. The author recommends compacting the cement-treated layer into a single layer, regardless of its thickness. According to Austroads (2017) the construction and compaction in single layers eliminate the early pavement deterioration that can result when sublayers are not bound together.

In South Africa, in general, the maximum cement-treated layer to be constructed and compacted in single layers is 200 mm, but it depends on the ability of the roller to compact the layer. Moreover, There is no guarantee that the construction of two 100 mm layers there will be good bond between the layers.

In case of a cement-treated layer being greater than 200 mm, the construction is done in two layers. According to Visser (2017) the cement-treated layer is constructed in two layers, as it is difficult to compact 250 mm of material without breaking down the particles.

When the cement-treated layers is constructed in two layers, in some cases, the layer is partially constructed and then compacted with a pad-foot or sheep-foot roller, leaving indentations that will assist with bond. The balance of the layer is then placed and compacted with a pad-foot and vibratory roller. In such a case one must take core samples and test the core in three parts for density.

In Unites States, according to Caltrans (2010) whenever cement-treated layer is spread and compacted in more than one layer, each lower layer is compacted to the required degree of compaction before placing the next layer.

2.5.5 Moisture Content

According to Balbo (1993), the water and cement ratio is a conditioning factor for the strength gain of the cement-treated layer. However, the Brazilian specifications do not mention this peculiarity of the mixture (Balbo, 2007). Furthermore, according to the author, if it is not possible to carry out a complete dosage study of the mixture, the mixture can be prepared with a moisture content of 1.0 % below that of the reference (optimum moisture content), fixing the cement content between 3.0 % and 4.0 % by weight.

Klinsky and Faria (2015) concluded that the reduction of the moisture content to around 1 % below the optimum moisture content tends to increase the strength and stiffness of the cement-treated layer, while the increase in moisture content reduces these mechanical parameters.

The recommendations made by the main organizations in Brazil (DNIT, 2017 and DER/SP, 2005c) and in South Africa (SANRAL, 2014) are presented in Table 2-26.

Table 2-26: Moisture content requirements in Brazil and in South Africa

Organization	Country	Moisture content requirements
DNIT (2017)	Brazil	The moisture content of the cement-treated layer, immediately before compaction, must be within the range of -2.0% to +1.0%, in relation to the optimum moisture content obtained from compaction in the laboratory.
DER/SP (2005c)	Brazil	
SANRAL (2014)	South Africa	Stabilised materials should be compacted at a moisture content below 80% of saturation, to reduce cracking in the stabilized layers.

2.5.6 Processing Time

In Brazil, (DER/SP, 2005c) and DNIT (2017) recommend that the time of mixing and compaction should not be longer than the beginning of the cement setting.

In South Africa, according to TRH13 (1985) mixing and compaction should be efficient to minimize the decrease in density and strength due the early reactions between stabiliser, water and soil. In case of utilisation of Portland cement, the maximum time is 6 hours for completion of compaction and finishing after the stabilising agent comes into contact with soil.

In Australia, Hamory (1977) mentioned in Yeo (2011) evaluated in a mix with 2 % cement the relationship to delay between mixing and compaction immediately after mixing and after 24 hours of mixing. The specimens were compacted to 100 % optimum moisture content and tested immediately after curing without dry back. The results of this assessment are presented in Figure 2-12.

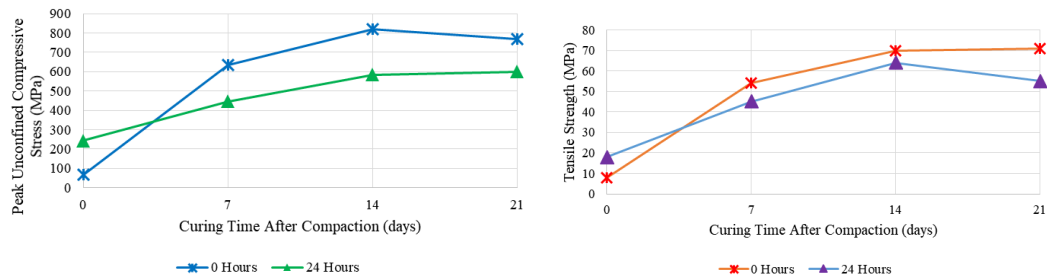


Figure 2-12: Strength parameters of cement stabilised limestone compacted at 0 and 24 hours delay (Adapted from Yeo, 2011)

The results show that a delay in compaction increases the initial strength of the specific material, which in turn suggests that field techniques may be employed to address cracking tendencies of stiff pavements (Hamory, 1977 mentioned in Yeo, 2011).

It is noteworthy that the adequate performance of the cement-treated layer depends on a range of different construction parameters, as well as the processing time of the mixture, the type and amount of cement, moisture content, compaction techniques, and curing also play an important role in achieving acceptable strengths in the cement-treated layer when it is built.

2.5.7 Curing

Brazilian specifications recommend the application of a curing membrane of cationic spray grade bitumen emulsion immediately after compacting the layer (DER/SP, 2005c and DNIT, 2017). DER/SP (2005c) furthermore recommends that the cement-treated layer should be properly moistened before applying the curing bitumen emulsions and emphasise that the cement-treated layer must be removed and redone in case of rain before the curing bitumen emulsions.

DER/SP (2005c) and DNIT (2017) also prohibit any traffic over the cement-treated layer, but do not define the number of days. However, the specifications underscore that in exceptional cases, the supervisory engineering staff may authorize the opening to traffic as long as the cement-treated layer presents the resistance compatible with the load request and that bitumen emulsion is completely "broken" and "cured".

In South Africa, according to TRH13 (1986), after the treated layer is completed it should be protected against drying for 7 days and traffic should be not allowed on the layer during this period. TRH13 also recommends that one of the following curing methods should be used:

- Frequent light water spraying to ensure that the layer and even the surface remain continuously damp; a full, heavy water bowser may damage the layer and light or half-full bowsers or side spraying should be used. A layer of sand about 40 mm thick will improve the moisture retention. The surface of the layer must not be subjected to wetting and drying cycles since this has a detrimental effect on the treated layer;
- Watering and covering with plastic sheeting;
- Application of a curing membrane consisting of spray-grade emulsion, and
- Covering the treated material while it is still damp with material that may be required for the new layer; this must be carried out in such a way that the treated layer is not damaged.

2.5.8 Deflectometry Control

In Brazil, deflectometry control has been employed in quality control during the construction of new pavements throughout the territory. The idea behind the incorporating deflectometry control when constructing pavements is that, controlling the deformability is as important as controlling the degree of compaction of the layer because the deformability directly influences the fatigue process of the pavement as a whole. Control of the deflectometry level of each layer, limits the total deflection of the structure, and thus, increases the probability of reaching an acceptable deflection level for the structure.

Deflection measurements are carried out at all layers in the constructive process, and in case of the deflections measured in the field being greater than the deflections expected in the design, different actions need to be taken urgently before the next layer is placed.

The Brazilian specifications do not present any references on which deflectometry level must be reached in each of the layers of the pavement structure, including for the final layer of earthworks. In the cement-treated layer, deflection measurements with Benkelman beam or FWD must be performed after 28 days of curing (DER/SP, 2005c). The deflections measured in the field are compared with the deflections predicted in the project, thus enabling the verification of the elastic behaviour of the cement-treated layer in-situ through back-calculations. Even with the recommendation, in Brazil, deflection measurements are often carried out 7 days after the layer is compacted.

2.5.9 Laboratory and field tests for the acceptance control

Quality control plays a significant part during the material selection and construction. Inadequate quality control with test results that do not meet the design requirements in terms of characteristics and thickness of the selected materials results in social and economic losses.

The laboratory and in-situ tests conducted on cement-treated layer for quality control in Brazil and in South Africa are listed in Table 2-27.

Table 2-27: Laboratory and field tests for cement-treated layers in Brazil and in South Africa (Adapted from DER, 2005c; DNIT, 2017 and SANRAL, 2014)

Component	Aspect to be Controlled	Type of Control	Country		Test Method	
			Brazil	South Africa	Brazil	South Africa
Compaction	Maximum dry density	MDD	x	x	NBR-7182 (DER/SP, 2005c) DNIT 164/2003-ME (DNIT, 2017)	SANS 3001–GR51
	Density	Sand replacement	x	x	NBR-7185 (DER/SP, 2005c) and DNER-ME 092/94 (DNIT, 2017)	SANS 3001–GR35
		Nuclear	-	x	-	SANS 3001–GR35
	Moisture Content	Gravimetric analysis	x	x	DNER-ME 088/94 (DER/SP, 2005c and DNIT, 2017)	SANS 3001–GR20
Layer Placement	Layer Thickness	Measurement	x	x	-	-
Material Properties	Grading	Sieve analysis	x	x	NBR NM 248 (DER/SP, 2005c and DNIT, 2017)	SANS 3001–GR1
		Soil mortar analysis				
	Atterberg Limits	Liquid limit	-	x	-	SANS 3001–GR10, 11 & 12
		Linear shrinkage Plasticity Index				
	Strength	UCS, ITS	x	x	NBR-5739 and NBR-7222 (DER/SP, 2005c) DNER-ME 180/94 and DNER-ME 181/94 (DNIT, 2017)	SANS 3001–GR51, 52, 53 and 54
Stabilizer Content	Distribution and quantity of added stabilizer	Laboratory determination of calcium content	-	x	-	SANS 3001–GR58

2.6 Inverted pavement performance

2.6.1 Rutting

In TMH9 (1992), rut depth is defined as the maximum deformation measured under a 2 m straightedge placed transversely across the rut. The presence, severity and shape of rutting provides valuable insight concerning a pavement's condition. Wide, even shaped ruts, illustrated in Figure 2-13, indicate that the weakness in the pavement is located in the lower pavement layers.

On highways where traffic is channelled, permanent deformation is usually manifested in wheel tracks. According to Cortes (2010) the plastic deformations are typically the result of densification experienced by the unbound aggregate layer under service traffic load triggered by inadequate compaction. Permanent deformation of granular material – manifested as rutting and shoving, particularly along the outer wheel path near the pavement shoulder – results from the material

having insufficient stability to cope with the prevailing loading and environmental conditions (Austroads, 2017).



Figure 2-13: Wide subgrade rutting (SANRAL, 2014)

Rasoulia et al. (2000) analysed the performance life of nine test lanes by the amount of ESALs received at failure. The failure criteria were primarily rutting of 1 in. (25 mm) and cracking density of 1.5 linear ft/ft² (5 m/m²) in 50 % of the tested area. SANRAL (2014) gives guidelines for interpreting rutting data (Table 2-28).

Table 2-27: Structural Interpretation of Rut Depths (SANRAL, 2014)

Rut depth	Interpretation
< 10 mm	Sound
10 to 20 mm	Warning
> 20 mm	Severe

In Brazil, in general, there is a variation in the interpretation of rut depth, and this variation is given according to road class, the states, and the different standard organizations. DNIT (2005) recommends that for monitoring purposes, the rut depth must be less than or equal to 5 mm. The São Paulo State Transport Agency (ARTESP) recommends that the rut depth must be less than or equal to 7 mm. The Parana State Department of Traffic (DER/PR) recommends that the rut depth must be less than or equal to 10 mm.

2.6.2 Deflection

According to SANRAL (2014) the interpretation of FWD deflection results are widely used to evaluate pavements and give crude estimates of the remaining life. The evolution of the structural

evaluation process with the use of FWD has enabled a better understanding and characterisation of the elastic behaviour of inverted pavements (De Almeida et al., 2019a).

In general surface resilient deflection is a good indicator of the state of cementitious layers (Figure 2-14); low deflections indicate high moduli and vice versa. However, in Phase III (equivalent granular phase) the resilient deflection will not necessarily be a good indicator of large deformation, since this depends on the moisture sensitivity of the material (erodibility) (De Beer, 1985).

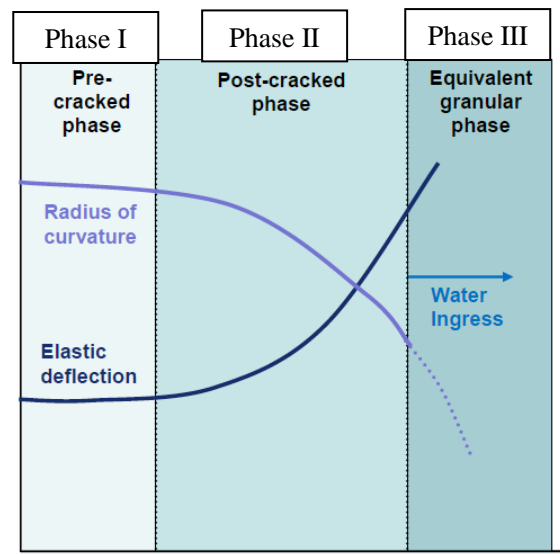


Figure 2-14: Elastic deflection and radius of curvature (SANRAL, 2014)

In South Africa, deflection bowl parameters for analysing the deflection bowl were developed. The deflection bowl can be used to identify weak areas in the depth of a pavement (Table 2-29). According to Horak (2008), the deflection bowl can be basically divided into three distinct zones, Zone 01, Zone 02, and Zone 03. Figure 2-15 illustrates these zones.

Table 2-28: Deflection bowl parameters (Adapted from SANRAL, 2014 and Horak, 2008)

Parameter	Formula	Zones
D₀ - Maximum Deflection	D ₀	1, 2 e 3
RoC - Radius of curvature	$R = \frac{L^2}{2D_0(1 - \frac{D_{200}}{D_0})}$	1
BLI - Base layer index	BLI = D ₀ - D ₃₀₀	1
MLI - Middle layer index	MLI = D ₃₀₀ - D ₆₀₀	2
LLI - Lower layer index	LLI = D ₆₀₀ - D ₉₀₀	3

Where: D₀, D₂₅₀, D₃₀₀, D₆₀₀, D₉₀₀ (mm), L: 200 mm for the FWD

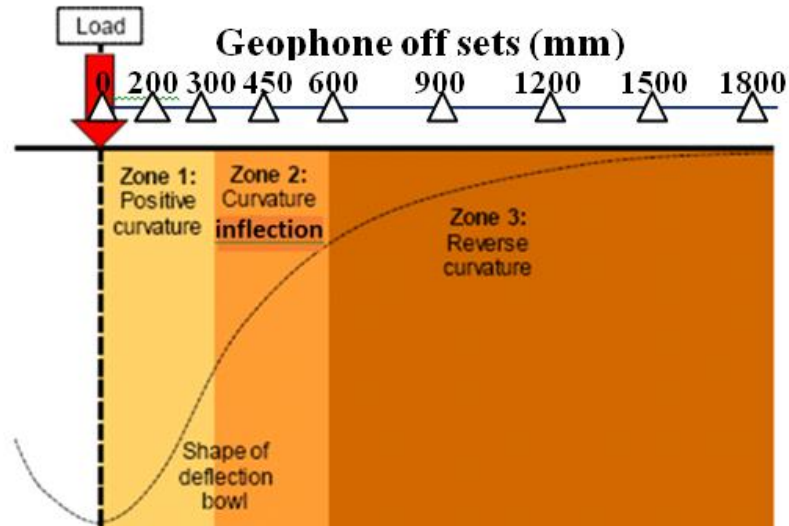


Figure 2-15: Deflection Bowl (Horak, 2008)

Horak (2008) suggested criteria for assessing pavements in terms of sound, warning and severe, shown in Table 2-30. By using this assessment criterion, deficiencies in the structural layers are identified. De Almeida et al. (2019a) applied the criteria suggested by Horak (2008) and concluded that these parameters are a good way to evaluate inverted pavement response and suggested a range of moduli (Table 2-30) linked to these deflection bowl parameters.

Table 2-30: Deflection bowl parameter structural condition rating criteria (Adapted from Horak, 2008 and De Almeida et al., 2019a)

Structural Condition Rating		D_0	BLI	MLI	LLI
		Asphalt Surface Layer Asphalt Concrete	Base Unbound base layer	Subbase Cement-treated layer	Selected Subgrade + Subgrade
Sound	Deflection Bowl Parameters (μm)	<200	<100	<50	<40
	Modulus (MPa)	$E \geq 3\ 100$	$E \geq 200$	$E \geq 7\ 000$	$E \geq 180$
Warning	Deflection Bowl Parameters (μm)	200 – 400	100 – 300	50 – 100	40 – 80
	Modulus (MPa)	$2\ 100 < E \leq 3\ 100$	$100 < E \leq 200$	$2\ 000 < E \leq 7\ 000$	$50 < E \leq 180$
Severe	Deflection Bowl Parameters (μm)	>400	>300	>100	>80
	Modulus (MPa)	$E \leq 2\ 100$	$E \leq 100$	$E \leq 2000$	$E \leq 50$

One of the most common analysis methods of deflection data is to backcalculate material response parameters for each layer within the pavement structure from deflection bowl measurements (Von Quintus and Killingsworth, 1997). Although the concept of back-calculation is known among designers, the process of obtaining elasticity moduli for the pavement layers is complicated, since

this process involves several unknowns, in addition to the moduli of the various pavement layers and their interaction with each other.

According to Smith et al. (2017) researchers and professionals have developed over the years numerous approaches to calculate the elasticity moduli of the layers of the pavements, as well as several programs to perform the calculations.

The choice of software in the back-calculation process is extremely important for obtaining reliable results that characterize the elastic behaviour of materials. De Almeida et al. (2019b) performed a comparative analysis between the back-calculated moduli obtained with different softwares such as Evercalc ©, Elsym-5, BakFAA and BackMeDiNa, concluding the moduli obtained by Elsym-5 and BakFAA presented the best structural response.

2.6.3 Influence of the subgrade modulus

According to Balbo (1993), an aspect that interferes a lot with the compaction of cement-treated layers is the deformability of the underlying layers. Le Coz and Paute (1978) mentioned in Balbo (1993) present several results obtained in the field. In Figure 2-16 the results obtained in the mentioned study are presented, where it is clear that the lower the deformability of the layer underlying the cement-treated layer, the greater the densities obtained at the bottom of this layer after compaction.

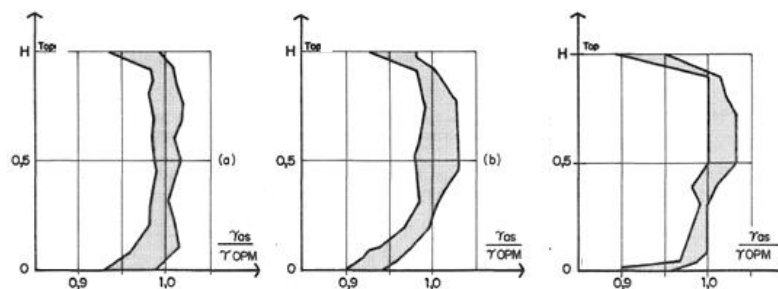


Figure 2-16: a) cemented layer over cemented layer b) cemented layer over subgrade and c) cemented layer over unbound base layer (Adapted from Balbo, 1993)

As the strength of subgrade materials is influenced by compaction and moisture content, consideration should be given during design to the likely construction densities and moisture conditions specified for the construction of the subgrade (Austroads, 2017).

2.6.4 Influence of the cement-treated layer modulus

According to Suzuki (1992), the increase in modular values of cement-treated layer improves the structural performance of inverted as a whole, with the exception of the cement-treated layer itself, which tends to have higher tensile strain that can lead to early rupture of this layer due to fatigue.

Furthermore, according to Suzuki (1992), the cement-treated base stiffness improves the elastic modulus of the unbound base layer and consequently, the horizontal tensile strain in the bottom of the asphalt layer decreases.

2.6.5 Influence of the cement-treated layer thickness

According to Suzuki (1992), the critical level of tensile strains in the bottom of the cement-treated layer is more affected by the increase in thickness of the unbound base layers and the cement-treated layer itself than by increases in the modulus of all layers of the pavement structure. The maximum compressive stress in the subgrade decreases as a result of the increase in the cement-treated base thickness (Cortes, 2010).

Thinner cement-treated layers cause an increase in both compressive stress at the top and tensile stress at the bottom of the cement-treated layers. The responses of the asphalt concrete and unbound base layers are largely unaffected by the thickness of the cement-treated layer as long as this layer remains intact, Papadopoulos and Santamarina (2015).

According to Balbo (1993), a thinner cement-treated layer will quickly induce the fatigue process, if it does not almost immediately rupture the material at the beginning of the service life of the pavement. Balbo (1993) accentuates that that variations (downwards) in the thickness of the compacted cement-treated layer should not be tolerated.

2.6.6 Influence of the unbound base modulus

The unbound base layer placed between the asphalt concrete layer and the cement-treated layer tends to have a higher elastic modulus than normal, due to the confinement effect. According to Suzuki (1992) the increase of the modular value causes a decrease in the indicators D_0 , ϵ_t , ϵ and ϵ_v while providing an increase in the results of parameters RoC , $RoC \times D_0$ and RoC / D_0 , thus demonstrating that this effect is quite beneficial for the performance of the inverted pavement. In

addition, according to the author, the parameters D_0 , ε_t , ε and ε_v tend to increase rapidly when the unbound base layer modulus is less than 300 MPa.

According to Papadopoulos and Santamarina (2015), the unbound base layer acts as a cushioning layer to support the asphalt concrete layer, relieve tension from the cement-treated layer and is under compression everywhere.

2.6.7 Influence of unbound base thickness

According to Cortes (2010) the maximum tensile strain in the cement-treated layer can be reduced by increasing the asphalt concrete layer thickness, increasing the unbound aggregate base thickness, and/or increasing the cement-treated base thickness. Furthermore, according to Cortes (2010) the fatigue life of the asphalt concrete layer is inversely proportional to the thickness of the unbound base layer. Thicker unbound base layers increase the bending of the asphalt layer, but decrease bending stresses in the cement-treated layer (Papadopoulos and Santamarina, 2015).

According to Suzuki (1992) for fixing the unbound thickness, the following aspects should be analysed, regarding the upper and lower limits:

- It should not be too thick, for economic and structural reasons; an increase in the thickness of the unbound base layer increases the thickness of the asphalt concrete layer, and increases the risk permanent deformations in the surface of the pavement,
- It should not be too thin, to prevent the spread of thermal shrinkage cracks in the underlying treated layer. This limit should be in the order of 100 mm, and
- The unbound thickness of 150 mm has more capacity to absorb the reflection of shrinkage cracks than smaller thicknesses.

The initial cracks in the cement-treated layer do not usually reflect through an unbound base layer (G1, G2 or G3) of 150 mm or more (TRH13, 1986).

2.6.8 Influence of the asphalt concrete modulus

According to Cortes (2010) stiffness of the asphalt concrete layer has a strong influence on the predicted maximum tensile strain in the asphalt concrete layer and the cement-treated base, and the maximum compressive stress in the unbound aggregate base. The response of the asphalt concrete layer is sensitive to the thickness of the unbound base layer.

According to Suzuki (1992) the high modulus of the asphalt layer reduces stresses, deformations and deviations at any point in the structure. Moreover, according to the author, among the variables considered in the pavement performance, the asphalt modulus is the least important parameter.

2.6.9 Influence of asphalt concrete thickness

According to Cortes (2010) an increase in the thickness of the asphalt concrete layer leads to higher fatigue resistance in the asphalt concrete layer, and the cement-treated base. Thicker asphalt layers also reduce the magnitude of the maximum compressive stress in the unbound aggregate base, which is associated to rutting. However, a comparison between the mechanical performance of typical conventional flexible pavements and inverted base pavement structures show that thin asphalt layers offer sufficient structural capacity in inverted pavement structures.

For Papadopoulos and Santamarina (2015) thin-asphalt layers deform more uniformly and experience lower tension than thick layers, but do not reduce the vertical contact stress, which is felt by the unbound base with almost the same intensity.

According to Austroads (2017) to reduce the risk of reflective cracking the pavement should provide a minimum cover equivalent to 175 mm of asphalt over the cemented material or lean-mix concrete. Granular material can be used as cover either solely in conjunction with asphalt, subject to the following criterion:

$$(0.75 \times \text{thickness of granular material cover}) + (\text{thickness of asphalt cover}) \geq 175 \text{ mm}$$

According to Suzuki (1992), asphalt thicknesses are always more interesting for inverted pavement, since all parameters are improved with the increase of the thickness of the layer. Furthermore, for the author, considering that one of the major problems of the inverted pavements is the cracks reflection on the surface, it is important to protect the cement-treated layer.

2.7 Summary

The literature review sought the basic knowledge necessary for the development of this study. To achieve this, the literature review began with the design procedures for inverted pavement, concluding that the concept of pavement design, which is very similar between countries with a few changes on the materials and local conditions.

In the sequence, the main factors that influence the mechanical behaviour of the cement-treated layer was addressed. It was found that the strength parameters are influenced and determined by material variables, such as the type and cement content, grain size distribution, type of aggregate, moisture content, compaction, and curing.

In addition, the contribution of each layer (thickness and modulus) to pavement performance as a whole was approached as well. According to the literature review, all layers play an important role in the behaviour of the inverted pavement, however, the support layer underlying the cement-treated layer, and the unbound base are the central components of the pavement structure.

In general, the main Brazilian specifications for cement-treated layer allow designers to make most decisions based on their experience, and these decisions range from the definition of the subgrade modulus to authorising that the cement-treated layer may be open to traffic. The South African specifications, unlike the Brazilian specifications, are more specific, showing instructions that must be followed by designers, at least in the pavement design phase. In the execution phase, the South African specifications also have gaps, which must be filled in accordance with the current contract or by the designers based on experience.

In conclusion, even with the employment of inverted pavements worldwide, South Africa being a world reference in procedures and techniques, the scarcity of publications that explore in-depth factors that directly affect the mechanical behaviour of the cement-treated layer and the inverted pavement as a whole was noted.

3. EXPERIMENTAL WORK

Experimental work forms a part of this study, in addition to the theoretical aspect. The theoretical and experimental studies seek to understand the mechanical behaviour of an inverted pavement, identifying and characterizing the variables directly related to structural behaviour of inverted pavement.

The experimental work is divided into five different sections: test section selection, field measurements, in-situ tests, laboratory tests, and evaluation of the tests carried out during the construction in the quality control of test sections selected (Figure 3-1).

The deflection and traffic data, as well as the tests carried out during the quality control in the construction of both test sections were provided by CCR Engelog, which is the company responsible for the maintenance and monitoring of the Bandeirantes Highway (SP-348), where the test sections scope of this study are located. The tests carried out and the procedures followed in each one of the different test sections are detailed in the following sections.

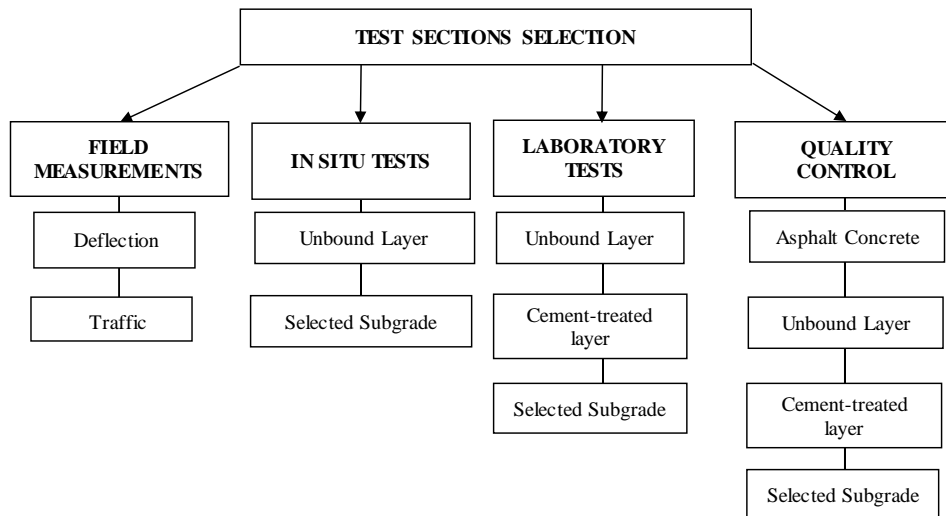


Figure 3-1: Flow diagram of the Experimental work

3.1 Test sections selection

As a scope of this study, two test sections located along the Bandeirantes Highway (SP-348) were selected, each one with a length of 320 m. Both sections were built based on the same design principles, but they have been presented through different structural performances since their implementation back in 2001, and this difference has only increased over time. During the selection of the tests, care was taken to reduce the effect of external variables. Both test sections

are located in a similar topographic region, this does not include curves or ramps, and the traffic of both test sections is the same order of magnitude. Figure 3-2 shows the location of the selected test sections on the map.

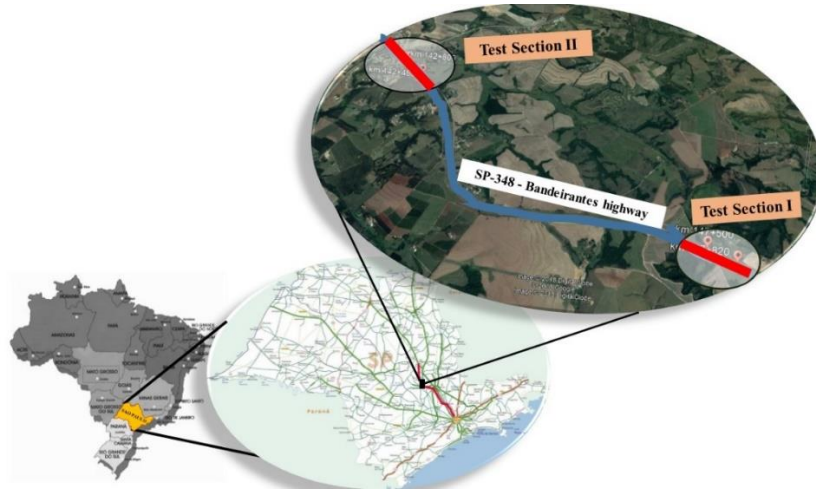


Figure 3-2: Test Sections' locations

Table 3-1 presents the main information about the location and length of the test sections covered in this study. Figure 3-3 shows the overview of these test sections.

Table 3-1: Details of the location of the test sections

Test Sections	Location		Lengh (m)	Direction
	Start station	End station		
I	147+480	147+800	320	North
II	142+480	142+800	320	South



Figure 3-3: a) Test section I (T-I) overview and b) Test section II (T-II) overview

According to the Technical Design Report (MC-01.348.000-0-P00_003-R0, 2000), provided by CCR Engelog, the inverted pavement structure of both test sections was built following executive procedures of Brazilian standards and authorities (Highway Development S/A– DERSA). The elastic properties for each of these layers, concerning their materials, thicknesses, elastic moduli and Poisson's Ratio were selected by the designer. The highway cross section is shown in Figure 3-4 and the proprieties of the materials are shown in and Table 3-2.

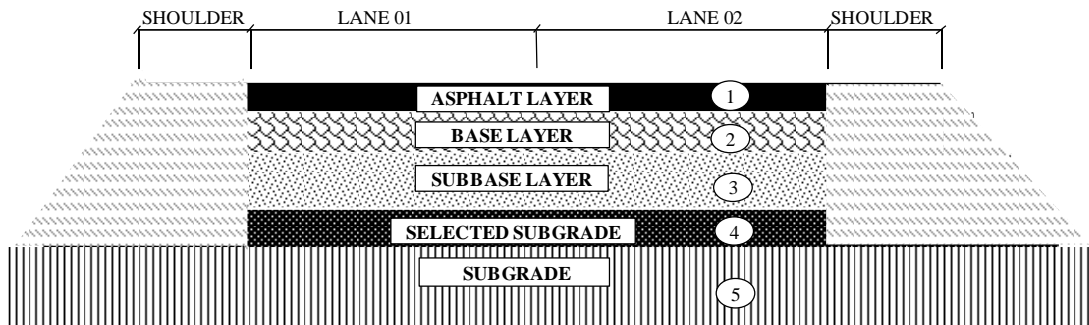


Figure 3-4: Cross section of the Bandeirantes Highway (SP-348)

Table 3-2: Test sections I and II materials properties

ID	Layer	Thickness (mm)	Poisson's Ratio	Modulus (MPa)
1	Asphalt Asphalt Concrete	120	0.30	4 000
2	Base Unbound base layer	150	0.35	250
3	Subbase Cement-treated layer	180	0.25	12 000
4	Selected Subgrade	150	0.40	150
5	Subgrade	Semi-infinite	0.40	70

For the prediction of pavement performance, including the adoption of modulus for each of the layers, the designer used the data obtained in the experimental section of inverted pavement executed on the Santos Dumont highway (SP-075), the same section mentioned in Section 2.2.1.

During the execution of T-I and T-II, there was a concern about ensuring adequate and homogeneous support for the pavement structure, therefore, the in-situ subgrade was ripped and recompacted in three layers of 200 mm thick each. Thus, at the end of the earthworks phase, the

subgrade of both test sections should present a modulus greater than or equal to 70 MPa and an expansion less than or equal to 2 %, in the minimum thickness of 600 mm.

3.2 Field Measurements

Field measurement gives a lot of information about the pavement without having to take field samples from the pavement for laboratory testing, besides being more representative in the evaluation of the actual conditions of the pavement. From the data obtained in the field over the years, it is possible to understand and accurately characterise the existing conditions of the pavement, and thus draw inferences on its behaviour. In this section of the dissertation, results and procedures adopted for conducting deflection and traffic measurement are presented.

3.2.1 Deflection measurement

Deflection testing simulates the effects of traffic on the pavement. From understanding of the effects of loading and the interpretation of the deflection bowl generated during the measurement, it is possible to analyse the performance of the pavement as a whole and identify the influence of each layer on the maximum deflection.

Deflection measurement using a FWD is the most common method in Brazil and worldwide. The FWD (Figure 3-5) applies a dynamic load that simulates the load of a moving wheel. The displacements generated by the load applied on the pavement surface are measured by geophones, generating a deflection bowl. In Brazil, normally, the geophones are spaced at zero (D_0) (under the centre of the FWD loading plate, which itself has a diameter of 300 mm), 200 mm (D_{200}), 300 mm (D_{300}), 450 mm (D_{450}), 600 mm (D_{600}), 900 mm (D_{900}) and 1200 mm (D_{1200}).

The geophone directly underneath the load of the FWD (D_0) measures the largest deflection, and all layers contribute to this deflection. The second geophone measures the deformation of the pavement at 200 mm from the load application point (D_{200}). The geophone furthest from the load (D_{1200}) measures a deflection that is generated mostly from the subgrade.

As part of this work, the deflection measurements of test sections T-I and T-II were taken every two years in the period between 2003 and 2016 using an FWD. The deflections were measured every 40 m in the heavy traffic lane (lane 2). The deflections results were obtained from the drop of weight equal to 40 kN (566 kPa contact stress) and the geophones were spaced as presented

above. The results of the deflection measurement carried out with the FWD are presented in Figures 3-6 to Figure 3-12.



Figure 3-5: FWD Equipment (SANRAL, 2014)

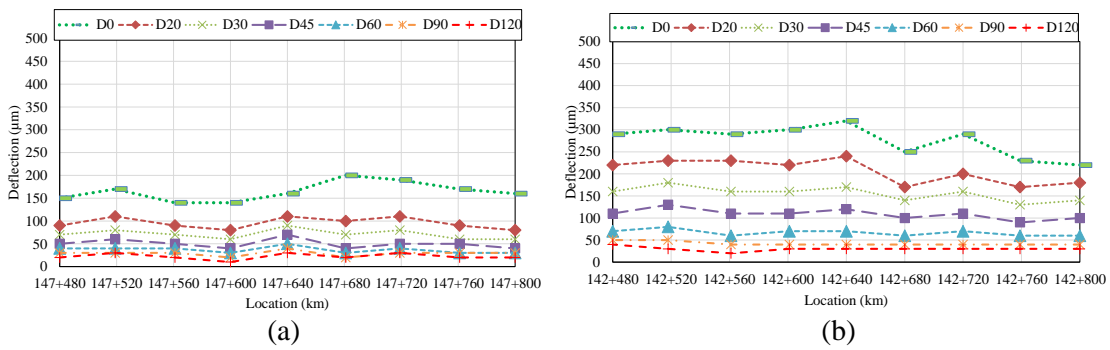


Figure 3-6: a) T-I - Deflection measurement carried out in 2003 b) T-II - Deflection measurement carried out in 2003

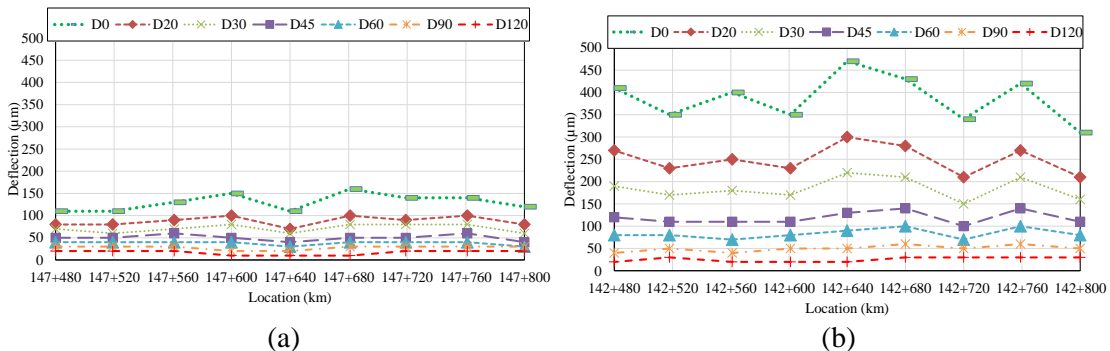
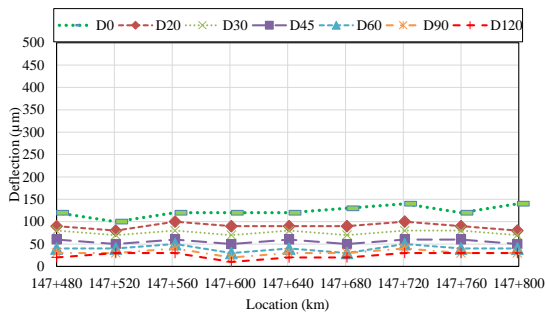
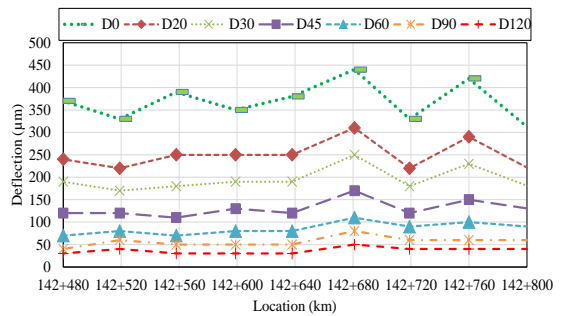


Figure 3-7: a) T-I - Deflection measurement carried out in 2005 b) T-II - Deflection measurement carried out in 2005

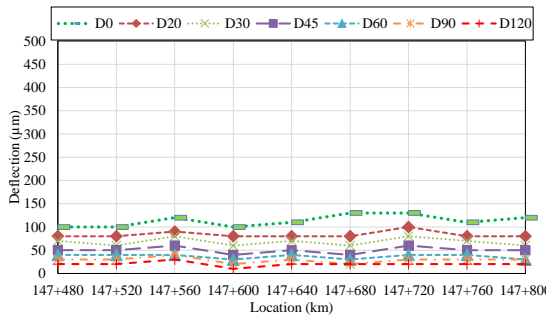


(a)

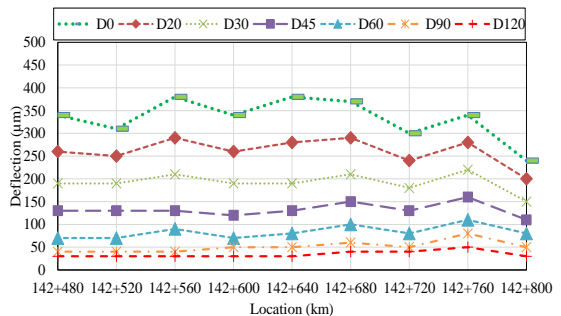


(b)

Figure 3-8: a) T-I - Deflection measurement carried out in 2007 b) T-II - Deflection measurement carried out in 2007

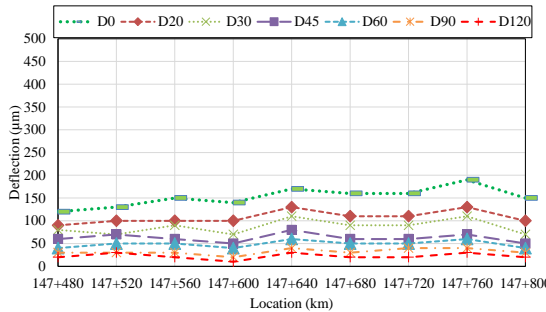


(a)

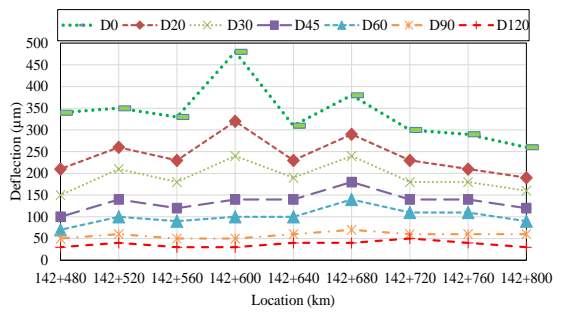


(b)

Figure 3-9: a) T-I - Deflection measurement carried out in 2009 b) T-II - Deflection measurement carried out in 2009

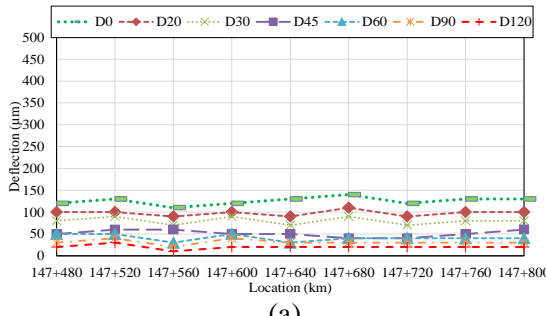


(a)

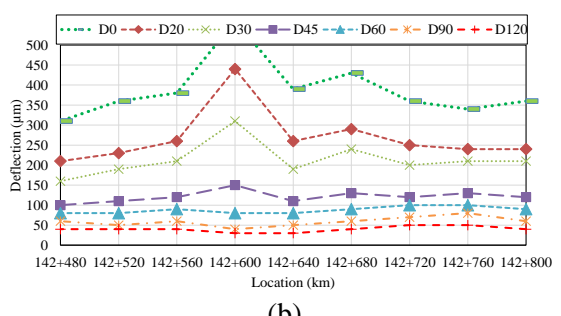


(b)

Figure 3-10: a) T-I - Deflection measurement carried out in 2012 b) T-II - Deflection measurement carried out in 2012



(a)



(b)

Figure 3-11: a) T-I - Deflection measurement carried out in 2014 b) T-II - Deflection measurement carried out in 2014

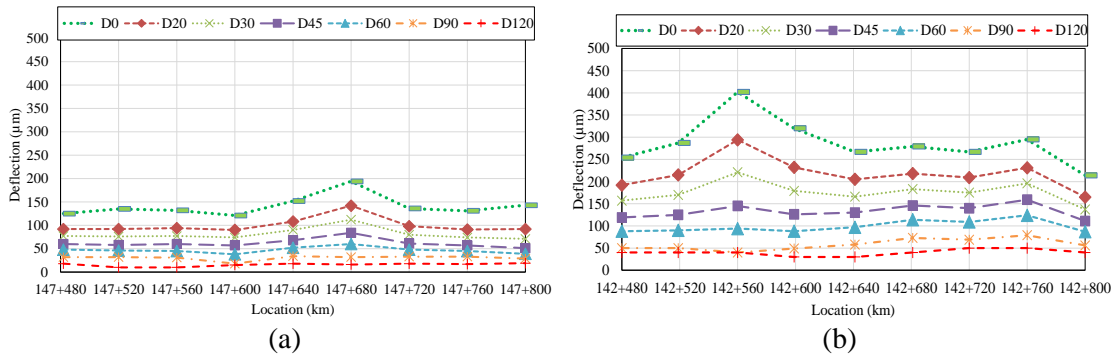


Figure 3-12: a) T- I - Deflection measurement carried out in 2016 b) T-II - Deflection measurement carried out in 2016

Due to the large amount and homogeneity of data, a decision was made to choose a representative (actual measured) deflection bowl for each year of measurement to carry out the analysis for this study. To determine the most representative deflection bowls measured in the field annually, the differences between the annual deflection bowl averages and the actual deflection bowls measured in the field were calculated. These differences were measured using the Root Mean Square Error (RMSE).

The RMSE (Equation 3.1) is a measure often used to calculate the difference between predicted values (annual average of the deflection bowls) and observed values (actual deflection bowl). These deviations are called residuals if calculations were performed over the data sample that was used for estimation and are called errors (or prediction errors) if computed out-of-sample.

$$\text{RMSE (\%)} = \left[\sum_{i=1}^n \left(\frac{100 \times (D_{\text{Average}} - D_{\text{Actual}})}{D_{\text{Actual}}} \right)^2 \right]^{\frac{1}{2}} \quad (\text{Equation 3.1})$$

Where:

D_{Average} : Annual average deflection bowl

D_{Actual} : Annual actual deflection bowl

The deflection bowl measured in both test sections T-I and T-II are shown in Figure 3-13 and Figure 3-14.

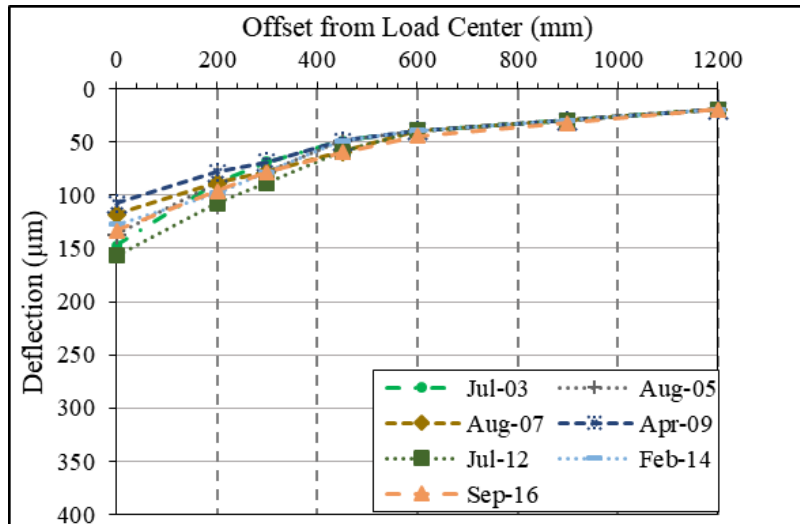


Figure 3-13: Test-Section I – Deflection bowls

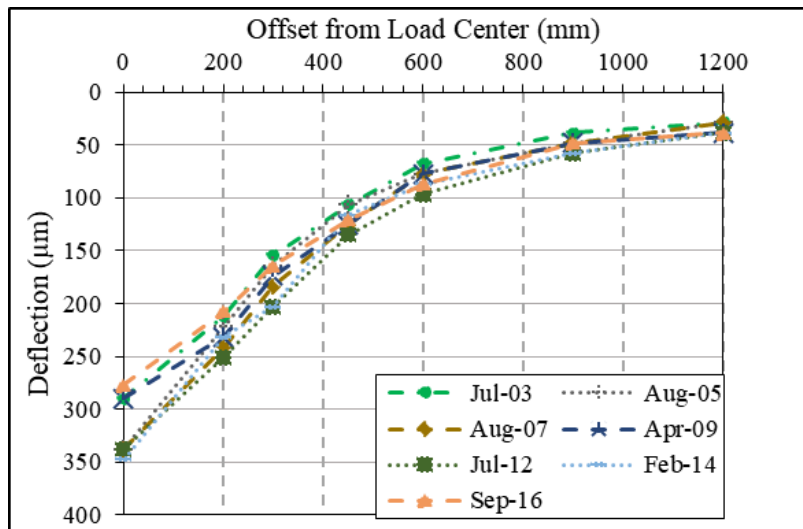


Figure 3-14: Test-Section II – Deflection bowls

According to Chen et al. (2000) temperature is one of the most important parameters that affect FWD measurements. Since FWD measurements are collected at different temperatures, temperature correction needs to be applied in the analysis. Motta and Medina (1988) mentioned in Júnior (2018) the temperature correction must be variable in relation to the type of pavement structure and the climate of the region. According to the authors, the temperature correction is not considered to be of great relevance for cases such as Brazil, which has characteristics of a tropical climate and generally thin asphalt layered structures. Chen et al. (2000) and Park et al. (2001) proposed temperature correction equations to correct the deflections measured at 25 °C. The first researchers proposed a correction equation for asphalt concrete layer thicknesses greater than 178 mm, and the second researchers for asphalt concrete layer thicknesses greater than 180 mm.

Adjusting the temperature as a function of the asphalt thickness is not easy. Some researchers have observed the inapplicability of temperature correction factors for asphalt thicknesses less than 180 mm (Chen et al., 2000 and Park et al., 2001). According to Zheng et al. (2019) the best trend found with the increase in asphalt pavement thickness among temperature correction was in the pavement structure with the asphalt layer greater than 150 mm. Song and Zeng (2017) proposed temperature correction coefficients. The authors performed the deflection tests on four pavement structures with the asphalt layer thickness varying from 150 mm to 335 mm.

Kim et al. (1995) showed the temperature adjustment factors proposed by AASHTO for pavements with granular or asphalt-treated base for thickness varying to 2 in (50.8 mm) from 12 in (304.8 mm). According to the authors, it has been reported by many practitioners that the AASHTO procedure is inaccurate, especially at temperatures over 38°C (100°F).

After widely research, no suitable temperature adjustment factors were found in the available literature for the studied structures. As the thickness of the asphalt concrete surface of both test sections is less than 150 mm and part of the temperatures measured are close or greater than 38 °C (Table 3-3) the correction of the deflections as a function of the temperature will not be done. As temperatures over the measurement years in both test sections are relatively similar, the analysis and results are not expected to be compromised.

Table 3-3 shows the temperatures measured at the surface of the asphalt concrete layer of the representative basins during the measurement of deflection in test sections T-I and T-II.

Table 3-3: Pavement surface temperature measured in test sections T-I and T-II

Data	Test-section I	Test-section II
	Temperature of the pavement (°C)	
Jul-03	36	27
Aug-05	37	33
Aug-07	33	41
Apr-09	33	39
Jul-12	36	25
Feb-14	36	39
Sep-16	40	33

The effect of the seasonal rainfall on pavement strength shall be considered as a factor when measuring pavement deflections in tropical climates. According to Smith and Jones (1980), periods of rain or dry weather can cause changes in moisture conditions under pavements, thereby affecting the overall stiffness of the structure and the deflection measured on it. Furthermore, according to the authors, it is important to measure pavement deflections at the end of the wettest period of the year, since this is when the pavement is weakest.

The majority of the deflection measurement in this research was carried out between July and September, where maximum precipitation reached 49 mm (4 % in relation to the annual rainfall of 1 321 mm) (Figure 3-15). In others months, monthly rainfall reached 23.9 mm and 40.6 mm, in April 2009 and February 2014, respectively. No rainfall was reported in the test sections during the deflection measurement or the three days before testing.

The period between November and January has the highest rainfall in the Limeira region (a town located 10 km away from the test sections), and from January, the volume of rainfall begins to decrease (Figure 3-16). The measurements carried out in April 2009 and February 2014, even after the rainy seasons, did not show significant increases in deflections in relation to the other years of measurement (Figures 3-5 to Figure 3-11), and this may be associated with the low volumes of precipitation that occurred in the aforementioned years even in the rainfall seasons.

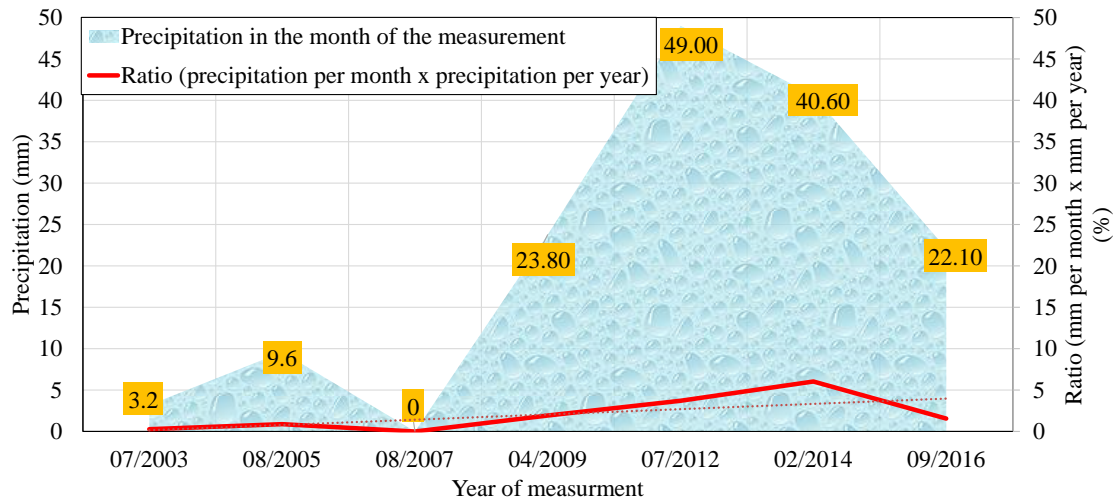


Figure 3-15: Precipitation in the month of the measurement (Adapted from CIAGRO, 2020)

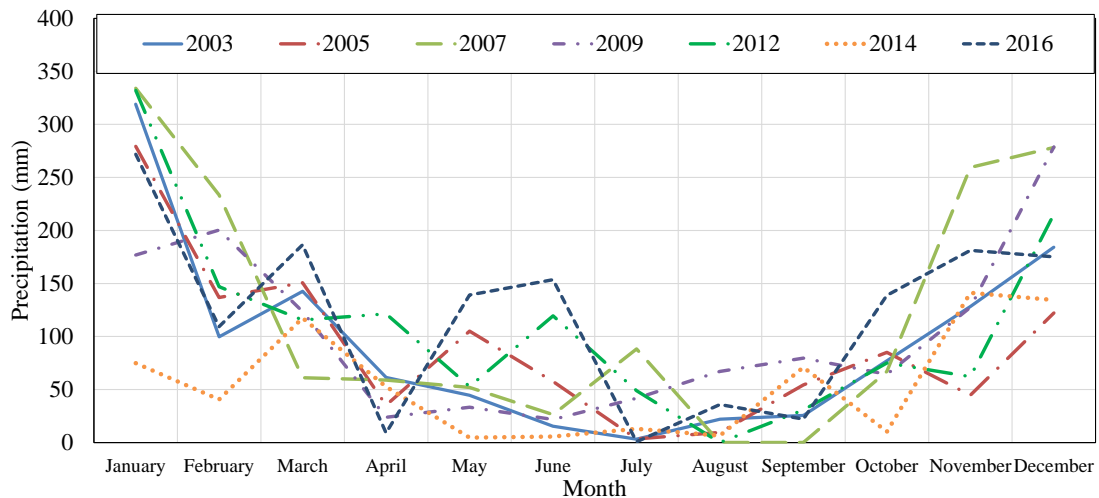


Figure 3-16: Annual precipitation in Limeira (Adapted from CIAGRO, 2020)

3.2.2 Traffic Measurement

The study of traffic is one of the most important steps in the development of a pavement project since the solutions adopted need to be structurally adequate to the expected requests. The effect of vehicle loading on the pavement is relatively small when considering each vehicle or loading individually. However, the cumulative effect of many such loads causes distress in the pavement. An understanding of the short-term effects of loading on a pavement provides a good background for how the cumulative effects manifest and are modelled.

In this research, to analyse the performance of both test sections pavement under a load over time, the measurement of traffic was needed. CCR Engelog provided the composition (counts and classification) of vehicles. Data were collected for each year of study between January and December. The average annual daily traffic composition for both test sections (line 2 of each one) are shown in Table 3-4 and Table 3-5 and the most common Brazilian commercial vehicles spectrum classes and silhouettes are illustrated in Table 3-6.

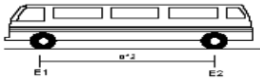
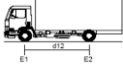

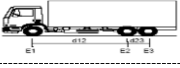
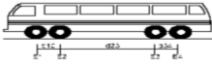
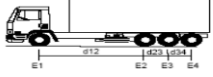



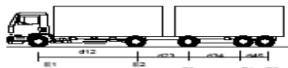

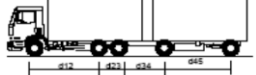
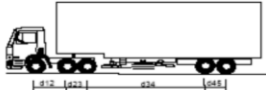



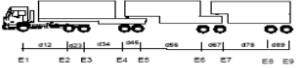
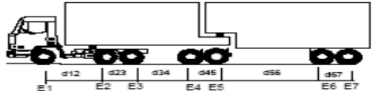
Table 3-4: Test-Section I – Average annual daily traffic for the base year

Vehicle classes	Total	2CB	3CB	4CB	2C	3C	4C	2S1	2S2	2S3	3S2	3S3	3S2C4	3S2S2	2C2	2C3	3C2	3C3	3C4
No. of Axles		2	3	4	2	3	4	3	4	5	5	6	9	7	4	5	5	6	7
2003	693	121	22	0	121	100	41	100	41	39	39	17	6	3	9	10	10	12	2
2005	907	153	28	0	153	126	60	126	60	46	46	31	7	10	13	11	11	20	6
2007	1124	185	33	0	185	148	77	148	77	56	56	49	9	15	17	14	14	33	8
2009	1273	209	37	0	209	168	87	168	87	64	64	56	10	17	19	16	16	37	9
2012	1690	278	50	0	278	223	115	223	115	84	84	74	14	23	26	21	21	49	12
2014	1816	299	53	0	299	239	124	239	124	90	90	80	15	24	28	23	23	53	13
2016	1482	244	43	0	244	195	101	195	101	74	74	65	12	20	22	19	19	43	11

Table 3-5: Test-Section II - Average annual daily traffic for the base year

Daily heavy vehicle volume per lane for the base year																			
Vehicle classes	Total	2CB	3CB	4CB	2C	3C	4C	2S1	2S2	2S3	3S2	3S3	3S2C4	3S2S2	2C2	2C3	3C2	3C3	3C4
No. of Axles		2	3	4	2	3	4	3	4	5	5	6	9	7	4	5	5	6	7
2003	775	117	20	0	117	90	31	90	31	79	79	35	0	10	7	20	20	24	5
2005	1372	149	30	0	149	133	51	133	51	142	142	113	0	79	11	36	36	75	42
2007	1273	182	28	0	182	126	68	126	68	87	87	95	0	66	15	22	22	64	35
2009	1556	256	46	0	256	205	106	205	106	78	78	68	12	21	24	19	19	46	11
2012	2062	339	61	0	339	272	140	272	140	103	103	91	17	27	31	26	26	60	15
2014	2220	365	65	0	365	293	151	293	151	111	111	97	18	29	34	28	28	65	16
2016	1810	298	53	0	298	239	123	239	123	90	90	79	15	24	27	23	23	53	13

Table 3-6: Most common Brazilian commercial vehicles spectrum: classes and silhouettes (Adapted from DNIT, 2006b)

Vehicle classes					
Buses	2CB		Light trucks	2C	
	3CB		Medium heavy trucks	3C	
	4CB		Heavy trucks	4C	
Semi-trailers	2S1		Trailers	2C2	
	2S2			2C3	
	2S3			3C2	
	3S2			3C3	
	3S3			3C4	
	3S2C4				
	3S2S2				

From knowledge of the composition (counts and classification) of traffic it was possible to calculate the equivalent standard axles, in Brazil known as “N”. The calculation of “N” is given by Equation 3.2. The standard axle load is an 80 kN single axle load with a dual wheel configuration.

$$N = 365 * V_p * F_v * F_r$$

(Equation 3.2)

Where:

N = Equivalent Number of standard axles (80 kN)

V_P = Annual average daily traffic

F_V = Vehicle Factor

F_R = Regional Factor (was adopted F_R equal to 1, the value adopted often in Brazil)

The Vehicle Factor (F_V) is a factor that converts different truckloads to an equivalent number of standard axles. For each type of vehicle, there is a different factor. In this research, the Vehicle Factors (Equation 3.3) used to calculate the Number “N” were recommended by the American Association of State Highway and Transportation Officials (AASHTO) and the United States Army Corps of Engineers (USACE) methodologies, as recommended by DNIT (2006b).

$$F_V = F_E * F_{LEF} \quad \text{(Equation 3.3)}$$

Where:

F_E = Axle Factor

F_{LEF} = Load Equivalency Factor

Changes to the legal axle load and the level of enforcement affect the F_V . In the determination of the Number “N”, based on the experience of the AutoBAn Concessionaire consideration was made that 20 % of commercial vehicles travel empty and 80 % travel full in all the years of analysis. The Permissible axle load limits changed over time as shown in Table 3-7.

Table 3-7: Permissible axle load limits changes

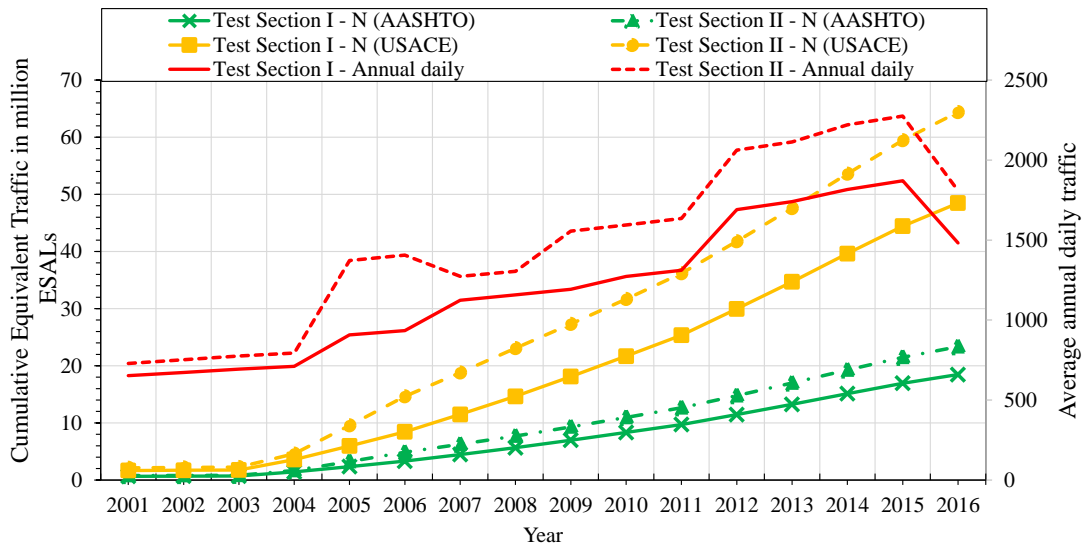
Year	Permissible axle load limits
2003	5%
2005	5%
2007	5%
2009	5%
2012	7.5%
2014	7.5%
2016	10%

When numbers and classification of vehicles were known, it became possible to calculate the Equivalent Number of standard axles (80 kN) for each year of analysis, according to the AASHTO and USACE methodologies for both test sections T-I and T-II. To calculate the cumulative traffic, a growth rate of 3.0 % was considered for each year when no data collected, such as 2001, 2002, 2004, 2006, 2008, 2010, 2011, 2013 and 2014. The cumulative equivalent traffic and the average annual daily traffic obtained are shown in Table 3-8 and in Figure 3-17.

Table 3-8: Cumulative Equivalent Traffic in million ESALs

Year	Test section I			Test section II		
	Average annual daily traffic	N _{AASHTO}	N _{USACE}	Average annual daily traffic	N _{AASHTO}	N _{USACE}
2001 ¹	652	0.66	1.66	729	0.78	2.13
2002	672	0.68	1.71	752	0.80	2.20
2003	693	0.70	1.76	775	0.83	2.27
2004	710	1.43	3.58	794	1.68	4.60
2005	907	2.35	5.97	1372	3.25	9.54
2006	934	3.31	8.43	1406	4.87	14.63
2007	1124	4.46	11.49	1273	6.26	18.79
2008	1158	5.66	14.64	1305	7.70	23.08
2009	1192	6.97	18.11	1556	9.30	27.31
2010	1273	8.32	21.68	1595	10.95	31.67
2011	1311	9.71	25.35	1635	12.65	36.16
2012	1690	11.45	29.96	2062	14.78	41.78
2013	1741	13.25	34.69	2114	16.97	47.56
2014	1816	15.12	39.64	2220	19.26	53.60
2015	1870	16.94	44.43	2276	21.48	59.46
2016	1482	18.46	48.47	1810	23.34	64.39

¹ Year of opening traffic

**Figure 3-17: Cumulative Equivalent Traffic in million ESALs for both test sections**

3.3 Materials characterization of the test sections

Two inspection pits were opened in the heavy traffic line (line 2) in each one of the test sections (Figure 3-18) to verify the thicknesses of the layers, evaluate possible anomalies found through visual analysis. In addition, tests in-situ were carried out in each of the inspection pits, and samples were collected to carry out tests in the laboratory.

Samples were collected from the unbound base layer, cement-treated layer, and selected subgrade. No samples from the asphalt concrete layer were collected, because in 2015, 50 % of the asphalt concrete layer in T-I was replaced, and in T-II the replacement covered 100 %, thus, the results obtained from the asphalt concrete layer would not give the answers expected in this research.



Figure 3-18: a) IP-01 opened in Test Section I b) IP-02 opened in Test Section I c) IP-03 opened in Test Section II c) IP-04 opened in Test Section II

The thicknesses of the layers identified in both inspection pits for each test section are summarized in Table 3-9, and in Figure 3-19 is possible to identify where the layers are placed. The samples extracted in both inspection pits, from the cement-treated layer in T-I were completely intact. The cement-treated layer found in T-II presented disaggregation in the last 30 mm in the bottom layer of both inspection pits.

Table 3-9: Layer thickness identified in both test-sections

ID	Layer	Test Section I		Test Section II	
		PI-01	PI-02	PI-03	PI-04
Thickness (mm)					
1	Asphalt Asphalt Concrete	140	140	140	135
2	Base Unbound base layer	80	90	120	130
3	Subbase Cement-treated layer	190	180	180*	180*
4	Selected Subgrade	180	185	160	140
5	Subgrade	-	-	-	-

*The last 30 mm in the bottom of the cement-treated layer presented disaggregation

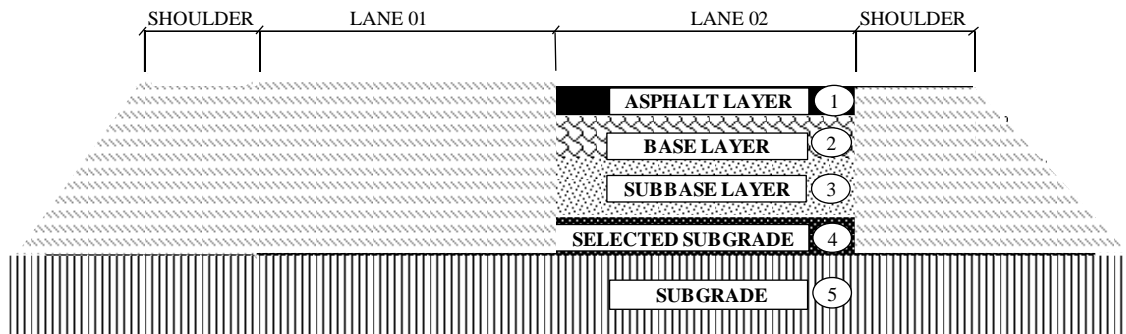


Figure 3-19: Cross section of the test sections T-I and T-II

3.3.1 In-situ and laboratory trial planning

Tests performed in-situ and in the laboratory in both test sections are shown in Table 3-10.

Table 3-10: Tests carried out in-situ and in laboratory

Test	Layer	Test performed
In-situ	Unbound base	Density (Sand-Cone Method)
	Selected Subgrade	Density (Sand-Cone Method)
		Soil Strength (DCP)
Laboratory	Unbound base	Gradation test
		Dynamic Modulus
		Resilient modulus
	Cement-treated base	Flexural modulus
		Unconfined compressive strength
		Indirect tensile strength
		Flexural tensile strength
	Selected Subgrade	Californian Bearing Ratio (CBR)
		Atterberg Limits
		Soil Classification (HRB-AASHTO, TRH14 and MCT)
Resilient modulus		

In addition to the collection of samples from the granular layer and selected subgrade, six cylindrical specimens were collected in the cement-treated layer in each of the inspection pits. The specimens collected were 100 mm in diameter and height varying according to the thickness found in the cement-treated layer (Figure 3-20). Prismatic specimens with dimensions of approximately 400 mm x 400 mm and height variable were also extracted from the cement-treated layer (Figure 3-21).

**Figure 3-20: Preparation of cylindrical specimens collected from both test sections**

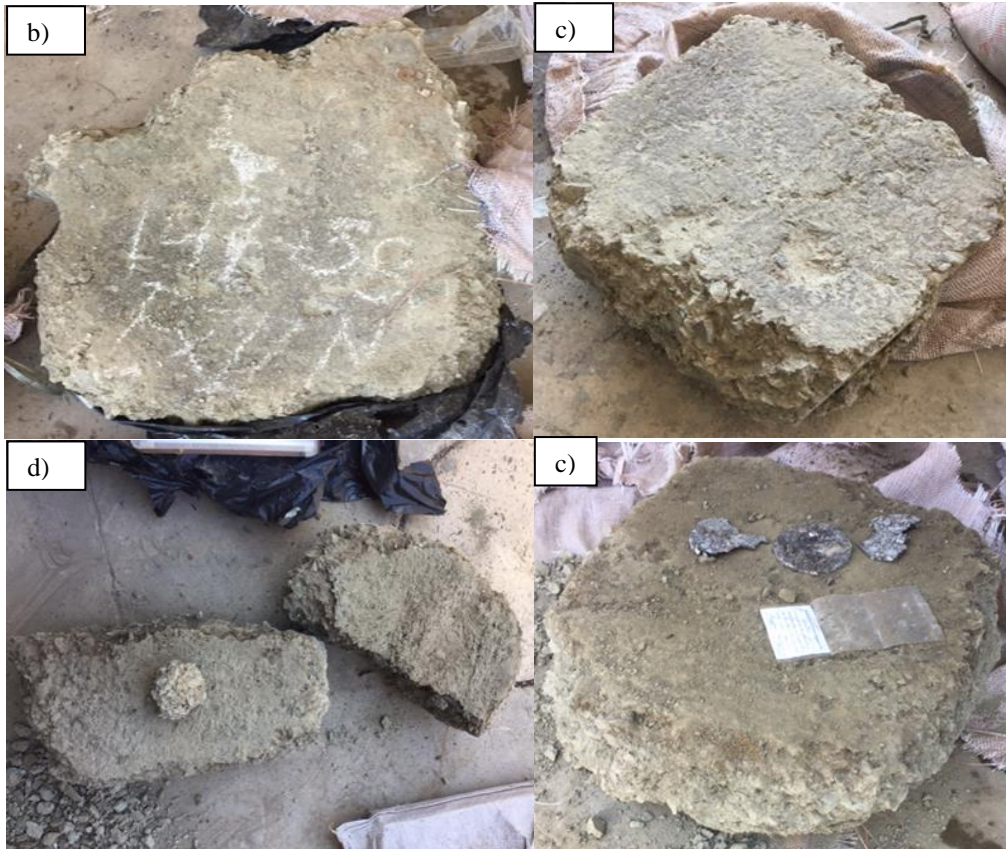


Figure 3-21: a) Prismatic specimen collected in IP-01 b) Prismatic specimen collected in IP-02 c) Prismatic specimen collected in IP-03 d) Prismatic specimen collected in IP-04

From the collection of the cylindrical specimens of the cement-treated layer, the tests described in Tables 3-11 and 3-12 were performed. In addition to the tests described in the following tables, tests were performed to obtain the Flexural modulus and Flexural tensile strength using prismatic specimens. Descriptions of the procedures and practices adopted during the tests are covered in Section 3.6.

Table 3-11: Laboratory trial planning in Test Section – I

Sample ID	Location	Height (mm)	Test
1	IP-01	191.2	Dynamic Modulus and USC
2	IP-01	197.6	Dynamic Modulus and USC
3	IP-01	176.8	Resilient Modulus and ITS
4	IP-01	198.2	Dynamic Modulus and USC
5	IP-01	194.2	Resilient Modulus and ITS
6	IP-01	117.6	Resilient Modulus and ITS
1	IP-02	180.4	Dynamic Modulus and USC
2	IP-02	180.0	Resilient Modulus and ITS
3	IP-02	178.2	Dynamic Modulus and USC
4	IP-02	175.8	Resilient Modulus and ITS
5	IP-02	181.4	Dynamic Modulus and USC
6	IP-02	182.2	Resilient Modulus and ITS

Table 3-12: Laboratory trial planning in Test Section – II

Sample ID	Location	Height (mm)	Test
1	IP-03	153.8	Dynamic Modulus and USC
2	IP-03	165.6	Dynamic Modulus and USC
3	IP-03	151.2	Resilient Modulus and ITS
4	IP-03	160.2	Dynamic Modulus and USC
5	IP-03	128.8	Resilient Modulus and ITS
6	IP-03	141.2	Resilient Modulus and ITS
1	IP-04	184.2	Dynamic Modulus and USC
2	IP-04	150.2	Resilient Modulus and ITS
3	IP-04	175.6	Dynamic Modulus and USC
4	IP-04	123.6	Resilient Modulus and ITS
5	IP-04	167.8	Dynamic Modulus and USC
6	IP-04	159.8	Resilient Modulus and ITS

3.4 In-situ tests carried out in the test sections

The performance of in-situ tests is extremely important to evaluate the performance of materials in the field, since sometimes the expected behaviour in the laboratory may not be achieved in the field.

In-situ tests are necessary to understand the behaviour of the materials during and after the construction of pavements. In this section of the dissertation, results and procedures adopted to obtain the density and soil strength by using the Sand-Cone Method and the DCP are presented respectively.

In-situ tests were carried out on the inspections pit opened in the test sections. The IP-01 was opened in T-I one day after a period of heavy rainfall, and, for this reason, the results obtained in IP-01 may not fully represent the in-situ characteristics of the materials.

3.4.1 Density

Soil compaction is performed with the intention of increasing bearing capacity and reducing settlement. There are several methods to evaluate natural or compacted soils in terms of the relative compaction of the subgrade and several layers of the pavement. In Brazil, the Sand-Cone Method is widely used because it is relatively simple and inexpensive when compared with other methods available.

The Sand-Cone Method requires that a test hole be excavated in the field (approximately the thickness of the compacted layer) and the mass of soil, coarse or granular material is removed from the hole and measured. The test hole is then filled with the standard sand, using a plastic jar as shown in Figure 3-22. Knowing the sand density used to fill the test hole it is possible to calculate the volume of the sand required to fill the hole, and consequently, the volume of the hole becomes known. Thus, with the information on the volume of the test hole and the weight of the excavated material is possible to calculate the bulk density of the requested material. In general, the bulk density is equal to the weight of the excavated material divided by the volume of the excavated material.

Through the Sand-Cone Method it is also possible to obtain the moisture content and the dry density. Both are very important parameters to evaluate the degree of compaction achieved during the construction process.

In this research the bulk density, dry density, and moisture content were determined using the Sand-Cone Method. The procedures recommended in DNER-ME 092/94 were followed. The results obtained are shown in Table 3-13.

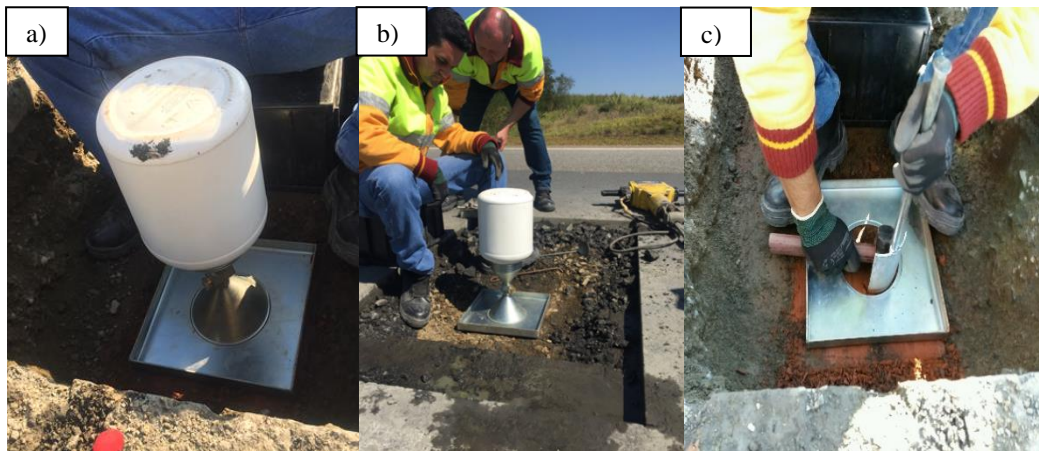


Figure 3-22: a) The sand-cone device b) and c) Determination of the density of the unbound base and selected subgrade in-situ by the Sand-Cone Method

Table 3-13: Test results obtained in-situ by the Sand-Cone Method

Layer	Test	Test Section I		Test Section II	
		IP-01	IP-02	IP-03	IP-04
Selected Subgrade	Moisture Content %	12.9	14.3	9.2	9.8
	Bulk Density kg/m ³	2 129	2 171	2 053	2 083
	Dry Density kg/m ³	1 886	1 900	1 880	1 898
Base Layer	Moisture Content %	3.9	3.3	4.4	5.0
	Bulk Density kg/m ³	2 315	2 265	2 370	2 329
Unbound base	Dry Density kg/m ³	2 228	2 193	2 271	2 217

3.4.2 Soil Strength

The normalised strength distribution of a pavement structure is defined as the decrease in the strength of layers as they increase in depth. Thus, if the decrease in strength is progressive and without any discontinuity, the layer is considered balanced.

One way to measure and analyse the strength of different pavement layers, identify thickness, and location of underlying soil layers is by using the DCP. The DCP is a hand-held device (Figure 3-23) that consists of a steel hardened 60° cone fitted to the end of a 16 mm steel rod.

Conducting a DCP test involves repeated hammering to drive the cone on the lower shaft into the underlying pavement layers. Typically, after each hammer blow, the penetration of the cone is measured and recorded. The material's strength is determined by measuring the penetration of the lower shaft into the material after each hammed drop. This value is recorded in milometers per blow and is known as the DCP index (DPCI).

Two DCP tests were carried out in the selected subgrade in each of the inspection pits opened in both test sections T-I and T-II, totalling 8 tests. The tests were carried out in the selected subgrade to gauge the structural capacity of the pavement and to estimate in-situ materials properties.



Figure 3-23: Dynamic Cone Penetrometer (DCP) test

The visual representation of the progress made in penetration of the DCP through the pavement in both test sections are shown in Figure 3-24 to Figure 3-27.

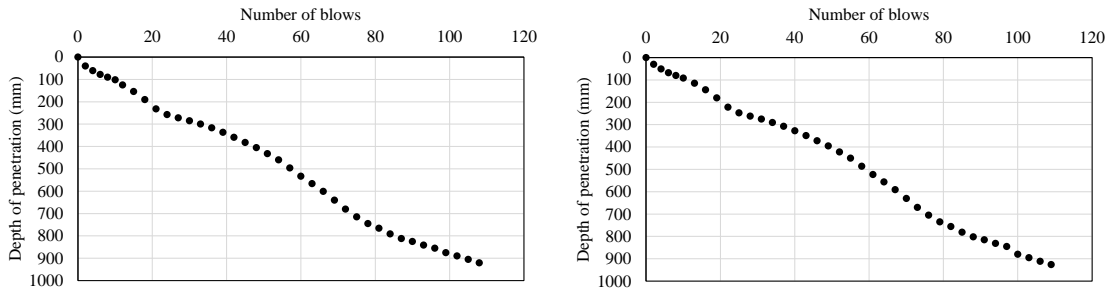


Figure 3-24: DCP field curves obtained in Test section I - IP-01

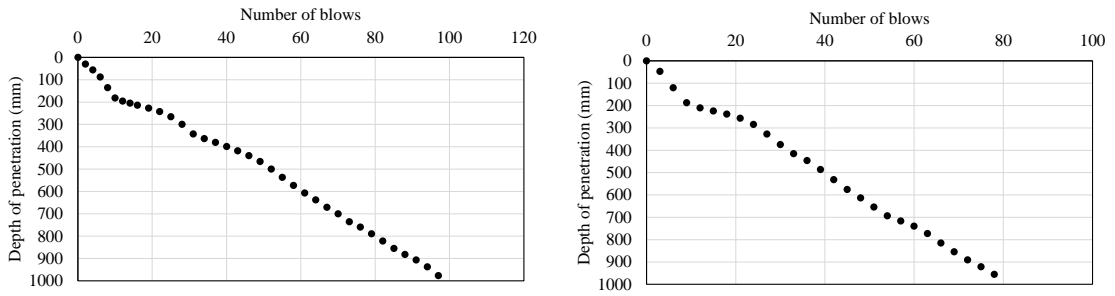


Figure 3-25: DCP field curves obtained in Test section I - IP-02

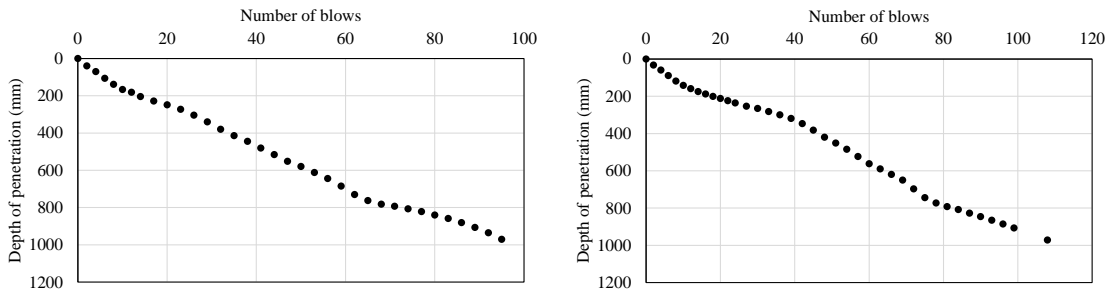


Figure 3-26: DCP field curves obtained in Test section II - IP-03

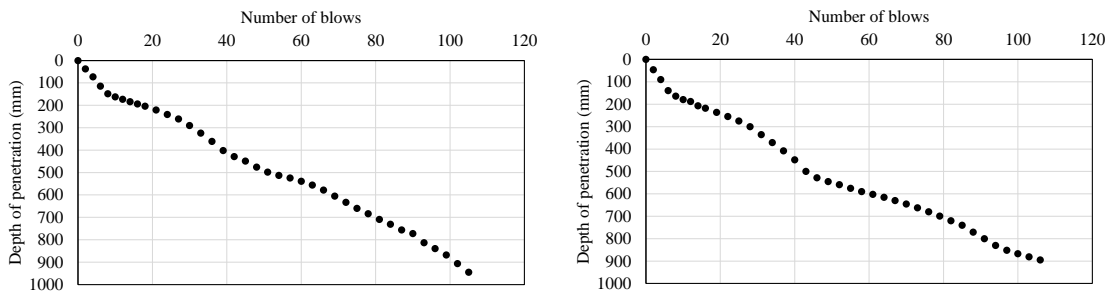


Figure 3-27: DCP field curves obtained in Test section II – IP-04

From the representation of the DCP field curve it is possible to visualize some slopes called DCP number (DN). The DN is defined as the penetration of the instrument through a specific pavement layer as measured in mm per blow. When the DN value is constant, it means uniform material properties. Its variation (slope) means a change in the property of the material (moisture content or its apparent specific mass) or a change of layer. The variations and analysis of strength are discussed in Chapter 6.

3.5 Laboratory tests carried out in the unbound base

As discussed in Section 2.2.3, 2.6.6 and 2.6.7, the unbound base layer plays a fundamental role in pavement behaviour, indicated by many researchers as a central component of the inverted pavement service life. Its modular variations in thickness are very dependent on the grading of crushed stone and moisture. Thus, besides the tests carried in-situ, gradation tests were carried out in the unbound base layer, as well.

3.5.1 Gradation Test

The gradation test is relatively simple, but it is one of the most important tests in road building. This test can compromise the structural behaviour of the work and cause results of compaction and strength to be indeterminable.

Materials were collected from the unbound base layer in both inspection pits in each test sections. Particle size distribution curves were obtained according to the procedures recommended by the specifications in DNER ME 080-94, in both section tests and are shown in Figure 3-28 and Figure 3-29.

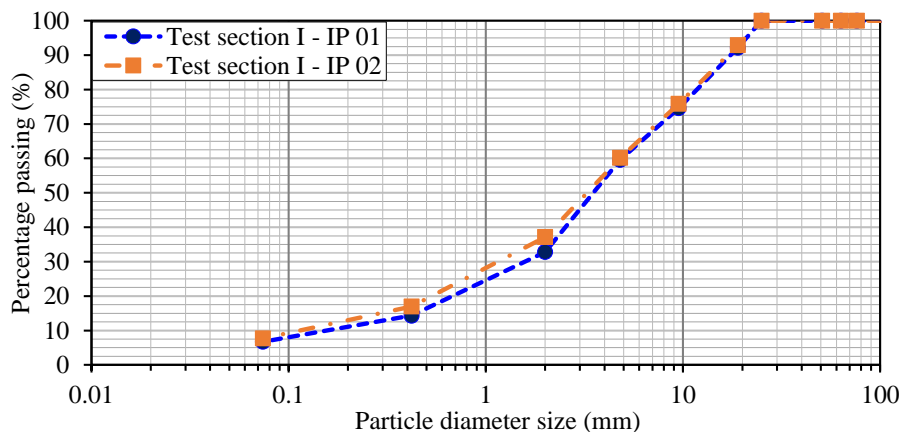


Figure 3-28: Particle size distribution curves obtained in T-I

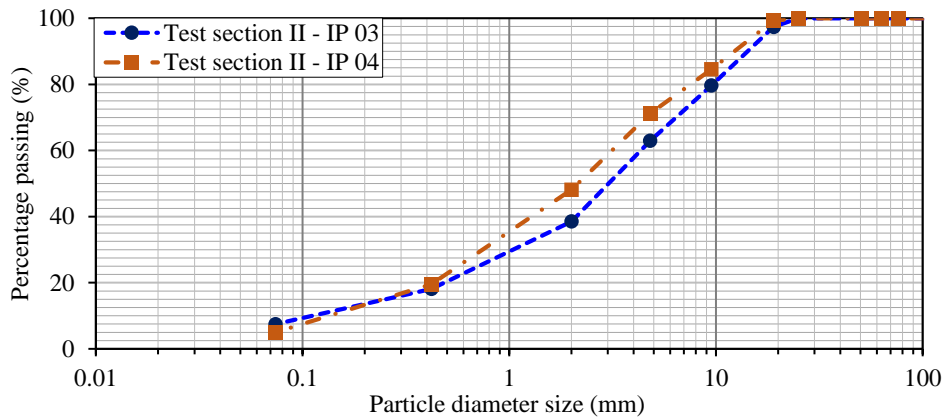


Figure 3-29: Particle size distribution curves obtained in T-II

3.6 Laboratory tests carried out in the cement-treated layer

All layers of the inverted pavement are important. Each one plays a different role and they need to work together for the pavement to behave properly under load over time. Therefore, as has been discussed in this document, many variables can compromise the behaviour of the cement-treated layer, and there are several ways to evaluate this performance. Some tests are more complex, others simple, but all of them give results, and these results need to be carefully evaluated.

In this section details the procedures followed during the performance of tests carried out in the cement-treated layer, as well as the results. It is important to note that some tests such as Dynamic Modulus and UCS tests were performed using the entire breadth of the specimens collected in the field. As discussed previously, the cement-treated layer found in T-II presented disaggregation in the last 30 mm in the bottom layer of both inspection pits so; the test results may not represent the real behaviour of the layer.

3.6.1 Dynamic Modulus

In this research, to obtain the dynamic moduli, the tests were performed according to the recommendations of AASHTO T 342-11. In this test, three Linear Variable Differential Transformers (LVDTs) were installed along the axial direction of the specimen to measure its displacements.

The specimens tested had a diameter of 100 mm and variable height (Table 3-14), according to the thickness identified in the field. The tests were conducted at a temperature of 21 °C and the loading frequencies were 25; 10; 5; 1; 0.5 and 0.1 Hz.

For verification purposes, two of the specimens collected from IP-03 and one from IP-04 were broken down before the end of the test. The additional Dynamic Moduli results obtained for the different loading frequencies are shown in Table 3-14. The analysis of the results is presented in Chapter 6.

Table 3-14: Dynamic moduli results obtained in both test sections

Test Section	Sample ID	Height (mm)	Diameter (mm)	Dynamic Modulus (MPa)					
				Reduced Frequency (Hz)					
				25	10	5	1	0.5	0.1
Section I IP-01	1	191.2	100.0	5 432	5 214	4 908	4 343	4 079	3 994
	2	197.6	100.0	5 401	5 236	4 863	4 301	4 071	4 008
	4	198.2	100.0	4 944	4 644	4 325	3 792	3 591	3 546
Section I IP-02	1	180.4	100.0	9 671	9 351	9 033	8 597	8 349	8 174
	3	178.2	100.0	9 385	8 883	8 415	7 760	7 465	7 253
	5	181.4	100.0	11 555	11 176	10 819	10 349	10 106	9 846
Section II IP-03	1	153.8	100.0	The sample was broken during the test					
	2	165.6	100.0	7 907	7 587	7 151	6 203	5 905	5 590
	4	160.2	100.0	The sample was broken during the test					
Section II IP-04	1	184.2	100.0	4 717	4 921	4 729	4 234	4 027	3 827
	3	175.6	100.0	The sample was broken during the test					
	5	167.8	100.0	4 649	4 727	4 572	4 296	4 043	4 361

3.6.2 Resilient Modulus

In this work, the obtainment of the resilient moduli of the cement-treated layer met the standardized specifications by DNIT 135/2010. The tests were conducted at a temperature of 25 °C. The load used was fixed at 1 000 N and the Poisson's Ratio was assumed to be 0.20.

In this test, two LVDTs were installed along the axial direction of the specimen to measure the displacements. The cylindrical specimens collected in both test sections had a slice of their length cut off, to meet the specifications of DNIT 135/2010. Thus, the test specimens had a diameter of 100 mm and height around 660 mm. The results obtained are shown in Table 3-15. The analysis of the results is presented in Chapter 6.

Table 3-15: Resilient moduli results obtained in both test sections

Location	Sample ID	Height (mm)	Diameter (mm)	Resilient Modulus (MPa)
Test Section I IP-01	3	63.6	100	13 205
	5	64.4	100	13 180
	6	65.0	100	10 762
Test Section I IP-02	2	66.1	100	13 037
	4	65.5	100	14 374
	6	65.9	100	4 879
Test Section II IP-03	3	66.1	100	5 938
	5	65.5	100	5 488
	6	65.3	100	5 971
Test Section II IP-04	2	67.5	100	8 101
	4	67.2	100	7 881
	6	67.3	100	8 719

3.6.3 Flexural Modulus

To obtain the Flexural Moduli for the cement-treated layer, prismatic specimens were extracted from each of the inspection pits, and then the specimens were cut so that the dimensions meet the specifications for carrying out the tests. The dimensions of the tested specimens varied around 100 mm x 100 mm x 400 mm as shown in Table 3-16. In this test, the recommendations made in ASTM C 1609 were followed.

In this test, the four-point flexural test was carried out. This test is very similar to the three-point bending flexural test (Recommended in ASTM C 1609), the principal difference is the addition of a fourth bearing. The portion of the beam between the two loading points is put under maximum stress, as opposed to only the material right under the central bearing as in the case of three-point bending. The results obtained are shown in Table 3-16. The analysis of the results is presented in Chapter 6.

Table 3-16: Flexural Modulus results obtained in both test sections

Location	Beam	Test Position	Height (mm)	Width (mm)	Length (mm)	Flexural Modulus (MPa)
Test Section I IP-01	1	A	100.5	100.5	378.0	14 480
	1	B				13 653
	2	A	106.2	95.3	400.0	8 270
	2	B				9 202
	3	A	101.5	107.9	418.0	11 975
	3	B				8 015
Test Section I IP-02	1	A	97.2	102.0	405.0	11 817
	1	B				11 747
	2	A	98.1	101.8	398.0	11 239
	2	B				11 183
Test Section II IP-03	1	A	94.3	114.3	400.0	7 519
	1	B				7 455
	2	A	103.3	111.8	395.0	6 013
	2	B				13 495
Test Section II IP-04	1	A	102.7	105.1	400.0	6 035
	1	B				4 368
	2	A	103.1	107.9	372.0	4 874
	2	B				6 301

3.6.4 Unconfined Compressive Strength

The UCS is normally used to fix the cement content necessary to meet the strength criteria of the cement-treated layer. The UCS tests were performed on the same specimens used to perform the dynamic modulus tests (discussed in Section 3.6.1). Thus, the specimens tested had a diameter of 100 mm and variable height (Table 3-17), according to the thickness identified in the field.

The procedure recommended by the ABNT NBR-5739 standard was employed, with a loading speed of (45 ± 15) MPa/s. Mindful that during the dynamic modulus test, two of the specimens collected from IP-03 and one from IP-04 were broken down during the test, the results are shown in Table 3-17. The analysis of the results is presented in Chapter 6.

Table 3-17: UCS results obtained in both test sections

Test Section	Sample ID	Height (mm)	Diameter (mm)	UCS (MPa)
Test Section I IP-01	1	191.2	100.0	2.46
	2	197.6	100.0	1.70
	4	198.2	100.0	2.22
Test Section I IP-02	1	180.4	100.0	2.61
	3	178.2	100.0	2.85
	5	181.4	100.0	2.68
Test Section II IP-03	1	153.8	100.0	The sample was broken during the test
	2	165.6	100.0	1.96
	4	160.2	100.0	The sample was broken during the test
Test Section II IP-04	1	184.2	100.0	1.83
	3	175.6	100.0	The sample was broken during the test
	5	167.8	100.0	2.68

3.6.5 Indirect Tensile Strength

The ITS of the cement-treated layer is considered as a significant material property for designing pavement structures, and tests such as Flexural Tensile Strength and Indirect Tensile Strength have been employed to evaluate the parameter of the cement-treated layer.

To obtain the ITS parameter, the same specimens used in the resilient moduli were employed, thus, the test specimens had a diameter of 100 mm and height around 660 mm (Table 3-19).

This test is practical, easy, economical and can be performed in almost all laboratories. The procedure recommended by the DNIT 136/2010 standard was employed, the breaking speed used was 1.27mm / min, usually used on other road materials. The results obtained are shown in Table 3-18. The analysis of the results is presented in Chapter 6.

Table 3-18: ITS results obtained in both test sections

Location	Sample ID	Height (mm)	Diameter (mm)	Tensile Strength (MPa)
Test Section I IP-01	3	63.6	100	0.55
	5	64.4	100	0.61
	6	65.0	100	0.65
Test Section I IP-02	2	66.1	100	0.62
	4	65.5	100	0.65
	6	65.9	100	0.41
Test Section II IP-03	3	66.1	100	0.56
	5	65.5	100	0.52
	6	65.3	100	0.54
Test Section II IP-04	2	67.5	100	0.59
	4	67.2	100	0.55
	6	67.3	100	0.62

3.6.6 Flexural Tensile Strength

For some researchers, the f_t parameter simulates the field conditions better than the test obtained through cylindrical specimens, as is the case of ITS. According to TRH13 (1986) the flexural test is sometimes preferred because it represents the condition of a cement-treated layer in the pavement when it is subjected to a wheel load.

To carried out the flexural tensile strength tests in this research, were used the same prismatic specimens to obtain the flexural moduli, following the same procedures recommended by ASTM C 1609. The results obtained are shown in Table 3-19. The analysis of the results is presented in Chapter 6.

Table 3-19: f_t results obtained in both test sections

Location	Beam	Test Position	Height (mm)	Width (mm)	Length (mm)	f_t (MPa)
Test Section I IP-01	1	A	100.5	100.5	378.0	0.88
	1	B				
	2	A	106.2	95.3	400.0	0.75
	2	B				
	3	A	101.5	107.9	418.0	0.67
	3	B				
Test Section I IP-02	1	A	97.2	102.0	405.0	1.40
	1	B				
	2	A	98.1	101.8	398.0	1.30
	2	B				
Test Section II IP-03	1	A	94.3	114.3	400.0	1.60
	1	B				
	2	A	103.3	111.8	395.0	1.60
	2	B				
Test Section II IP-04	1	A	102.7	105.1	400.0	0.80
	1	B				
	2	A	103.1	107.9	372.0	0.80
	2	B				

3.7 Laboratory tests carried out in the selected subgrade

This section details the procedures followed during the performance of tests carried out in the selected subgrade, as well as the results. Material was collected from the selected subgrade that made it possible to obtain the CBR, Atterberg limits, soil classification and resilient modulus.

Bearing in mind that the IP-01 located in T-I was the first inspection pit inspected in this research. Unfortunately, the company responsible for the collection of the samples did not have enough material to recompose the IP-01 after collecting the material from the selected subgrade layer, for this reason, the material was not collected and the expected tests for the IP-01 were not carried

out. Figure 3-31 shows the samples collected from the selected subgrade in IP-02, IP-03 and IP-04.



Figure 3-30: a) Selected subgrade samples collected from IP-02 b) Selected subgrade samples collected from IP-03 b) Selected subgrade samples collected from IP-04

3.7.1 California Bearing Ratio

Many pavement design procedures are based on subgrade support, as they directly affect the pavement design thickness, composition, and performance. Therefore, subgrade support is key for good performance of the pavement.

The CBR is one of the most common parameters around the world used in designing pavement, from that parameter it is possible to evaluate the extent of support provided by the material applied as subgrade and additional layers. To obtain the CBR values for both test sections, procedures recommended in DNER-ME 049/94 were followed. Normal Brazilian specifications were applied during the compaction of the specimen. The results are presented in Table 3-20. The analysis of the results is presented in Chapter 6.

Table 3-20: Bearing parameters obtained for the subgrade

Test	Test Section I		Test Section II	
	IP-01	IP-02	IP-03	IP-04
CBR %	-	16	58	28
Expansion %	-	0.1	0.2	0.1
Dry Density kg/m ³	-	1 833	1 934	1 954
Optimum Moisture Content %	-	14.8	10.9	10.5

3.7.2 Atterberg Limits

Water and traffic are a pavements' worst enemy. Understanding how the pavement behaves under these two variables is essential to ensure an appropriate service life for the pavement. Through

the Atterberg Limits, it is possible to analyse the behavioural changes of the soil when it is exposed to water. The Atterberg Limits measures the critical water contents that define transitions between the solid, plastic, and liquid states of given soil material. The points at which soil changes from one state to another are arbitrarily defined by simple tests called the Liquid Limit test and Plastic Limit test.

To obtain the Liquid Limit and Plastic Limit, procedures recommended by DNER ME-122/94 and DNER ME-082/94 were followed, respectively. The Plasticity Index is found by the difference of the Liquid Limit and the Plastic Limit. The results are present in Table 3-21. The analysis of the results is presented in Chapter 6.

Table 3-21: Atterberg Limits obtained for the selected subgrade

Test	Test Section I		Test Section II	
	IP-01	IP-02	IP-03	IP-04
Liquid Limit %	-	32	23	19
Plastic Limit %	-	17	12	13
Plasticity Index %	-	15	11	6

3.7.3 Resilient Modulus

The Resilient Modulus is one of the most critical variables to mechanistic pavement design. Though the Resilient Modulus is possible to characterize material under a variety of temperatures and stress states that simulate the conditions in a pavement subjected to moving wheel loads.

For the purposes of this research, the minimum and maximum Resilient Moduli were obtained at optimum moisture. The tests were carried out according to the procedures recommend in AASHTO-TP46 and AASHTO-T307. The results are shown in Table 3-22. The analysis of the results is presented in Chapter 6.

Table 3-22: Resilient Modulus for the selected subgrade

Test	Test Section I		Test Section II	
	IP-01	IP-02	IP-03	IP-04
Resilient Modulus (MPa)	-	146	51	97

3.7.4 Soil Classification

When soil classification is done it means that the soil has been separated into classes or groups, each one having similar characteristics and potentially similar behaviour. In the engineering of pavements, it is important and necessary to know which kind of soil has been used as a subgrade,

selected subgrade or in the further layers. From that knowledge, it is possible to predict behaviour and control the mechanical properties of the soil found in the field or chosen from a soil deposit.

In this research, the material inspected from the selected subgrade was classified through HRB-AASHTO, MCT (Miniature Compacted Tropical classification) and TRH14 methodologies. The HRB-AASHTO soil classification is broadly accepted, in its classification system the soil is divided into two large groups: Granular materials (A1 to A3 - 35 % or less passing the 0.075 mm sieve) and Silt-clay materials (A4 – A7 - >35 % passing the 0.075 mm sieve). According to the Mechanistic-Empirical Pavement Design Guide (2008) the materials classified between A1-A3 are most often used as subbase or as underlying layers and the materials classified between A4-A7 are most often used as subgrade.

The MCT classification is a method developed especially for tropical soils and is for this reason well applied in Brazil. According to Santos (2006), due to the MCT Classification, soils traditionally considered unsuitable for use in paving works have been able to have their geotechnical properties reassessed and thus be successfully used as base material, sub-base and sub-grade of many Brazilian pavements. The MCT classification divides the soil into two principal groups: lateritic soils (L) and non-lateritic soils (N). DER / SP (2006a) recommends that the soils appropriate for the selected subgrade have lateritic behaviour (LA, LA' and LG ') of the MCT classification, proposed by Nogami and Villibor (1995).

In South Africa, the TRH14 classification system is widely used. In the TRH14 system, the untreated or granular materials are classified as: Graded crushed stone (G1, G2 and G3), Natural gravels (G4, G5 and G6), Gravel-soil (G7, G8, G9 and G10), waterbound macadam and Dump rock. TRH14 (1985) presents where the materials are most often used in the layers in the pavement. According to Guidelines (TRH14, 1985), G5 and G6 are used as a subbase, G6, G7, G8 and G9 are used as a selected layer and G8, G9 and G10 as a subgrade.

In the HRB-AASHTO classification, procedures recommended in AASHTO M-145/91 were followed and for the MCT classification, procedures recommended in DNER-ME 259/96 were followed. The TRH14 classification followed the requirements on materials contained in Appendix A of Chapter 4 SANRAL (2014). The results obtained are shown in Table 3-23. The analysis of the results is presented in Chapter 6.

Table 3-23: Soil classification for the selected subgrade

Test	Test Section I		Test Section II	
	IP-01	IP-02	IP-03	IP-04
HRB-AASHTO Soil Classification	-	(A-6) - IG (5)	(A2-4) - IG (0)	(A2-6) - IG (0)
MCT Soil Classification	-	LG'	NA'	NA'
TRH14 Classification	-	G7	G6	G6

3.8 Tests carried out during quality control in 2001

The test sections studied in this research are located along Bandeirantes Highway (SP-348), as mentioned in Section 3.1. Due to the extension of the highway, the construction was divided into lots, and, the test sections were located in different lots. Thus, the construction and consequently the quality control was carried out by different companies.

This section presents the results of quality control performed in both tests sections. It should be noted that the test results presented in this dissertation do not fully represent the quality control performed during the construction of both test sections. CCR Engelog provided all files related to the tests carried out during the quality control, but some of them were damaged over to time.

3.8.1 Deflectometry control recommended in the Technical Design Report

According to the Technical Design Report (MC-01.348.000-0-P00_003-R0, 2000), the company responsible for designing the pavement structures of both test sections, recommended a deflectometry control for the execution of each layer (Figure 3-32). As discussed in Section 2.5.8, the deflectometry control has been employed in quality control during the construction of new pavements.

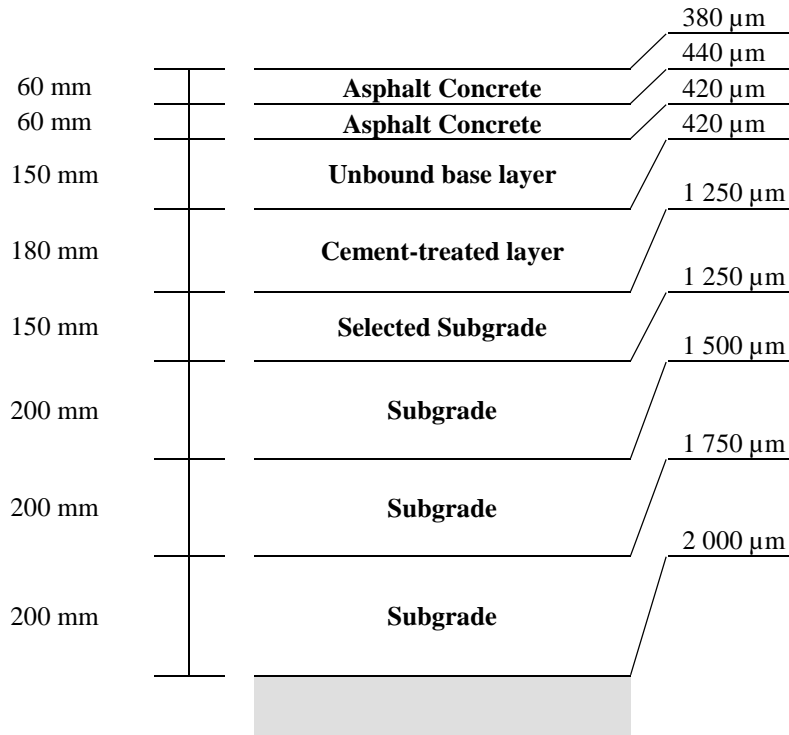


Figure 3-31: Deflectometry control recommended during the construction of both test sections

3.8.2 Deflectometry performed in the Quality Control

During quality control, deflections were measured at the top of each layer using a Benkelman Beam. At that stage of quality control, the main goal was to reach the deflection level recommended by the designer (Figure 3-31). The deflections were measured every 20 meters in the right wheel path, centre line, and left wheel path (Figure 3-32). The highest deflection obtained in each point of measurement was noted. The average of the deflections measured, the standard deviation and the coefficient of variation for each layer in both test sections T-I and T-II are shown in Table 3-24.

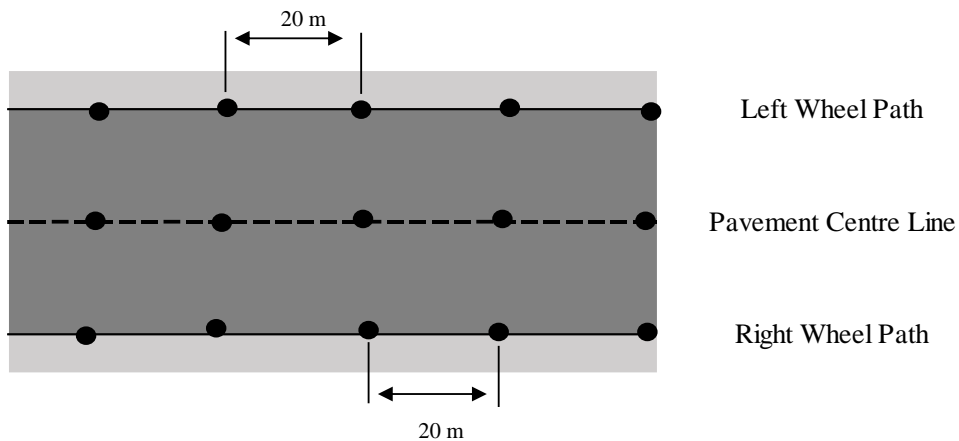


Figure 3-32: Deflection measurement Locations

The deflections obtained at the top of the subgrade were measured in the last layer of earthworks. As mentioned in Section 3.1 the subgrade of both test sections was ripped and recompact in three layers of 200 mm thick each.

Table 3-24: Deflections measured at the top of each layer

Layer	Test Section	Average Deflection (μm)	Standard deviation (μm)	Coefficient of Variation
Asphalt	I	220	55	25 %
Asphalt Concrete	II	280	58	21 %
Base	I	250	71	28 %
Unbound base layer	II	310	73	24 %
Subbase	I	150	23	15 %
Cement-treated layer	II	410	167	41 %
Selected Subgrade	I	420	109	26 %
	II	560	108	19 %
Subgrade	I	420	123	29 %
	II	890	108	12 %

3.8.3 Compaction

During quality control tests were carried out using the Sand-Cone Method. The tests were carried out in the unbound base layer, cement-treated base layer, selected subgrade and subgrade. Results obtained from the tests during the construction process are shown in Table 3-25 for both test section T-I and T-II.

Table 3-25: Test results obtained in-situ by the sand-cone method during the quality control

Layer	Test	Test Section I			Test Section II		
		Average	σ	CV	Average	σ	CV
Subgrade	Moisture Content %	17	0.2	1 %	13	4.3	33 %
	Bulk Density kg/m ³	2 106	6.1	0 %	2 163	53.6	2 %
	Dry Density kg/m ³	1 793	1.5	0 %	1 915	116.3	6 %
	Optimum Moisture Content % (Laboratory)	17	0.3	2 %	13	3.6	28 %
	Dry Density kg/m ³ (Laboratory)	1 760	1.2	0 %	1 894	125.4	7 %
	Compaction Degree %	102	0.6	1 %	101	0.6	1 %
Selected Subgrade	Moisture Content %	18	1.2	7 %	10	1.1	11 %
	Bulk Density kg/m ³	2 160	37.5	2 %	2 163	7.8	0 %
	Dry Density kg/m ³	1 835	1.4	0 %	1 915	16.3	1 %
	Optimum Moisture Content % (Laboratory)	17	0.0	0 %	10	1.1	10 %
	Dry Density kg/m ³ (Laboratory)	1 807	38.2	2 %	1 968	19.8	1 %
	Compaction Degree %	101	0.3	0 %	100	0.0	0 %
Subbase	Moisture Content %	9	0.4	4 %	8	0.1	2 %
	Bulk Density kg/m ³	2 608	30.2	1 %	2 467	13.6	1 %
	Dry Density kg/m ³	2 402	23.9	1 %	2 284	11.7	1 %
Cement-treated layer	Optimum Moisture content % (Laboratory)	9	0.0	0 %	8	0.0	0 %
	Dry Density kg/m ³ (Laboratory)	2 378	0.0	0 %	2 237	0.0	0 %
	Compaction Degree %	100	0.3	0 %	102	0.4	0 %
Base Layer	Moisture Content %	8	0.5	7 %	8	0.3	4 %
	Bulk Density kg/m ³	2 579	47.2	2 %	2 534	21.0	1 %
	Dry Density kg/m ³	2 399	33.4	1 %	2 355	15.1	1 %
Unbound base layer	Optimum Moisture Content % (Laboratory)	8	0.0	0 %	8	0.0	0 %
	Dry density kg/m ³ (Laboratory)	2 362	0.0	0 %	2 336	0.0	0 %
	Compaction Degree %	102	1.5	1 %	101	0.6	1 %

3.8.4 Cement Content

According to the quality control provided, the cement content used in the cement-treated layer of the T- I varied between 2.8 % and 3.2 %. Information related to the cement content adopted in the cement-treated layer was not found in files related to T-II. However, it is believed that the same content used in T-I was used in T-II.

It should be reiterated once again that the results presented in this research do not fully represent the test performed during the quality control of both test sections. Some parts of the results were lost or damaged over to time.

3.8.5 Unconfined Compressive Strength and Indirect Tensile Strength

As part of the quality control, samples were collected in the cement-treated layer to obtain information of strength in-situ of the cement-treated layers. The collected samples were ruptured 7 and 28 days after their collection. The results of the UCS and ITS are shown in Table 3-26. The results were obtained in the intermediate energy.

Table 3-26: UCS and ITS test results obtained during the quality control

Test Section	Cement Content %	UCS (MPa) 7 days			USC (MPa) 28 days			ITS (MPa) 28 days		
		Average	σ	cv	Average	σ	cv	Average	σ	cv
I	2.8	3.62	0.01	0%	5.4	0.3	6%	0.95	0.02	2%
	3.1	3.56	1.12	31%	5.4	0.4	7%	0.90	0.07	8%
	3.2	4.30	0.33	8%	6.6	0.3	5%	1.12	0.02	2%
II	-	3.26	0.27	8%	5.1	0.3	5%	0.71	0.01	2%

3.8.6 Curing

The analysis of curing time in quality control is fundamental to understanding the behaviour of the layers individually and of the pavement as a whole. For many researchers, knowledge about the curing time is essential, since different curing times provide different strengths, as discussed in Sections 2.3.7 and 2.6.7.

According to the results provided, it was not possible to find information regarding curing bitumen emulsions or curing time in general. Nevertheless, from the deflectometry control performed on each of the layers, it is possible to make assumptions about the release time of the layers, since the deflectometry control is done on top of the compacted layer. Furthermore, according to DER (2005c), in the cement-treated layer, deflection measurements with Benkelman beam or FWD must be performed after 28 days of curing. Although, in Brazil the practice of performing deflectometry measurements after 7 days of curing quite common.

Table 3-28 shows the dates that deflectometry control was performed on top of each layer in both test sections.

Table 3-27: Deflectometry control date carried out in both test sections

Layer	Test Section	Deflection control date
Asphalt	I	17/09/2001
Asphalt Concrete	II	14/10/2001
Base	I	19/07/2001
Unbound base layer	II	13/09/2001
Subbase	I	28/06/2001
Cement-treated layer	II	28/08/2001
Selected Subgrade	I	20/06/2001
	II	21/07/2001
Subgrade	I	28/06/2001
	II	13/07/2001

4. ANALYSIS OF THE PAVEMENT PERFORMANCE OF BOTH TEST SECTION

This chapter details the analysis of the results of the deflections obtained in 2001 during the quality control of both test sections as well as the deflections measured between 2003 and 2016 during the pavement monitoring. In 2001, deflections were measured at the top of each layer using Benkelman Beam, whereas FWD equipment was used for the measurements carried out between 2003 and 2016 as shown in Sections 3.2.1 and 3.8.2.

This chapter also presents a parametric numerical study, where the main objective was to understand the interdependence of the variation of the thickness and modulus in the performance of inverted pavements.

As a general comment, during the analysis of the deflection measurements carried out using FWD, a change in the structural behaviour of the pavements was noticed in the measurements made in 2012 and 2016. For these behavioural changes, the following comments can be made:

- Between 2010 and 2011, periodical maintenance was carried out on the lots in which the test sections were inserted, which justifies the changes of the structural condition of the pavements in both test sections reported in the deflectometry data in 2012, and
- In 2015, both test sections presented permanent deformations. In T-I, 50 % of the asphalt concrete layer surface was replaced. The replacement was done of the upper 70 mm of the surface. In T-II, 100 % of the asphalt concrete layer was replaced, including the whole asphalt concrete surface (140 mm).

4.1 Analysis of back-calculation modulus

In this research, the back-calculation of both pavement structures was performed with the Elsym-5. In the back-calculation process, the maximum error allowed was 10 % between the measured and calculated deflection bowls, and the structures identified in IP-02 (Test Section I) and IP-03 (Test Section II) were adopted.

Furthermore, as discussed in Section 3.3, the last 30 mm in the bottom of the cement-treated layer presented disaggregation, therefore the cement-treated layer of test section II was not working to its full thickness. Thus, in the back-calculation process, the 30 mm disaggregated were disregarded from the analysis, to avoid false results. According to Von Quintus and Killingsworth,

(1997) 10 % difference in thickness can result in more than a 20 % change in the calculated modulus.

The structures and Poisson's Ratios adopted are shown in Table 4.1. The adoption of Poisson's Ratio is in accordance with the values normally used for Brazilian materials, as presented in the Literature Review carried out in this work (Chapter 2). In addition, in the back-calculation process, the subgrade and the selected subgrade were treated as a unique layer, reducing the number of interactions and increasing the reliability of the back-calculated modulus.

Table 4-1: Structure and Poisson's Ratio adopted in the back-calculation process

Layer	Test Section I	Test Section II	Poisson's Ratio
	Thickness (mm)		
Asphalt Surface Layer Asphalt Concrete	140	140	0.30
Base Layer Unbound base layer	90	120	0.35
Subbase Cement-treated layer	180	150*	0.25
Selected Subgrade + Subgrade	Semi-infinite	Semi-infinite	0.40

*Intact thickness identified in the inspection pits.

In the back-calculation process, thousands of structures were simulated, varying the modulus intervals until finding the best fit between the measured deflection bowls and the simulated deflection bowls. During the back-calculation process it was observed that:

- The infrastructure equivalent modulus (selected subgrade + subgrade) contributes much more to obtain the cement-treated modulus than to obtain the asphalt concrete modulus;
- The subgrade or infrastructure equivalent modulus is independent. The layers above the infrastructure contribute almost nothing in obtaining the subgrade modulus;
- The elastic behaviour of the cement-treated layer is dependent on the support of the underlying layer;
- The modulus of the unbound base layer varies depending on the modulus of the cement-treated layer and the asphalt concrete, mainly as a function of the cement-treated layer modulus because it is directly supported;
- The asphalt concrete modulus depends directly on the unbound base layer modulus;
- The elastic behaviour of the structure as a whole is interdependent. The elastic behaviour of the layers is conditioned by the support of the layer immediately below, and

- Different combinations of moduli can result in the same deflection bowl.

Figures 4-1, 4-2, 4-3 and 4-4 show the back-calculated moduli obtained for the test sections T-I and T-II. For the sake of comparison, the elastic moduli considered in the pavement design of the test sections were added. To facilitate the analysis between the back-calculated moduli and the design moduli, the equivalent design modulus for the infrastructure (selected subgrade + subgrade) was calculated for both test sections.

In general, from the back-calculations of the infrastructure of both sections (Figure 4-1), it can be concluded that:

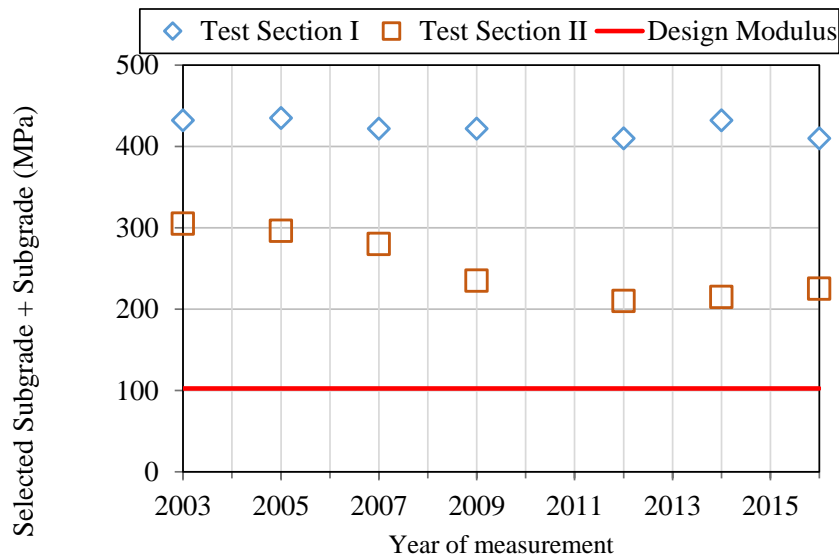


Figure 4-1: Back-calculated moduli of the infrastructure layers of both test sections

- The bearing capacity of the infrastructure of both test sections T-I and T-II is above of the projected capacity, and therefore the central deflections of both sections are still low for the traffic active after 15 years of service;
- The infrastructure of T-I presents a much better bearing capacity than the infrastructure of T-II. The differences in the elastic behaviour of both test sections reached almost 100 % from 2009, and
- The elastic behaviour of the infrastructure of T-I is practically homogeneous and stable over the years. In T-II, the infrastructure moduli present a heterogeneous behaviour with a tendency to decrease over the years.

Among the many factors that can be linked to the performance differences of both test sections, the difference in the support capacity of the infrastructure may be a conditioning factor. As discussed in the Literature Review (Chapter 2), Papadopoulos and Santamarina (2017), Adaska and Luhr (2004) and SANRAL (2014) emphasise the importance of a good support capacity of the infrastructure layer for good performance of the pavement as a whole. Le Coz and Paute (1978) mentioned in Balbo (1993), Balbo (1993), and Austroads (2017) the importance of the support of the infrastructure for the performance of the upper layer, especially in the case of cement-treated layers.

In general, from the back-calculation of the cement-treated layers (Figure 4-2) of both sections, it can be concluded that:

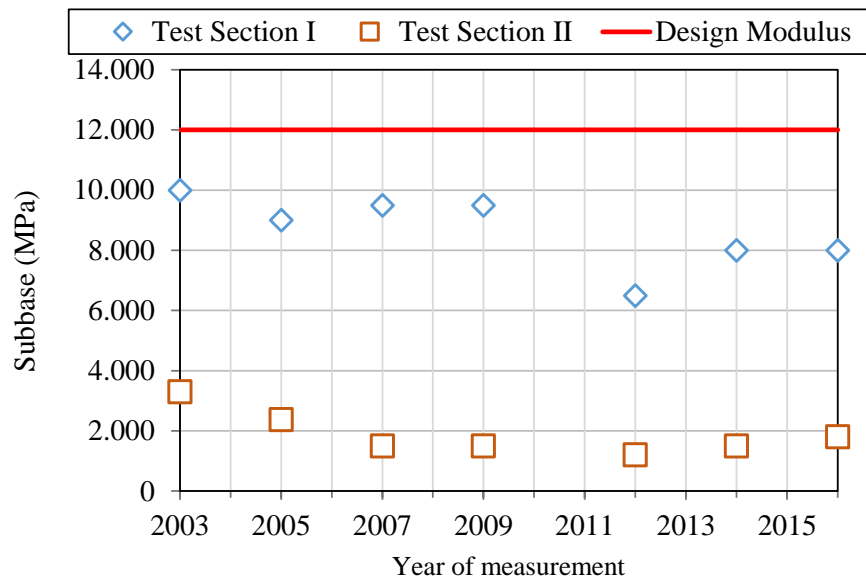


Figure 4-2: Back-calculated moduli of the cement-treated layers of both test sections

- a) The back-calculated moduli obtained for both test sections show a huge discrepancy. In T-I, the back-calculated moduli remain constant until 2009, presenting an elastic behaviour close to what was projected in the pavement design. Changes in the elastic behaviour of the cement-treated layer in 2012 and 2016 may reflect the maintenance actions carried out in 2010-2011 and 2015 as previously discussed, and
- b) During the first year of monitoring, in 2003, the cement-treated layer of T-II already presented a modular performance well below projections, and this performance continued to drop over the years. Changes in the elastic behaviour of the cement-treated layer in 2012 and 2016 in T-I was also noted.

In general, from the back-calculations of the unbound base layers (Figure 4-3) of both sections, it can be concluded that:

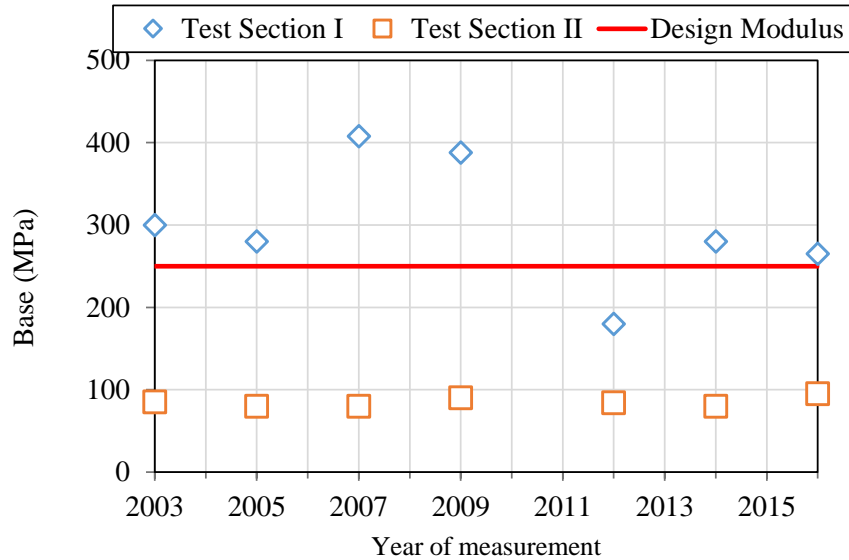


Figure 4-3: Back-calculated moduli of the unbound base layers of both test sections

- a) In T-I, the elastic behaviour of the unbound base follows the same oscillatory trend observed in the behaviour of the cement-treated layer (Figure 4-2). In other words, as the cement-treated layer modulus increases, the unbound base modulus increases, as the cement-treated layer modulus decreases, the unbound base modulus decreases;
- b) In T-I, the unbound base moduli performed better than the designed modulus in almost every years, except in 2012. It is also noticed that the granular behaviour of the unbound base did not vary significantly over the years since the cement-treated layer offers the necessary support for the proper functioning of the layer, and
- c) In T-II, the unbound base presents a stable and less than expected behaviour over the years, giving the impression that the underlying layer (cement-treated layer) does not provide the unbound base with the minimum level of tension for it to perform in its state of confinement.

In general, from the back-calculation of the asphalt concrete layers (Figure 4-4) of both sections, it can be concluded that:

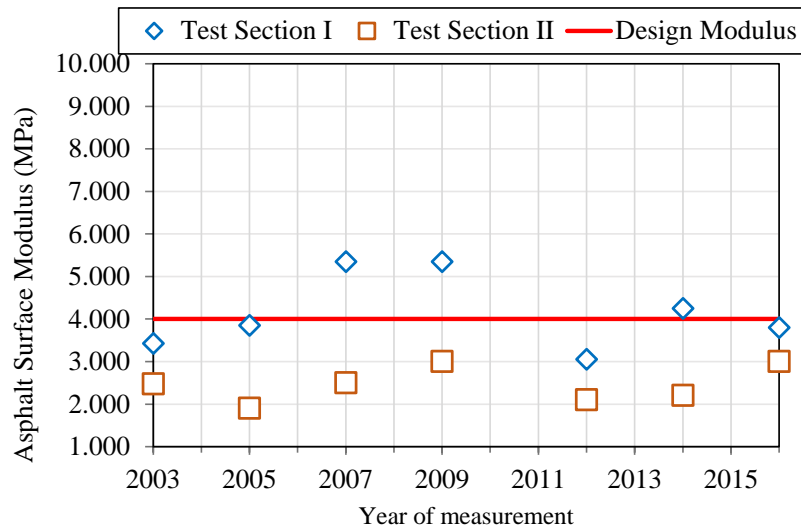


Figure 4-4: Back-calculated moduli of the asphalt concrete layers of both test sections

- a) In T-I, the asphalt concrete layer, in general, presents the expected modular behaviour and even better than expected in the pavement design. The moduli of the asphalt layer vary in accordance with the variation of the unbound base (Figure 4-3) in all the years analysed;
- b) In T-II, in contrast to the T-I, presents a modular behaviour below that expected in the design. The modular behaviour of T-II does not vary in accordance with the unbound base, but with the cement-treated layer (Figure 4-2), and
- c) In T-II, the support offered to the asphalt concrete layer by the unbound base seems neutral; it is as if the asphalt concrete layer was directly supported by the cement-treated layer.

4.2 Analysis of deflection bowl parameters

The deflection bowl parameters for both test sections were calculated. The deflection bowl parameters were associated with the back-calculated moduli of the respective layers. The assessment criteria of cement-treated layers are in accordance with Table 2-25 (Chapter 2).

The applicability of deflection bowl parameters in assessing the structural condition of Brazilian inverted pavements was discussed in Section 2.6.2. From the analysis of the Figures (from 4-5 to 4-7) it is possible to identify a good correlation between the back-calculated moduli and the deflection bowl parameters. As the deflection bowl parameters increase, the moduli decrease. This behaviour was observed in all analyses.

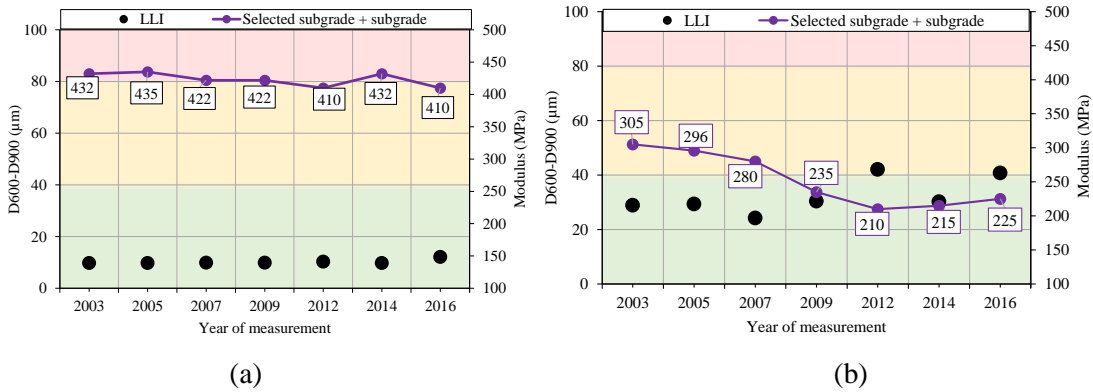


Figure 4-5: a) T-I - LLI parameters and infrastructure moduli, and b) T-II - LLI parameters and infrastructure moduli

The structural condition indicators (Modulus and LLI) of the infrastructure layers (Figure 4-5) present great disparities in both test sections. The LLI parameters obtained for the T-I show homogeneous behaviour and a “sound” classification in all years of analysis, whereas the LLI parameters obtained for the T-II, in addition to being superior to the parameters obtained for the T-I present heterogeneity and a growth trend over the years, reaching the “warning” region in 2012.

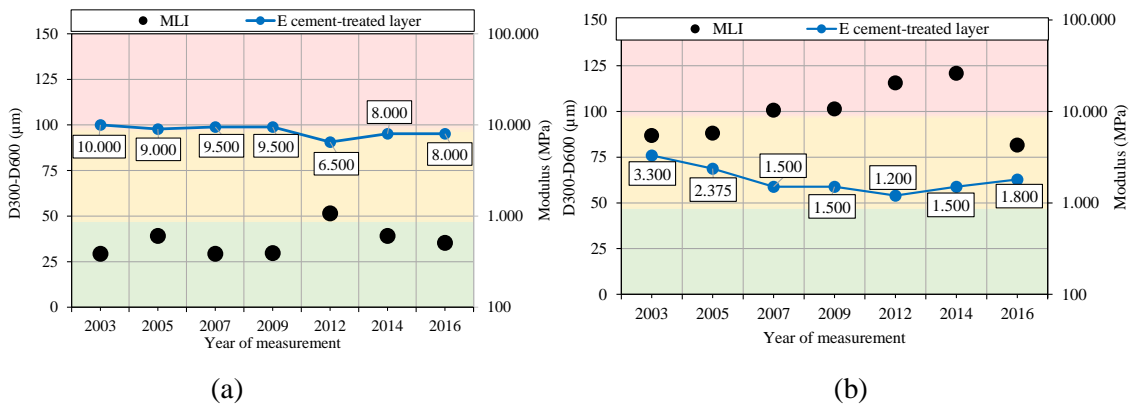


Figure 4-6: a) T-I - MLI parameters and cement-treated layer moduli, and b) T-II - MLI parameters and cement-treated layer moduli

The elastic behaviour of the cement-treated layer of T-I remains “sound” in practically all years of analysis (Figure 4-6.a) and within the limit of “sound” and “warning” in 2012. On the other hand, the elastic behaviour of the cement-treated layer of T-II (Figure 4-6.b) denotes a gradual loss of structural capacity since it was first monitored in 2003. The poor structural condition of T-II was also verified during the extraction of the specimens and found to present disaggregation in the last 30 mm of the bottom layer as previously discussed. The structural gain observed in

2016, as previously discussed, may be associated with the actions of rehabilitation carried out in the section under study.

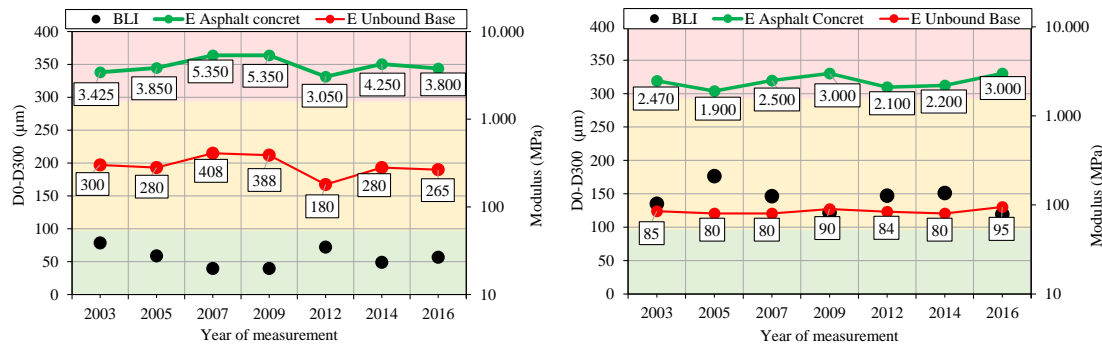


Figure 4-7: a) T-I - BLI parameters and asphalt concrete and unbound base moduli and b) T-II - BLI parameters and asphalt concrete and unbound base moduli

In Figure 4-7, the BLI parameter was associated with the back-calculated moduli of the asphalt concrete layer and unbound base, since it was verified that the modular performance of the asphalt concrete is directly linked to the integrity of the underlying layer.

In T-I, all calculated parameters were less than 100 μm, indicating a good structural condition, while the minimum modular values corresponded to 3 050 MPa and 180 MPa for the asphalt concrete and unbound base, respectively. In T-II, the BLI parameter calculated for all years was found to be in the ‘warning’ region, and the moduli of both the asphalt concrete and unbound base presented much lower levels than the moduli considered in the design.

4.3 Analysis of the cement-treated layer moduli as a function of traffic

As shown in Section 3.2.2, traffic in T-II is around 30 % higher than traffic in T-I, these differences were observed since the year of traffic opening in 2001. From the traffic data analysed, it was found that the Numbers “N” calculated using the USACE methodology were 37 % higher than the Numbers “N” calculated using the AASHTO methodology, with a standard deviation of less than 2 %.

In order to analyse the behaviour of cement-treated layers as a function of time (traffic), the deflection measurements obtained in 2012 in T-I and 2016 in T-II were not considered because they present dispersions in relation to the other years due to the actions of maintenance that preceded the measurements in the years mentioned.

From the back-calculated moduli obtained year by year, it was possible to describe the behaviour of cement-treated layers as a function of traffic through functions (Figure 4-8). In T-I, the function

that best described the behaviour of cement-treated layers effective modulus as a function of traffic was the Linear Function. In the Linear Function, when the rate of change is constant, it results in an $R^2 = 1$ or -1 . In T-I, the R^2 is equal to 0.814 indicating a reasonable constancy in the rate of change of effective modulus of the cement-treated layer as a function of time.

In T-II, the function that best describes the behaviour of the cement-treated layers as a function of traffic was the Exponential Function. The Exponential Function describes the exponential decay of the cement-treated layer as a function of the traffic, where the rate of change in the exponential function is the exponential function itself.

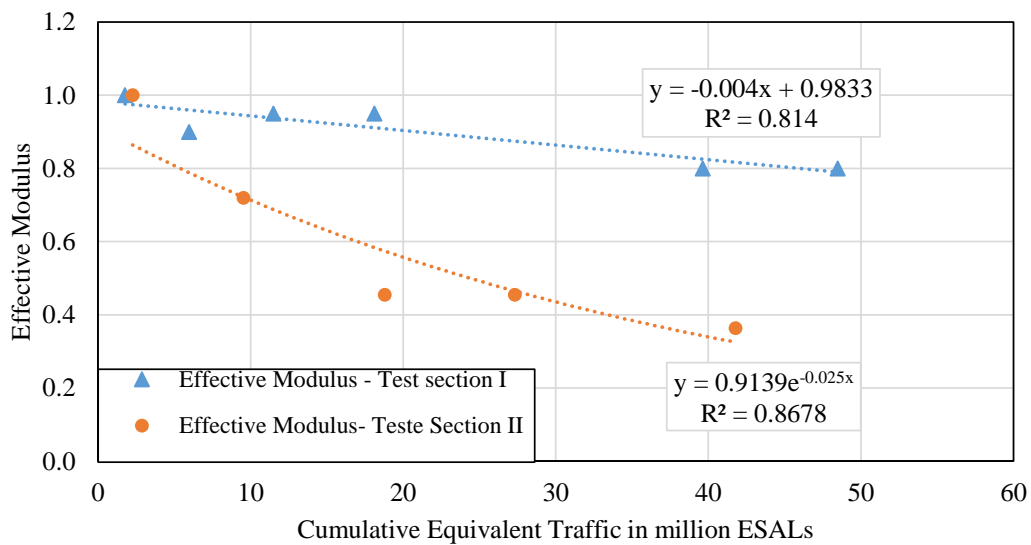


Figure 4-8: Analysis of the integrity of the cement-treated layer as a function of traffic

As discussed in Section 2.4.1, the effective modulus of the cement-treated layer changes over time, presenting three distinct and defined phases. It is not known when the transition through these phases happens exactly, however, once the integrity of the cement-treated layer is compromised, the degradation process of the cement-treated layer is accelerated exponentially due to traffic, as shown in Figure 4-8.

From analysis of Figure 4-8 it does not seem like the cement-treated layer of T-II underwent a natural process of degradation due to traffic. Its signalled behaviour gives the impression that this layer has been exposed to traffic for a much longer period. This level of exposure is not possible since both test sections were built in the same year and the acting loads are not very different. Failure in the design of the cement-treated mixture, associated with executive techniques and low support capacity of the underlying layer may be responsible for the behaviour observed.

4.4 Analysis of deflections obtained during quality control

To analyse the deflections measured at the top of the layers of both test sections during quality control, the individual structural gain of each layer was evaluated. Table 4-2 shows the structural gains predicted by the company responsible for the dimensioning of the test sections, and structural gains actually achieved when the test sections were built.

Table 4-2: Structural gains obtained in the deflectometry measurement

Layer	Deflectometry Control recommended for both test sections		Deflectometry Control obtained			
			Test Section I		Test Section II	
	Deflection (μm)	Structural gain	Deflection (μm)	Structural gain	Deflection (μm)	Structural gain
Asphalt Concrete	380	10 %	220	12 %	280	10 %
Unbound base	420	0 %	250	-67 %	310	24 %
Cement-treated layer	420	66 %	150	64 %	410	27 %
Selected Subgrade	1 250	17 %	420	0 %	560	37 %
Subgrade	1 500	-	420	-	890	-

The deflectometry control recommended by the company predicted a 17 % structural gain after the construction of the selected subgrade. In T-I, there was no improvement after the construction of this layer, since the deflections measured in both subgrade and selected subgrade were 420 μm . In T-II, 37 % was gained after the construction of the selected subgrade.

The largest structural gain, 66 %, was predicted for the cement-treated layer. In T-I, structural gain reached was 64 %, being very close to gain the predicted, which may indicate that mechanical properties predicted in the design of the cement-treated layer were achieved in the field. In T-II, the structural gain of the cement-treated layer represents 27 % in relation to the underlying layer, which is even lower than the structural gain achieved with the construction of the selected subgrade.

For the unbound base, no structural gains were foreseen in the project. However, a structural loss was expected, because the pavement would become unbalanced if constructed with a modulus much lower than the modulus in the underlying layer. This structural loss is identified in T-I, where there is a 67 % structural reduction in relation to the previous layer. In T-II, this structural loss was not identified, meaning that the underlying layer does not provide the necessary support for the pavement to be unbalanced.

For the asphalt concrete layer, the expected structural gain was 10 % in relation to the remaining structure. In both test sections this gain was achieved, being 12 % in T-I and 10 % in T-II.

When building a new pavement, the concern of the supervision team is to obtain deflections lower than the deflection level recommended by the designer, often focusing only on the deflections measured at the top of the asphalt concrete layer. However, more important than the punctual assessment of the deflections obtained is to analyse whether the individual structural gain expected in the project is being achieved in the field. When individual structural gains are achieved in the field it means that the resistance parameters considered in the project have also been achieved.

To better understand the individual structural gains of each of the layers of the test sections, equivalent moduli were calculated for the remaining layers as a function of the deflection measured at the top of the layers. To find the correlation (Equation 4.1) of the equivalent modulus as a function of the deflection measured at the top of the layer, 601 structures were simulated in Elsym5. In the simulations, the structures had homogeneous, isotropic and semi-infinite characteristics. The range of moduli varied from 20 MPa to 320 MPa, considering a step of 0.5 MPa. The Poisson's Ratio used in the analysis was 0.40. The structures simulated and their outcomes are attached in Appendix A.

$$E_{Eq} = 12\,669D^{-1} \quad (R^2=1) \quad \text{(Equation 4.1)}$$

Where:

E_{Eq} : Equivalent modulus

D: Deflection measured at the top of the layer

The individual structural gains obtained through the analysis of equivalent moduli (Table 4-3) were the same as those obtained in the analysis of deflections (Table 4-2), thus showing the confidence in the Equation 4.1 application.

Table 4-3: Structural gain obtained through the equivalent modulus

Layer	Resilient Parameters recommended for both test sections		Resilient Parameters obtained			
			Test Section I		Test Section II	
	Equivalent Modulus (MPa)	Structural gain	Equivalent Modulus (MPa)	Structural gain	Equivalent Modulus (MPa)	Structural gain
Asphalt Concrete	333	10 %	575.9	12 %	452.5	10 %
Unbound base	302	0 %	506.8	-67 %	408.7	24 %
Cement-treated layer	302	66 %	844.6	64 %	309.0	27 %
Selected Subgrade	101	17 %	301.6	0 %	226.2	37 %
Subgrade	85	-	301.6	-	142.3	-

From analysis of the individual structural gain of the layers of the pavements of the test sections, the following statements can be concluded:

- a) The performance of the cement-treated layer is highly dependent on the support of the underlying layers. The cement-treated layers, both projected and executed in the T-I present practically the same individual structural gains, but with completely divergent equivalent moduli, and this behaviour may be attributed to the difference in support from the underlying layers;
- b) Similar equivalent moduli can mean different structures and performances. The structures of T-I and T-II showed different levels of structural gains and, consequently, different equivalent moduli, however, the final equivalent moduli are of a similar order. This behaviour may be attributed to the fact that in T-I there was a gain (execution of the cement-treated layer) and loss (execution of the unbound base), whereas in T-II the gains, even if not foreseen, were small and gradual resulting in similar equivalent moduli, and
- c) Although the differences between the final equivalent modulus expected in design and obtained in T-I are clear, the individual structural gain of the layers is similar. The individual structural gain of T-II is completely different from what was designed.

Another important factor that must be observed during deflectometry control is the variation coefficient obtained during the tests for each layer. The coefficient of variation is a measure of dispersion and provides the variation of the data obtained in relation to the average; that is, the lower the coefficient of variation, the more homogeneous the sample is. The coefficients of variation obtained during the quality control of both test sections are shown in Table 4-4.

Table 4-4: Coefficient of variation obtained during deflectometry control

Layer	Test Section	Coefficient of variation
Asphalt	I	25 %
Asphalt Concrete	II	21 %
Base	I	28 %
Unbound base	II	24 %
Subbase	I	15 %
Cement-treated layer	II	41 %
Selected Subgrade	I	26 %
	II	19 %
Subgrade	I	29 %
	II	12 %

For some mathematicians, a data set is considered homogeneous when the variation coefficient is less than or equal to 25 %, for others this limit can be extended to 30 %. However, with the homogeneity limit ranging between 25 % or 30 %, the variation coefficient obtained for the cement-treated layer of T-II was 41 % (Table 4-4), leading to the conclusion that this layer showed the most variations in the results obtained.

4.5 Analysis of the influence of thickness and modulus in the performance of the inverted pavement

As discussed in the Literature Review (Chapter 2), both the thickness and modulus of the unbound base and the cement-treated layer played the most important roles in the behaviour of the inverted pavement, besides the support provided by the underlying layer to the cement-treated layer.

As has been discussed in this chapter, the greatest physical and mechanical differences identified in T-I and T-II and are in the infrastructure (selected subgrade + subgrade), cement-treated layer, and unbound base. In Figure 4-9, the designed structure, and the structures constructed in the T-I and T-II are presented. It should be noted, as discussed in previously, the cement-treated layer of T-II was built at the design thickness but presented segregation in the last 30 mm in the bottom, therefore the workable thickness of T-II is 150 mm and not 180 mm.

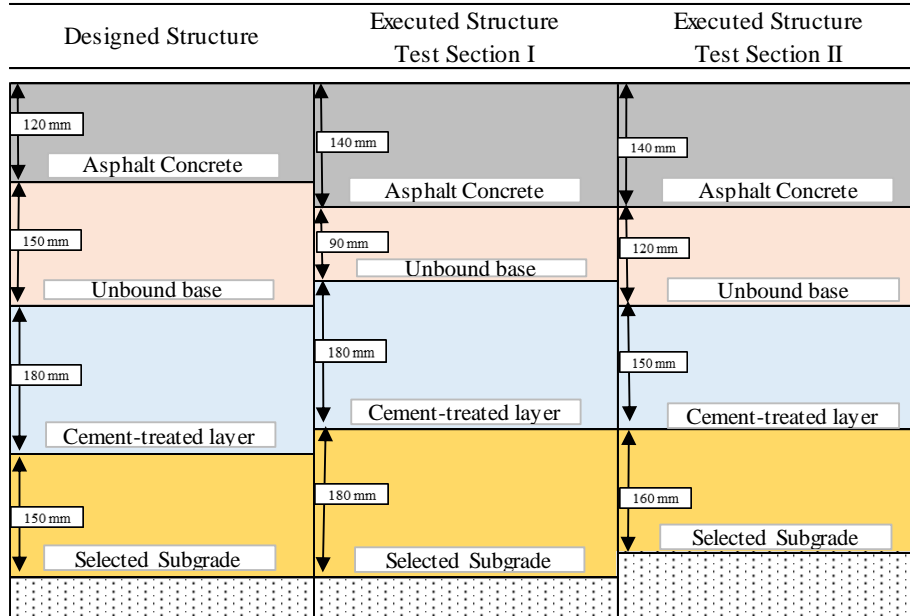


Figure 4-9: Designed structure and executed structures

To understand the influence of the thickness and modulus of the layers on the behaviour of the inverted pavement as a whole, a parametric numerical study was developed using the program Elsym-5. Altogether 960 structures were simulated, varying the moduli and thicknesses values. In the parametric numerical study, both the thickness and modulus of the asphalt layer were fixed, since this was the layer that showed the least difference in relation to the project, both test sections are 140 mm thick. Furthermore, according to Suzuki (1992) among the variables involved in the performance of the inverted pavement, the asphalt layer is the least influential.

The range of moduli and thicknesses were determined according to the physical characteristics identified in both test sections, covering the minimum and maximum limits of thicknesses and moduli found in T-I and T-II. Table 4-5 summarizes the characteristics of the simulated structures. The structures simulated and their outcomes are attached in Appendix B.

Table 4-5: Characteristics of the simulated structures

Layer	Thickness (mm)	Poisson's Ratio	Elastic Modulus (MPa)
Asphalt Concrete	140	0.30	3 000
Unbound base	90 - 100 -110 – 120	0.35	100 - 200 - 300 - 400
Cement-treated layer	150 - 160 -170 – 180	0.25	2 000 – 4 000 – 6 000 – 7 000 – 8 000 – 9 000 – 10 000
Infra. (Selected Subgrade + Subgrade)	Semi-infinite	0.40	200 - 300 - 400

From the simulations performed in the parametric numerical study, it was possible to generate Figure 4-10 and Figure 4-11 and make the following conclusions:

- Surface deflections, horizontal tensile strains in the bottom of the asphalt concrete layer (ϵ_t) and horizontal tensile strains in the bottom of the cement-treated layer (ϵ) decrease with the increase of the elastic modulus of the infrastructure layer;
- Surface deflections and ϵ_t increase with the increase in the thickness of the unbound base, but these same parameters decrease with the increase in the elastic modulus of the unbound base;
- Surface deflections, ϵ_t and ϵ decrease with increasing thickness of the cement-treated layer;
- The parameter ϵ increases and the vertical compressive strains at the surface of the subgrade (ϵ_v) decreases with the increase in the elastic modulus of the cement-treated layer. The elastic modulus of the cement-treated layer, among all the studied parameters, is mainly responsible for the variation of parameter ϵ ;
- The elastic modulus of the cement-treated layer has very little influence on the surface deflections and ϵ_t ;
- The thickness of the unbound influence more the parameter ϵ than its elastic modulus;
- Greater thicknesses and elastic moduli of the unbound base and the cement-treated layer result in a decrease of ϵ_v ;
- The parameter ϵ_v varies mainly according to its own elastic modulus, and then according to the elastic modulus of the cement-treated layer, and
- Among all the variables studied, the variation of ϵ_t is directly influenced by the thickness and elastic modulus of the unbound base, followed by the elastic modulus of the infrastructure layer.

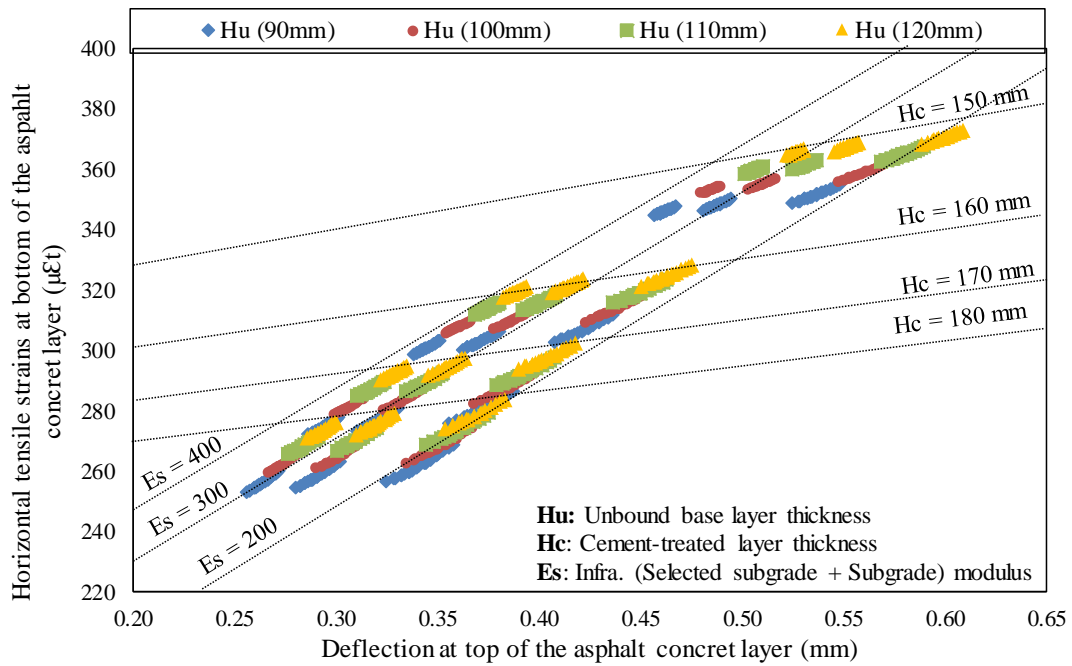


Figure 4-10: Parametric Numerical Study – Variation of D_0 and $\mu\epsilon_t$

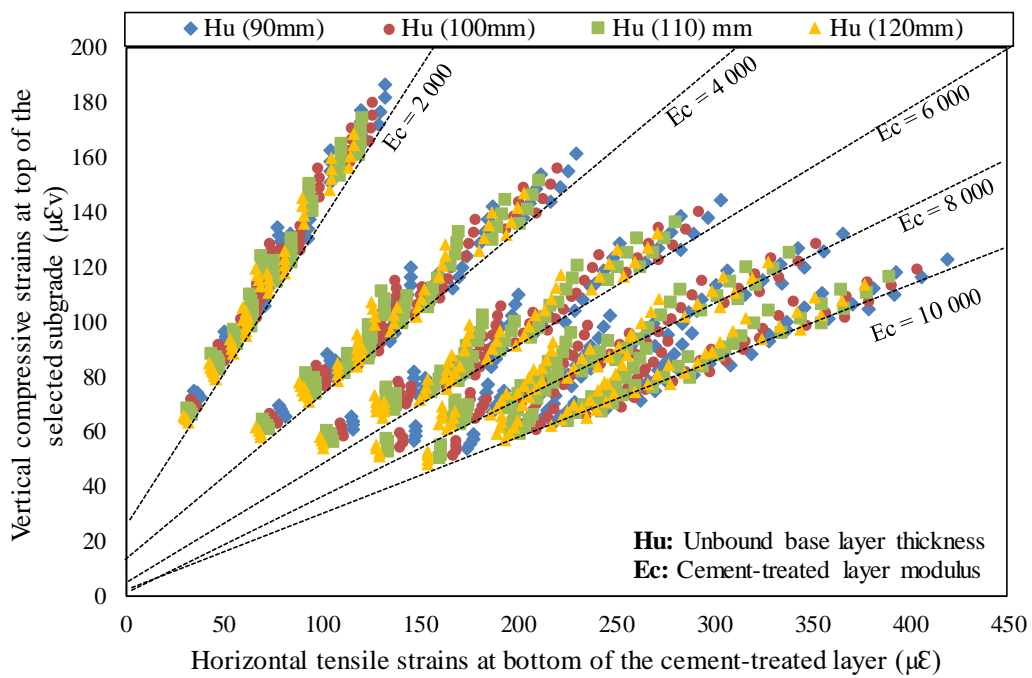
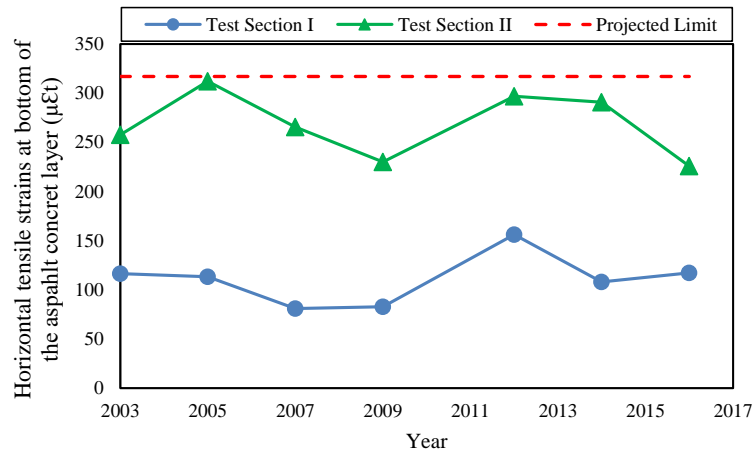


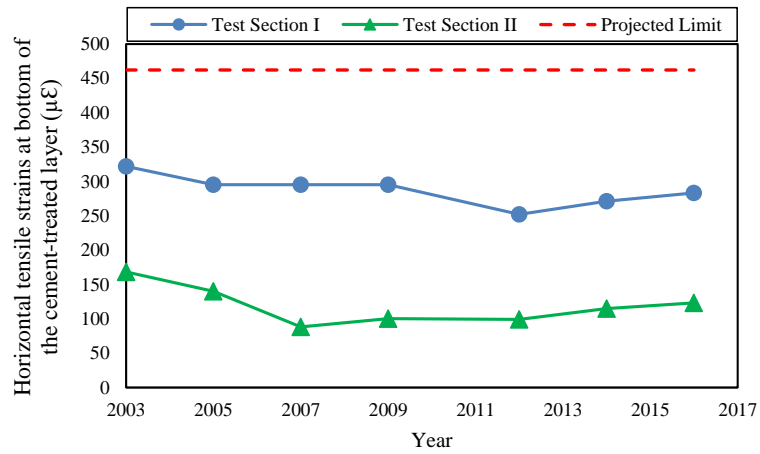
Figure 4-11: Parametric Numerical Study – Variation of $\mu\epsilon$ and $\mu\epsilon_v$

The statements found through the parametric numerical study allow comparing the performance of multiple inverted pavement structures in terms of the critical pavement response parameters (ϵ_t , ϵ_v , ϵ) in addition to allowing a critical analysis of the performance of both test sections according to their thickness and modulus identified. Figure 4-12, presents the parameters (ϵ_t , ϵ_v , ϵ) calculated

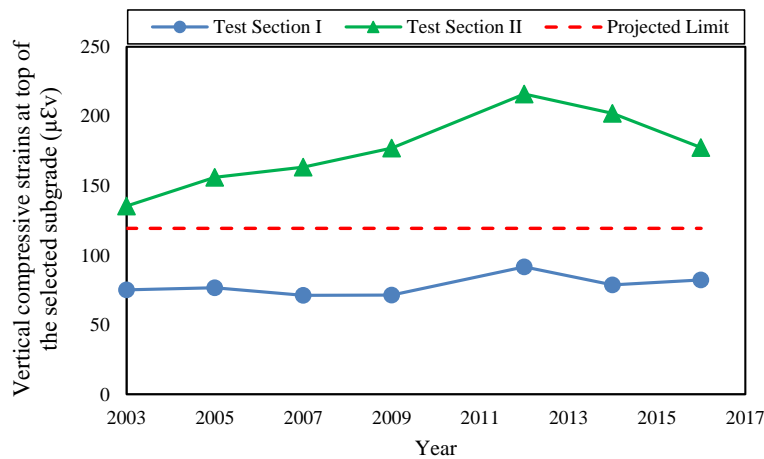
in the design of the test sections and the parameters calculated year by year considering the thicknesses identified in-situ and the back-calculated moduli.



(a)



(b)



(c)

Figure 4-12: a) Variation of ϵ_t as a function of time, b) Variation of ϵ as a function of time, and c) Variation of ϵ_v as a function of time

Figure 4-12.a shows the ε_t projected to the asphalt concrete layer and the ε_t acting in both test sections. In both test sections, the acting ε_t is lower than the expected in the design, and the parameters ε_t obtained year by year for T-I are better than the parameters obtained for T-II. The following considerations can be:

- Increasing the thickness of asphalt concrete decreases parameter ε_t . The concrete asphalt thicknesses of both test sections are greater than the thickness expected in the pavement design;
- Increasing the modulus of the infrastructure decreases the parameter ε_t . T-I has a much better bearing capacity than T-II, and both sections have better bearing capacity than expected in the pavement design;
- The increase in thickness of the cement-treated layer decreases the parameter ε_t . Even though in both test sections the cement-treated layers were built in the total design thicknesses, the cement-treated layer of T-II is not working in its entire thickness. In other words, while the workable thickness of the cement-treated layer of T-I is 180 mm, the workable thickness of T-II is 150 mm
- The smaller thickness and the greater moduli of the unbound base of T-I also contribute to the difference in the parameter ε_t between both test sections.

Figure 4-12.b shows the parameter ε expected in the pavement design of both test section and ε parameters acting in the bottom of the cement-treated layers. In both test sections, the parameter ε is inferior to what is expected in the pavement design, and the parameters obtained year by year for T-II are better than the parameters obtained for T-I. For these behaviours, the following considerations can be made:

- The main factor that directly affects the parameter ε is the modulus of the cement-treated layer itself. Smaller moduli result in a decrease in the parameter ε . The difference in modulus of both test sections is huge, while the moduli of the cement-treated layer of T-I vary around 9 000 MPa (Figure 4-2), the moduli of the T-II are below 2 000 MPa in the vast majority (Figure 4-2). The same concept is applied for the parameter ε projected. The back-calculated moduli for the cement-treated layer of both test sections did not reach the 12 000 MPa, modulus considered in the project.

Figure 4-12.c shows the parameter ε_v projected for the infrastructure and the parameters ε_v actually acting at the surface of the infrastructure of both test sections. The parameters ε_v obtained

in T-II in all years of study are superior to the parameter ε_v provided in the pavement design and also to the parameters ε_v obtained for T-I. The following considerations can be made:

- The layers overlying the infrastructure layers act as a shield, protecting the underlying layers from the actions of traffic loads. As some of the layers overlying the infrastructure layer no longer work as planned, the lower layers feel the reflection, and consequently, the resistance decreases, thus increasing the parameters ε_v , and
- Even though the infrastructure layer moduli of T-II are greater than the designed modulus, the upper layers are not working as planned, since the cement-treated layer works with smaller modulus and thickness than projected, and the unbound base has very low moduli, thus increasing the parameters ε_v .

5. ANALYSIS AND DISCUSSION OF TESTS CARRIED OUT IN-SITU AND LABORATORY IN QUALITY CONTROL

This chapter presents the analyses and discussions of the test results carried in-situ and the laboratory on the unbound base, cement-treated layer, selected subgrade and subgrade during the quality control of both test section.

As discussed in Section 3.8 the test results presented in this dissertation do not fully represent the quality control performed during the construction of both test sections. CCR Engelog provided all files related to the tests carried out during the quality control, but some of them were damaged over to time.

5.1 Compaction characteristics of both test section

5.1.1 Dry density obtained in the laboratory and the field

Figure 5-1 shows the dry density values obtained in the laboratory, the results obtained in-situ and the degrees of compaction achieved. In general, the dry densities obtained in-situ are higher than the densities obtained in the laboratory in all analysed layers, however, the level of significance does not exceed 2 % in all analyses, which demonstrates the proximity of the results obtained in the field and in-situ. As the dry densities obtained in the laboratory and in-situ were reached, consequently the minimum degree of compaction required by the Brazilian specifications was also reached in all layers, varying between 100 % and 102 %.

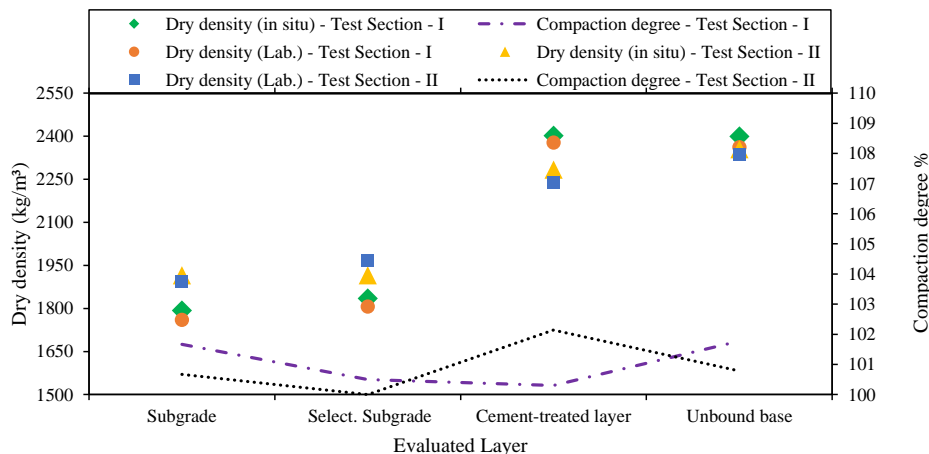


Figure 5-1: Test results obtained in-situ by the sand-cone method during the quality control

The dry densities obtained both in the laboratory and in-situ for the selected subgrade and subgrade are slightly higher in T-II, showing that the materials used on the selected subgrade and

subgrade of both test sections have different physical properties. Normally, under comparable conditions, the more clayey the soil is, the lower its density, thus implying that both the selected subgrade and subgrade materials from T-I have more clay characteristics than the materials used in T-II.

Both dry densities obtained in the laboratory and in-situ for the unbound base are quite similar in both test sections. Normally when the densities of granular materials are similar to the properties of the aggregates such mineralogy, gradation, particle shape, texture, angularity, Atterberg limits, and per cent passing the No. 0.075 mm sieve are also similar.

Among all the layers evaluated, the biggest differences, when comparing the dry densities obtained in-situ-between both test sections, were verified in the cement-treated layer. The dry density of the cement-treated layer of T-II is 6 % less than the dry density achieved in T-I. One of the possible reasons for the difference in density may be the difference in the properties of the aggregates, since the Brazilian specifications recommend the physical requirements for the materials, but do not mention the mineralogy of the materials, and as discussed in Section 2.3 different aggregates provide different densities.

The cement content is also a key factor in determining the dry density of the cement-treated layer. As presented in Section 3.8.4, while the variations of the cement content used in the cement-treated layer of the T- I ranged between 2.8 % and 3.2 %, the information related to the cement content adopted in the cement-treated layer was not found in files related to T-II.

It should also be noted, as presented in Section 3.3, the cement-treated layer found in T-II presented disaggregation in the last 30 mm in the bottom layer of both inspection pits. Pathologies of this type can be linked to many factors such as the type of aggregate, its gradation and the degree of compaction which mainly governs the aggregate structure, cement content, fines content, moisture content, curing time, and curing condition as covered in Section 2.3.

5.1.2 Moisture content in the compaction process

In the compaction stage, the optimum moisture content was reached in all layers in the field, as shown in Table 5-1. At optimum moisture content, the materials reach the highest dry density, that is, if the moisture content used to compact the layer is greater or less than the optimum moisture content, the soil will not reach its maximum degree of compaction.

Table 5-1: Moisture content in the compaction Process

Test Section	Parameter	Subgrade	Selected Subgrade	Cement-treated layer	Unbound base
I	Moisture Content (in-situ) %	17	18	9	8
	Optimum Moisture content (Lab.) %	17	17	9	8
II	Moisture Content (in-situ) %	13	10	8	8
	Optimum Moisture content (Lab.) %	13	10	8	8

In all layers, during the compaction stage, the moisture content used was equal or very similar to the optimum moisture content obtained in the laboratory. Still, according to the data obtained, it is clear that the higher the dry density (Figure 5-1), the lower the moisture content required (Table 5-1). Even with the proximity of the dry densities obtained for the selected subgrade and subgrade of both test sections, a large discrepancy in the optimum moisture content values is verified.

5.2 Comparative analysis of densities obtained in-situ in 2001 and 2017

As discussed in Section 3.4.1, the verification of densities and moisture content in-situ was carried out in the selected subgrade and the unbound base for each inspection, pits opened in both test sections. In Figure 5-2, the densities (dry density and Bulk density) obtained in-situ in 2017 were compared with the densities obtained in 2001 during the quality control of both test sections.

In general, the Bulk density is greater than dry density in all tests performed. The bulk density represents the natural states of the soil that includes water. In the dry density, the moisture content is not considered which makes the dry density lower than the bulk density.

The results obtained in 2017 for the selected subgrade and the unbound base were found to be similar to the density results obtained during the quality control in 2001. For the unbound base, a small increase in dry density is observed in relation to 2001. The increase in unbound density can be linked to the consolidation period, since after the opening of the highway to traffic, the particles continue to be rearranged, thus reducing voids, and consequently causing an increase in density.

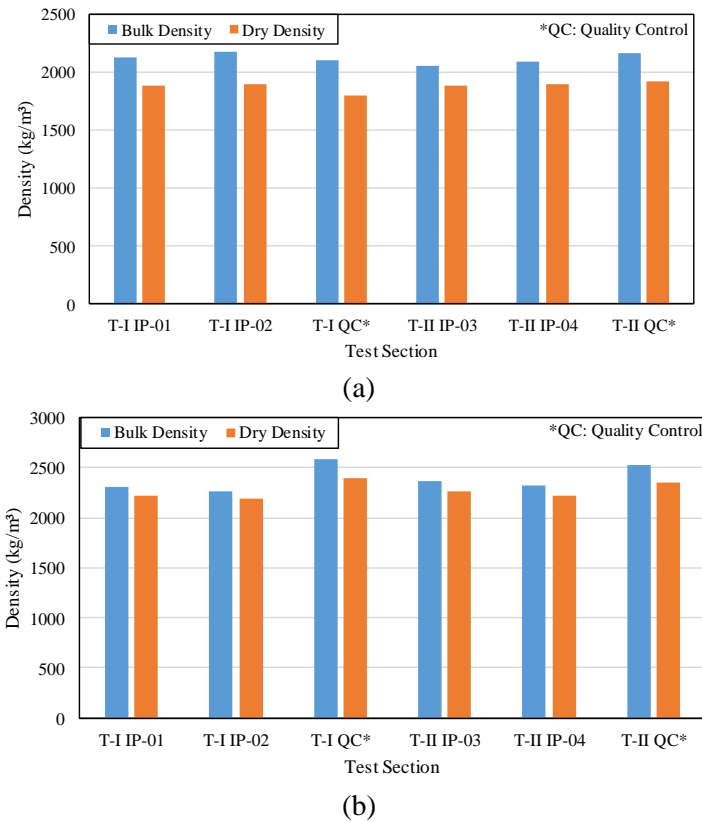


Figure 5-2: a) Comparison of bulk and dry density of the selected subgrade b) Comparison of bulk and dry density of the unbound base

5.3 Analysis of the strength parameters obtained for the cement-treated layer

As discussed in Section 3.8.5, samples were collected from the cement-treated layers just after their compaction. The rupture of the samples was carried out 7 and 28 days after their collection. The specification of force in the state of São Paulo (DER/SP, 2006a), where the test sections were built, indicates maximum and minimum strength limits (USC and ITS) for the cement-treated layer as shown in Section 2.5.2.

The specimens collected in T-I presented varying cement content (2.8 to 3.1). No information related to the cement content used was found in the cement-treated layer of T-II. Figure 5-3 and Figure 5-4 show the UCS and ITS resistances obtained at 28 days as a function of their cement content.

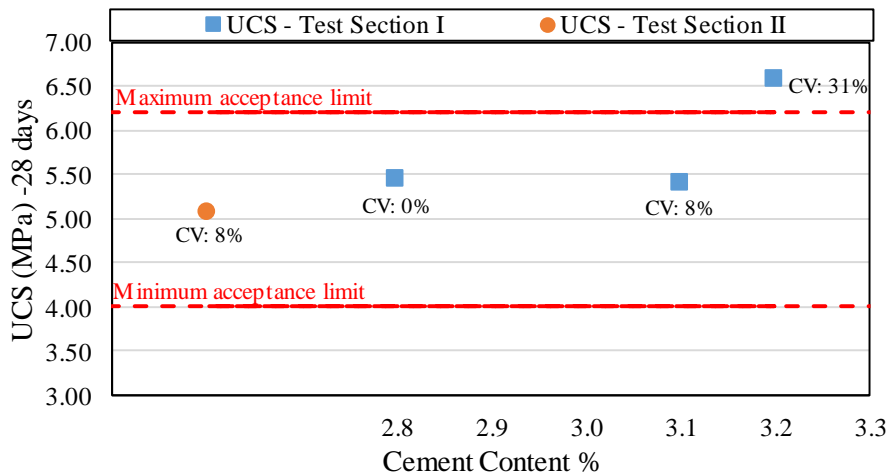


Figure 5-3: UCS as a function of cement content in both test sections

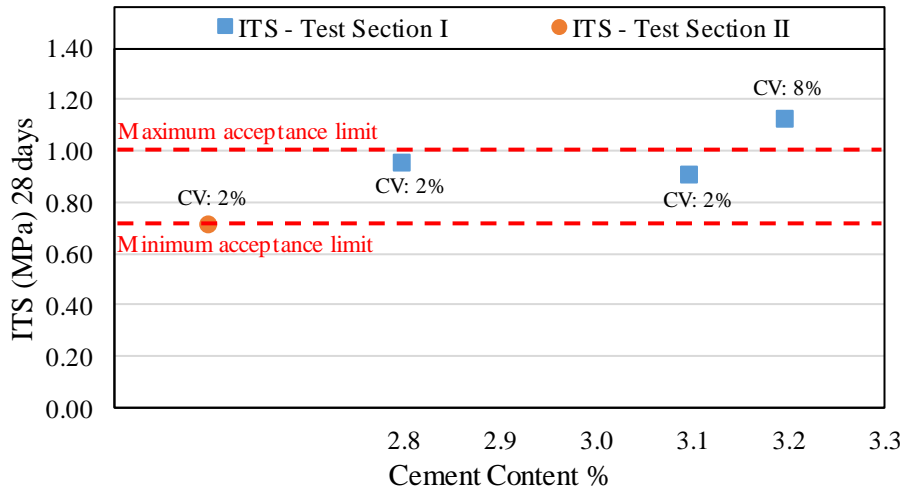


Figure 5-4: ITS as a function of cement content in both test sections

The resistances obtained in T-II show coefficients of variation of 8 % for UCS and 2 % for ITS, demonstrating the sample homogeneity. Furthermore, the lowest resistances (UCS and ITS) obtained were in the cement-treated layer of T-II.

For some authors, there is a conflict in meeting the minimum resistance of USC and ITS, since it is more difficult to achieve ITS than UCS, and the UCS results are usually higher than the upper limit specified. In case of conflict, SANRAL (2014) recommends that the ITS criteria is met, once the durability of the stabilised materials depends more on the ITS than the UCS

5.3.1 Relationship between the strength parameter UCS and curing time

As discussed in Sections 2.3.7 and 2.5.7, the curing process is a conditioning factor for the strength gain of the cement-treated layer. Since the cement content used in the mixture of the cement-treated layer of T-I is known, it was possible to verify the increase in strength relating to cement content as well as the number of days of cure (Figure 5-5).

At 7 days of cure, 66 % of the resistances obtained at 28 days were reached for all cement percentages. The resistances obtained for 2.8 % and 3.1 % of cement content are practically equal, whereas the resistances obtained with 3.2% of cement content present the higher values.

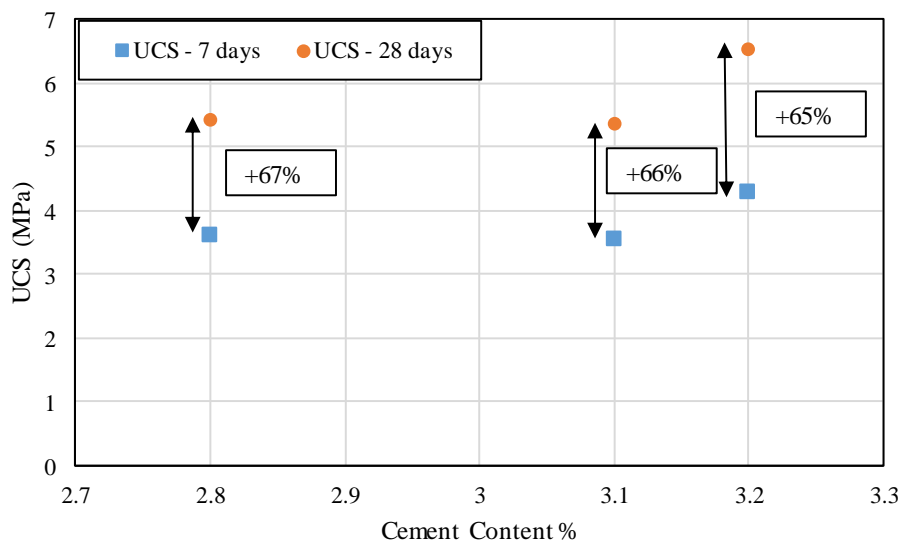


Figure 5-5: Analysis of the relationship between the strength parameter UCS and curing time

5.3.2 Relationship between UCS and ITS

As discussed in Section 2.4.3, several researchers have developed correlations to obtain the tensile strength value from UCS. From the resistance parameters (UCS and ITS) obtained at 28 days, it was possible to draw a linear function (Figure 5-6). According to the data obtained from quality control of the cement-treated layer of T-I, the ITS represents 17 % of the UCS value.

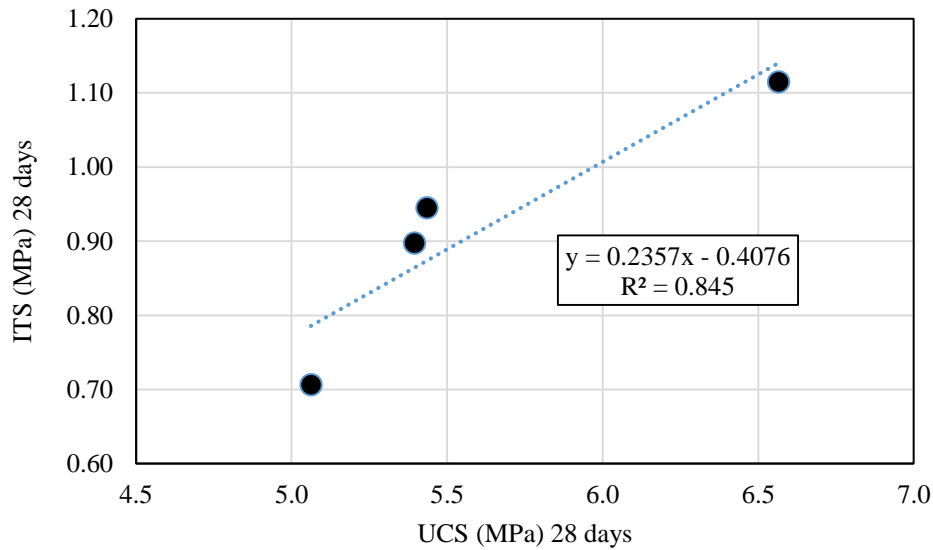


Figure 5-6: The relationship between UCS and ITS

5.3.3 Analysis of the influence of curing of the cement-treated layers on the performance of test sections

The analysis of the curing time of the cement-treated layers would be of great help to understand why the test sections, especially the cement-treated layers, have shown different behaviours, since the curing time directly influences the strength of the cement-treated layer, as discussed in Sections 2.3.7 and 2.5.7.

As it was not possible to find information regarding curing bitumen emulsions or curing time in general, hence the decision to analyse and maybe make some assumptions considering the release time of the layers, since the deflectometry control is done on top of the compacted layer. From the date of deflectometry control (Table 5-2) it was possible to make some comments:

Table 5-2: Analysis of the release time of the layers

Layer	Test - Section I		Test - Section II	
	Deflection control date	Release time (Days)	Deflection control date	Release time (Days)
Selected Subgrade	20/06/2001	-	21/07/2001	-
Cement-treated layer	28/06/2001	8	28/08/2001	38
BGS	19/07/2001	21	13/09/2001	16

Test-Section I - The time elapsed between the deflectometry control performed at the top of the selected subgrade and the cement-treated layer was 8 days. 21 days after the execution of the deflectometry control of the cement-treated layer, the control of the unbound base was being carried out. Thus, in less than 7 days, the cement-treated layer was already open to traffic to carry out deflectometry control, and in less than 28 days, the cement-treated layer and unbound base were built.

Test-Section II - The time elapsed between the deflectometry control performed at the top of the selected subgrade and the cement-treated layer was 38 days. In this interval, there would be enough time to build the cement layer and perform the deflectometry control in 28 days after compaction according to the recommendations (Section 2.5.7). However, it is not possible to say whether this actually happened. There may have been a delay in the work, resulting in a delay of 38 days.

In conclusion, there is a possibility that the cement-treated layer of T-II has been cured according to Brazilian specifications (28 days of curing). In T-I, this possibility does not exist. Emphasis on that, even with the recommendations, in Brazil, deflection measurements are often carried out 7 days after the layer is compacted.

6. ANALYSIS AND DISCUSSIONS OF RESULTS CARRIED OUT IN LABORATORY IN 2017

This chapter presents the analyses and discussions of test results carried in out in the laboratory for the unbound base, cement-treated layer and selected subgrade in 2017 in both test sections as shown in Chapter 3 (Section 3.5 to 3.7).

In addition to analysis of convergences and divergences of the results obtained for both test sections, the test results were compared to test results obtained during quality control and what was suggested in the project of the pavement of both test sections.

6.1 Analysis of tests carried out on the subgrade and selected subgrade

The results of the tests presented in Section 3.7 are discussed in this section. Analysing different soil properties is complicated, especially when you have many different results. When the results are tilted in the same direction, it is much easier to analyse and make an assertive diagnosis, but when not, many uncertainties are created.

Unfortunately, the failure to collect material from the selected subgrade at IP-01 to perform laboratory tests, made the analysis even more complex to make generics conclusions.

6.1.1 Analysis of soil classification

According to the HRB-AASHTO Soil Classification, TRH14 Classification and MCT Soil Classification, the material collected from the selected subgrade of both test sections would have different applications. The soils classified by the HRB-AASHTO and TRH14 methodologies showed similarities. In both classifications, the material collected from the selected subgrade of T-II showed better bearing capacity than the material collected from the T-I (Table 6-1).

The soils classified using the MCT methodology present a condition that is opposite to the HRB-AASHTO and TRH14 classifications (Table 6-1). According to the MCT methodology, the material collected from the selected subgrade of T-I has better bearing capacity than the material collected from T-II. The better performance of the infrastructure layers (selected subgrade and subgrade) of T-I had already been verified in the analyses and discussions carried out in Chapters 4 and 5.

Table 6-1: Material application according to the classification

HRB-AASHTO Soil Classification	T-I			A-6
	T-II	A-2-4 A-2-6		
TRH14 Soil Classification	T-I		G7	
	T-II	G6		
MCT Soil Classification	T-I		LG'	
	T-II			NA'
Application	Base	Subbase	Selected Subgrade	Subgrade

According to Nogami and Villibor (1995), the use of the HRB-AASHTO soil classification presents limitations for the classification of tropical soil, as is the case in Brazil, since in the HRB-AASHTO classification both the Atterberg Limits as to the per cent passing the No. 0.075 mm sieve are crucial indexes in the classification of the soil. For the authors, experience in both the laboratory and the field has revealed that the limits of LL and IP do not apply for tropical environmental conditions. Furthermore, the authors highlight that; these indexes cannot be used to forecast their expansive characteristics.

Some designers have noticed that, in countries with a tropical climate, traditional classifications that are based on the grain size distribution and Atterberg Limits when applied to soils present serious discrepancies. In the TRH14 classification, the Atterberg limits and the per cent passing the No. 0.075 mm sieve are also crucial factors for soil classification; therefore, following the same line of thought as Nogami and Villibor (1995) and designers experience, the TRH14 classification, as well as the HRB-AASHTO classification, may also have limitations in the classification of tropical soils.

6.1.2 Analysis of soil strength as a function of Soil classification

The CBR values show a completely different bearing capacity when the resilient moduli obtained in the laboratory for the selected subgrade (Figure 6-1) are observed. For many researchers, the CBR values may, in many circumstances, not adequately reflect the quality of the soil-aggregate, especially those of types that are poorer in fines and little or non-cohesive.

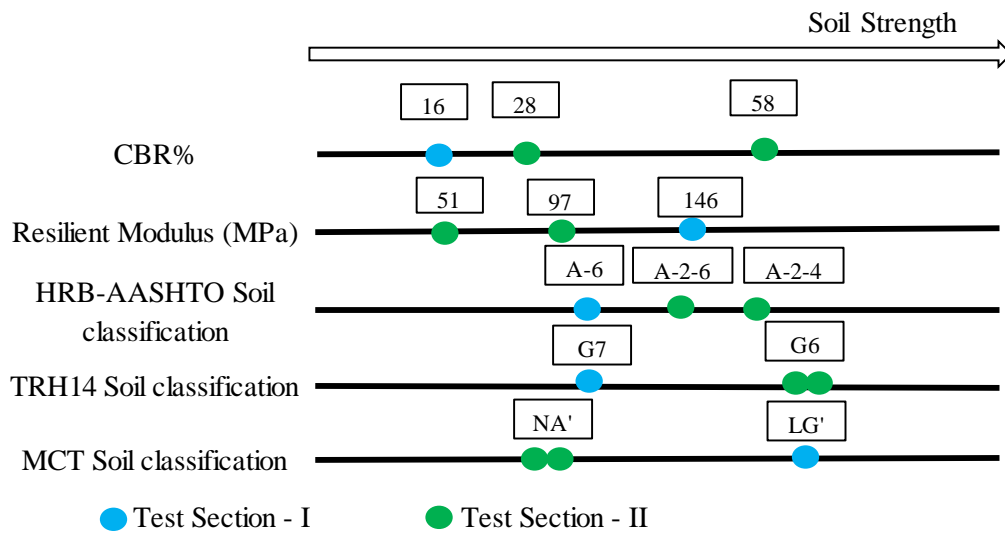


Figure 6-1: Analysis of soil strength as a function of Soil classification

According to Figure 6-1, the soils classified by the HRB-AASHTO and TRH14 methodologies follow the same tendency for bearing capacity as identified in the CBR values, in other words, the bearing capacity of the selected subgrade of T-I is less than capacity identified in T-II. Nevertheless, soils classified by the MCT methodology show a condition similar to the values of the resilient modulus obtained in the laboratory.

Normally, it is expected that both the CBR values and the values of resilient moduli obtained for lateritic soils (T-I) will be greater than the results obtained for non-lateritic soils (T-II), in agreement with the MCT classification. In the results obtained in both test sections, the CBR values for T-II are higher than the values obtained for T-I. This behaviour had already been identified by Ferri (2018) in his thesis and by some Brazilian designers during the geotechnical investigation. However, unfortunately, there are not many studies regarding the behaviour of non-lateritic soils, so it is very difficult to make behavioural predictions when this soil is used as a pavement layer.

6.1.3 Resilient modulus as a function of CBR

There are many correlations for estimating resilient modulus through CBR. Perhaps the most famous correlation between the resilient modulus and CBR used is $MR = CBR \times 10$ (in MPa) proposed by Heukelom and Foster (1960). Dione et al (2014) in their literature review found that the CBR is not suitable for estimating the resilient modulus. For the authors, the CBR is a measure

of strength so it is not correlated with the resilient modulus which is a measure of stiffness, and strongly dependent on the stress state.

If it is necessary to obtain the soil resilient modulus as a function of the CBR, it is important to apply equations that take into account the type of soil classified using the appropriate methodology. In this research, the Equation 6.1 and Equation 6.2 both recommended by DER/SP (2006a) were applied.

Recommended for lateritic soils (LA' and LG) - Applied in T-I:

$$MR = 22 * CBR^{0.8} \text{ in (MPa)} \quad (\text{Equation 6.1})$$

Recommended for sandy or non-cohesive soils – Applied in T-II:

$$MR = 14 * CBR^{0.7} \text{ in (MPa)} \quad (\text{Equation 6.2})$$

The application of the Equations 6.1 and 6.2, did not result in satisfactory values (Table 6-2), since the resilient moduli obtained by the correlations are completely different from the resilient moduli obtained at the laboratory, especially for soils classified as non-lateritic (IP-03 and IP-04 – T-II). Ferri (2018) did not identify good correlations to obtain resilient moduli as a function of the CBR for Brazilian lateritic and non-lateritic soils.

Table 6-2: Resilient modulus as a function of the CBR and MCT soil classification

Test	Test Section I		Test Section II	
	IP-01	IP-02	IP-03	IP-04
CBR %	-	16	58	28
Resilient Modulus (CBR) (MPa)		202	240	144
Resilient Modulus (Lab.) (MPa)		149	51	97

Even with the reduced number of CBR tests and resilient moduli, no direct relationship was identified between the CBR values and resilient moduli. Therefore, it is recommended that the resilient modulus test be performed to measure the resistance of the materials used. Even with prior knowledge of soil classification, the use of correlations can lead to erroneous results, compromising the integrity of the pavement as a whole.

6.1.4 Comparison of laboratory resilient moduli with back-calculated moduli

In this research, the back-calculated moduli obtained in the infrastructure layer were adjusted by the application of the factor equal to 0.35, according to recommendations made by the Guide for Mechanistic-Empirical Pavement Design Guide of AASHTO (2008).

Figure 6-2 shows the back-calculated moduli obtained from the deflection measured at the top of the selected subgrade during the quality control (column A), the back-calculated moduli obtained from the deflection measurement carried out year by year (column B), and the resilient moduli obtained in the laboratory for the selected subgrade (column C).

By applying the adjustment factor, the proximity of the back-calculated moduli to the moduli obtained in the laboratory can be seen in both test sections. The application of the adjustment factor is necessary since it has been documented in the literature and verified in this dissertation that the back-calculated moduli calculated do not match the measurements made in the laboratory.

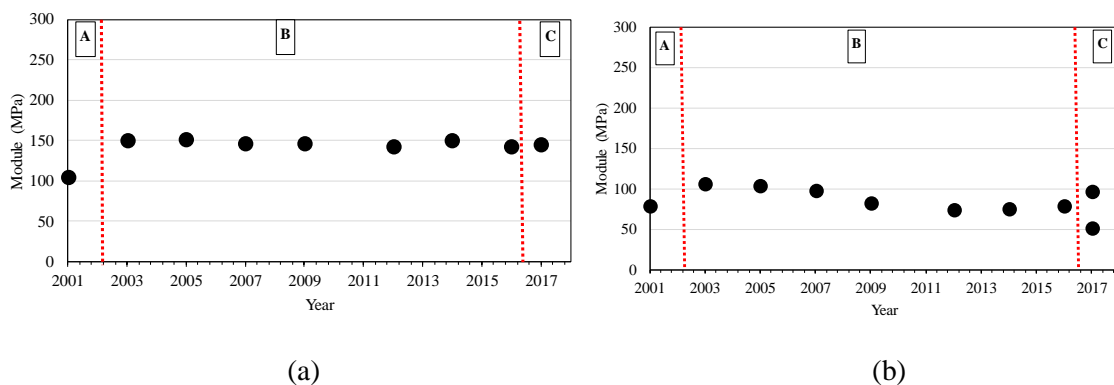


Figure 6-2: a) Laboratory resilient moduli and back-calculated moduli - Test section I and, b) Laboratory resilient moduli and back-calculated moduli - Test section II

It is also noted that the back-calculated moduli obtained from measurements made in 2001 are lower than the back-calculated moduli obtained in the following years, and this is due to the fact that the pavement structure was being built and would be open to traffic, going through the consolidation phase. The deflections measured during construction are usually higher than the deflections measured during subsequent monitoring, resulting in a decrease of the back-calculated moduli.

As discussed in Chapter 4 and Chapter 5, there is a considerable difference in the infrastructure (selected subgrade +subgrade) bearing capacity of both test sections. The resilient moduli

obtained in the laboratory for the selected subgrade from both test sections also reported this difference in bearing capacity.

6.1.5 Dynamic Penetration Cone analysis

To facilitate the analysis, an average penetration index was calculated, obtained from the four DCP tests (two in each inspection pit) performed in each test section. A coverage area was also drawn, obtained by, subtracting and adding the standard deviation to the mean (Figure 6-3).

The coverage region involves practically all the results obtained in both test sections, thus verifying the homogeneity of the tested material. In T-I, the thickness of the selected subgrade is a little greater than the thickness of the selected subgrade of T-II, as verified when the inspection wells were opened, it also presents greater resistance. Variations in the strength of the subgrade as a function of depth in both sections vary in the same order. The values of the resistances and their variations are shown in Table 6-3.

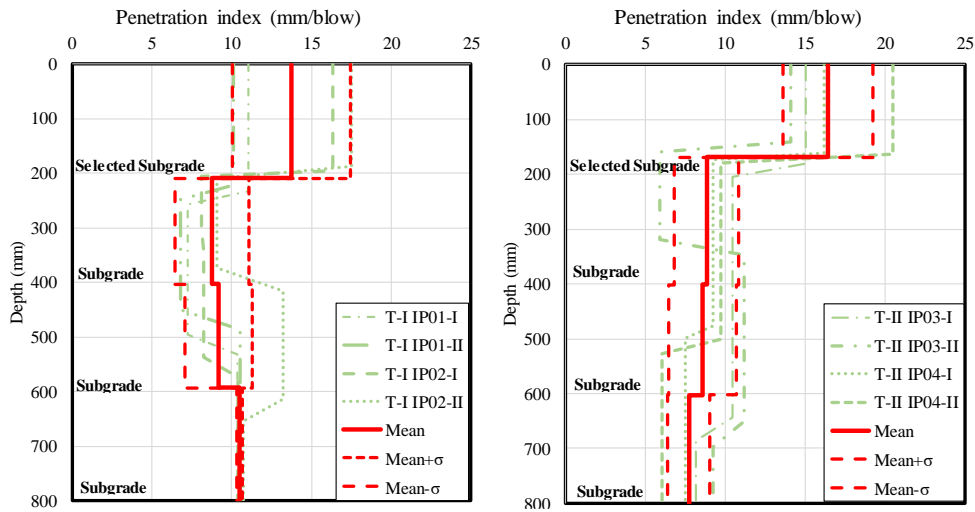


Figure 6-3: Layer-strength diagram of both test sections

Table 6-3: Strength of the selected subgrade and subgrade of both test sections obtained by DCP

Layer	Test section - I					Test section - II				
	Mean	σ	cv	Mean+ σ	Mean- σ	Mean	σ	cv	Mean+ σ	Mean- σ
Selected Subgrade	13.7	3.7	27%	17.5	10.0	16.5	2.8	17%	19.3	13.7
Subgrade 3 layer	8.8	2.3	26%	11.1	6.5	8.8	2.0	23%	10.9	6.8
Subgrade 2 layer	9.2	2.1	23%	11.3	7.1	8.6	2.1	25%	10.7	6.5
Subgrade 1 layer	10.5	0.2	2%	10.7	10.3	7.7	1.3	17%	9.1	6.4

In the analysed profiles, the strength of both selected subgrades has lower resistance than the underlying layers (subgrade). The earthmoving layers of the subgrade have a continuous resistance as the test deepens. Furthermore, according to the results, the strength of both subgrades are quite similar, however, the subgrade of T-II presents a slightly better resistance than the resistances obtained for T-I.

6.1.6 Comparison of $CBR_{\text{Laboratory}}$ with CBR_{DCP}

From the analysis of the strength profile of both test sections, it was possible to obtain the CBR in-situ (Table 6-4). There are several models for obtaining the CBR in-situ through corrections with the DN. In this study, Equation 6.3, developed by Kleyn (1984) was chosen for this analysis.

$$CBR = 410 * DN^{-1.27} \quad \text{(Equation 6.3)}$$

Where:

DN: DCP number (DN) in mm/blow

The CBR obtained from the application of Equation 6.3 for T-I (Table 6-4) is similar to the CBR value obtained in the laboratory. However, the CBR obtained for T-II is completely different from the CBR obtained in the laboratory. Dal Pai (2005) observed the coherence of the values of DN and CBR obtained in laboratories for lateritic soils, and the lack of conclusive results for non-lateritic soils, the same observations were made in this dissertation

Table 6-4: Comparison of $CBR_{\text{Laboratory}}$ with CBR_{DCP}

Layer	Test section - I			Test section - II		
	Mean	Mean+ σ	Mean- σ	Mean	Mean+ σ	Mean- σ
CBR (DCP)	14.7	10.8	21.9	11.7	9.6	14.8
CBR (Lab)	16.0	-	-	58	-	-
				28	-	-

During the manual analysis of the results, it was realised that the definition of strength through the identification of slopes is a process that requires a lot of sensitivity since small distortions during the definition of slopes can result in completely different results.

6.2 Analyses of the grain size distribution in the unbound base

In the unbound base, besides the Gradation test, in-situ density was also carried out as already discussed in section 5.1.1. According to Figure 6-4, in addition to the grain size distribution identified in the unbound base of both test sections, the grading envelope indicated in the pavement design of both test sections is also shown.

The samples collected in T-I, in both inspection pits, show little difference when compared. Comparing the samples collected in T-I with the grading envelope recommended in the design, it is clear that the number of coarse aggregates that pass through the No. 25 mm, No. 19 mm, and No. 9.5 mm sieve is slightly higher than the allowed limit. However, fine aggregates meet the minimum limit of the grading envelope.

In T-II, the amount of coarse aggregates also exceeds the upper limit of the recommended envelope, but in more sieves and a larger quantity than T-I. In IP-03, the limits are exceeded until the No. 4.75 mm sieve, and in IP-04, the limits are exceeded until the No. 2.0 mm sieve. As in T-I, the minimum limits are met in sieves No. 0.42 mm and No. 0.075 mm.

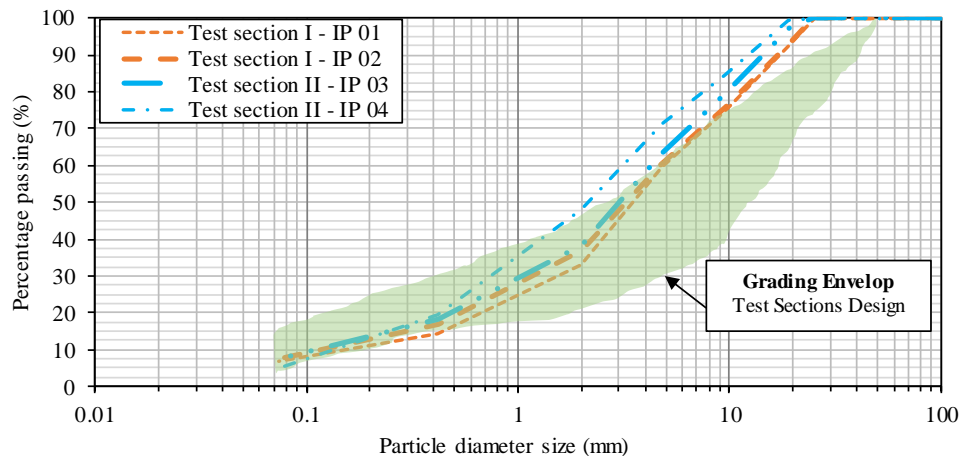


Figure 6-4: Grain size distribution of the unbound base executed in both test sections

The grain size distribution of the unbound base, as discussed in Section 2.2.3, plays a critical role in the performance of the inverted pavement. A larger quantity of coarse aggregates requires a bigger quantity of fine aggregates, ensuring that the voids are filled up and the layers are compacted perfectly.

Both test sections, mainly in T-II, present a quantity of coarse aggregates above the maximum limit of the project envelope, and a quantity of fine aggregates that meets the minimum limit of the particle size envelope, resulting in a disharmonious distribution. Since if the number of coarse aggregate increases, the amount of fines aggregate should also increase to fill the voids.

As presented in Chapter 4, the presence of permanent deformations was verified in both test sections, especially in T-II. The occurrence of these pathologies may be linked to many factors such as mineralogy, moisture content, thickness, as well as the grain size distribution of the unbound base.

Furthermore, the low values of the back-calculated moduli obtained for the unbound base of T-II may also be associated with the imbalance between coarse and fine aggregates. According to Cortes (2010), the unbound base stiffness initially increases with higher fines fraction as a result of an increase in coordination number caused by pore-filling fines.

6.3 Analysis of the strength parameters of the cement-treated layer

6.3.1 Elastic response analyses

In Figure 6-5 and Figure 6-6 the average of the dynamic moduli at the various frequencies, the flexural moduli, the resilient moduli and the back-calculated moduli for the cement-treated layers of both test sections are shown.

Before using the average as a criterion for assessing the stiffness of the cement-treated layers, the coefficients of variation were calculated to verify whether the results were homogeneous and whether the use of the average would be feasible. The calculated coefficients of variation varied as follows:

- a) Dynamic Moduli - The coefficient of variation increased as the frequency increased - ranging between 11 % and 16 % for T-I, and between 20 % and 32 % for T-II;
- b) Resilient Moduli - The coefficient of variation obtained was 10 % for both test sections, and
- c) Flexural Moduli - The coefficient of variation obtained was 19 % for both test sections.

In the dynamic moduli obtained for T-II, the highest variations were observed. Unfortunately, as discussed in Section 3.6.1, three of the six specimens were ruptured before the tests were

completed, so the sample analysed in this work contains only three specimens with varying thickness. Section 6.3.2 discusses the influence of the thickness of the specimen in obtaining the dynamic modulus.

Even if the 180 mm thickness was identified in the field for the cement-treated layers of both test sections, when the specimens are extracted, a small thickness variation is common, often depending on the size of the aggregate used. For this reason, the specimens used in obtaining dynamic moduli have varying levels of thicknesses. To obtain the average of the dynamic moduli of the T-I, the results obtained for the specimens with a height of 181.4 mm, 180.4 mm and 178.2 mm were considered.

In Figure 6-5, the moduli obtained for T-I are shown. The resilient moduli presented the highest values, followed by the flexural moduli. The dynamic moduli, obtained for the different frequencies, are more similar to the back-calculated moduli.

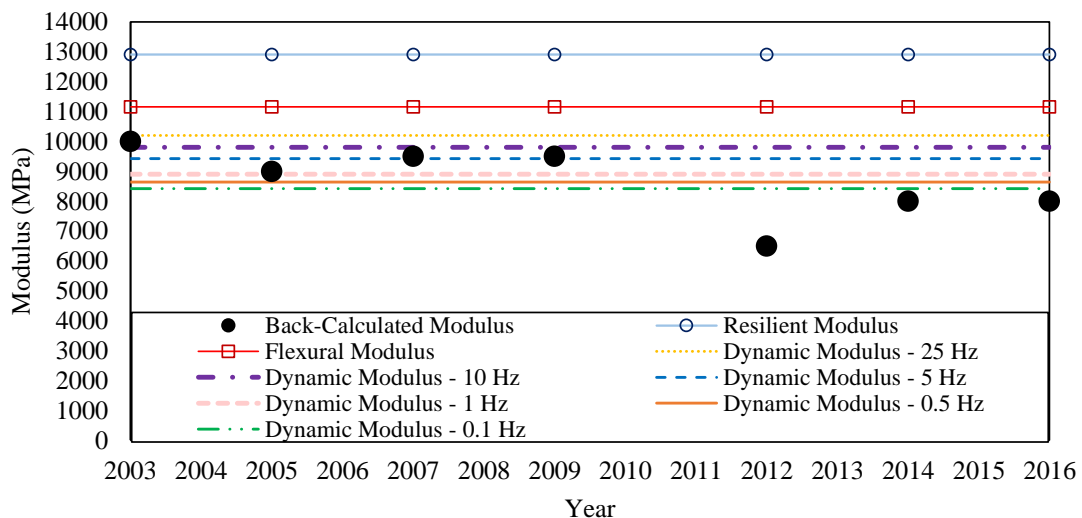


Figure 6-5: Lab. and back-calculated moduli obtained for the cement-treated layer in T-I

In Figure 6-6, the resilient moduli, as in T-I, presented the highest values, followed by the flexural moduli. In general, the moduli obtained in the laboratory for T-II are not very different from each other, but they differ considerably from the back-calculated moduli.

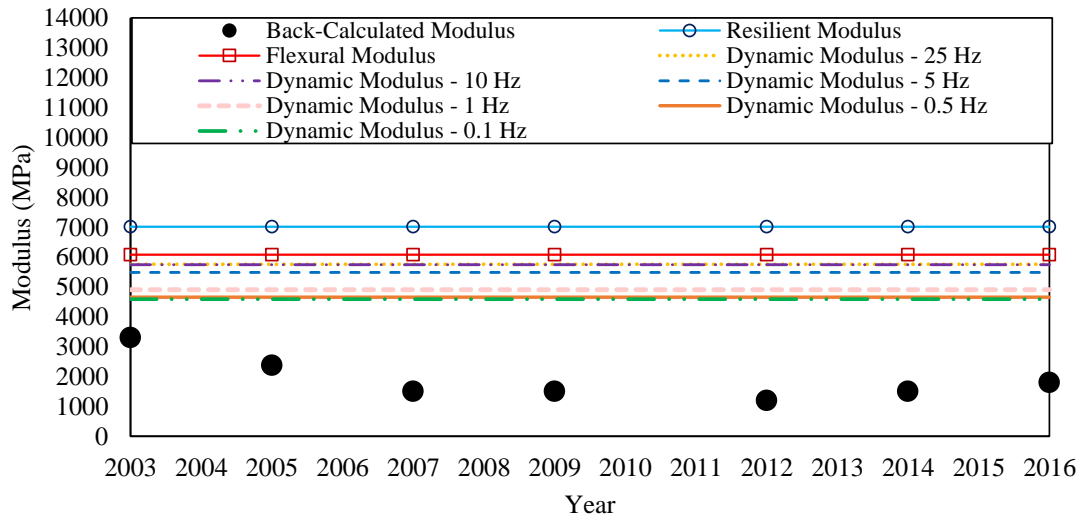


Figure 6-6: Lab. and back-calculated moduli obtained for the cement-treated layer in T-II

In general, the dynamic, resilient and flexural moduli obtained for T-I are greater than the moduli obtained for T-II. While the moduli of the T-I oscillate between 8 424 MPa and 12 912 MPa, the moduli obtained of T-II oscillate between 4 593 MPa and 7 016 MPa.

It should be noted that the values of the moduli obtained in the laboratory for the cement-treated layer of T-II (Figure 6-6) may not represent the performance condition of the layer in its entire thickness; since the samples extracted had presented disaggregation in the last 30 mm of the bottom layer, and the moduli were obtained from the intact fraction of the cement-treated layer. The specimens extracted in T-I were intact, thereby, possibly, the test results represent the performance condition of the cement-treated layer.

6.3.2 Influence of the thickness and frequency in the Dynamic Modulus results

The dynamic moduli obtained by the different frequencies are presented in the form of a graph (Figure 6-7). From the analysis of the graphs, the following comments can be made:

- As the frequency increases, the dynamic moduli increase in both test sections, and
- Less thicknesses provide greater dynamic moduli.

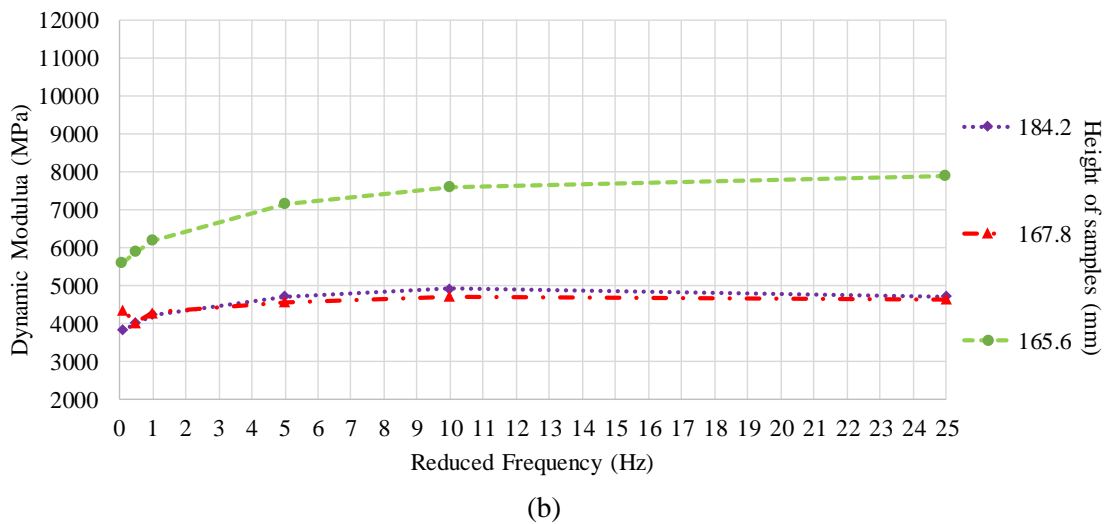
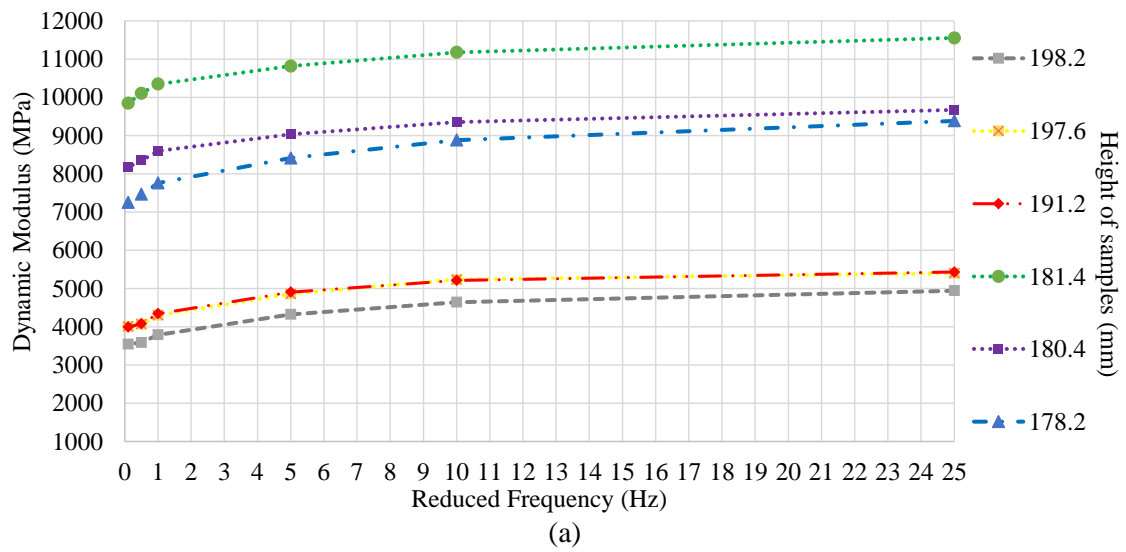


Figure 6-7: a) Dynamic moduli results obtained in T-I and b) Dynamic moduli results obtained in T-II

6.3.3 UCS and Tensile strength analyses

Figure 6-8 shows the UCS, ITS and f_t results obtained for the cement-treated layer of both sections, as previously presented in Section 3.6. The maximum and minimum strength limits (UCS and ITS) for the cement-treated layer according to the specification in force in the state of São Paulo (DER / SP, 2006a) are also shown in the Figure 6-8. As a comparison, the UCS and ITS results obtained during the quality control of both sections are presented as well, as previously shown in Section 5.3.

In general, the strength parameters (UCS, ITS and f_t) obtained for both test sections are quite similar, at times the parameters obtained for T-II are better than the strength parameters obtained

for T-I (Figure 6-8.c). This result in strength performance was not expected, since, in all the analyses performed, the cement-treated layer in T-I proved to be stiffer and with a better structural condition, when compared to T-II. Thus, it was expected that the strength parameters obtained for T-I would be better than the strength parameters obtained for T-II. Furthermore, in both test sections, the UCS and ITS parameters, in addition to being similar, do not meet the minimum strength limits, previously met when the quality control was carried out in 2001 (Section 5.3).

The similarities and low strength observed in the USC, IT and f_t tests for both test sections, associated with the differences observed in the results of tests carried out in 2001, may be attributed to the following factors:

- a) Losses of resistance due to microcracking in the handling of the specimens, both in transport and in modulus tests. As previously mentioned, in the tests carried out in 2017, the same specimens were used to obtain the moduli and strength parameters (UCS, ITS and f_t). Perhaps the integrity of the specimens collected was the same when the tests of strength were performed, because they were damaged in the handling;
- b) Condition of moisture or seasoning of the specimens preceding the rupture;
- c) The dimensions of the specimens tested in 2017 are different from the dimensions of the specimens tested in 2001, and
- d) The curing of the cement-treated layer of both test sections may have been different from the curing of the specimens moulded in 2001.

No studies were found in the literature that report loss of strength caused by the factors previously mentioned. It remains to be seen whether some of these factors mentioned and whether the strength of the materials may result in regression after a certain age, and whether the loading history should be considered in this analysis cause the loss of strength.

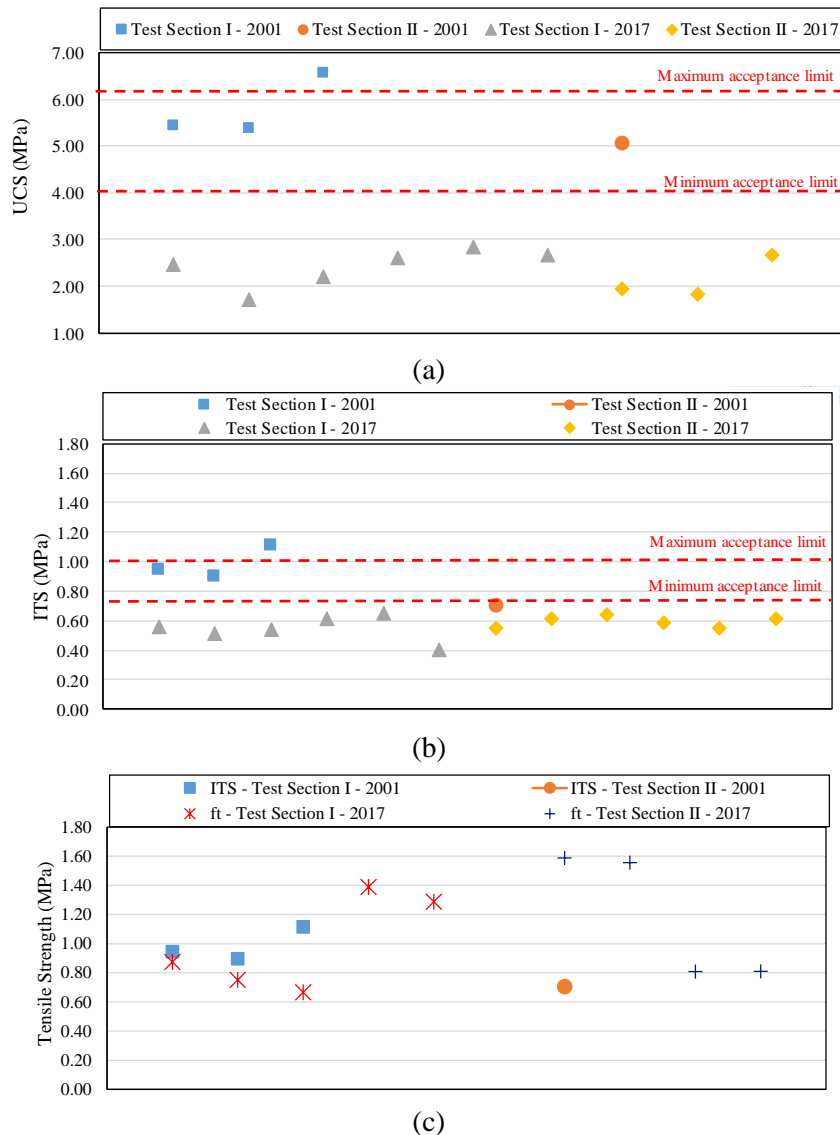


Figure 6-8: a) UCS obtained in both test section, b) ITS obtained in both test section and c) f_t obtained in both test section

6.3.4 The relationship between UCS and tensile strength

No satisfactory correlations were found between UCS and ITS, UCS and f_t and ITS and f_t from the tests results obtained in 2017. From the test results obtained, ITS values represent around 24 % of the UCS value, f_t represents around 55 % of the UCS values, and ITS represents around 50 % of the f_t value.

In the strength parameters obtained in 2001, as noted in Section 5.3.2, it was possible to draw a liner function (ITS as a function of UCS) with R^2 greater than 0.8. Furthermore, according to the data obtained from quality control of the cement-treated layer of T-I, the ITS represents 17 % of the UCS value.

7. CONCLUSIONS AND RECOMMENDATIONS

7.1 Conclusions

The main objective of this study was to understand the mechanical behaviour of the inverted pavement, especially for the cement-treated used as a subbase layer. To this end, the main objective was divided into three interdependent sub-objectives. The first one sought to identify and characterize the variables directly related to structural behaviour of inverted pavements; the second one sought to make a comparative analysis of the design, materials, construction and quality control methods adopted by Brazil and South Africa; and the last one, from the understanding obtained throughout this research, sought to recommend some procedures for the inverted pavement structures on the basis of the Brazilian test sections.

Based on the analyses and discussions carried out throughout this research, the variables directly related to the structural behaviour of inverted pavements were identified as follows:

- a) Bearing capacity of the selected subgrade and subgrade – The elastic behaviour of the layers is conditioned by the support of the layer immediately below, and the performance of the cement-treated layer is highly dependent on the support of the underlying layers. The bearing capacity of both selected subgrade and subgrade of T-I was better than the bearing capacity of T-II as indicated in the deflection bowl parameters, in the back-calculated moduli, in the resilient moduli obtained in the laboratory, and in the MCT classification. The difference in bearing capacity of the selected subgrade and subgrade was a strong variable related to the difference in the performance of both test sections;
- b) Modulus of the cement-treated layer – The increase in the elastic modulus of the cement-treated layer increases the parameter ϵ , but decreases the vertical compressive strains at the surface of the subgrade, and improves the elastic modulus of the unbound base layer and consequently the horizontal tensile strains in the bottom of the asphalt layer decrease. In the test sections studied, both the back-calculated moduli and the moduli obtained in the laboratory showed a huge discrepancy. In all the analyses performed, the cement-treated layer in T-I proved to be stiffer and with a better structural condition when compared to T-II;
- c) Thickness of the cement-treated layer – The thickness of the cement-treated layers also plays a fundamental role in the performance of the inverted pavement. The parameters D_0 , ϵ_t , ϵ and ϵ_v decrease with increasing thickness of the cement-treated layer. Thinner layers have increased horizontal tensile strains in the bottom of the cement-treated layer, bringing the action of loads

closer to the subgrade. The workable thickness of the cement-treated layer of T-II was 150 mm due to the 30 mm of segregation identified in the bottom of the layers, while T-I was working to its full thickness (180 mm), which could be an important factor in the difference in the performance of both test sections;

d) Elastic modulus of the unbound base – The increase of the modular value causes a decrease in the parameters D_0 , ε_t , ε and ε_v , providing better performance to the inverted pavements as a whole. Among all the variables studied, the variation of ε_t is directly influenced by the thickness and elastic modulus of the unbound base, followed by the elastic modulus of the infrastructure layer. The unbound base certainly contributed to the difference in behaviour of both test sections, and

e) Construction Techniques – Construction Techniques – Good techniques and serious quality control can lead to different results, directly reflecting on the pavement's service life. The analysis of the test carried out in 2001 during the quality control indicated that there were possible problems in the cement-treated layer of T-II, either in the design of the cement mixture or the construction techniques adopted.

Based on the Literature Review carried out in this research, it was possible to highlight the main differences from the design, materials, construction and quality control carried out on inverted pavements in Brazil and South Africa. These differences are shown as follows:

a) Bearing capacity of the subgrade – The South African flexible pavement design emphasises the importance of a good foundation - Most of the main Brazilian specifications do not indicate the minimum bearing capacity for the subgrade when it is done, the indication is a minimum CBR of 2 %, while the South African specifications indicate a minimum CBR of 15 % for the subgrade;

b) Grain size distribution - In general, in South Africa, the grading envelopes indicated for granular materials used as a base and in the composition of the cement-treated layer are more graduated (the number of sieves used in the gradation is higher) and allow a smaller variation in particle size (the minimum and maximum ranges are narrower) than the materials used in Brazil. In South Africa, the grading envelope used in cement-treated layer C2 has almost the same maximum limits as the Brazilian B material. The big difference between the grading envelopes of both materials is in the minimum limits, the grading envelope of C2 allows more fine aggregates in grading envelope than the B material;

c) Type of cement - South Africa uses special cement for road paving while in Brazil a type of cement intended for road construction has not yet been developed. The absence of a suitable cement for application in road paving in Brazil, linked to grain size distribution is perhaps an important factor in the differences in strength (modulus, USC and ITS) obtained for the cement-treated layers in the South African and Brazilian highway pavements, whereas the cement content used in both countries are quite similar, and

Quality control - The laboratory and in-situ tests conducted on the cement-treated layer for quality control in Brazil and South Africa are quite similar. The biggest difference is in the determination of the cement content of the cement-treated layer. In Brazil, the determination of the cement content for the cement-treated layer is obtained by the ratio between the mass difference of the mixture, with cement and without cement, by the mass of the mixture without cement, multiplied by 100. In South Africa, to determine the percentage of lime or cement necessary to satisfy the demand of clay minerals in soils and gravels the Initial Consumption of Stabilizer (ICS) has been applied.

Based on the analyses and discussions carried out throughout this research, it was possible to recommend the following procedures for the inverted pavement structures on the basis of the Brazilian test sections.

a) Selected subgrade and subgrade:

- I. Good bearing capacity - The resilient behaviour of the cement-treated layer is dependent on the support of the underlying layer, therefore, when dimensioning pavements, it is recommended that the use of a good quality infrastructure layer be considered, thus offering the cement-treated layer the necessary support for its proper functioning;
- II. Minimum modulus - According to the test carried out in this research and the finding available in the literature review, the modulus adopted to the selected subgrade and subgrade to design procedures of the inverted pavement should be equal or greater than 150 MPa;
- III. Adjustment factor - The back-calculated moduli are good and reliable indicators of resistance, however, it is essential to apply adjustment factors, since the back-calculated moduli do not match the measurements made in the laboratory;
- IV. Resilient tests - As no direct correlations were found to obtaining resilient modulus through CBR, when the analyse of the material, preferably resilient tests should be performed instead of using values obtained in correlations, and

- V. Type of soil - In case of obtaining CBR values through DCP tests, it is important to be aware of the type of soil. As reported in the available literature, the coherence between the values of DN and CBR obtained in laboratories for lateritic soils (T-I) and the incoherence for no-lateritic soils (T-II) was also verified in this work.
- b) Unbound Base Layer
- I. Minimum modulus - According to the results obtained and the analysis performed, elastic modulus less than 200 MPa increases significantly the parameters D_0 , ε_t , ε and ε_v , and
 - II. Grading envelopes - The increase in the elastic module of the unbound layer, in addition to the confinement stresses, may increase by increasing the gradation and the amount of fine aggregates in the grading envelopes suggested in the Brazilian specifications.
- c) Cement-treated Layer
- I. Minimum modulus - The adoption of elastic modulus less than 10 000 MPa as a design input may lead to a significant design risk, considering technical specifications, design procedures, material properties for cement-treated layer, and construction parameters adopted in Brazil;
 - II. Minimum thickness - For Brazilian circumstances, in which the cement-treated layers are very stiff, thicknesses less than 180 mm may cause the premature failure of the layer, and consequently of the pavement as a whole, and
 - III. Integrity evaluation - For Brazilian circumstances, cement-treated layers with elastic modulus less than 7 000 MPa may be an indication that the integrity of the layer is compromised.
- d) Quality Control
- I. Structural gain - The analysis of the structural gain calculated from the deflection measurements made at the top of each layer during the quality control is a good parameter to verify if the constructed layers are showing the performance expected in the project. When individual structural gains are achieved in the field it means that the resistance parameters considered in the project have also been achieved;
 - II. Coefficient of variation - Deflections measured during quality control must be carefully evaluated. The acceptance layer criterion is based only on achieving the required maximum deflection and can hide construction flaws. Therefore, it is recommended that

whenever quality control is carried out, the homogeneity of the measures collected from the variation coefficient is verified. A coefficient of variation less than 30 % may be a good indicator of homogeneity;

- III. Deflectometry control - The deflectometry control should be seen as a complement to quality control. It is important to carry out laboratory tests during material selection and construction of all layers. In this research, for example, from the available data obtained from quality control, it was not possible to obtain answers that would in fact explain the reasons why the test sections have shown different behaviours, and
- IV. Specimens - Care needs to be taken in the collection, transport, and preparation of the specimens to avoid wrong results. There is a risk of damaging specimens and so causing unrealistic results when specimens are collected in the field and moulded in the laboratory to meet the pre-defined dimensions of the tests.

7.2 Recommendations

In light of the conclusions made, the following recommendations are made:

- It is recommended to study particle size distribution, shape, maximum grain size and fine aggregates in the resilient response of the unbound base, to avoid the appearance of permanent deformation and recurrent pathology in inverted pavements;
- It is recommended to study the physical and chemical properties of the types of cement used in road paving in Brazil and South Africa;
- It is recommend to study the influence of the type of aggregate and its gradation in obtaining the strength parameters of the cement-treated layer, and
- It recommend to conduct an in-depth study of the properties of non-lateritic soils to avoid erroneous assumptions, jeopardizing the credibility of the pavement designs.

8. REFERENCES

- AASHTO TP46. 1994. *Standard Test Method for Determining the Resilient Modulus of Soils and Aggregate Materials*. American Association of State Highway and Transportation Officials, Washington, D.C.
- AASHTO T307. 2007. *Standard method of test for resilient modulus of subgrade soils and untreated base/subbase materials*. American Association of State Highway and Transportation Officials, Washington, D.C.
- AASHTO T342. 2001. *Standard Method of Test for Determining Dynamic Modulus of Hot-Mix Asphalt Concrete Mixtures*. American Association of State Highway and Transportation Officials, Washington, D.C.
- AASHTO. Mechanistic-Empirical Pavement Design Guide. 2008. Interim Edition. A Manual of Practice. Washington, D. C. USA: AASHTO.
- ABCP. 2002. *Guia básico de utilização do cimento Portland*. Boletim Técnico. BT-106. Associação Brasileira de Cimento Portland. Sao Paulo.
- Adaska, W.S. and Luhr, D.R., 2004. *Control of reflective cracking in cement stabilized pavements*. Paper presented at 5th International RILEM conference. pp. 309-316. Limoges, France.
- Alberto, V.M. 2018. *Contribuição à avaliação da eficiência na escolha de estruturas de Pavimentos Flexíveis, semirrígidos e invertidas*. Masters dissertation. University of São Paulo. Sao Paulo, Brazil.
- Alessio, C. 2016. *Use of local available material for inverted pavement technique*. PhD thesis. University of Studies of Cagliari. Cagliari, Italy.
- ASTM C1609/C1609M. 2012. *Standard test method for flexural performance of fiber-reinforced concrete (Using beam with third-point loading)*. ASTM International, West Conshohocken, PA.
- Austrroads. 2017. *Guide to Pavement Technology Part 2: Pavement Structural Design*. 4th Edition. Austrroads Ltd. Sydney, Australia.
- Balbo, J.T. 1993. *Estudo das propriedades mecânicas das misturas de brita e cimento e sua aplicação aos pavimentos semi-rígidos*. PhD thesis. University of São Paulo. Sao Paulo, Brazil.
- Balbo, J.T., 2006. *Britas graduadas tratadas com cimento: uma avaliação de sua durabilidade sob o enfoque de porosidade, tenacidade e fratura*. TRANSPORTES, v. 14, n. 1, pp. 45-53.
- Balbo, J. T. 2007. *Pavimentação Asfáltica: Materiais, Projetos e Restauração*. 1st ed. Oficina de textos. Sao Paulo, Brazil.
- Caltrans. 2010. *Standard Specifications*. Department of Transportation. State of California. United States.

Chen, D.H., Bilyeu, J., Lin, H.H. and Murphy, M., 2000. *Temperature correction on falling weight deflectometer measurements*. Transportation Research Record: Journal of the Transportation Research Board, v. 1716, n. 1, pp.30-39.

CIIAGRO, 2020. *Centro Integrado de Informações Agrometeorológicas (CIIAGRO)*. Accessed: 21 July 2020 < <http://www.ciiagro.sp.gov.br/>>.

Cordani, U. G.; Teixeira, W.; Toledo, M. C.; Fairchild, T. 2000. *O planeta Terra e suas origens*. Oficina de textos. Sao Paulo, Brazil.

Cortes, D. D. 2010. *Inverted base pavement structures*. PhD thesis. School of Civil and Environmental Engineering, Georgia Institute of Technology. Georgia, United States.

Cortes, D. D.; Shin, H.; Santamarina, J. C. 2012. Numerical simulation of inverted pavement systems. *Journal of Transportation Engineering*, v. 138, n. 12, pp. 1507-1519.

Cortes, D. D., Santamarina, J. C. 2012. *Inverted Base Pavement in LaGrange, Georgia: Characterization and Preliminary Numerical Analyses*. TRB 91st Annual meeting. Washington DC, United States.

Corté, J., Goux, M. 1996. *Design of pavement structures: the French technical guide*. Transportation Research Record: Journal of the Transportation Research Board, v. 1539, n.1, pp.116–124.

Dal Pai, C. M. 2005. *Investigação geotécnica de vias urbanas empregando o método das pastilhas e o penetrômetro dinâmico de cone-DCP*. Masters dissertation. Federal University of Santa Catarina. Santa Catarina, Brazil.

De Almeida, D.C., Brondino, N.C.M., Vicente, P.R.F. and Jacintho, A.E.P. 2019a. *Avaliação de pavimentos semirrígidos invertidos no brasil através da curvatura da bacia de deflexões*. 33th Congresso de Pesquisa e Ensino em Transporte da ANPET. Balneario Camboriu, Santa Catarina.

De Almeida, D.C., Klinsky, L. M. G., Vicente, P.R.F. and Jacintho, A.E.P. 2019b. *Comparação entre valores de módulos elásticos retroanalizados por diferentes softwares em pavimentos semirrígidos invertidos*. 33th Congresso de Pesquisa e Ensino em Transporte da ANPET. Balneario Camboriu, Santa Catarina.

De Beer, M 1985. *Behaviour of cementitious subbase layers in bitumen base road structures*. Masters dissertation. University of Pretoria. Pretoria, South Africa.

De Beer, M. and Maina, J.W., 2008. *Some fundamental definitions of the elastic parameters for homogeneous isotropic linear elastic materials in pavement design and analysis*. Proceedings of the 27th Southern African Transport Conference. Pretoria, South Africa, pp. 282-293.

Departamento de Estradas de Rodagem. 2005. *DER/PR ES-P 01/05. Especificação de Serviço: Pavimentação – Regularização do subleito*. Parana: DER/PR.

Departamento de Estradas de Rodagem. 2005a. *DER/SP ET-DE-P00/001. Especificação Técnica: Melhoria e Preparo do Subleito*. Sao Paulo: DER/SP.

Departamento de Estradas e Rodagens. 2005b. *DER/SP ET-DE-P00/008. Especificação Técnica: Sub-base ou Base de brita graduada*. Sao Paulo: DER/SP.

Departamento de Estradas e Rodagens. 2005c. *DER/SP ET-DE-P00/009. Especificação Técnica: Sub-base ou Base de brita graduada tratada com cimento - BGTC*. Sao Paulo: DER/SP.

Departamento de Estradas de Rodagem. 2006a. *DER/SP IP-DE-P00/001. Instrução de Projeto: Projeto de Pavimentação*. Sao Paulo: DER/SP.

Departamento de Estradas de Rodagem. 2006b. *DER/SP IP-DE-P00/002. Instrução de Projeto: Projeto de Restauração de Pavimento*. Sao Paulo: DER/SP.

Departamento Nacional de Estrada de Rodagem. 1994. DNER-ME 049-94. *Solos - Determinação do índice de suporte Califórnia utilizando amostras não trabalhadas – Método de Ensaio*. Rio de Janeiro: DNER/IPR.

Departamento Nacional de Estrada de Rodagem. 1994. DNER-ME 080-94. *Solos - Análise granulométrica por peneiramento – Método de Ensaio*. Rio de Janeiro: DNER/IPR.

Departamento Nacional de Estrada de Rodagem. 1994. DNER-ME 082-94. *Solos – Determinação do limite de liquidez – Método de Ensaio*. Rio de Janeiro: DNER/IPR.

Departamento Nacional de Estrada de Rodagem. 1994. DNER-ME 092-94. *Solos – Determinação da massa específica aparente “in situ”, com emprego do Frasco de Areia – Método de Ensaio*. Rio de Janeiro: DNER/IPR.

Departamento Nacional de Estrada de Rodagem. 1994. DNER-ME 122-94. *Solos – Determinação do limite de plasticidade – Método de Ensaio*. Rio de Janeiro: DNER/IPR.

Departamento Nacional de Infraestrutura de Transportes. 2005. *Manual de Conservação Rodoviária*. Rio de Janeiro: DNIT.

Departamento Nacional de Infraestrutura de Transportes. 2006a. *Manual de Pavimentação*. Rio de Janeiro: DNIT.

Departamento Nacional de Infraestrutura de Transportes. 2006b. *Manual de Estudos de Tráfego*. Rio de Janeiro: DNIT.

Departamento Nacional de Infraestrutura de Transportes. 2009. DNIT ES. *Especificação de Serviço: Pavimentação – Sub-base ou Base de brita graduada simples*. Rio de Janeiro: DNIT.

Departamento Nacional de Infraestrutura de Transportes. 2010. *DNIT 137/2010 - ES. Especificação de Serviço: Pavimentação – Regularização do subleito*. Rio de Janeiro: DNIT.

Departamento Nacional de Infraestrutura de Transportes. 2010. DNIT 135/2010. *Misturas asfálticas - Determinação do módulo de resiliência – Método de Ensaio*. Rio de Janeiro: DNIT.

Departamento Nacional de Infraestrutura de Transportes. 2010. DNIT 136/2010. *Misturas asfálticas - Determinação da resistência à tração por compressão diametral – Método de Ensaio*. Rio de Janeiro: DNIT.

Departamento Nacional de Infraestrutura de Transportes. 2017. DNIT ES. *Especificação de Serviço: Pavimentação – Sub-base ou Base de brita graduada tratada com cimento*. Rio de Janeiro: DNIT.

Desenvolvimento Rodoviário S/A. 1997. *DERSA/SP ET-P00/039. Especificação Técnica de Pavimentação: Brita Graduada*. Sao Paulo: DERSA/SP.

Dione, A., Fall, M., Berthaud, Y., Benboudjama, F., & Michou, A. (2014). Implementation of Resilient Modulus–CBR relationship in Mechanistic Pavement Design. *Sciences Appliquées et de l'Ingénieur*, v. 1, n. 2, p. 65-71, 2014.

Etzi, A. 2015. *Granite By-Products for Inverted Pavement Technique*. PhD thesis. University of Studies of Cagliari. Cagliari, Italy.

Ferri, S. 2013. *Critérios de aceitação e controle da qualidade da execução de camadas de fundação de pavimentos novos através de métodos deflectométricos*. Masters dissertation. University of Sao Paulo. Sao Paulo, Brazil.

Ferri, S. 2018. *Contribuições ao estudo do comportamento mecânico de solos de subleito para fins de projeto de pavimentos asfálticos*. PhD thesis. University of São Paulo. Sao Paulo, Brazil.

FHWA. 1997. *User Guidelines for Waste and Byproduct Materials in Pavement Construction – Stabilized Base – Application Description*. Federal Highway Administration. Publication Number FHWA-RD-97-148. United States.

Frost, J. David. 2017. *Long-term Performance of Granular Bases Including the Effect of Wet-Dry Cycles on Inverted Base Pavement Performance*. No. FHWA-GA-17-1510. Georgia. Department of Transportation. Office of Research.

Heukelom W. and Foster. 1960. Dynamic Testing of Pavement. *Journal of the Structural Division*, v. 86, n. 1, pp. 1-28.

Horak, Emile. 2008. Benchmarking the structural condition of flexible pavements with deflection bowl parameters. *Journal of the South African Institution of Civil Engineering*, v. 50, n. 2, pp. 2-9.

Horne, D., Belancio, G., Carradine, S. A., Gaj, S., Hallin, J., Jackson, N. and Zink, R. 1997. *South African pavement and other highway technologies and practices*. Federal Highway Administration US Department of Transportation.

Hossain, M. S., Nair, H., Ozyildirim, H. C. 2017. *Determination of mechanical properties for cement-treated aggregate base* (No. FHWA/VTRC 17-R21). Virginia Transportation Research Council.

Johnson, C. W. 1961. *Comparative Studies of Combinations of Treated and Untreated Bases and Subbases for Flexible Pavements*. Highway Research Board Bulletin, v. 289, pp 44-61.

Júnior, J.S., 2018. *Aplicação do novo método de dimensionamento de pavimentos asfálticos a trechos de uma rodovia federal*. Masters dissertation. Federal University of Rio de Janeiro. Rio de Janeiro, Brazil.

Kim, Y. R., Hibbs, B. O., and Lee, Y. C. 1995. *Temperature correction of deflections and backcalculated asphalt concrete moduli*. Transportation Research Record: Journal of the Transportation Research Board, v.1473, pp. 55-62.

Kleyn, E.G. 1984. *Aspects of pavement evaluation and design as determined with the aid of the Dynamic Cone Penetrometer (In Afrikaans)*. Masters dissertation. University of Pretoria. Pretoria, South Africa.

Klinsky, L. M. G., and Faria, V. C. 2018. *Avaliação do tipo de cimento e de compactação nos parâmetros mecânicos da brita graduada tratada com cimento*. ANTT, Centro de Pesquisas Rodoviárias, CCR NovaDutra.

Klinsky, L. M. G., and Faria, V. C. 2015. *Estudo da Influência do Teor de Cimento Portland, da Energia de Compactação e da Umidade no Comportamento Mecânico da Brita Graduada Tratada com Cimento (BGTC) para duas gêneses de agregados*. ANTT, Centro de Pesquisas Rodoviárias, CCR NovaDutra.

Kleyn, E. 2012. *Successful G1 crushed stone basecourse construction*. 31st Southern African Transport Conference. Pretoria, South Africa.

Lekarp, F., Isacsson, U. and Dawson, A. 2000. State of the art. I: Resilient response of unbound aggregates. *Journal of Transportation Engineering*, v. 126, n.1, pp. 66-75.

Lewis, D. E., Ledford, K., Georges, T., and Jared, D. M. 2012. *Construction and Performance of Inverted Pavements in Georgia*. TRB 91st Annual meeting. Washington DC, United States.

Li, Y., Metcalf, J. B., Romanoschi, S. A., and Rasoulian, M. (1999). *Performance and failure modes of Louisiana asphalt pavements with soil-cement bases under full-scale accelerated loading*. Transportation Research Record: Journal of the Transportation Research Board, v.1673, n. 1, pp. 9-15.

Macêdo, J. D. 1996. *Interpretação de ensaios deflectométricos para avaliação estrutural de pavimentos flexíveis*. PhD thesis. Federal University of Rio de Janeiro. Rio de Janeiro, Brazil.

Maree, J. H., Van Zyl, N. J. W., and Freeme, C. R. 1982. *Effective Moduli and Stress Dependence of Pavement Materials as Measured in Some Heavy-Vehicle Simulator Tests*. Transportation Research Record: Journal of the Transportation Research Board. n. 852, pp. 52-60.

Massenlli, G. S. R.; Paiva, C. E. L. 2019. *Influencia de la deflexión superficial en pavimentos flexibles con subrasante de baja resistencia*. Ingeniare. Revista Chilena de Ingeniería, v. 27, n.4. pp. 613-624.

- Metcalf, J. B., Romanoschi, S. A., Li, Y., and Rasoulia, M. 1999. *The First Full-Scale Accelerated Pavement Test in Louisiana: Development and Findings*. Proceedings of the 1st International Conference on Accelerated Pavement Testing. Reno, Nevada.
- Motta, L.M.G.; Ubaldo, M. O., 2014. *Discussão Sobre Valores de Módulo de Resiliência de Brita Graduada Tratada com Cimento (BGTC)*. In: Anais da 43^a Reunião Anual de Pavimentação, Maceio-AL, Brasil.
- Murphy, Harry W.; Baran, E. T.; Gordon, R. G. 1980. *Cement Treated Bases for Pavement*. Institution of Engineers, Australia Queensland Division Tech Pap, v. 21, n. 29, pp. 35-43.
- NBR 5739/2007. 2007. *Concreto - Ensaio de compressão de corpos-de-prova cilíndricos*. Rio de Janeiro, ABNT - Associação Brasileira de Normas Técnicas.
- Nogami, J.S. and Villibor, D.F. 1995. *Pavimentação de Baixo Custo com Solos Lateríticos*. 1st ed. Villibor. Sao Paulo, Brazil.
- Norling, L. T. 1973. *Minimizing reflective cracks in soil-cement pavements: a status report of laboratory studies and field practices*. 52nd Annual Meeting of the Highway Research Board. Highway Research Board, n. 442, pp. 22- 33.
- Paige-Green, P., and Netterberg, F. 2004. *Cement stabilization of road pavement materials: laboratory testing programme phase 1*. Confidential Contract Report CR-2003/42 prepared for Cement and Concrete Institute by CSIR Transportek. Pretoria.
- Papadopoulos, E. 2014. *Performance of unbound aggregate bases and implications for inverted base pavements*. PhD thesis. Georgia Institute of Technology. Georgia, United States.
- Papadopoulos, E.; Santamarina, J. C. 2015. Analysis of inverted base pavements with thin-asphalt layers. *International Journal of Pavement Engineering*, v. 17, n. 7, pp. 590-601.
- Papadopoulos, E. and Santamarina, J.C., 2017. Inverted base pavements: construction and performance. *International Journal of Pavement Engineering*, v. 20, n. 6, pp. 697-703.
- Park, D.Y., Buch, N. and Chatti, K., 2001. *Effective layer temperature prediction model and temperature correction via falling weight deflectometer deflections*. Transportation Research Record: Journal of the Transportation Research Board, v. 1764, n 1, pp.97-111.
- Pinto, S. et al. 1988. *Avaliação do desempenho dos trechos experimentais do Instituto de Pesquisas Rodoviárias/DNER com utilização de cinza volante e cal*. 23^a Reunião de Pavimentação, v.1. pp. 65-86.
- Prefeitura do município de São Paulo. 2004. *Instrução de Projeto 05: Dimensionamento de Pavimentos Flexíveis Tráfego Meio Pesado, Pesado, Muito Pesado e Faixa Exclusiva de Ônibus*. São Paulo: Secretaria de Infraestrutura Urbana.
- Rasoulia, M., Becnel, B. and Keel, G. 2000. *Stone interlayer pavement design*. Transportation Research Record: Journal of the Transportation Research Board, v. 1709, n. 1, pp. 60-68.

Rodrigues, W.A. 2018. *Relatório de fiscalização*. Tribunal de contas da união n. 012.533/2018-1. São Paulo.

Rust, F. C., Mahoney, J. P., Sorenson, J. B. 1998. *An international view of pavement engineering*. Meeting of the Bearing Capacity of Roads and Airfields Conference. Trondheim, Norway.

Salviano, W. R. A. and Motta, L. M. G. 2015. *Análise do controle construtivo de um trecho de pavimento semirrígido por deflexão*. 44^a RAPv - Reunião Anual de Pavimentação. Foz do Iguaçu.

Santos, E. F. D. 2006. *Estudo comparativo de diferentes sistemas de classificações geotécnicas aplicadas aos solos tropicais*. PhD thesis. University of Sao Paulo. São Paulo, Brazil.

Silva, C. F. S. C. 2014. *Análise de tensões em pavimentos a partir de modelo físico instrumentado*. Masters dissertation. Federal University of Rio de Janeiro. Rio de Janeiro, Brazil.

Smith, H.R. and Jones, C.R., 1980. *Measurement of pavement deflections in tropical and sub-tropical climates*. Transport and Road Research Laboratory. Crowthorne, Berkshire.

Smith, K. D., Bruinsma, J. E., Wade, M. J., Chatti, K., Vandebossche, J., & Yu, H. T. 2017. *Using Falling Weight Deflectometer Data with Mechanistic-Empirical Design and Analysis, Volume I* (No. FHWA-HRT-16-009). United States. Federal Highway Administration.

Song, X. J., and Zeng, M. I. 2017. Temperature Correction Method for Asphalt Pavement Dynamic Deflection. *Journal of Highway and Transportation Research and Development*, v. 11, n.1, pp. 33-37.

Suzuki, C.Y. 1992. *Contribuição ao estudo de pavimentos rodoviários com estrutura invertida (sub-base cimentada)*. PhD thesis. University of Sao Paulo. Sao Paulo, Brazil.

Technical design report, 2000. *MC-01.348.000-0-P00_003-R0*, São Paulo, 2000.

The South African National Roads Agency Ltd (SANRAL). 2014. *South African Pavement Engineering Manual*. 2nd edition. South Africa: SANRAL.

Terrell, R.G., Cox, B.R., Stokoe, K.H., Allen, J.J. and Lewis, D. 2003. *Field evaluation of the stiffness of unbound aggregate base layers in inverted flexible pavements*. Transportation Research Record: Journal of the Transportation Research Board, v.1837, n. 1, pp.50-60.

Theyse HL, De Beer M, Rust FC. 1996. *Overview of South African mechanistic pavement design method*. Transportation Research Record: Journal of the Transportation Research Board, v. 1539, n.1, pp. 6-17.

TMH9. 1992. *Pavement Management Systems: Standard Visual Assessment Manual for Flexible Pavements*. Technical Methods for Highways. Committee of State Road Authorities, Pretoria.

TRH4. 1996. *Structural design of flexible pavements for interurban and rural roads*. Draft. Pretoria: Department of Transport. (Technical Recommendations for Highways; TRH4).

TRH13. 1986. *Cement stabilizers in road construction*. Draft. Pretoria: Department of Transport. (Technical Recommendations for Highways; TRH13)

TRH14. 1985. *Guidelines for Road Construction Materials*. Draft. Pretoria: Department of Transport. (Technical Recommendations for Highways; TRH14).

Tutumluer, E. and Barksdale, R. D. 1995. *Inverted flexible pavement response and performance*. Transportation Research Record: Journal of the Transportation Research Board. v.1485, pp.102-110.

Uzan, J. 1985. *Characterization of granular material*. Transportation Research Record: Journal of the Transportation Research Board v. 1022, n. 1, pp.52-59.

Visser, A.T., 2017. *Potential of South African road technology for application in China*. Journal of traffic and transportation engineering (English edition), v. 4, n. 2, pp.113-117.

Von Quintus, H. L., and Killingsworth, B.1997. *Design pamphlet for the backcalculation of pavement layer moduli in support of the 1993 AASHTO Guide for the Design of Pavement Structures* (No. FHWA-RD-97-076). United States. Federal Highway Administration. Office of Engineering Research and Development.

Weber, R. C. 2013. *Avaliação das trajetórias de umedecimento e secagem na deformabilidade elástica de solos compactados*. Masters dissertation. Federal University of Rio Grande do Sul. Porto Alegre, Brazil.

Xuan, D. X. 2012. *Cement treated recycled crushed concrete and masonry aggregates for pavements*. PhD thesis. Delft University of Technology. Netherlands.

YEO, Y. S. 2011. *Characterization of Cement Treated Crushed Rock Basecourse for Western Australian Roads*. PhD thesis. University of Curtin. Bentley, Australia.

Zheng, Y., Zhang, P., and Liu, H. 2019. Correlation between pavement temperature and deflection basin form factors of asphalt pavement. *International Journal of Pavement Engineering*, v.20, n. 8, pp.874-883.

APPENDIX A

CORRELATION BETWEEN EQUIVALENT MODULUS AND DEFLECTION MEASURED AT THE
TOP OF THE LAYER

N° of simulations	Thickness (mm)	Poisson's Ratio	Modulus (MPa)	Point of analysis	Elastic Deflection (z) μm
1	0 (Semi-infinite)	0.4	20.00	0.1	633.5
2	0 (Semi-infinite)	0.4	20.50	0.1	618.1
3	0 (Semi-infinite)	0.4	21.00	0.1	603.4
4	0 (Semi-infinite)	0.4	21.50	0.1	589.3
5	0 (Semi-infinite)	0.4	22.00	0.1	575.9
6	0 (Semi-infinite)	0.4	22.50	0.1	563.1
7	0 (Semi-infinite)	0.4	23.00	0.1	550.9
8	0 (Semi-infinite)	0.4	23.50	0.1	539.2
9	0 (Semi-infinite)	0.4	24.00	0.1	528.0
10	0 (Semi-infinite)	0.4	24.50	0.1	517.2
11	0 (Semi-infinite)	0.4	25.00	0.1	506.8
12	0 (Semi-infinite)	0.4	25.50	0.1	496.9
13	0 (Semi-infinite)	0.4	26.00	0.1	487.3
14	0 (Semi-infinite)	0.4	26.50	0.1	478.1
15	0 (Semi-infinite)	0.4	27.00	0.1	469.3
16	0 (Semi-infinite)	0.4	27.50	0.1	460.8
17	0 (Semi-infinite)	0.4	28.00	0.1	452.5
18	0 (Semi-infinite)	0.4	28.50	0.1	444.6
19	0 (Semi-infinite)	0.4	29.00	0.1	436.9
20	0 (Semi-infinite)	0.4	29.50	0.1	429.5
21	0 (Semi-infinite)	0.4	30.00	0.1	422.4
22	0 (Semi-infinite)	0.4	30.50	0.1	415.4
23	0 (Semi-infinite)	0.4	31.00	0.1	408.7
24	0 (Semi-infinite)	0.4	31.50	0.1	402.2
25	0 (Semi-infinite)	0.4	32.00	0.1	396.0
26	0 (Semi-infinite)	0.4	32.50	0.1	389.9
27	0 (Semi-infinite)	0.4	33.00	0.1	384.0
28	0 (Semi-infinite)	0.4	33.50	0.1	378.2
29	0 (Semi-infinite)	0.4	34.00	0.1	372.7
30	0 (Semi-infinite)	0.4	34.50	0.1	367.3
31	0 (Semi-infinite)	0.4	35.00	0.1	362.0
32	0 (Semi-infinite)	0.4	35.50	0.1	356.9
33	0 (Semi-infinite)	0.4	36.00	0.1	352.0
34	0 (Semi-infinite)	0.4	36.50	0.1	347.1
35	0 (Semi-infinite)	0.4	37.00	0.1	342.5
36	0 (Semi-infinite)	0.4	37.50	0.1	337.9
37	0 (Semi-infinite)	0.4	38.00	0.1	333.4
38	0 (Semi-infinite)	0.4	38.50	0.1	329.1
39	0 (Semi-infinite)	0.4	39.00	0.1	324.9
40	0 (Semi-infinite)	0.4	39.50	0.1	320.8
41	0 (Semi-infinite)	0.4	40.00	0.1	316.8
42	0 (Semi-infinite)	0.4	40.50	0.1	312.9
43	0 (Semi-infinite)	0.4	41.00	0.1	309.0
44	0 (Semi-infinite)	0.4	41.50	0.1	305.3

N° of simulations	Thickness (mm)	Poisson's Ratio	Modulus (MPa)	Point of analysis	Elastic Deflection (z) μm
45	0 (Semi-infinite)	0.4	42.00	0.1	301.7
46	0 (Semi-infinite)	0.4	42.50	0.1	298.1
47	0 (Semi-infinite)	0.4	43.00	0.1	294.7
48	0 (Semi-infinite)	0.4	43.50	0.1	291.3
49	0 (Semi-infinite)	0.4	44.00	0.1	288.0
50	0 (Semi-infinite)	0.4	44.50	0.1	284.7
51	0 (Semi-infinite)	0.4	45.00	0.1	281.6
52	0 (Semi-infinite)	0.4	45.50	0.1	278.5
53	0 (Semi-infinite)	0.4	46.00	0.1	275.5
54	0 (Semi-infinite)	0.4	46.50	0.1	272.5
55	0 (Semi-infinite)	0.4	47.00	0.1	269.6
56	0 (Semi-infinite)	0.4	47.50	0.1	266.8
57	0 (Semi-infinite)	0.4	48.00	0.1	264.0
58	0 (Semi-infinite)	0.4	48.50	0.1	261.3
59	0 (Semi-infinite)	0.4	49.00	0.1	258.6
60	0 (Semi-infinite)	0.4	49.50	0.1	256.0
61	0 (Semi-infinite)	0.4	50.00	0.1	253.4
62	0 (Semi-infinite)	0.4	50.50	0.1	250.9
63	0 (Semi-infinite)	0.4	51.00	0.1	248.4
64	0 (Semi-infinite)	0.4	51.50	0.1	246.0
65	0 (Semi-infinite)	0.4	52.00	0.1	243.7
66	0 (Semi-infinite)	0.4	52.50	0.1	241.3
67	0 (Semi-infinite)	0.4	53.00	0.1	239.1
68	0 (Semi-infinite)	0.4	53.50	0.1	236.8
69	0 (Semi-infinite)	0.4	54.00	0.1	234.6
70	0 (Semi-infinite)	0.4	54.50	0.1	232.5
71	0 (Semi-infinite)	0.4	55.00	0.1	230.4
72	0 (Semi-infinite)	0.4	55.50	0.1	228.3
73	0 (Semi-infinite)	0.4	56.00	0.1	226.3
74	0 (Semi-infinite)	0.4	56.50	0.1	224.3
75	0 (Semi-infinite)	0.4	57.00	0.1	222.3
76	0 (Semi-infinite)	0.4	57.50	0.1	220.4
77	0 (Semi-infinite)	0.4	58.00	0.1	218.5
78	0 (Semi-infinite)	0.4	58.50	0.1	216.6
79	0 (Semi-infinite)	0.4	59.00	0.1	214.8
80	0 (Semi-infinite)	0.4	59.50	0.1	213.0
81	0 (Semi-infinite)	0.4	60.00	0.1	211.2
82	0 (Semi-infinite)	0.4	60.50	0.1	209.4
83	0 (Semi-infinite)	0.4	61.00	0.1	207.7
84	0 (Semi-infinite)	0.4	61.50	0.1	206.0
85	0 (Semi-infinite)	0.4	62.00	0.1	204.4
86	0 (Semi-infinite)	0.4	62.50	0.1	202.7
87	0 (Semi-infinite)	0.4	63.00	0.1	201.1
88	0 (Semi-infinite)	0.4	63.50	0.1	199.5
89	0 (Semi-infinite)	0.4	64.00	0.1	198.0

N° of simulations	Thickness (mm)	Poisson's Ratio	Modulus (MPa)	Point of analysis	Elastic Deflection (z) μm
90	0 (Semi-infinite)	0.4	64.50	0.1	196.4
91	0 (Semi-infinite)	0.4	65.00	0.1	194.9
92	0 (Semi-infinite)	0.4	65.50	0.1	193.4
93	0 (Semi-infinite)	0.4	66.00	0.1	192.0
94	0 (Semi-infinite)	0.4	66.50	0.1	190.5
95	0 (Semi-infinite)	0.4	67.00	0.1	189.1
96	0 (Semi-infinite)	0.4	67.50	0.1	187.7
97	0 (Semi-infinite)	0.4	68.00	0.1	186.3
98	0 (Semi-infinite)	0.4	68.50	0.1	185.0
99	0 (Semi-infinite)	0.4	69.00	0.1	183.6
100	0 (Semi-infinite)	0.4	69.50	0.1	182.3
101	0 (Semi-infinite)	0.4	70.00	0.1	181.0
102	0 (Semi-infinite)	0.4	70.50	0.1	179.7
103	0 (Semi-infinite)	0.4	71.00	0.1	178.5
104	0 (Semi-infinite)	0.4	71.50	0.1	177.2
105	0 (Semi-infinite)	0.4	72.00	0.1	176.0
106	0 (Semi-infinite)	0.4	72.50	0.1	174.8
107	0 (Semi-infinite)	0.4	73.00	0.1	173.6
108	0 (Semi-infinite)	0.4	73.50	0.1	172.4
109	0 (Semi-infinite)	0.4	74.00	0.1	171.2
110	0 (Semi-infinite)	0.4	74.50	0.1	170.1
111	0 (Semi-infinite)	0.4	75.00	0.1	168.9
112	0 (Semi-infinite)	0.4	75.50	0.1	167.8
113	0 (Semi-infinite)	0.4	76.00	0.1	166.7
114	0 (Semi-infinite)	0.4	76.50	0.1	165.6
115	0 (Semi-infinite)	0.4	77.00	0.1	164.6
116	0 (Semi-infinite)	0.4	77.50	0.1	163.5
117	0 (Semi-infinite)	0.4	78.00	0.1	162.4
118	0 (Semi-infinite)	0.4	78.50	0.1	161.4
119	0 (Semi-infinite)	0.4	79.00	0.1	160.4
120	0 (Semi-infinite)	0.4	79.50	0.1	159.4
121	0 (Semi-infinite)	0.4	80.00	0.1	158.4
122	0 (Semi-infinite)	0.4	80.50	0.1	157.4
123	0 (Semi-infinite)	0.4	81.00	0.1	156.4
124	0 (Semi-infinite)	0.4	81.50	0.1	155.5
125	0 (Semi-infinite)	0.4	82.00	0.1	154.5
126	0 (Semi-infinite)	0.4	82.50	0.1	153.6
127	0 (Semi-infinite)	0.4	83.00	0.1	152.7
128	0 (Semi-infinite)	0.4	83.50	0.1	151.7
129	0 (Semi-infinite)	0.4	84.00	0.1	150.8
130	0 (Semi-infinite)	0.4	84.50	0.1	150.0
131	0 (Semi-infinite)	0.4	85.00	0.1	149.1
132	0 (Semi-infinite)	0.4	85.50	0.1	148.2
133	0 (Semi-infinite)	0.4	86.00	0.1	147.3
134	0 (Semi-infinite)	0.4	86.50	0.1	146.5

N° of simulations	Thickness (mm)	Poisson's Ratio	Modulus (MPa)	Point of analysis	Elastic Deflection (z) μm
135	0 (Semi-infinite)	0.4	87.00	0.1	145.6
136	0 (Semi-infinite)	0.4	87.50	0.1	144.8
137	0 (Semi-infinite)	0.4	88.00	0.1	144.0
138	0 (Semi-infinite)	0.4	88.50	0.1	143.2
139	0 (Semi-infinite)	0.4	89.00	0.1	142.4
140	0 (Semi-infinite)	0.4	89.50	0.1	141.6
141	0 (Semi-infinite)	0.4	90.00	0.1	140.8
142	0 (Semi-infinite)	0.4	90.50	0.1	140.0
143	0 (Semi-infinite)	0.4	91.00	0.1	139.2
144	0 (Semi-infinite)	0.4	91.50	0.1	138.5
145	0 (Semi-infinite)	0.4	92.00	0.1	137.7
146	0 (Semi-infinite)	0.4	92.50	0.1	137.0
147	0 (Semi-infinite)	0.4	93.00	0.1	136.2
148	0 (Semi-infinite)	0.4	93.50	0.1	135.5
149	0 (Semi-infinite)	0.4	94.00	0.1	134.8
150	0 (Semi-infinite)	0.4	94.50	0.1	134.1
151	0 (Semi-infinite)	0.4	95.00	0.1	133.4
152	0 (Semi-infinite)	0.4	95.50	0.1	132.7
153	0 (Semi-infinite)	0.4	96.00	0.1	132.0
154	0 (Semi-infinite)	0.4	96.50	0.1	131.3
155	0 (Semi-infinite)	0.4	97.00	0.1	130.6
156	0 (Semi-infinite)	0.4	97.50	0.1	130.0
157	0 (Semi-infinite)	0.4	98.00	0.1	129.3
158	0 (Semi-infinite)	0.4	98.50	0.1	128.6
159	0 (Semi-infinite)	0.4	99.00	0.1	128.0
160	0 (Semi-infinite)	0.4	99.50	0.1	127.3
161	0 (Semi-infinite)	0.4	100.00	0.1	126.7
162	0 (Semi-infinite)	0.4	100.50	0.1	126.1
163	0 (Semi-infinite)	0.4	101.00	0.1	125.5
164	0 (Semi-infinite)	0.4	101.50	0.1	124.8
165	0 (Semi-infinite)	0.4	102.00	0.1	124.2
166	0 (Semi-infinite)	0.4	102.50	0.1	123.6
167	0 (Semi-infinite)	0.4	103.00	0.1	123.0
168	0 (Semi-infinite)	0.4	103.50	0.1	122.4
169	0 (Semi-infinite)	0.4	104.00	0.1	121.8
170	0 (Semi-infinite)	0.4	104.50	0.1	121.3
171	0 (Semi-infinite)	0.4	105.00	0.1	120.7
172	0 (Semi-infinite)	0.4	105.50	0.1	120.1
173	0 (Semi-infinite)	0.4	106.00	0.1	119.5
174	0 (Semi-infinite)	0.4	106.50	0.1	119.0
175	0 (Semi-infinite)	0.4	107.00	0.1	118.4
176	0 (Semi-infinite)	0.4	107.50	0.1	117.9
177	0 (Semi-infinite)	0.4	108.00	0.1	117.3
178	0 (Semi-infinite)	0.4	108.50	0.1	116.8
179	0 (Semi-infinite)	0.4	109.00	0.1	116.2

N° of simulations	Thickness (mm)	Poisson's Ratio	Modulus (MPa)	Point of analysis	Elastic Deflection (z) μm
180	0 (Semi-infinite)	0.4	109.50	0.1	115.7
181	0 (Semi-infinite)	0.4	110.00	0.1	115.2
182	0 (Semi-infinite)	0.4	110.50	0.1	114.7
183	0 (Semi-infinite)	0.4	111.00	0.1	114.2
184	0 (Semi-infinite)	0.4	111.50	0.1	113.6
185	0 (Semi-infinite)	0.4	112.00	0.1	113.1
186	0 (Semi-infinite)	0.4	112.50	0.1	112.6
187	0 (Semi-infinite)	0.4	113.00	0.1	112.1
188	0 (Semi-infinite)	0.4	113.50	0.1	111.6
189	0 (Semi-infinite)	0.4	114.00	0.1	111.1
190	0 (Semi-infinite)	0.4	114.50	0.1	110.7
191	0 (Semi-infinite)	0.4	115.00	0.1	110.2
192	0 (Semi-infinite)	0.4	115.50	0.1	109.7
193	0 (Semi-infinite)	0.4	116.00	0.1	109.2
194	0 (Semi-infinite)	0.4	116.50	0.1	108.8
195	0 (Semi-infinite)	0.4	117.00	0.1	108.3
196	0 (Semi-infinite)	0.4	117.50	0.1	107.8
197	0 (Semi-infinite)	0.4	118.00	0.1	107.4
198	0 (Semi-infinite)	0.4	118.50	0.1	106.9
199	0 (Semi-infinite)	0.4	119.00	0.1	106.5
200	0 (Semi-infinite)	0.4	119.50	0.1	106.0
201	0 (Semi-infinite)	0.4	120.00	0.1	105.6
202	0 (Semi-infinite)	0.4	120.50	0.1	105.2
203	0 (Semi-infinite)	0.4	121.00	0.1	104.7
204	0 (Semi-infinite)	0.4	121.50	0.1	104.3
205	0 (Semi-infinite)	0.4	122.00	0.1	103.9
206	0 (Semi-infinite)	0.4	122.50	0.1	103.4
207	0 (Semi-infinite)	0.4	123.00	0.1	103.0
208	0 (Semi-infinite)	0.4	123.50	0.1	102.6
209	0 (Semi-infinite)	0.4	124.00	0.1	102.2
210	0 (Semi-infinite)	0.4	124.50	0.1	101.8
211	0 (Semi-infinite)	0.4	125.00	0.1	101.4
212	0 (Semi-infinite)	0.4	125.50	0.1	101.0
213	0 (Semi-infinite)	0.4	126.00	0.1	100.6
214	0 (Semi-infinite)	0.4	126.50	0.1	100.2
215	0 (Semi-infinite)	0.4	127.00	0.1	99.8
216	0 (Semi-infinite)	0.4	127.50	0.1	99.4
217	0 (Semi-infinite)	0.4	128.00	0.1	99.0
218	0 (Semi-infinite)	0.4	128.50	0.1	98.6
219	0 (Semi-infinite)	0.4	129.00	0.1	98.2
220	0 (Semi-infinite)	0.4	129.50	0.1	97.8
221	0 (Semi-infinite)	0.4	130.00	0.1	97.5
222	0 (Semi-infinite)	0.4	130.50	0.1	97.1
223	0 (Semi-infinite)	0.4	131.00	0.1	96.7
224	0 (Semi-infinite)	0.4	131.50	0.1	96.4

N° of simulations	Thickness (mm)	Poisson's Ratio	Modulus (MPa)	Point of analysis	Elastic Deflection (z) μm
225	0 (Semi-infinite)	0.4	132.00	0.1	96.0
226	0 (Semi-infinite)	0.4	132.50	0.1	95.6
227	0 (Semi-infinite)	0.4	133.00	0.1	95.3
228	0 (Semi-infinite)	0.4	133.50	0.1	94.9
229	0 (Semi-infinite)	0.4	134.00	0.1	94.6
230	0 (Semi-infinite)	0.4	134.50	0.1	94.2
231	0 (Semi-infinite)	0.4	135.00	0.1	93.9
232	0 (Semi-infinite)	0.4	135.50	0.1	93.5
233	0 (Semi-infinite)	0.4	136.00	0.1	93.2
234	0 (Semi-infinite)	0.4	136.50	0.1	92.8
235	0 (Semi-infinite)	0.4	137.00	0.1	92.5
236	0 (Semi-infinite)	0.4	137.50	0.1	92.2
237	0 (Semi-infinite)	0.4	138.00	0.1	91.8
238	0 (Semi-infinite)	0.4	138.50	0.1	91.5
239	0 (Semi-infinite)	0.4	139.00	0.1	91.2
240	0 (Semi-infinite)	0.4	139.50	0.1	90.8
241	0 (Semi-infinite)	0.4	140.00	0.1	90.5
242	0 (Semi-infinite)	0.4	140.50	0.1	90.2
243	0 (Semi-infinite)	0.4	141.00	0.1	89.9
244	0 (Semi-infinite)	0.4	141.50	0.1	89.6
245	0 (Semi-infinite)	0.4	142.00	0.1	89.2
246	0 (Semi-infinite)	0.4	142.50	0.1	88.9
247	0 (Semi-infinite)	0.4	143.00	0.1	88.6
248	0 (Semi-infinite)	0.4	143.50	0.1	88.3
249	0 (Semi-infinite)	0.4	144.00	0.1	88.0
250	0 (Semi-infinite)	0.4	144.50	0.1	87.7
251	0 (Semi-infinite)	0.4	145.00	0.1	87.4
252	0 (Semi-infinite)	0.4	145.50	0.1	87.1
253	0 (Semi-infinite)	0.4	146.00	0.1	86.8
254	0 (Semi-infinite)	0.4	146.50	0.1	86.5
255	0 (Semi-infinite)	0.4	147.00	0.1	86.2
256	0 (Semi-infinite)	0.4	147.50	0.1	85.9
257	0 (Semi-infinite)	0.4	148.00	0.1	85.6
258	0 (Semi-infinite)	0.4	148.50	0.1	85.3
259	0 (Semi-infinite)	0.4	149.00	0.1	85.0
260	0 (Semi-infinite)	0.4	149.50	0.1	84.8
261	0 (Semi-infinite)	0.4	150.00	0.1	84.5
262	0 (Semi-infinite)	0.4	150.50	0.1	84.2
263	0 (Semi-infinite)	0.4	151.00	0.1	83.9
264	0 (Semi-infinite)	0.4	151.50	0.1	83.6
265	0 (Semi-infinite)	0.4	152.00	0.1	83.4
266	0 (Semi-infinite)	0.4	152.50	0.1	83.1
267	0 (Semi-infinite)	0.4	153.00	0.1	82.8
268	0 (Semi-infinite)	0.4	153.50	0.1	82.6
269	0 (Semi-infinite)	0.4	154.00	0.1	82.3

N° of simulations	Thickness (mm)	Poisson's Ratio	Modulus (MPa)	Point of analysis	Elastic Deflection (z) μm
270	0 (Semi-infinite)	0.4	154.50	0.1	82.0
271	0 (Semi-infinite)	0.4	155.00	0.1	81.8
272	0 (Semi-infinite)	0.4	155.50	0.1	81.5
273	0 (Semi-infinite)	0.4	156.00	0.1	81.2
274	0 (Semi-infinite)	0.4	156.50	0.1	81.0
275	0 (Semi-infinite)	0.4	157.00	0.1	80.7
276	0 (Semi-infinite)	0.4	157.50	0.1	80.5
277	0 (Semi-infinite)	0.4	158.00	0.1	80.2
278	0 (Semi-infinite)	0.4	158.50	0.1	79.9
279	0 (Semi-infinite)	0.4	159.00	0.1	79.7
280	0 (Semi-infinite)	0.4	159.50	0.1	79.4
281	0 (Semi-infinite)	0.4	160.00	0.1	79.2
282	0 (Semi-infinite)	0.4	160.50	0.1	79.0
283	0 (Semi-infinite)	0.4	161.00	0.1	78.7
284	0 (Semi-infinite)	0.4	161.50	0.1	78.5
285	0 (Semi-infinite)	0.4	162.00	0.1	78.2
286	0 (Semi-infinite)	0.4	162.50	0.1	78.0
287	0 (Semi-infinite)	0.4	163.00	0.1	77.7
288	0 (Semi-infinite)	0.4	163.50	0.1	77.5
289	0 (Semi-infinite)	0.4	164.00	0.1	77.3
290	0 (Semi-infinite)	0.4	164.50	0.1	77.0
291	0 (Semi-infinite)	0.4	165.00	0.1	76.8
292	0 (Semi-infinite)	0.4	165.50	0.1	76.6
293	0 (Semi-infinite)	0.4	166.00	0.1	76.3
294	0 (Semi-infinite)	0.4	166.50	0.1	76.1
295	0 (Semi-infinite)	0.4	167.00	0.1	75.9
296	0 (Semi-infinite)	0.4	167.50	0.1	75.7
297	0 (Semi-infinite)	0.4	168.00	0.1	75.4
298	0 (Semi-infinite)	0.4	168.50	0.1	75.2
299	0 (Semi-infinite)	0.4	169.00	0.1	75.0
300	0 (Semi-infinite)	0.4	169.50	0.1	74.8
301	0 (Semi-infinite)	0.4	170.00	0.1	74.5
302	0 (Semi-infinite)	0.4	170.50	0.1	74.3
303	0 (Semi-infinite)	0.4	171.00	0.1	74.1
304	0 (Semi-infinite)	0.4	171.50	0.1	73.9
305	0 (Semi-infinite)	0.4	172.00	0.1	73.7
306	0 (Semi-infinite)	0.4	172.50	0.1	73.5
307	0 (Semi-infinite)	0.4	173.00	0.1	73.2
308	0 (Semi-infinite)	0.4	173.50	0.1	73.0
309	0 (Semi-infinite)	0.4	174.00	0.1	72.8
310	0 (Semi-infinite)	0.4	174.50	0.1	72.6
311	0 (Semi-infinite)	0.4	175.00	0.1	72.4
312	0 (Semi-infinite)	0.4	175.50	0.1	72.2
313	0 (Semi-infinite)	0.4	176.00	0.1	72.0
314	0 (Semi-infinite)	0.4	176.50	0.1	71.8

N° of simulations	Thickness (mm)	Poisson's Ratio	Modulus (MPa)	Point of analysis	Elastic Deflection (z) μm
315	0 (Semi-infinite)	0.4	177.00	0.1	71.6
316	0 (Semi-infinite)	0.4	177.50	0.1	71.4
317	0 (Semi-infinite)	0.4	178.00	0.1	71.2
318	0 (Semi-infinite)	0.4	178.50	0.1	71.0
319	0 (Semi-infinite)	0.4	179.00	0.1	70.8
320	0 (Semi-infinite)	0.4	179.50	0.1	70.6
321	0 (Semi-infinite)	0.4	180.00	0.1	70.4
322	0 (Semi-infinite)	0.4	180.50	0.1	70.2
323	0 (Semi-infinite)	0.4	181.00	0.1	70.0
324	0 (Semi-infinite)	0.4	181.50	0.1	69.8
325	0 (Semi-infinite)	0.4	182.00	0.1	69.6
326	0 (Semi-infinite)	0.4	182.50	0.1	69.4
327	0 (Semi-infinite)	0.4	183.00	0.1	69.2
328	0 (Semi-infinite)	0.4	183.50	0.1	69.1
329	0 (Semi-infinite)	0.4	184.00	0.1	68.9
330	0 (Semi-infinite)	0.4	184.50	0.1	68.7
331	0 (Semi-infinite)	0.4	185.00	0.1	68.5
332	0 (Semi-infinite)	0.4	185.50	0.1	68.3
333	0 (Semi-infinite)	0.4	186.00	0.1	68.1
334	0 (Semi-infinite)	0.4	186.50	0.1	67.9
335	0 (Semi-infinite)	0.4	187.00	0.1	67.8
336	0 (Semi-infinite)	0.4	187.50	0.1	67.6
337	0 (Semi-infinite)	0.4	188.00	0.1	67.4
338	0 (Semi-infinite)	0.4	188.50	0.1	67.2
339	0 (Semi-infinite)	0.4	189.00	0.1	67.0
340	0 (Semi-infinite)	0.4	189.50	0.1	66.9
341	0 (Semi-infinite)	0.4	190.00	0.1	66.7
342	0 (Semi-infinite)	0.4	190.50	0.1	66.5
343	0 (Semi-infinite)	0.4	191.00	0.1	66.3
344	0 (Semi-infinite)	0.4	191.50	0.1	66.2
345	0 (Semi-infinite)	0.4	192.00	0.1	66.0
346	0 (Semi-infinite)	0.4	192.50	0.1	65.8
347	0 (Semi-infinite)	0.4	193.00	0.1	65.7
348	0 (Semi-infinite)	0.4	193.50	0.1	65.5
349	0 (Semi-infinite)	0.4	194.00	0.1	65.3
350	0 (Semi-infinite)	0.4	194.50	0.1	65.2
351	0 (Semi-infinite)	0.4	195.00	0.1	65.0
352	0 (Semi-infinite)	0.4	195.50	0.1	64.8
353	0 (Semi-infinite)	0.4	196.00	0.1	64.7
354	0 (Semi-infinite)	0.4	196.50	0.1	64.5
355	0 (Semi-infinite)	0.4	197.00	0.1	64.3
356	0 (Semi-infinite)	0.4	197.50	0.1	64.2
357	0 (Semi-infinite)	0.4	198.00	0.1	64.0
358	0 (Semi-infinite)	0.4	198.50	0.1	63.8
359	0 (Semi-infinite)	0.4	199.00	0.1	63.7

N° of simulations	Thickness (mm)	Poisson's Ratio	Modulus (MPa)	Point of analysis	Elastic Deflection (z) μm
360	0 (Semi-infinite)	0.4	199.50	0.1	63.5
361	0 (Semi-infinite)	0.4	200.00	0.1	63.4
362	0 (Semi-infinite)	0.4	200.50	0.1	63.2
363	0 (Semi-infinite)	0.4	201.00	0.1	63.0
364	0 (Semi-infinite)	0.4	201.50	0.1	62.9
365	0 (Semi-infinite)	0.4	202.00	0.1	62.7
366	0 (Semi-infinite)	0.4	202.50	0.1	62.6
367	0 (Semi-infinite)	0.4	203.00	0.1	62.4
368	0 (Semi-infinite)	0.4	203.50	0.1	62.3
369	0 (Semi-infinite)	0.4	204.00	0.1	62.1
370	0 (Semi-infinite)	0.4	204.50	0.1	62.0
371	0 (Semi-infinite)	0.4	205.00	0.1	61.8
372	0 (Semi-infinite)	0.4	205.50	0.1	61.7
373	0 (Semi-infinite)	0.4	206.00	0.1	61.5
374	0 (Semi-infinite)	0.4	206.50	0.1	61.4
375	0 (Semi-infinite)	0.4	207.00	0.1	61.2
376	0 (Semi-infinite)	0.4	207.50	0.1	61.1
377	0 (Semi-infinite)	0.4	208.00	0.1	60.9
378	0 (Semi-infinite)	0.4	208.50	0.1	60.8
379	0 (Semi-infinite)	0.4	209.00	0.1	60.6
380	0 (Semi-infinite)	0.4	209.50	0.1	60.5
381	0 (Semi-infinite)	0.4	210.00	0.1	60.3
382	0 (Semi-infinite)	0.4	210.50	0.1	60.2
383	0 (Semi-infinite)	0.4	211.00	0.1	60.1
384	0 (Semi-infinite)	0.4	211.50	0.1	59.9
385	0 (Semi-infinite)	0.4	212.00	0.1	59.8
386	0 (Semi-infinite)	0.4	212.50	0.1	59.6
387	0 (Semi-infinite)	0.4	213.00	0.1	59.5
388	0 (Semi-infinite)	0.4	213.50	0.1	59.4
389	0 (Semi-infinite)	0.4	214.00	0.1	59.2
390	0 (Semi-infinite)	0.4	214.50	0.1	59.1
391	0 (Semi-infinite)	0.4	215.00	0.1	58.9
392	0 (Semi-infinite)	0.4	215.50	0.1	58.8
393	0 (Semi-infinite)	0.4	216.00	0.1	58.7
394	0 (Semi-infinite)	0.4	216.50	0.1	58.5
395	0 (Semi-infinite)	0.4	217.00	0.1	58.4
396	0 (Semi-infinite)	0.4	217.50	0.1	58.3
397	0 (Semi-infinite)	0.4	218.00	0.1	58.1
398	0 (Semi-infinite)	0.4	218.50	0.1	58.0
399	0 (Semi-infinite)	0.4	219.00	0.1	57.9
400	0 (Semi-infinite)	0.4	219.50	0.1	57.7
401	0 (Semi-infinite)	0.4	220.00	0.1	57.6
402	0 (Semi-infinite)	0.4	220.50	0.1	57.5
403	0 (Semi-infinite)	0.4	221.00	0.1	57.3
404	0 (Semi-infinite)	0.4	221.50	0.1	57.2

N° of simulations	Thickness (mm)	Poisson's Ratio	Modulus (MPa)	Point of analysis	Elastic Deflection (z) μm
405	0 (Semi-infinite)	0.4	222.00	0.1	57.1
406	0 (Semi-infinite)	0.4	222.50	0.1	57.0
407	0 (Semi-infinite)	0.4	223.00	0.1	56.8
408	0 (Semi-infinite)	0.4	223.50	0.1	56.7
409	0 (Semi-infinite)	0.4	224.00	0.1	56.6
410	0 (Semi-infinite)	0.4	224.50	0.1	56.4
411	0 (Semi-infinite)	0.4	225.00	0.1	56.3
412	0 (Semi-infinite)	0.4	225.50	0.1	56.2
413	0 (Semi-infinite)	0.4	226.00	0.1	56.1
414	0 (Semi-infinite)	0.4	226.50	0.1	55.9
415	0 (Semi-infinite)	0.4	227.00	0.1	55.8
416	0 (Semi-infinite)	0.4	227.50	0.1	55.7
417	0 (Semi-infinite)	0.4	228.00	0.1	55.6
418	0 (Semi-infinite)	0.4	228.50	0.1	55.5
419	0 (Semi-infinite)	0.4	229.00	0.1	55.3
420	0 (Semi-infinite)	0.4	229.50	0.1	55.2
421	0 (Semi-infinite)	0.4	230.00	0.1	55.1
422	0 (Semi-infinite)	0.4	230.50	0.1	55.0
423	0 (Semi-infinite)	0.4	231.00	0.1	54.9
424	0 (Semi-infinite)	0.4	231.50	0.1	54.7
425	0 (Semi-infinite)	0.4	232.00	0.1	54.6
426	0 (Semi-infinite)	0.4	232.50	0.1	54.5
427	0 (Semi-infinite)	0.4	233.00	0.1	54.4
428	0 (Semi-infinite)	0.4	233.50	0.1	54.3
429	0 (Semi-infinite)	0.4	234.00	0.1	54.2
430	0 (Semi-infinite)	0.4	234.50	0.1	54.0
431	0 (Semi-infinite)	0.4	235.00	0.1	53.9
432	0 (Semi-infinite)	0.4	235.50	0.1	53.8
433	0 (Semi-infinite)	0.4	236.00	0.1	53.7
434	0 (Semi-infinite)	0.4	236.50	0.1	53.6
435	0 (Semi-infinite)	0.4	237.00	0.1	53.5
436	0 (Semi-infinite)	0.4	237.50	0.1	53.4
437	0 (Semi-infinite)	0.4	238.00	0.1	53.2
438	0 (Semi-infinite)	0.4	238.50	0.1	53.1
439	0 (Semi-infinite)	0.4	239.00	0.1	53.0
440	0 (Semi-infinite)	0.4	239.50	0.1	52.9
441	0 (Semi-infinite)	0.4	240.00	0.1	52.8
442	0 (Semi-infinite)	0.4	240.50	0.1	52.7
443	0 (Semi-infinite)	0.4	241.00	0.1	52.6
444	0 (Semi-infinite)	0.4	241.50	0.1	52.5
445	0 (Semi-infinite)	0.4	242.00	0.1	52.4
446	0 (Semi-infinite)	0.4	242.50	0.1	52.3
447	0 (Semi-infinite)	0.4	243.00	0.1	52.1
448	0 (Semi-infinite)	0.4	243.50	0.1	52.0
449	0 (Semi-infinite)	0.4	244.00	0.1	51.9

N° of simulations	Thickness (mm)	Poisson's Ratio	Modulus (MPa)	Point of analysis	Elastic Deflection (z) μm
450	0 (Semi-infinite)	0.4	244.50	0.1	51.8
451	0 (Semi-infinite)	0.4	245.00	0.1	51.7
452	0 (Semi-infinite)	0.4	245.50	0.1	51.6
453	0 (Semi-infinite)	0.4	246.00	0.1	51.5
454	0 (Semi-infinite)	0.4	246.50	0.1	51.4
455	0 (Semi-infinite)	0.4	247.00	0.1	51.3
456	0 (Semi-infinite)	0.4	247.50	0.1	51.2
457	0 (Semi-infinite)	0.4	248.00	0.1	51.1
458	0 (Semi-infinite)	0.4	248.50	0.1	51.0
459	0 (Semi-infinite)	0.4	249.00	0.1	50.9
460	0 (Semi-infinite)	0.4	249.50	0.1	50.8
461	0 (Semi-infinite)	0.4	250.00	0.1	50.7
462	0 (Semi-infinite)	0.4	250.50	0.1	50.6
463	0 (Semi-infinite)	0.4	251.00	0.1	50.5
464	0 (Semi-infinite)	0.4	251.50	0.1	50.4
465	0 (Semi-infinite)	0.4	252.00	0.1	50.3
466	0 (Semi-infinite)	0.4	252.50	0.1	50.2
467	0 (Semi-infinite)	0.4	253.00	0.1	50.1
468	0 (Semi-infinite)	0.4	253.50	0.1	50.0
469	0 (Semi-infinite)	0.4	254.00	0.1	49.9
470	0 (Semi-infinite)	0.4	254.50	0.1	49.8
471	0 (Semi-infinite)	0.4	255.00	0.1	49.7
472	0 (Semi-infinite)	0.4	255.50	0.1	49.6
473	0 (Semi-infinite)	0.4	256.00	0.1	49.5
474	0 (Semi-infinite)	0.4	256.50	0.1	49.4
475	0 (Semi-infinite)	0.4	257.00	0.1	49.3
476	0 (Semi-infinite)	0.4	257.50	0.1	49.2
477	0 (Semi-infinite)	0.4	258.00	0.1	49.1
478	0 (Semi-infinite)	0.4	258.50	0.1	49.0
479	0 (Semi-infinite)	0.4	259.00	0.1	48.9
480	0 (Semi-infinite)	0.4	259.50	0.1	48.8
481	0 (Semi-infinite)	0.4	260.00	0.1	48.7
482	0 (Semi-infinite)	0.4	260.50	0.1	48.6
483	0 (Semi-infinite)	0.4	261.00	0.1	48.6
484	0 (Semi-infinite)	0.4	261.50	0.1	48.5
485	0 (Semi-infinite)	0.4	262.00	0.1	48.4
486	0 (Semi-infinite)	0.4	262.50	0.1	48.3
487	0 (Semi-infinite)	0.4	263.00	0.1	48.2
488	0 (Semi-infinite)	0.4	263.50	0.1	48.1
489	0 (Semi-infinite)	0.4	264.00	0.1	48.0
490	0 (Semi-infinite)	0.4	264.50	0.1	47.9
491	0 (Semi-infinite)	0.4	265.00	0.1	47.8
492	0 (Semi-infinite)	0.4	265.50	0.1	47.7
493	0 (Semi-infinite)	0.4	266.00	0.1	47.6
494	0 (Semi-infinite)	0.4	266.50	0.1	47.6

N° of simulations	Thickness (mm)	Poisson's Ratio	Modulus (MPa)	Point of analysis	Elastic Deflection (z) μm
495	0 (Semi-infinite)	0.4	267.00	0.1	47.5
496	0 (Semi-infinite)	0.4	267.50	0.1	47.4
497	0 (Semi-infinite)	0.4	268.00	0.1	47.3
498	0 (Semi-infinite)	0.4	268.50	0.1	47.2
499	0 (Semi-infinite)	0.4	269.00	0.1	47.1
500	0 (Semi-infinite)	0.4	269.50	0.1	47.0
501	0 (Semi-infinite)	0.4	270.00	0.1	46.9
502	0 (Semi-infinite)	0.4	270.50	0.1	46.8
503	0 (Semi-infinite)	0.4	271.00	0.1	46.8
504	0 (Semi-infinite)	0.4	271.50	0.1	46.7
505	0 (Semi-infinite)	0.4	272.00	0.1	46.6
506	0 (Semi-infinite)	0.4	272.50	0.1	46.5
507	0 (Semi-infinite)	0.4	273.00	0.1	46.4
508	0 (Semi-infinite)	0.4	273.50	0.1	46.3
509	0 (Semi-infinite)	0.4	274.00	0.1	46.2
510	0 (Semi-infinite)	0.4	274.50	0.1	46.2
511	0 (Semi-infinite)	0.4	275.00	0.1	46.1
512	0 (Semi-infinite)	0.4	275.50	0.1	46.0
513	0 (Semi-infinite)	0.4	276.00	0.1	45.9
514	0 (Semi-infinite)	0.4	276.50	0.1	45.8
515	0 (Semi-infinite)	0.4	277.00	0.1	45.7
516	0 (Semi-infinite)	0.4	277.50	0.1	45.7
517	0 (Semi-infinite)	0.4	278.00	0.1	45.6
518	0 (Semi-infinite)	0.4	278.50	0.1	45.5
519	0 (Semi-infinite)	0.4	279.00	0.1	45.4
520	0 (Semi-infinite)	0.4	279.50	0.1	45.3
521	0 (Semi-infinite)	0.4	280.00	0.1	45.3
522	0 (Semi-infinite)	0.4	280.50	0.1	45.2
523	0 (Semi-infinite)	0.4	281.00	0.1	45.1
524	0 (Semi-infinite)	0.4	281.50	0.1	45.0
525	0 (Semi-infinite)	0.4	282.00	0.1	44.9
526	0 (Semi-infinite)	0.4	282.50	0.1	44.9
527	0 (Semi-infinite)	0.4	283.00	0.1	44.8
528	0 (Semi-infinite)	0.4	283.50	0.1	44.7
529	0 (Semi-infinite)	0.4	284.00	0.1	44.6
530	0 (Semi-infinite)	0.4	284.50	0.1	44.5
531	0 (Semi-infinite)	0.4	285.00	0.1	44.5
532	0 (Semi-infinite)	0.4	285.50	0.1	44.4
533	0 (Semi-infinite)	0.4	286.00	0.1	44.3
534	0 (Semi-infinite)	0.4	286.50	0.1	44.2
535	0 (Semi-infinite)	0.4	287.00	0.1	44.2
536	0 (Semi-infinite)	0.4	287.50	0.1	44.1
537	0 (Semi-infinite)	0.4	288.00	0.1	44.0
538	0 (Semi-infinite)	0.4	288.50	0.1	43.9
539	0 (Semi-infinite)	0.4	289.00	0.1	43.8

N° of simulations	Thickness (mm)	Poisson's Ratio	Modulus (MPa)	Point of analysis	Elastic Deflection (z) μm
540	0 (Semi-infinite)	0.4	289.50	0.1	43.8
541	0 (Semi-infinite)	0.4	290.00	0.1	43.7
542	0 (Semi-infinite)	0.4	290.50	0.1	43.6
543	0 (Semi-infinite)	0.4	291.00	0.1	43.5
544	0 (Semi-infinite)	0.4	291.50	0.1	43.5
545	0 (Semi-infinite)	0.4	292.00	0.1	43.4
546	0 (Semi-infinite)	0.4	292.50	0.1	43.3
547	0 (Semi-infinite)	0.4	293.00	0.1	43.3
548	0 (Semi-infinite)	0.4	293.50	0.1	43.2
549	0 (Semi-infinite)	0.4	294.00	0.1	43.1
550	0 (Semi-infinite)	0.4	294.50	0.1	43.0
551	0 (Semi-infinite)	0.4	295.00	0.1	43.0
552	0 (Semi-infinite)	0.4	295.50	0.1	42.9
553	0 (Semi-infinite)	0.4	296.00	0.1	42.8
554	0 (Semi-infinite)	0.4	296.50	0.1	42.7
555	0 (Semi-infinite)	0.4	297.00	0.1	42.7
556	0 (Semi-infinite)	0.4	297.50	0.1	42.6
557	0 (Semi-infinite)	0.4	298.00	0.1	42.5
558	0 (Semi-infinite)	0.4	298.50	0.1	42.5
559	0 (Semi-infinite)	0.4	299.00	0.1	42.4
560	0 (Semi-infinite)	0.4	299.50	0.1	42.3
561	0 (Semi-infinite)	0.4	300.00	0.1	42.2
562	0 (Semi-infinite)	0.4	300.50	0.1	42.2
563	0 (Semi-infinite)	0.4	301.00	0.1	42.1
564	0 (Semi-infinite)	0.4	301.50	0.1	42.0
565	0 (Semi-infinite)	0.4	302.00	0.1	42.0
566	0 (Semi-infinite)	0.4	302.50	0.1	41.9
567	0 (Semi-infinite)	0.4	303.00	0.1	41.8
568	0 (Semi-infinite)	0.4	303.50	0.1	41.8
569	0 (Semi-infinite)	0.4	304.00	0.1	41.7
570	0 (Semi-infinite)	0.4	304.50	0.1	41.6
571	0 (Semi-infinite)	0.4	305.00	0.1	41.5
572	0 (Semi-infinite)	0.4	305.50	0.1	41.5
573	0 (Semi-infinite)	0.4	306.00	0.1	41.4
574	0 (Semi-infinite)	0.4	306.50	0.1	41.3
575	0 (Semi-infinite)	0.4	307.00	0.1	41.3
576	0 (Semi-infinite)	0.4	307.50	0.1	41.2
577	0 (Semi-infinite)	0.4	308.00	0.1	41.1
578	0 (Semi-infinite)	0.4	308.50	0.1	41.1
579	0 (Semi-infinite)	0.4	309.00	0.1	41.0
580	0 (Semi-infinite)	0.4	309.50	0.1	40.9
581	0 (Semi-infinite)	0.4	310.00	0.1	40.9
582	0 (Semi-infinite)	0.4	310.50	0.1	40.8
583	0 (Semi-infinite)	0.4	311.00	0.1	40.7
584	0 (Semi-infinite)	0.4	311.50	0.1	40.7

N° of simulations	Thickness (mm)	Poisson's Ratio	Modulus (MPa)	Point of analysis	Elastic Deflection (z) μm
585	0 (Semi-infinite)	0.4	312.00	0.1	40.6
586	0 (Semi-infinite)	0.4	312.50	0.1	40.6
587	0 (Semi-infinite)	0.4	313.00	0.1	40.5
588	0 (Semi-infinite)	0.4	313.50	0.1	40.4
589	0 (Semi-infinite)	0.4	314.00	0.1	40.4
590	0 (Semi-infinite)	0.4	314.50	0.1	40.3
591	0 (Semi-infinite)	0.4	315.00	0.1	40.2
592	0 (Semi-infinite)	0.4	315.50	0.1	40.2
593	0 (Semi-infinite)	0.4	316.00	0.1	40.1
594	0 (Semi-infinite)	0.4	316.50	0.1	40.0
595	0 (Semi-infinite)	0.4	317.00	0.1	40.0
596	0 (Semi-infinite)	0.4	317.50	0.1	39.9
597	0 (Semi-infinite)	0.4	318.00	0.1	39.9
598	0 (Semi-infinite)	0.4	318.50	0.1	39.8
599	0 (Semi-infinite)	0.4	319.00	0.1	39.7
600	0 (Semi-infinite)	0.4	319.50	0.1	39.7
601	0 (Semi-infinite)	0.4	320.00	0.1	39.6

APPENDIX B

PARAMETRIC NUMERICAL STUDY

Simul.	Thickness (mm)			Poisson's Ratio				Modulus (MPa)				Point of analyses (mm)				D0 (μm)	$\mu\epsilon_t$	$\mu\epsilon$	$\mu\epsilon_v$	
	AC	Base	Subbase	Seleted Sub.	AC	Base	Subbase	Seleted Sub.	AC	Base	Subbase	Seleted Sub.								
1	140	90	150	0	0.3	0.35	0.25	0.40	3000	100	2000	200	0.1	139.9	229.9	380.1	54.8	354.8	77	134.3
2	140	90	150	0	0.3	0.35	0.25	0.40	3000	100	2000	300	0.1	139.9	229.9	380.1	49.5	350.1	50	96.2
3	140	90	150	0	0.3	0.35	0.25	0.40	3000	100	2000	400	0.1	139.9	229.9	380.1	46.7	347.6	35	75.0
4	140	90	150	0	0.3	0.35	0.25	0.40	3000	100	4000	200	0.1	139.9	229.9	380.1	54.3	353.3	145	119.9
5	140	90	150	0	0.3	0.35	0.25	0.40	3000	100	4000	300	0.1	139.9	229.9	380.1	49.2	349.2	103	87.9
6	140	90	150	0	0.3	0.35	0.25	0.40	3000	100	4000	400	0.1	139.9	229.9	380.1	46.5	346.9	78	69.7
7	140	90	150	0	0.3	0.35	0.25	0.40	3000	100	6000	200	0.1	139.9	229.9	380.1	54.0	352.3	200	109.9
8	140	90	150	0	0.3	0.35	0.25	0.40	3000	100	6000	300	0.1	139.9	229.9	380.1	48.9	348.6	147	81.7
9	140	90	150	0	0.3	0.35	0.25	0.40	3000	100	6000	400	0.1	139.9	229.9	380.1	46.3	346.5	115	65.4
10	140	90	150	0	0.3	0.35	0.25	0.40	3000	100	8000	200	0.1	139.9	229.9	380.1	53.7	351.5	247	102.2
11	140	90	150	0	0.3	0.35	0.25	0.40	3000	100	8000	300	0.1	139.9	229.9	380.1	48.8	348.1	185	76.8
12	140	90	150	0	0.3	0.35	0.25	0.40	3000	100	8000	400	0.1	139.9	229.9	380.1	46.2	346.1	148	62.0
13	140	90	150	0	0.3	0.35	0.25	0.40	3000	100	10000	200	0.1	139.9	229.9	380.1	53.4	350.9	289	96.1
14	140	90	150	0	0.3	0.35	0.25	0.40	3000	100	10000	300	0.1	139.9	229.9	380.1	48.6	347.7	219	72.8
15	140	90	150	0	0.3	0.35	0.25	0.40	3000	100	10000	400	0.1	139.9	229.9	380.1	46.1	345.8	177	59.1
16	140	90	150	0	0.3	0.35	0.25	0.40	3000	200	2000	200	0.1	139.9	229.9	380.1	43.6	311.6	104	162.4
17	140	90	150	0	0.3	0.35	0.25	0.40	3000	200	2000	300	0.1	139.9	229.9	380.1	38.0	306.3	70	119.0
18	140	90	150	0	0.3	0.35	0.25	0.40	3000	200	2000	400	0.1	139.9	229.9	380.1	35.1	303.3	51	94.1
19	140	90	150	0	0.3	0.35	0.25	0.40	3000	200	4000	200	0.1	139.9	229.9	380.1	42.9	309.1	187	142.3
20	140	90	150	0	0.3	0.35	0.25	0.40	3000	200	4000	300	0.1	139.9	229.9	380.1	37.6	304.6	137	106.8
21	140	90	150	0	0.3	0.35	0.25	0.40	3000	200	4000	400	0.1	139.9	229.9	380.1	34.8	302.0	107	85.9
22	140	90	150	0	0.3	0.35	0.25	0.40	3000	200	6000	200	0.1	139.9	229.9	380.1	42.5	307.5	252	128.7
23	140	90	150	0	0.3	0.35	0.25	0.40	3000	200	6000	300	0.1	139.9	229.9	380.1	37.3	303.6	191	98.0
24	140	90	150	0	0.3	0.35	0.25	0.40	3000	200	6000	400	0.1	139.9	229.9	380.1	34.6	301.3	153	79.7
25	140	90	150	0	0.3	0.35	0.25	0.40	3000	200	8000	200	0.1	139.9	229.9	380.1	42.1	306.3	307	118.6
26	140	90	150	0	0.3	0.35	0.25	0.40	3000	200	8000	300	0.1	139.9	229.9	380.1	37.1	302.8	237	91.2
27	140	90	150	0	0.3	0.35	0.25	0.40	3000	200	8000	400	0.1	139.9	229.9	380.1	34.4	300.7	193	74.8
28	140	90	150	0	0.3	0.35	0.25	0.40	3000	200	10000	200	0.1	139.9	229.9	380.1	41.8	305.4	355	110.7
29	140	90	150	0	0.3	0.35	0.25	0.40	3000	200	10000	300	0.1	139.9	229.9	380.1	36.9	302.2	277	85.8
30	140	90	150	0	0.3	0.35	0.25	0.40	3000	200	10000	400	0.1	139.9	229.9	380.1	34.3	300.2	229	70.7
31	140	90	150	0	0.3	0.35	0.25	0.40	3000	300	2000	200	0.1	139.9	229.9	380.1	38.7	286.5	120	177.5
32	140	90	150	0	0.3	0.35	0.25	0.40	3000	300	2000	300	0.1	139.9	229.9	380.1	33.1	281.0	84	132.0
33	140	90	150	0	0.3	0.35	0.25	0.40	3000	300	2000	400	0.1	139.9	229.9	380.1	30.1	277.9	62	105.3
34	140	90	150	0	0.3	0.35	0.25	0.40	3000	300	4000	200	0.1	139.9	229.9	380.1	38.0	283.3	212	154.0
35	140	90	150	0	0.3	0.35	0.25	0.40	3000	300	4000	300	0.1	139.9	229.9	380.1	32.6	278.8	159	117.3
36	140	90	150	0	0.3	0.35	0.25	0.40	3000	300	4000	400	0.1	139.9	229.9	380.1	29.7	276.1	125	95.3
37	140	90	150	0	0.3	0.35	0.25	0.40	3000	300	6000	200	0.1	139.9	229.9	380.1	37.4	281.3	283	138.5
38	140	90	150	0	0.3	0.35	0.25	0.40	3000	300	6000	300	0.1	139.9	229.9	380.1	32.3	277.5	218	107.0
39	140	90	150	0	0.3	0.35	0.25	0.40	3000	300	6000	400	0.1	139.9	229.9	380.1	29.5	275.1	177	87.8
40	140	90	150	0	0.3	0.35	0.25	0.40	3000	300	8000	200	0.1	139.9	229.9	380.1	37.0	279.9	343	127.1
41	140	90	150	0	0.3	0.35	0.25	0.40	3000	300	8000	300	0.1	139.9	229.9	380.1	32.0	276.4	269	99.1
42	140	90	150	0	0.3	0.35	0.25	0.40	3000	300	8000	400	0.1	139.9	229.9	380.1	29.3	274.3	222	82.0
43	140	90	150	0	0.3	0.35	0.25	0.40	3000	300	10000	200	0.1	139.9	229.9	380.1	36.7	278.7	393	118.2
44	140	90	150	0	0.3	0.35	0.25	0.40	3000	300	10000	300	0.1	139.9	229.9	380.1	31.8	275.7	312	92.8
45	140	90	150	0	0.3	0.35	0.25	0.40	3000	300	10000	400	0.1	139.9	229.9	380.1	29.2	273.7	261	77.2
46	140	90	150	0	0.3	0.35	0.25	0.40	3000	400	2000	200	0.1	139.9	229.9	380.1	35.8	268.6	132	186.8
47	140	90	150	0	0.3	0.35	0.25	0.40	3000	400	2000	300	0.1	139.9	229.9	380.1	30.2	263.2	94	140.5
48	140	90	150	0	0.3	0.35	0.25	0.40	3000	400	2000	400	0.1	139.9	229.9	380.1	27.2	260.0	70	112.9
49	140	90	150	0	0.3	0.35	0.25	0.40	3000	400	4000	200	0.1	139.9	229.9	380.1	35.0	264.9	230	161.2
50	140	90	150	0	0.3	0.35	0.25	0.40	3000	400	4000	300	0.1	139.9	229.9	380.1	29.6	260.5	174	124.1
51	140	90	150	0	0.3	0.35	0.25	0.40	3000	400	4000	400	0.1	139.9	229.9	380.1	26.8	257.8	139	101.5
52	140	90	150	0	0.3	0.35	0.25	0.40	3000	400	6000	200	0.1	139.9	229.9	380.1	34.4	262.6	304	144.4
53	140	90	150	0	0.3	0.35	0.25	0.40	3000	400	6000	300	0.1	139.9	229.9	380.1	29.3	258.9	237	112.7
54	140	90	150	0	0.3	0.35	0.25	0.40	3000	400	6000	400	0.1	139.9	229.9	380.1	26.5	256.6	194	93.2
55	140	90	150	0	0.3	0.35	0.25	0.40	3000	400	8000	200	0.1	139.9	229.9	380.1	34.0	261.0	366	132.2
56	140	90	150	0	0.3	0.35	0.25	0.40	3000	400	8000	300	0.1	139.9	229.9	380.1	29.0	257.8	291	104.1
57	140	90	150	0	0.3	0.35	0.25	0.40	3000	400	8000	400	0.1	139.9	229.9	380.1	26.3	255.7	242	86.7
58	140	90	150	0	0.3	0.35	0.25	0.40	3000	400	10000	200	0.1	139.9	229.9	380.1	33.6	259.7	419	122.6
59	140	90	150	0	0.3	0.35	0.25	0.40	3000	400	10000	300	0.1	139.9	229.9	380.1	28.7	256.8	337	97.3
60	140	90	150	0	0.3	0.35	0.25	0.40	3000	400	10000	400	0.1	139.9	229.9	380.1	26.1	255.0	283	81.5

Simul.	Thickness (mm)				Poisson's Ratio				Modulus (MPa)				Point of analyses (mm)				D0 (μm)	$\mu\epsilon_t$	$\mu\epsilon$	$\mu\epsilon_v$
	AC	Base	Subbase	Seleted Sub.	AC	Base	Subbase	Seleted Sub.	AC	Base	Subbase	Seleted Sub.								
61	140	90	160	0	0.3	0.35	0.25	0.40	3000	100	2000	200	0.1	139.9	229.9	390.1	54.7	354.3	78	131.8
62	140	90	160	0	0.3	0.35	0.25	0.40	3000	100	2000	300	0.1	139.9	229.9	390.1	49.4	349.8	51	94.8
63	140	90	160	0	0.3	0.35	0.25	0.40	3000	100	2000	400	0.1	139.9	229.9	390.1	46.7	347.4	36	74.1
64	140	90	160	0	0.3	0.35	0.25	0.40	3000	100	4000	200	0.1	139.9	229.9	390.1	54.1	352.7	145	116.6
65	140	90	160	0	0.3	0.35	0.25	0.40	3000	100	4000	300	0.1	139.9	229.9	390.1	49.0	348.8	104	85.9
66	140	90	160	0	0.3	0.35	0.25	0.40	3000	100	4000	400	0.1	139.9	229.9	390.1	46.4	346.6	79	68.3
67	140	90	160	0	0.3	0.35	0.25	0.40	3000	100	6000	200	0.1	139.9	229.9	390.1	53.7	351.7	199	106.1
68	140	90	160	0	0.3	0.35	0.25	0.40	3000	100	6000	300	0.1	139.9	229.9	390.1	48.8	348.2	147	79.3
69	140	90	160	0	0.3	0.35	0.25	0.40	3000	100	6000	400	0.1	139.9	229.9	390.1	46.2	346.2	116	63.8
70	140	90	160	0	0.3	0.35	0.25	0.40	3000	100	8000	200	0.1	139.9	229.9	390.1	53.4	350.8	244	98.2
71	140	90	160	0	0.3	0.35	0.25	0.40	3000	100	8000	300	0.1	139.9	229.9	390.1	48.6	347.6	184	74.2
72	140	90	160	0	0.3	0.35	0.25	0.40	3000	100	8000	400	0.1	139.9	229.9	390.1	46.1	345.8	148	60.2
73	140	90	160	0	0.3	0.35	0.25	0.40	3000	100	10000	200	0.1	139.9	229.9	390.1	53.1	350.1	284	91.9
74	140	90	160	0	0.3	0.35	0.25	0.40	3000	100	10000	300	0.1	139.9	229.9	390.1	48.4	347.2	218	70.1
75	140	90	160	0	0.3	0.35	0.25	0.40	3000	100	10000	400	0.1	139.9	229.9	390.1	46.0	345.5	177	57.1
76	140	90	160	0	0.3	0.35	0.25	0.40	3000	200	2000	200	0.1	139.9	229.9	390.1	43.4	310.8	104	158.7
77	140	90	160	0	0.3	0.35	0.25	0.40	3000	200	2000	300	0.1	139.9	229.9	390.1	37.9	305.8	71	116.8
78	140	90	160	0	0.3	0.35	0.25	0.40	3000	200	2000	400	0.1	139.9	229.9	390.1	35.0	303.0	52	92.6
79	140	90	160	0	0.3	0.35	0.25	0.40	3000	200	4000	200	0.1	139.9	229.9	390.1	42.7	308.2	185	137.6
80	140	90	160	0	0.3	0.35	0.25	0.40	3000	200	4000	300	0.1	139.9	229.9	390.1	37.4	304.1	137	103.8
81	140	90	160	0	0.3	0.35	0.25	0.40	3000	200	4000	400	0.1	139.9	229.9	390.1	34.7	301.6	107	83.8
82	140	90	160	0	0.3	0.35	0.25	0.40	3000	200	6000	200	0.1	139.9	229.9	390.1	42.2	306.6	249	123.6
83	140	90	160	0	0.3	0.35	0.25	0.40	3000	200	6000	300	0.1	139.9	229.9	390.1	37.1	303.0	189	94.6
84	140	90	160	0	0.3	0.35	0.25	0.40	3000	200	6000	400	0.1	139.9	229.9	390.1	34.5	300.8	153	77.2
85	140	90	160	0	0.3	0.35	0.25	0.40	3000	200	8000	200	0.1	139.9	229.9	390.1	41.8	305.4	301	113.3
86	140	90	160	0	0.3	0.35	0.25	0.40	3000	200	8000	300	0.1	139.9	229.9	390.1	36.9	302.2	234	87.6
87	140	90	160	0	0.3	0.35	0.25	0.40	3000	200	8000	400	0.1	139.9	229.9	390.1	34.3	300.2	191	72.1
88	140	90	160	0	0.3	0.35	0.25	0.40	3000	200	10000	200	0.1	139.9	229.9	390.1	41.4	304.4	346	105.3
89	140	90	160	0	0.3	0.35	0.25	0.40	3000	200	10000	300	0.1	139.9	229.9	390.1	36.7	301.5	272	82.1
90	140	90	160	0	0.3	0.35	0.25	0.40	3000	200	10000	400	0.1	139.9	229.9	390.1	34.1	299.7	226	67.9
91	140	90	160	0	0.3	0.35	0.25	0.40	3000	300	2000	200	0.1	139.9	229.9	390.1	38.5	285.6	120	173.0
92	140	90	160	0	0.3	0.35	0.25	0.40	3000	300	2000	300	0.1	139.9	229.9	390.1	32.9	280.4	84	129.2
93	140	90	160	0	0.3	0.35	0.25	0.40	3000	300	2000	400	0.1	139.9	229.9	390.1	30.0	277.4	63	103.4
94	140	90	160	0	0.3	0.35	0.25	0.40	3000	300	4000	200	0.1	139.9	229.9	390.1	37.7	282.2	209	148.6
95	140	90	160	0	0.3	0.35	0.25	0.40	3000	300	4000	300	0.1	139.9	229.9	390.1	32.4	278.1	158	113.7
96	140	90	160	0	0.3	0.35	0.25	0.40	3000	300	4000	400	0.1	139.9	229.9	390.1	29.6	275.6	125	92.7
97	140	90	160	0	0.3	0.35	0.25	0.40	3000	300	6000	200	0.1	139.9	229.9	390.1	37.1	280.2	278	132.6
98	140	90	160	0	0.3	0.35	0.25	0.40	3000	300	6000	300	0.1	139.9	229.9	390.1	32.0	276.7	215	103.0
99	140	90	160	0	0.3	0.35	0.25	0.40	3000	300	6000	400	0.1	139.9	229.9	390.1	29.4	274.5	176	84.9
100	140	90	160	0	0.3	0.35	0.25	0.40	3000	300	8000	200	0.1	139.9	229.9	390.1	36.7	278.7	334	121.1
101	140	90	160	0	0.3	0.35	0.25	0.40	3000	300	8000	300	0.1	139.9	229.9	390.1	31.8	275.6	264	94.9
102	140	90	160	0	0.3	0.35	0.25	0.40	3000	300	8000	400	0.1	139.9	229.9	390.1	29.1	273.7	218	78.8
103	140	90	160	0	0.3	0.35	0.25	0.40	3000	300	10000	200	0.1	139.9	229.9	390.1	36.3	277.6	382	112.1
104	140	90	160	0	0.3	0.35	0.25	0.40	3000	300	10000	300	0.1	139.9	229.9	390.1	31.5	274.8	305	88.5
105	140	90	160	0	0.3	0.35	0.25	0.40	3000	300	10000	400	0.1	139.9	229.9	390.1	29.0	273.1	256	74.0
106	140	90	160	0	0.3	0.35	0.25	0.40	3000	400	2000	200	0.1	139.9	229.9	390.1	35.5	267.5	132	181.8
107	140	90	160	0	0.3	0.35	0.25	0.40	3000	400	2000	300	0.1	139.9	229.9	390.1	30.0	262.5	94	137.2
108	140	90	160	0	0.3	0.35	0.25	0.40	3000	400	2000	400	0.1	139.9	229.9	390.1	27.1	259.4	70	110.6
109	140	90	160	0	0.3	0.35	0.25	0.40	3000	400	4000	200	0.1	139.9	229.9	390.1	34.7	263.7	226	155.2
110	140	90	160	0	0.3	0.35	0.25	0.40	3000	400	4000	300	0.1	139.9	229.9	390.1	29.4	259.7	172	120.1
111	140	90	160	0	0.3	0.35	0.25	0.40	3000	400	4000	400	0.1	139.9	229.9	390.1	26.6	257.2	138	98.6
112	140	90	160	0	0.3	0.35	0.25	0.40	3000	400	6000	200	0.1	139.9	229.9	390.1	34.1	261.4	297	138.1
113	140	90	160	0	0.3	0.35	0.25	0.40	3000	400	6000	300	0.1	139.9	229.9	390.1	29.0	258.0	233	108.3
114	140	90	160	0	0.3	0.35	0.25	0.40	3000	400	6000	400	0.1	139.9	229.9	390.1	26.3	255.9	192	89.9
115	140	90	160	0	0.3	0.35	0.25	0.40	3000	400	8000	200	0.1	139.9	229.9	390.1	33.6	259.7	356	125.7
116	140	90	160	0	0.3	0.35	0.25	0.40	3000	400	8000	300	0.1	139.9	229.9	390.1	28.7	256.8	284	99.5
117	140	90	160	0	0.3	0.35	0.25	0.40	3000	400	8000	400	0.1	139.9	229.9	390.1	26.1	255.0	237	83.2
118	140	90	160	0	0.3	0.35	0.25	0.40	3000	400	10000	200	0.1	139.9	229.9	390.1	33.2	258.5	406	116.2
119	140	90	160	0	0.3	0.35	0.25	0.40	3000	400	10000	300	0.1	139.9	229.9	390.1	28.5	255.9	328	92.6
120	140	90	160	0	0.3	0.35	0.25	0.40	3000	400	10000	400	0.1	139.9	229.9	390.1	25.9	254.3	277	77.9

Simul.	Thickness (mm)				Poisson's Ratio				Modulus (MPa)				Point of analyses (mm)				D0 (μm)	$\mu\epsilon_t$	$\mu\epsilon$	$\mu\epsilon_v$
	AC	Base	Subbase	Seleted Sub.	AC	Base	Subbase	Seleted Sub.	AC	Base	Subbase	Seleted Sub.								
121	140	90	170	0	0.3	0.35	0.25	0.40	3000	100	2000	200	0.1	139.9	229.9	400.1	54.5	353.9	79	129.3
122	140	90	170	0	0.3	0.35	0.25	0.40	3000	100	2000	300	0.1	139.9	229.9	400.1	49.3	349.6	52	93.4
123	140	90	170	0	0.3	0.35	0.25	0.40	3000	100	2000	400	0.1	139.9	229.9	400.1	46.6	347.2	37	73.2
124	140	90	170	0	0.3	0.35	0.25	0.40	3000	100	4000	200	0.1	139.9	229.9	400.1	53.9	352.2	145	113.2
125	140	90	170	0	0.3	0.35	0.25	0.40	3000	100	4000	300	0.1	139.9	229.9	400.1	48.9	348.5	104	83.9
126	140	90	170	0	0.3	0.35	0.25	0.40	3000	100	4000	400	0.1	139.9	229.9	400.1	46.3	346.4	80	66.9
127	140	90	170	0	0.3	0.35	0.25	0.40	3000	100	6000	200	0.1	139.9	229.9	400.1	53.5	351.0	197	102.4
128	140	90	170	0	0.3	0.35	0.25	0.40	3000	100	6000	300	0.1	139.9	229.9	400.1	48.6	347.8	147	77.0
129	140	90	170	0	0.3	0.35	0.25	0.40	3000	100	6000	400	0.1	139.9	229.9	400.1	46.1	345.9	116	62.1
130	140	90	170	0	0.3	0.35	0.25	0.40	3000	100	8000	200	0.1	139.9	229.9	400.1	53.1	350.2	241	94.3
131	140	90	170	0	0.3	0.35	0.25	0.40	3000	100	8000	300	0.1	139.9	229.9	400.1	48.4	347.2	183	71.7
132	140	90	170	0	0.3	0.35	0.25	0.40	3000	100	8000	400	0.1	139.9	229.9	400.1	46.0	345.5	148	58.3
133	140	90	170	0	0.3	0.35	0.25	0.40	3000	100	10000	200	0.1	139.9	229.9	400.1	52.8	349.5	280	88.0
134	140	90	170	0	0.3	0.35	0.25	0.40	3000	100	10000	300	0.1	139.9	229.9	400.1	48.3	346.8	215	67.5
135	140	90	170	0	0.3	0.35	0.25	0.40	3000	100	10000	400	0.1	139.9	229.9	400.1	45.8	345.2	176	55.2
136	140	90	170	0	0.3	0.35	0.25	0.40	3000	200	2000	200	0.1	139.9	229.9	400.1	43.2	310.1	104	154.9
137	140	90	170	0	0.3	0.35	0.25	0.40	3000	200	2000	300	0.1	139.9	229.9	400.1	37.8	305.4	72	114.4
138	140	90	170	0	0.3	0.35	0.25	0.40	3000	200	2000	400	0.1	139.9	229.9	400.1	35.0	302.7	53	91.0
139	140	90	170	0	0.3	0.35	0.25	0.40	3000	200	4000	200	0.1	139.9	229.9	400.1	42.4	307.4	183	132.9
140	140	90	170	0	0.3	0.35	0.25	0.40	3000	200	4000	300	0.1	139.9	229.9	400.1	37.3	303.5	136	100.8
141	140	90	170	0	0.3	0.35	0.25	0.40	3000	200	4000	400	0.1	139.9	229.9	400.1	34.6	301.2	107	81.7
142	140	90	170	0	0.3	0.35	0.25	0.40	3000	200	6000	200	0.1	139.9	229.9	400.1	41.9	305.7	244	118.6
143	140	90	170	0	0.3	0.35	0.25	0.40	3000	200	6000	300	0.1	139.9	229.9	400.1	36.9	302.4	187	91.3
144	140	90	170	0	0.3	0.35	0.25	0.40	3000	200	6000	400	0.1	139.9	229.9	400.1	34.3	300.4	152	74.8
145	140	90	170	0	0.3	0.35	0.25	0.40	3000	200	8000	200	0.1	139.9	229.9	400.1	41.4	304.5	294	108.2
146	140	90	170	0	0.3	0.35	0.25	0.40	3000	200	8000	300	0.1	139.9	229.9	400.1	36.7	301.5	230	84.2
147	140	90	170	0	0.3	0.35	0.25	0.40	3000	200	8000	400	0.1	139.9	229.9	400.1	34.1	299.7	189	69.5
148	140	90	170	0	0.3	0.35	0.25	0.40	3000	200	10000	200	0.1	139.9	229.9	400.1	41.1	303.5	337	100.2
149	140	90	170	0	0.3	0.35	0.25	0.40	3000	200	10000	300	0.1	139.9	229.9	400.1	36.4	300.9	267	78.5
150	140	90	170	0	0.3	0.35	0.25	0.40	3000	200	10000	400	0.1	139.9	229.9	400.1	34.0	299.2	222	65.3
151	140	90	170	0	0.3	0.35	0.25	0.40	3000	300	2000	200	0.1	139.9	229.9	400.1	38.2	284.7	120	168.5
152	140	90	170	0	0.3	0.35	0.25	0.40	3000	300	2000	300	0.1	139.9	229.9	400.1	32.8	279.8	84	126.3
153	140	90	170	0	0.3	0.35	0.25	0.40	3000	300	2000	400	0.1	139.9	229.9	400.1	29.9	277.0	63	101.3
154	140	90	170	0	0.3	0.35	0.25	0.40	3000	300	4000	200	0.1	139.9	229.9	400.1	37.4	281.2	206	143.2
155	140	90	170	0	0.3	0.35	0.25	0.40	3000	300	4000	300	0.1	139.9	229.9	400.1	32.2	277.4	156	110.1
156	140	90	170	0	0.3	0.35	0.25	0.40	3000	300	4000	400	0.1	139.9	229.9	400.1	29.5	275.1	125	90.1
157	140	90	170	0	0.3	0.35	0.25	0.40	3000	300	6000	200	0.1	139.9	229.9	400.1	36.8	279.1	272	127.0
158	140	90	170	0	0.3	0.35	0.25	0.40	3000	300	6000	300	0.1	139.9	229.9	400.1	31.8	275.9	212	99.1
159	140	90	170	0	0.3	0.35	0.25	0.40	3000	300	6000	400	0.1	139.9	229.9	400.1	29.2	273.9	174	82.0
160	140	90	170	0	0.3	0.35	0.25	0.40	3000	300	8000	200	0.1	139.9	229.9	400.1	36.3	277.7	325	115.4
161	140	90	170	0	0.3	0.35	0.25	0.40	3000	300	8000	300	0.1	139.9	229.9	400.1	31.5	274.9	258	90.9
162	140	90	170	0	0.3	0.35	0.25	0.40	3000	300	8000	400	0.1	139.9	229.9	400.1	29.0	273.1	215	75.8
163	140	90	170	0	0.3	0.35	0.25	0.40	3000	300	10000	200	0.1	139.9	229.9	400.1	35.9	276.5	371	106.4
164	140	90	170	0	0.3	0.35	0.25	0.40	3000	300	10000	300	0.1	139.9	229.9	400.1	31.3	274.1	298	84.5
165	140	90	170	0	0.3	0.35	0.25	0.40	3000	300	10000	400	0.1	139.9	229.9	400.1	28.8	272.5	250	70.9
166	140	90	170	0	0.3	0.35	0.25	0.40	3000	400	2000	200	0.1	139.9	229.9	400.1	35.3	266.5	130	176.8
167	140	90	170	0	0.3	0.35	0.25	0.40	3000	400	2000	300	0.1	139.9	229.9	400.1	29.9	261.8	93	133.9
168	140	90	170	0	0.3	0.35	0.25	0.40	3000	400	2000	400	0.1	139.9	229.9	400.1	27.0	259.0	71	108.2
169	140	90	170	0	0.3	0.35	0.25	0.40	3000	400	4000	200	0.1	139.9	229.9	400.1	34.3	262.5	222	149.4
170	140	90	170	0	0.3	0.35	0.25	0.40	3000	400	4000	300	0.1	139.9	229.9	400.1	29.2	258.9	170	116.1
171	140	90	170	0	0.3	0.35	0.25	0.40	3000	400	4000	400	0.1	139.9	229.9	400.1	26.5	256.6	137	95.6
172	140	90	170	0	0.3	0.35	0.25	0.40	3000	400	6000	200	0.1	139.9	229.9	400.1	33.7	260.2	290	132.0
173	140	90	170	0	0.3	0.35	0.25	0.40	3000	400	6000	300	0.1	139.9	229.9	400.1	28.8	257.2	229	104.0
174	140	90	170	0	0.3	0.35	0.25	0.40	3000	400	6000	400	0.1	139.9	229.9	400.1	26.2	255.3	189	86.6
175	140	90	170	0	0.3	0.35	0.25	0.40	3000	400	8000	200	0.1	139.9	229.9	400.1	33.2	258.6	346	119.6
176	140	90	170	0	0.3	0.35	0.25	0.40	3000	400	8000	300	0.1	139.9	229.9	400.1	28.5	256.0	277	95.1
177	140	90	170	0	0.3	0.35	0.25	0.40	3000	400	8000	400	0.1	139.9	229.9	400.1	25.9	254.3	232	79.9
178	140	90	170	0	0.3	0.35	0.25	0.40	3000	400	10000	200	0.1	139.9	229.9	400.1	32.8	257.3	392	110.1
179	140	90	170	0	0.3	0.35	0.25	0.40	3000	400	10000	300	0.1	139.9	229.9	400.1	28.2	255.1	319	88.2
180	140	90	170	0	0.3	0.35	0.25	0.40	3000	400	10000	400	0.1	139.9	229.9	400.1	25.7	253.6	270	74.5

Simul.	Thickness (mm)			Poisson's Ratio				Modulus (MPa)				Point of analyses (mm)				D0 (μm)	$\mu\epsilon_t$	$\mu\epsilon$	$\mu\epsilon_v$	
	AC	Base	Subbase	Seleted Sub.	AC	Base	Subbase	Seleted Sub.	AC	Base	Subbase	Seleted Sub.								
181	140	90	180	0	0.3	0.35	0.25	0.40	3000	100	2000	200	0.1	139.9	229.9	410.1	54.4	353.4	79	126.7
182	140	90	180	0	0.3	0.35	0.25	0.40	3000	100	2000	300	0.1	139.9	229.9	410.1	49.2	349.3	53	91.8
183	140	90	180	0	0.3	0.35	0.25	0.40	3000	100	2000	400	0.1	139.9	229.9	410.1	46.5	347.0	38	72.2
184	140	90	180	0	0.3	0.35	0.25	0.40	3000	100	4000	200	0.1	139.9	229.9	410.1	53.7	351.6	144	109.9
185	140	90	180	0	0.3	0.35	0.25	0.40	3000	100	4000	300	0.1	139.9	229.9	410.1	48.8	348.1	104	81.8
186	140	90	180	0	0.3	0.35	0.25	0.40	3000	100	4000	400	0.1	139.9	229.9	410.1	46.2	346.1	81	65.5
187	140	90	180	0	0.3	0.35	0.25	0.40	3000	100	6000	200	0.1	139.9	229.9	410.1	53.2	350.4	195	98.7
188	140	90	180	0	0.3	0.35	0.25	0.40	3000	100	6000	300	0.1	139.9	229.9	410.1	48.5	347.4	146	74.7
189	140	90	180	0	0.3	0.35	0.25	0.40	3000	100	6000	400	0.1	139.9	229.9	410.1	46.0	345.6	116	60.5
190	140	90	180	0	0.3	0.35	0.25	0.40	3000	100	8000	200	0.1	139.9	229.9	410.1	52.8	349.5	237	90.5
191	140	90	180	0	0.3	0.35	0.25	0.40	3000	100	8000	300	0.1	139.9	229.9	410.1	48.3	346.8	182	69.3
192	140	90	180	0	0.3	0.35	0.25	0.40	3000	100	8000	400	0.1	139.9	229.9	410.1	45.8	345.2	147	56.6
193	140	90	180	0	0.3	0.35	0.25	0.40	3000	100	10000	200	0.1	139.9	229.9	410.1	52.5	348.8	274	84.1
194	140	90	180	0	0.3	0.35	0.25	0.40	3000	100	10000	300	0.1	139.9	229.9	410.1	48.1	346.4	213	64.9
195	140	90	180	0	0.3	0.35	0.25	0.40	3000	100	10000	400	0.1	139.9	229.9	410.1	45.7	344.9	174	53.4
196	140	90	180	0	0.3	0.35	0.25	0.40	3000	200	2000	200	0.1	139.9	229.9	410.1	43.0	309.4	104	151.1
197	140	90	180	0	0.3	0.35	0.25	0.40	3000	200	2000	300	0.1	139.9	229.9	410.1	37.7	304.9	72	112.1
198	140	90	180	0	0.3	0.35	0.25	0.40	3000	200	2000	400	0.1	139.9	229.9	410.1	34.9	302.4	53	89.3
199	140	90	180	0	0.3	0.35	0.25	0.40	3000	200	4000	200	0.1	139.9	229.9	410.1	42.2	306.6	181	128.4
200	140	90	180	0	0.3	0.35	0.25	0.40	3000	200	4000	300	0.1	139.9	229.9	410.1	37.1	303.0	135	97.8
201	140	90	180	0	0.3	0.35	0.25	0.40	3000	200	4000	400	0.1	139.9	229.9	410.1	34.5	300.8	107	79.5
202	140	90	180	0	0.3	0.35	0.25	0.40	3000	200	6000	200	0.1	139.9	229.9	410.1	41.6	304.9	240	113.9
203	140	90	180	0	0.3	0.35	0.25	0.40	3000	200	6000	300	0.1	139.9	229.9	410.1	36.8	301.8	185	88.1
204	140	90	180	0	0.3	0.35	0.25	0.40	3000	200	6000	400	0.1	139.9	229.9	410.1	34.2	299.9	150	72.5
205	140	90	180	0	0.3	0.35	0.25	0.40	3000	200	8000	200	0.1	139.9	229.9	410.1	41.1	303.6	287	103.4
206	140	90	180	0	0.3	0.35	0.25	0.40	3000	200	8000	300	0.1	139.9	229.9	410.1	36.5	300.9	226	80.8
207	140	90	180	0	0.3	0.35	0.25	0.40	3000	200	8000	400	0.1	139.9	229.9	410.1	34.0	299.3	187	67.0
208	140	90	180	0	0.3	0.35	0.25	0.40	3000	200	10000	200	0.1	139.9	229.9	410.1	40.7	302.6	328	95.4
209	140	90	180	0	0.3	0.35	0.25	0.40	3000	200	10000	300	0.1	139.9	229.9	410.1	36.2	300.3	261	75.2
210	140	90	180	0	0.3	0.35	0.25	0.40	3000	200	10000	400	0.1	139.9	229.9	410.1	33.8	298.8	218	62.7
211	140	90	180	0	0.3	0.35	0.25	0.40	3000	300	2000	200	0.1	139.9	229.9	410.1	38.0	283.8	119	164.0
212	140	90	180	0	0.3	0.35	0.25	0.40	3000	300	2000	300	0.1	139.9	229.9	410.1	32.7	279.3	84	123.4
213	140	90	180	0	0.3	0.35	0.25	0.40	3000	300	2000	400	0.1	139.9	229.9	410.1	29.8	276.6	63	99.3
214	140	90	180	0	0.3	0.35	0.25	0.40	3000	300	4000	200	0.1	139.9	229.9	410.1	37.1	280.2	203	138.0
215	140	90	180	0	0.3	0.35	0.25	0.40	3000	300	4000	300	0.1	139.9	229.9	410.1	32.0	276.7	154	106.6
216	140	90	180	0	0.3	0.35	0.25	0.40	3000	300	4000	400	0.1	139.9	229.9	410.1	29.4	274.6	124	87.5
217	140	90	180	0	0.3	0.35	0.25	0.40	3000	300	6000	200	0.1	139.9	229.9	410.1	36.5	278.2	265	121.6
218	140	90	180	0	0.3	0.35	0.25	0.40	3000	300	6000	300	0.1	139.9	229.9	410.1	31.6	275.2	208	95.3
219	140	90	180	0	0.3	0.35	0.25	0.40	3000	300	6000	400	0.1	139.9	229.9	410.1	29.1	273.4	171	79.2
220	140	90	180	0	0.3	0.35	0.25	0.40	3000	300	8000	200	0.1	139.9	229.9	410.1	36.0	276.7	316	109.9
221	140	90	180	0	0.3	0.35	0.25	0.40	3000	300	8000	300	0.1	139.9	229.9	410.1	31.3	274.2	252	87.1
222	140	90	180	0	0.3	0.35	0.25	0.40	3000	300	8000	400	0.1	139.9	229.9	410.1	28.8	272.6	211	72.9
223	140	90	180	0	0.3	0.35	0.25	0.40	3000	300	10000	200	0.1	139.9	229.9	410.1	35.6	275.6	359	101.0
224	140	90	180	0	0.3	0.35	0.25	0.40	3000	300	10000	300	0.1	139.9	229.9	410.1	31.1	273.4	290	80.6
225	140	90	180	0	0.3	0.35	0.25	0.40	3000	300	10000	400	0.1	139.9	229.9	410.1	28.6	272.0	245	67.9
226	140	90	180	0	0.3	0.35	0.25	0.40	3000	400	2000	200	0.1	139.9	229.9	410.1	35.0	265.5	129	171.8
227	140	90	180	0	0.3	0.35	0.25	0.40	3000	400	2000	300	0.1	139.9	229.9	410.1	29.7	261.1	93	130.6
228	140	90	180	0	0.3	0.35	0.25	0.40	3000	400	2000	400	0.1	139.9	229.9	410.1	26.9	258.5	71	105.8
229	140	90	180	0	0.3	0.35	0.25	0.40	3000	400	4000	200	0.1	139.9	229.9	410.1	34.0	261.5	217	143.8
230	140	90	180	0	0.3	0.35	0.25	0.40	3000	400	4000	300	0.1	139.9	229.9	410.1	29.0	258.1	167	112.2
231	140	90	180	0	0.3	0.35	0.25	0.40	3000	400	4000	400	0.1	139.9	229.9	410.1	26.3	256.0	135	92.7
232	140	90	180	0	0.3	0.35	0.25	0.40	3000	400	6000	200	0.1	139.9	229.9	410.1	33.4	259.1	283	126.2
233	140	90	180	0	0.3	0.35	0.25	0.40	3000	400	6000	300	0.1	139.9	229.9	410.1	28.6	256.4	224	99.9
234	140	90	180	0	0.3	0.35	0.25	0.40	3000	400	6000	400	0.1	139.9	229.9	410.1	26.0	254.7	186	83.5
235	140	90	180	0	0.3	0.35	0.25	0.40	3000	400	8000	200	0.1	139.9	229.9	410.1	32.9	257.5	335	113.8
236	140	90	180	0	0.3	0.35	0.25	0.40	3000	400	8000	300	0.1	139.9	229.9	410.1	28.3	255.2	270	91.0
237	140	90	180	0	0.3	0.35	0.25	0.40	3000	400	8000	400	0.1	139.9	229.9	410.1	25.8	253.7	227	76.6
238	140	90	180	0	0.3	0.35	0.25	0.40	3000	400	10000	200	0.1	139.9	229.9	410.1	32.5	256.3	379	104.4
239	140	90	180	0	0.3	0.35	0.25	0.40	3000	400	10000	300	0.1	139.9	229.9	410.1	28.0	254.3	309	84.0
240	140	90	180	0	0.3	0.35	0.25	0.40	3000	400	10000	400	0.1	139.9	229.9	410.1	25.6	253.0	263	71.2

Simul.	Thickness (mm)				Poisson's Ratio				Modulus (MPa)				Point of analyses (mm)				D0 (μm)	$\mu\epsilon_t$	$\mu\epsilon$	$\mu\epsilon_v$
	AC	Base	Subbase	Seleted Sub.	AC	Base	Subbase	Seleted Sub.	AC	Base	Subbase	Seleted Sub.								
241	140	100	150	0	0.3	0.35	0.25	0.40	3000	100	2000	200	0.1	139.9	239.9	390.1	56.9	361.4	73	128.7
242	140	100	150	0	0.3	0.35	0.25	0.40	3000	100	2000	300	0.1	139.9	239.9	390.1	51.6	356.9	47	91.9
243	140	100	150	0	0.3	0.35	0.25	0.40	3000	100	2000	400	0.1	139.9	239.9	390.1	48.9	354.5	33	71.5
244	140	100	150	0	0.3	0.35	0.25	0.40	3000	100	4000	200	0.1	139.9	239.9	390.1	56.5	360.1	137	115.4
245	140	100	150	0	0.3	0.35	0.25	0.40	3000	100	4000	300	0.1	139.9	239.9	390.1	51.3	356.1	97	84.3
246	140	100	150	0	0.3	0.35	0.25	0.40	3000	100	4000	400	0.1	139.9	239.9	390.1	48.7	353.9	73	66.6
247	140	100	150	0	0.3	0.35	0.25	0.40	3000	100	6000	200	0.1	139.9	239.9	390.1	56.1	359.2	191	105.9
248	140	100	150	0	0.3	0.35	0.25	0.40	3000	100	6000	300	0.1	139.9	239.9	390.1	51.1	355.5	139	78.5
249	140	100	150	0	0.3	0.35	0.25	0.40	3000	100	6000	400	0.1	139.9	239.9	390.1	48.5	353.5	109	62.7
250	140	100	150	0	0.3	0.35	0.25	0.40	3000	100	8000	200	0.1	139.9	239.9	390.1	55.8	358.4	236	98.8
251	140	100	150	0	0.3	0.35	0.25	0.40	3000	100	8000	300	0.1	139.9	239.9	390.1	51.0	355.1	176	74.0
252	140	100	150	0	0.3	0.35	0.25	0.40	3000	100	8000	400	0.1	139.9	239.9	390.1	48.4	353.2	140	59.5
253	140	100	150	0	0.3	0.35	0.25	0.40	3000	100	10000	200	0.1	139.9	239.9	390.1	55.6	357.8	277	93.0
254	140	100	150	0	0.3	0.35	0.25	0.40	3000	100	10000	300	0.1	139.9	239.9	390.1	50.8	354.7	209	70.2
255	140	100	150	0	0.3	0.35	0.25	0.40	3000	100	10000	400	0.1	139.9	239.9	390.1	48.3	352.9	168	56.8
256	140	100	150	0	0.3	0.35	0.25	0.40	3000	200	2000	200	0.1	139.9	239.9	390.1	45.0	317.7	98	156.2
257	140	100	150	0	0.3	0.35	0.25	0.40	3000	200	2000	300	0.1	139.9	239.9	390.1	39.5	312.6	67	114.1
258	140	100	150	0	0.3	0.35	0.25	0.40	3000	200	2000	400	0.1	139.9	239.9	390.1	36.6	309.8	48	90.0
259	140	100	150	0	0.3	0.35	0.25	0.40	3000	200	4000	200	0.1	139.9	239.9	390.1	44.4	315.5	178	137.3
260	140	100	150	0	0.3	0.35	0.25	0.40	3000	200	4000	300	0.1	139.9	239.9	390.1	39.1	311.2	130	102.6
261	140	100	150	0	0.3	0.35	0.25	0.40	3000	200	4000	400	0.1	139.9	239.9	390.1	36.3	308.7	101	82.4
262	140	100	150	0	0.3	0.35	0.25	0.40	3000	200	6000	200	0.1	139.9	239.9	390.1	43.9	314.0	241	124.5
263	140	100	150	0	0.3	0.35	0.25	0.40	3000	200	6000	300	0.1	139.9	239.9	390.1	38.8	310.2	182	94.4
264	140	100	150	0	0.3	0.35	0.25	0.40	3000	200	6000	400	0.1	139.9	239.9	390.1	36.1	308.0	145	76.6
265	140	100	150	0	0.3	0.35	0.25	0.40	3000	200	8000	200	0.1	139.9	239.9	390.1	43.6	313.0	294	114.9
266	140	100	150	0	0.3	0.35	0.25	0.40	3000	200	8000	300	0.1	139.9	239.9	390.1	38.6	309.5	226	88.0
267	140	100	150	0	0.3	0.35	0.25	0.40	3000	200	8000	400	0.1	139.9	239.9	390.1	35.9	307.5	184	72.0
268	140	100	150	0	0.3	0.35	0.25	0.40	3000	200	10000	200	0.1	139.9	239.9	390.1	43.2	312.1	341	107.4
269	140	100	150	0	0.3	0.35	0.25	0.40	3000	200	10000	300	0.1	139.9	239.9	390.1	38.4	308.9	265	82.9
270	140	100	150	0	0.3	0.35	0.25	0.40	3000	200	10000	400	0.1	139.9	239.9	390.1	35.8	307.0	218	68.2
271	140	100	150	0	0.3	0.35	0.25	0.40	3000	300	2000	200	0.1	139.9	239.9	390.1	39.8	292.3	115	171.1
272	140	100	150	0	0.3	0.35	0.25	0.40	3000	300	2000	300	0.1	139.9	239.9	390.1	34.2	287.1	79	126.8
273	140	100	150	0	0.3	0.35	0.25	0.40	3000	300	2000	400	0.1	139.9	239.9	390.1	31.3	284.1	58	101.0
274	140	100	150	0	0.3	0.35	0.25	0.40	3000	300	4000	200	0.1	139.9	239.9	390.1	39.1	289.4	203	148.9
275	140	100	150	0	0.3	0.35	0.25	0.40	3000	300	4000	300	0.1	139.9	239.9	390.1	33.7	285.1	151	113.0
276	140	100	150	0	0.3	0.35	0.25	0.40	3000	300	4000	400	0.1	139.9	239.9	390.1	30.9	282.5	119	91.6
277	140	100	150	0	0.3	0.35	0.25	0.40	3000	300	6000	200	0.1	139.9	239.9	390.1	38.6	287.6	272	134.2
278	140	100	150	0	0.3	0.35	0.25	0.40	3000	300	6000	300	0.1	139.9	239.9	390.1	33.4	283.8	208	103.3
279	140	100	150	0	0.3	0.35	0.25	0.40	3000	300	6000	400	0.1	139.9	239.9	390.1	30.7	281.6	169	84.6
280	140	100	150	0	0.3	0.35	0.25	0.40	3000	300	8000	200	0.1	139.9	239.9	390.1	38.2	286.3	329	123.3
281	140	100	150	0	0.3	0.35	0.25	0.40	3000	300	8000	300	0.1	139.9	239.9	390.1	33.2	282.9	257	95.8
282	140	100	150	0	0.3	0.35	0.25	0.40	3000	300	8000	400	0.1	139.9	239.9	390.1	30.5	280.9	211	79.1
283	140	100	150	0	0.3	0.35	0.25	0.40	3000	300	10000	200	0.1	139.9	239.9	390.1	37.8	285.2	378	114.8
284	140	100	150	0	0.3	0.35	0.25	0.40	3000	300	10000	300	0.1	139.9	239.9	390.1	33.0	282.2	299	89.9
285	140	100	150	0	0.3	0.35	0.25	0.40	3000	300	10000	400	0.1	139.9	239.9	390.1	30.4	280.3	249	74.6
286	140	100	150	0	0.3	0.35	0.25	0.40	3000	400	2000	200	0.1	139.9	239.9	390.1	36.7	274.2	126	180.4
287	140	100	150	0	0.3	0.35	0.25	0.40	3000	400	2000	300	0.1	139.9	239.9	390.1	31.1	269.0	89	135.2
288	140	100	150	0	0.3	0.35	0.25	0.40	3000	400	2000	400	0.1	139.9	239.9	390.1	28.2	265.9	66	108.5
289	140	100	150	0	0.3	0.35	0.25	0.40	3000	400	4000	200	0.1	139.9	239.9	390.1	35.9	270.8	220	156.1
290	140	100	150	0	0.3	0.35	0.25	0.40	3000	400	4000	300	0.1	139.9	239.9	390.1	30.6	266.5	166	119.8
291	140	100	150	0	0.3	0.35	0.25	0.40	3000	400	4000	400	0.1	139.9	239.9	390.1	27.8	264.0	132	97.7
292	140	100	150	0	0.3	0.35	0.25	0.40	3000	400	6000	200	0.1	139.9	239.9	390.1	35.4	268.7	292	140.2
293	140	100	150	0	0.3	0.35	0.25	0.40	3000	400	6000	300	0.1	139.9	239.9	390.1	30.2	265.1	227	109.0
294	140	100	150	0	0.3	0.35	0.25	0.40	3000	400	6000	400	0.1	139.9	239.9	390.1	27.5	262.9	185	89.9
295	140	100	150	0	0.3	0.35	0.25	0.40	3000	400	8000	200	0.1	139.9	239.9	390.1	35.0	267.2	352	128.5
296	140	100	150	0	0.3	0.35	0.25	0.40	3000	400	8000	300	0.1	139.9	239.9	390.1	30.0	264.0	278	100.8
297	140	100	150	0	0.3	0.35	0.25	0.40	3000	400	8000	400	0.1	139.9	239.9	390.1	27.3	262.0	231	83.8
298	140	100	150	0	0.3	0.35	0.25	0.40	3000	400	10000	200	0.1	139.9	239.9	390.1	34.6	266.1	404	119.3
299	140	100	150	0	0.3	0.35	0.25	0.40	3000	400	10000	300	0.1	139.9	239.9	390.1	29.7	263.2	323	94.3
300	140	100	150	0	0.3	0.35	0.25	0.40	3000	400	10000	400	0.1	139.9	239.9	390.1	27.1	261.4	271	78.8

Simul.	Thickness (mm)				Poisson's Ratio				Modulus (MPa)				Point of analyses (mm)				D0 (μm)	$\mu\epsilon_t$	$\mu\epsilon$	$\mu\epsilon_v$
	AC	Base	Subbase	Seleted Sub.	AC	Base	Subbase	Seleted Sub.	AC	Base	Subbase	Seleted Sub.								
301	140	100	160	0	0.3	0.35	0.25	0.40	3000	100	2000	200	0.1	139.9	239.9	400.1	56.8	361.0	74	126.5
302	140	100	160	0	0.3	0.35	0.25	0.40	3000	100	2000	300	0.1	139.9	239.9	400.1	51.6	356.7	48	90.7
303	140	100	160	0	0.3	0.35	0.25	0.40	3000	100	2000	400	0.1	139.9	239.9	400.1	48.9	354.3	34	70.7
304	140	100	160	0	0.3	0.35	0.25	0.40	3000	100	4000	200	0.1	139.9	239.9	400.1	56.3	359.5	138	112.2
305	140	100	160	0	0.3	0.35	0.25	0.40	3000	100	4000	300	0.1	139.9	239.9	400.1	51.2	355.8	98	82.4
306	140	100	160	0	0.3	0.35	0.25	0.40	3000	100	4000	400	0.1	139.9	239.9	400.1	48.6	353.7	75	65.4
307	140	100	160	0	0.3	0.35	0.25	0.40	3000	100	6000	200	0.1	139.9	239.9	400.1	55.9	358.6	190	102.4
308	140	100	160	0	0.3	0.35	0.25	0.40	3000	100	6000	300	0.1	139.9	239.9	400.1	51.0	355.2	140	76.3
309	140	100	160	0	0.3	0.35	0.25	0.40	3000	100	6000	400	0.1	139.9	239.9	400.1	48.4	353.2	110	61.2
310	140	100	160	0	0.3	0.35	0.25	0.40	3000	100	8000	200	0.1	139.9	239.9	400.1	55.6	357.8	234	95.0
311	140	100	160	0	0.3	0.35	0.25	0.40	3000	100	8000	300	0.1	139.9	239.9	400.1	50.8	354.7	176	71.6
312	140	100	160	0	0.3	0.35	0.25	0.40	3000	100	8000	400	0.1	139.9	239.9	400.1	48.3	352.9	141	57.8
313	140	100	160	0	0.3	0.35	0.25	0.40	3000	100	10000	200	0.1	139.9	239.9	400.1	55.3	357.1	273	89.1
314	140	100	160	0	0.3	0.35	0.25	0.40	3000	100	10000	300	0.1	139.9	239.9	400.1	50.6	354.3	208	67.7
315	140	100	160	0	0.3	0.35	0.25	0.40	3000	100	10000	400	0.1	139.9	239.9	400.1	48.2	352.6	168	55.0
316	140	100	160	0	0.3	0.35	0.25	0.40	3000	200	2000	200	0.1	139.9	239.9	400.1	44.8	317.0	99	152.7
317	140	100	160	0	0.3	0.35	0.25	0.40	3000	200	2000	300	0.1	139.9	239.9	400.1	39.4	312.2	67	112.0
318	140	100	160	0	0.3	0.35	0.25	0.40	3000	200	2000	400	0.1	139.9	239.9	400.1	36.5	309.5	49	88.6
319	140	100	160	0	0.3	0.35	0.25	0.40	3000	200	4000	200	0.1	139.9	239.9	400.1	44.1	314.7	177	132.8
320	140	100	160	0	0.3	0.35	0.25	0.40	3000	200	4000	300	0.1	139.9	239.9	400.1	38.9	310.6	130	99.9
321	140	100	160	0	0.3	0.35	0.25	0.40	3000	200	4000	400	0.1	139.9	239.9	400.1	36.2	308.3	102	80.4
322	140	100	160	0	0.3	0.35	0.25	0.40	3000	200	6000	200	0.1	139.9	239.9	400.1	43.6	313.2	238	119.6
323	140	100	160	0	0.3	0.35	0.25	0.40	3000	200	6000	300	0.1	139.9	239.9	400.1	38.6	309.6	181	91.2
324	140	100	160	0	0.3	0.35	0.25	0.40	3000	200	6000	400	0.1	139.9	239.9	400.1	36.0	307.6	145	74.3
325	140	100	160	0	0.3	0.35	0.25	0.40	3000	200	8000	200	0.1	139.9	239.9	400.1	43.2	312.1	289	109.9
326	140	100	160	0	0.3	0.35	0.25	0.40	3000	200	8000	300	0.1	139.9	239.9	400.1	38.4	308.9	223	84.7
327	140	100	160	0	0.3	0.35	0.25	0.40	3000	200	8000	400	0.1	139.9	239.9	400.1	35.8	307.0	182	69.5
328	140	100	160	0	0.3	0.35	0.25	0.40	3000	200	10000	200	0.1	139.9	239.9	400.1	42.9	311.2	333	102.2
329	140	100	160	0	0.3	0.35	0.25	0.40	3000	200	10000	300	0.1	139.9	239.9	400.1	38.2	308.3	261	79.4
330	140	100	160	0	0.3	0.35	0.25	0.40	3000	200	10000	400	0.1	139.9	239.9	400.1	35.7	306.6	215	65.6
331	140	100	160	0	0.3	0.35	0.25	0.40	3000	300	2000	200	0.1	139.9	239.9	400.1	39.5	291.4	115	166.9
332	140	100	160	0	0.3	0.35	0.25	0.40	3000	300	2000	300	0.1	139.9	239.9	400.1	34.1	286.5	80	124.2
333	140	100	160	0	0.3	0.35	0.25	0.40	3000	300	2000	400	0.1	139.9	239.9	400.1	31.2	283.7	59	99.2
334	140	100	160	0	0.3	0.35	0.25	0.40	3000	300	4000	200	0.1	139.9	239.9	400.1	38.8	288.4	200	143.8
335	140	100	160	0	0.3	0.35	0.25	0.40	3000	300	4000	300	0.1	139.9	239.9	400.1	33.6	284.4	150	109.6
336	140	100	160	0	0.3	0.35	0.25	0.40	3000	300	4000	400	0.1	139.9	239.9	400.1	30.8	282.0	119	89.2
337	140	100	160	0	0.3	0.35	0.25	0.40	3000	300	6000	200	0.1	139.9	239.9	400.1	38.2	286.6	267	128.6
338	140	100	160	0	0.3	0.35	0.25	0.40	3000	300	6000	300	0.1	139.9	239.9	400.1	33.2	283.1	206	99.5
339	140	100	160	0	0.3	0.35	0.25	0.40	3000	300	6000	400	0.1	139.9	239.9	400.1	30.6	281.0	167	81.8
340	140	100	160	0	0.3	0.35	0.25	0.40	3000	300	8000	200	0.1	139.9	239.9	400.1	37.8	285.2	321	117.6
341	140	100	160	0	0.3	0.35	0.25	0.40	3000	300	8000	300	0.1	139.9	239.9	400.1	33.0	282.2	252	91.9
342	140	100	160	0	0.3	0.35	0.25	0.40	3000	300	8000	400	0.1	139.9	239.9	400.1	30.4	280.3	208	76.1
343	140	100	160	0	0.3	0.35	0.25	0.40	3000	300	10000	200	0.1	139.9	239.9	400.1	37.5	284.2	368	109.1
344	140	100	160	0	0.3	0.35	0.25	0.40	3000	300	10000	300	0.1	139.9	239.9	400.1	32.7	281.5	293	85.8
345	140	100	160	0	0.3	0.35	0.25	0.40	3000	300	10000	400	0.1	139.9	239.9	400.1	30.2	279.8	245	71.5
346	140	100	160	0	0.3	0.35	0.25	0.40	3000	400	2000	200	0.1	139.9	239.9	400.1	36.4	273.2	126	175.7
347	140	100	160	0	0.3	0.35	0.25	0.40	3000	400	2000	300	0.1	139.9	239.9	400.1	31.0	268.3	89	132.2
348	140	100	160	0	0.3	0.35	0.25	0.40	3000	400	2000	400	0.1	139.9	239.9	400.1	28.1	265.4	67	106.3
349	140	100	160	0	0.3	0.35	0.25	0.40	3000	400	4000	200	0.1	139.9	239.9	400.1	35.6	269.7	217	150.4
350	140	100	160	0	0.3	0.35	0.25	0.40	3000	400	4000	300	0.1	139.9	239.9	400.1	30.4	265.8	164	115.9
351	140	100	160	0	0.3	0.35	0.25	0.40	3000	400	4000	400	0.1	139.9	239.9	400.1	27.6	263.4	131	95.0
352	140	100	160	0	0.3	0.35	0.25	0.40	3000	400	6000	200	0.1	139.9	239.9	400.1	35.0	267.6	286	134.1
353	140	100	160	0	0.3	0.35	0.25	0.40	3000	400	6000	300	0.1	139.9	239.9	400.1	30.0	264.3	223	104.8
354	140	100	160	0	0.3	0.35	0.25	0.40	3000	400	6000	400	0.1	139.9	239.9	400.1	27.3	262.2	183	86.8
355	140	100	160	0	0.3	0.35	0.25	0.40	3000	400	8000	200	0.1	139.9	239.9	400.1	34.6	266.1	343	122.3
356	140	100	160	0	0.3	0.35	0.25	0.40	3000	400	8000	300	0.1	139.9	239.9	400.1	29.7	263.2	272	96.5
357	140	100	160	0	0.3	0.35	0.25	0.40	3000	400	8000	400	0.1	139.9	239.9	400.1	27.1	261.4	227	80.5
358	140	100	160	0	0.3	0.35	0.25	0.40	3000	400	10000	200	0.1	139.9	239.9	400.1	34.2	264.9	391	113.2
359	140	100	160	0	0.3	0.35	0.25	0.40	3000	400	10000	300	0.1	139.9	239.9	400.1	29.5	262.4	315	89.9
360	140	100	160	0	0.3	0.35	0.25	0.40	3000	400	10000	400	0.1	139.9	239.9	400.1	27.0	260.8	265	75.4

Simul.	Thickness (mm)				Poisson's Ratio				Modulus (MPa)				Point of analyses (mm)				D0 (μm)	$\mu\epsilon_t$	$\mu\epsilon$	$\mu\epsilon_v$
	AC	Base	Subbase	Seleted Sub.	AC	Base	Subbase	Seleted Sub.	AC	Base	Subbase	Seleted Sub.								
361	140	100	170	0	0.3	0.35	0.25	0.40	3000	100	2000	200	0.1	139.9	239.9	410.1	56.6	360.5	75	124.1
362	140	100	170	0	0.3	0.35	0.25	0.40	3000	100	2000	300	0.1	139.9	239.9	410.1	51.5	356.4	49	89.3
363	140	100	170	0	0.3	0.35	0.25	0.40	3000	100	2000	400	0.1	139.9	239.9	410.1	48.8	354.2	35	69.9
364	140	100	170	0	0.3	0.35	0.25	0.40	3000	100	4000	200	0.1	139.9	239.9	410.1	56.1	359.0	138	109.1
365	140	100	170	0	0.3	0.35	0.25	0.40	3000	100	4000	300	0.1	139.9	239.9	410.1	51.1	355.4	99	80.5
366	140	100	170	0	0.3	0.35	0.25	0.40	3000	100	4000	400	0.1	139.9	239.9	410.1	48.5	353.4	76	64.1
367	140	100	170	0	0.3	0.35	0.25	0.40	3000	100	6000	200	0.1	139.9	239.9	410.1	55.6	358.0	189	98.9
368	140	100	170	0	0.3	0.35	0.25	0.40	3000	100	6000	300	0.1	139.9	239.9	410.1	50.9	354.8	140	74.1
369	140	100	170	0	0.3	0.35	0.25	0.40	3000	100	6000	400	0.1	139.9	239.9	410.1	48.4	353.0	110	59.7
370	140	100	170	0	0.3	0.35	0.25	0.40	3000	100	8000	200	0.1	139.9	239.9	410.1	55.3	357.2	231	91.3
371	140	100	170	0	0.3	0.35	0.25	0.40	3000	100	8000	300	0.1	139.9	239.9	410.1	50.7	354.3	175	69.2
372	140	100	170	0	0.3	0.35	0.25	0.40	3000	100	8000	400	0.1	139.9	239.9	410.1	48.2	352.6	141	56.2
373	140	100	170	0	0.3	0.35	0.25	0.40	3000	100	10000	200	0.1	139.9	239.9	410.1	55.0	356.5	269	85.3
374	140	100	170	0	0.3	0.35	0.25	0.40	3000	100	10000	300	0.1	139.9	239.9	410.1	50.5	353.9	206	65.2
375	140	100	170	0	0.3	0.35	0.25	0.40	3000	100	10000	400	0.1	139.9	239.9	410.1	48.1	352.3	168	53.2
376	140	100	170	0	0.3	0.35	0.25	0.40	3000	200	2000	200	0.1	139.9	239.9	410.1	44.6	316.3	99	149.2
377	140	100	170	0	0.3	0.35	0.25	0.40	3000	200	2000	300	0.1	139.9	239.9	410.1	39.2	311.8	68	109.8
378	140	100	170	0	0.3	0.35	0.25	0.40	3000	200	2000	400	0.1	139.9	239.9	410.1	36.4	309.2	50	87.1
379	140	100	170	0	0.3	0.35	0.25	0.40	3000	200	4000	200	0.1	139.9	239.9	410.1	43.8	313.9	175	128.5
380	140	100	170	0	0.3	0.35	0.25	0.40	3000	200	4000	300	0.1	139.9	239.9	410.1	38.8	310.1	130	97.0
381	140	100	170	0	0.3	0.35	0.25	0.40	3000	200	4000	400	0.1	139.9	239.9	410.1	36.1	307.9	102	78.4
382	140	100	170	0	0.3	0.35	0.25	0.40	3000	200	6000	200	0.1	139.9	239.9	410.1	43.3	312.4	234	114.9
383	140	100	170	0	0.3	0.35	0.25	0.40	3000	200	6000	300	0.1	139.9	239.9	410.1	38.4	309.1	179	88.1
384	140	100	170	0	0.3	0.35	0.25	0.40	3000	200	6000	400	0.1	139.9	239.9	410.1	35.8	307.2	144	72.0
385	140	100	170	0	0.3	0.35	0.25	0.40	3000	200	8000	200	0.1	139.9	239.9	410.1	42.9	311.2	283	105.1
386	140	100	170	0	0.3	0.35	0.25	0.40	3000	200	8000	300	0.1	139.9	239.9	410.1	38.2	308.3	220	81.4
387	140	100	170	0	0.3	0.35	0.25	0.40	3000	200	8000	400	0.1	139.9	239.9	410.1	35.7	306.6	181	67.1
388	140	100	170	0	0.3	0.35	0.25	0.40	3000	200	10000	200	0.1	139.9	239.9	410.1	42.6	310.3	325	97.4
389	140	100	170	0	0.3	0.35	0.25	0.40	3000	200	10000	300	0.1	139.9	239.9	410.1	38.0	307.7	256	76.1
390	140	100	170	0	0.3	0.35	0.25	0.40	3000	200	10000	400	0.1	139.9	239.9	410.1	35.5	306.1	212	63.1
391	140	100	170	0	0.3	0.35	0.25	0.40	3000	300	2000	200	0.1	139.9	239.9	410.1	39.3	290.6	114	162.6
392	140	100	170	0	0.3	0.35	0.25	0.40	3000	300	2000	300	0.1	139.9	239.9	410.1	33.9	286.0	80	121.5
393	140	100	170	0	0.3	0.35	0.25	0.40	3000	300	2000	400	0.1	139.9	239.9	410.1	31.1	283.3	60	97.3
394	140	100	170	0	0.3	0.35	0.25	0.40	3000	300	4000	200	0.1	139.9	239.9	410.1	38.5	287.5	198	138.7
395	140	100	170	0	0.3	0.35	0.25	0.40	3000	300	4000	300	0.1	139.9	239.9	410.1	33.4	283.8	149	106.3
396	140	100	170	0	0.3	0.35	0.25	0.40	3000	300	4000	400	0.1	139.9	239.9	410.1	30.7	281.5	119	86.7
397	140	100	170	0	0.3	0.35	0.25	0.40	3000	300	6000	200	0.1	139.9	239.9	410.1	37.9	285.6	261	123.3
398	140	100	170	0	0.3	0.35	0.25	0.40	3000	300	6000	300	0.1	139.9	239.9	410.1	33.0	282.5	203	95.8
399	140	100	170	0	0.3	0.35	0.25	0.40	3000	300	6000	400	0.1	139.9	239.9	410.1	30.4	280.5	166	79.1
400	140	100	170	0	0.3	0.35	0.25	0.40	3000	300	8000	200	0.1	139.9	239.9	410.1	37.5	284.2	313	112.2
401	140	100	170	0	0.3	0.35	0.25	0.40	3000	300	8000	300	0.1	139.9	239.9	410.1	32.7	281.5	247	88.1
402	140	100	170	0	0.3	0.35	0.25	0.40	3000	300	8000	400	0.1	139.9	239.9	410.1	30.2	279.8	205	73.3
403	140	100	170	0	0.3	0.35	0.25	0.40	3000	300	10000	200	0.1	139.9	239.9	410.1	37.1	283.2	357	103.6
404	140	100	170	0	0.3	0.35	0.25	0.40	3000	300	10000	300	0.1	139.9	239.9	410.1	32.5	280.8	286	82.0
405	140	100	170	0	0.3	0.35	0.25	0.40	3000	300	10000	400	0.1	139.9	239.9	410.1	30.0	279.2	240	68.6
406	140	100	170	0	0.3	0.35	0.25	0.40	3000	400	2000	200	0.1	139.9	239.9	410.1	36.2	272.2	125	170.9
407	140	100	170	0	0.3	0.35	0.25	0.40	3000	400	2000	300	0.1	139.9	239.9	410.1	30.8	267.7	89	129.1
408	140	100	170	0	0.3	0.35	0.25	0.40	3000	400	2000	400	0.1	139.9	239.9	410.1	28.0	265.0	67	104.1
409	140	100	170	0	0.3	0.35	0.25	0.40	3000	400	4000	200	0.1	139.9	239.9	410.1	35.3	268.6	213	144.9
410	140	100	170	0	0.3	0.35	0.25	0.40	3000	400	4000	300	0.1	139.9	239.9	410.1	30.2	265.0	162	112.2
411	140	100	170	0	0.3	0.35	0.25	0.40	3000	400	4000	400	0.1	139.9	239.9	410.1	27.5	262.8	130	92.2
412	140	100	170	0	0.3	0.35	0.25	0.40	3000	400	6000	200	0.1	139.9	239.9	410.1	34.7	266.5	279	128.3
413	140	100	170	0	0.3	0.35	0.25	0.40	3000	400	6000	300	0.1	139.9	239.9	410.1	29.8	263.5	219	100.8
414	140	100	170	0	0.3	0.35	0.25	0.40	3000	400	6000	400	0.1	139.9	239.9	410.1	27.2	261.6	181	83.7
415	140	100	170	0	0.3	0.35	0.25	0.40	3000	400	8000	200	0.1	139.9	239.9	410.1	34.2	265.0	333	116.4
416	140	100	170	0	0.3	0.35	0.25	0.40	3000	400	8000	300	0.1	139.9	239.9	410.1	29.5	262.4	266	92.3
417	140	100	170	0	0.3	0.35	0.25	0.40	3000	400	8000	400	0.1	139.9	239.9	410.1	27.0	260.8	223	77.3
418	140	100	170	0	0.3	0.35	0.25	0.40	3000	400	10000	200	0.1	139.9	239.9	410.1	33.8	263.8	379	107.3
419	140	100	170	0	0.3	0.35	0.25	0.40	3000	400	10000	300	0.1	139.9	239.9	410.1	29.3	261.6	306	85.7
420	140	100	170	0	0.3	0.35	0.25	0.40	3000	400	10000	400	0.1	139.9	239.9	410.1	26.8	260.1	259	72.2

Simul.	Thickness (mm)				Poisson's Ratio				Modulus (MPa)				Point of analyses (mm)				D0 (μm)	$\mu\epsilon_t$	$\mu\epsilon$	$\mu\epsilon_v$
	AC	Base	Subbase	Seleted Sub.	AC	Base	Subbase	Seleted Sub.	AC	Base	Subbase	Seleted Sub.								
421	140	100	180	0	0.3	0.35	0.25	0.40	3000	100	2000	200	0.1	139.9	239.9	420.1	56.5	360.1	75	121.7
422	140	100	180	0	0.3	0.35	0.25	0.40	3000	100	2000	300	0.1	139.9	239.9	420.1	51.4	356.2	50	87.9
423	140	100	180	0	0.3	0.35	0.25	0.40	3000	100	2000	400	0.1	139.9	239.9	420.1	48.7	354.0	36	69.0
424	140	100	180	0	0.3	0.35	0.25	0.40	3000	100	4000	200	0.1	139.9	239.9	420.1	55.9	358.5	138	106.0
425	140	100	180	0	0.3	0.35	0.25	0.40	3000	100	4000	300	0.1	139.9	239.9	420.1	51.0	355.1	99	78.6
426	140	100	180	0	0.3	0.35	0.25	0.40	3000	100	4000	400	0.1	139.9	239.9	420.1	48.4	353.2	77	62.8
427	140	100	180	0	0.3	0.35	0.25	0.40	3000	100	6000	200	0.1	139.9	239.9	420.1	55.4	357.4	187	95.5
428	140	100	180	0	0.3	0.35	0.25	0.40	3000	100	6000	300	0.1	139.9	239.9	420.1	50.7	354.4	139	72.0
429	140	100	180	0	0.3	0.35	0.25	0.40	3000	100	6000	400	0.1	139.9	239.9	420.1	48.3	352.7	111	58.2
430	140	100	180	0	0.3	0.35	0.25	0.40	3000	100	8000	200	0.1	139.9	239.9	420.1	55.0	356.6	228	87.8
431	140	100	180	0	0.3	0.35	0.25	0.40	3000	100	8000	300	0.1	139.9	239.9	420.1	50.5	353.9	174	66.9
432	140	100	180	0	0.3	0.35	0.25	0.40	3000	100	8000	400	0.1	139.9	239.9	420.1	48.1	352.4	140	54.5
433	140	100	180	0	0.3	0.35	0.25	0.40	3000	100	10000	200	0.1	139.9	239.9	420.1	54.7	355.9	264	81.7
434	140	100	180	0	0.3	0.35	0.25	0.40	3000	100	10000	300	0.1	139.9	239.9	420.1	50.3	353.5	204	62.8
435	140	100	180	0	0.3	0.35	0.25	0.40	3000	100	10000	400	0.1	139.9	239.9	420.1	48.0	352.1	167	51.5
436	140	100	180	0	0.3	0.35	0.25	0.40	3000	200	2000	200	0.1	139.9	239.9	420.1	44.4	315.7	99	145.6
437	140	100	180	0	0.3	0.35	0.25	0.40	3000	200	2000	300	0.1	139.9	239.9	420.1	39.1	311.4	68	107.6
438	140	100	180	0	0.3	0.35	0.25	0.40	3000	200	2000	400	0.1	139.9	239.9	420.1	36.4	308.9	50	85.6
439	140	100	180	0	0.3	0.35	0.25	0.40	3000	200	4000	200	0.1	139.9	239.9	420.1	43.6	313.1	173	124.2
440	140	100	180	0	0.3	0.35	0.25	0.40	3000	200	4000	300	0.1	139.9	239.9	420.1	38.6	309.6	129	94.3
441	140	100	180	0	0.3	0.35	0.25	0.40	3000	200	4000	400	0.1	139.9	239.9	420.1	36.0	307.6	102	76.5
442	140	100	180	0	0.3	0.35	0.25	0.40	3000	200	6000	200	0.1	139.9	239.9	420.1	43.0	311.6	230	110.4
443	140	100	180	0	0.3	0.35	0.25	0.40	3000	200	6000	300	0.1	139.9	239.9	420.1	38.3	308.6	177	85.1
444	140	100	180	0	0.3	0.35	0.25	0.40	3000	200	6000	400	0.1	139.9	239.9	420.1	35.7	306.8	143	69.8
445	140	100	180	0	0.3	0.35	0.25	0.40	3000	200	8000	200	0.1	139.9	239.9	420.1	42.6	310.4	277	100.5
446	140	100	180	0	0.3	0.35	0.25	0.40	3000	200	8000	300	0.1	139.9	239.9	420.1	38.0	307.8	216	78.3
447	140	100	180	0	0.3	0.35	0.25	0.40	3000	200	8000	400	0.1	139.9	239.9	420.1	35.5	306.2	178	64.7
448	140	100	180	0	0.3	0.35	0.25	0.40	3000	200	10000	200	0.1	139.9	239.9	420.1	42.2	309.5	316	92.8
449	140	100	180	0	0.3	0.35	0.25	0.40	3000	200	10000	300	0.1	139.9	239.9	420.1	37.8	307.2	251	72.9
450	140	100	180	0	0.3	0.35	0.25	0.40	3000	200	10000	400	0.1	139.9	239.9	420.1	35.4	305.7	209	60.7
451	140	100	180	0	0.3	0.35	0.25	0.40	3000	300	2000	200	0.1	139.9	239.9	420.1	39.1	289.8	114	158.4
452	140	100	180	0	0.3	0.35	0.25	0.40	3000	300	2000	300	0.1	139.9	239.9	420.1	33.8	285.5	80	118.8
453	140	100	180	0	0.3	0.35	0.25	0.40	3000	300	2000	400	0.1	139.9	239.9	420.1	31.0	282.9	60	95.3
454	140	100	180	0	0.3	0.35	0.25	0.40	3000	300	4000	200	0.1	139.9	239.9	420.1	38.2	286.6	194	133.7
455	140	100	180	0	0.3	0.35	0.25	0.40	3000	300	4000	300	0.1	139.9	239.9	420.1	33.2	283.2	147	102.9
456	140	100	180	0	0.3	0.35	0.25	0.40	3000	300	4000	400	0.1	139.9	239.9	420.1	30.6	281.1	118	84.3
457	140	100	180	0	0.3	0.35	0.25	0.40	3000	300	6000	200	0.1	139.9	239.9	420.1	37.6	284.7	255	118.1
458	140	100	180	0	0.3	0.35	0.25	0.40	3000	300	6000	300	0.1	139.9	239.9	420.1	32.8	281.8	199	92.3
459	140	100	180	0	0.3	0.35	0.25	0.40	3000	300	6000	400	0.1	139.9	239.9	420.1	30.3	280.0	163	76.4
460	140	100	180	0	0.3	0.35	0.25	0.40	3000	300	8000	200	0.1	139.9	239.9	420.1	37.1	283.3	305	107.0
461	140	100	180	0	0.3	0.35	0.25	0.40	3000	300	8000	300	0.1	139.9	239.9	420.1	32.5	280.9	242	84.4
462	140	100	180	0	0.3	0.35	0.25	0.40	3000	300	8000	400	0.1	139.9	239.9	420.1	30.1	279.3	202	70.5
463	140	100	180	0	0.3	0.35	0.25	0.40	3000	300	10000	200	0.1	139.9	239.9	420.1	36.8	282.3	347	98.5
464	140	100	180	0	0.3	0.35	0.25	0.40	3000	300	10000	300	0.1	139.9	239.9	420.1	32.3	280.1	279	78.3
465	140	100	180	0	0.3	0.35	0.25	0.40	3000	300	10000	400	0.1	139.9	239.9	420.1	29.9	278.7	235	65.8
466	140	100	180	0	0.3	0.35	0.25	0.40	3000	400	2000	200	0.1	139.9	239.9	420.1	35.9	271.3	124	166.2
467	140	100	180	0	0.3	0.35	0.25	0.40	3000	400	2000	300	0.1	139.9	239.9	420.1	30.7	267.1	89	126.0
468	140	100	180	0	0.3	0.35	0.25	0.40	3000	400	2000	400	0.1	139.9	239.9	420.1	27.9	264.5	67	101.8
469	140	100	180	0	0.3	0.35	0.25	0.40	3000	400	4000	200	0.1	139.9	239.9	420.1	35.0	267.6	209	139.5
470	140	100	180	0	0.3	0.35	0.25	0.40	3000	400	4000	300	0.1	139.9	239.9	420.1	30.0	264.3	160	108.5
471	140	100	180	0	0.3	0.35	0.25	0.40	3000	400	4000	400	0.1	139.9	239.9	420.1	27.4	262.3	129	89.4
472	140	100	180	0	0.3	0.35	0.25	0.40	3000	400	6000	200	0.1	139.9	239.9	420.1	34.4	265.5	272	122.8
473	140	100	180	0	0.3	0.35	0.25	0.40	3000	400	6000	300	0.1	139.9	239.9	420.1	29.6	262.8	215	96.9
474	140	100	180	0	0.3	0.35	0.25	0.40	3000	400	6000	400	0.1	139.9	239.9	420.1	27.0	261.1	178	80.8
475	140	100	180	0	0.3	0.35	0.25	0.40	3000	400	8000	200	0.1	139.9	239.9	420.1	33.9	264.0	323	110.9
476	140	100	180	0	0.3	0.35	0.25	0.40	3000	400	8000	300	0.1	139.9	239.9	420.1	29.3	261.7	260	88.3
477	140	100	180	0	0.3	0.35	0.25	0.40	3000	400	8000	400	0.1	139.9	239.9	420.1	26.8	260.2	218	74.2
478	140	100	180	0	0.3	0.35	0.25	0.40	3000	400	10000	200	0.1	139.9	239.9	420.1	33.5	262.8	367	101.9
479	140	100	180	0	0.3	0.35	0.25	0.40	3000	400	10000	300	0.1	139.9	239.9	420.1	29.0	260.9	298	81.7
480	140	100	180	0	0.3	0.35	0.25	0.40	3000	400	10000	400	0.1	139.9	239.9	420.1	26.6	259.6	253	69.1

Simul.	Thickness (mm)				Poisson's Ratio				Modulus (MPa)				Point of analyses (mm)				D0 (μm)	$\mu\epsilon_t$	$\mu\epsilon$	$\mu\epsilon_v$
	AC	Base	Subbase	Seleted Sub.	AC	Base	Subbase	Seleted Sub.	AC	Base	Subbase	Seleted Sub.								
481	140	110	150	0	0.3	0.35	0.25	0.40	3000	100	2000	200	0.1	139.9	249.9	400.1	59.0	367.4	69	123.8
482	140	110	150	0	0.3	0.35	0.25	0.40	3000	100	2000	300	0.1	139.9	249.9	400.1	53.7	363.1	44	88.1
483	140	110	150	0	0.3	0.35	0.25	0.40	3000	100	2000	400	0.1	139.9	249.9	400.1	51.0	360.8	31	68.5
484	140	110	150	0	0.3	0.35	0.25	0.40	3000	100	4000	200	0.1	139.9	249.9	400.1	58.5	366.2	131	111.3
485	140	110	150	0	0.3	0.35	0.25	0.40	3000	100	4000	300	0.1	139.9	249.9	400.1	53.4	362.4	92	81.0
486	140	110	150	0	0.3	0.35	0.25	0.40	3000	100	4000	400	0.1	139.9	249.9	400.1	50.8	360.3	70	64.0
487	140	110	150	0	0.3	0.35	0.25	0.40	3000	100	6000	200	0.1	139.9	249.9	400.1	58.2	365.4	182	102.4
488	140	110	150	0	0.3	0.35	0.25	0.40	3000	100	6000	300	0.1	139.9	249.9	400.1	53.2	361.9	133	75.7
489	140	110	150	0	0.3	0.35	0.25	0.40	3000	100	6000	400	0.1	139.9	249.9	400.1	50.7	359.9	103	60.3
490	140	110	150	0	0.3	0.35	0.25	0.40	3000	100	8000	200	0.1	139.9	249.9	400.1	57.9	364.7	227	95.7
491	140	110	150	0	0.3	0.35	0.25	0.40	3000	100	8000	300	0.1	139.9	249.9	400.1	53.1	361.5	168	71.4
492	140	110	150	0	0.3	0.35	0.25	0.40	3000	100	8000	400	0.1	139.9	249.9	400.1	50.6	359.6	133	57.3
493	140	110	150	0	0.3	0.35	0.25	0.40	3000	100	10000	200	0.1	139.9	249.9	400.1	57.7	364.2	266	90.2
494	140	110	150	0	0.3	0.35	0.25	0.40	3000	100	10000	300	0.1	139.9	249.9	400.1	52.9	361.1	200	67.9
495	140	110	150	0	0.3	0.35	0.25	0.40	3000	100	10000	400	0.1	139.9	249.9	400.1	50.5	359.4	161	54.8
496	140	110	150	0	0.3	0.35	0.25	0.40	3000	200	2000	200	0.1	139.9	249.9	400.1	46.3	323.2	94	150.5
497	140	110	150	0	0.3	0.35	0.25	0.40	3000	200	2000	300	0.1	139.9	249.9	400.1	40.8	318.4	63	109.6
498	140	110	150	0	0.3	0.35	0.25	0.40	3000	200	2000	400	0.1	139.9	249.9	400.1	38.0	315.7	45	86.3
499	140	110	150	0	0.3	0.35	0.25	0.40	3000	200	4000	200	0.1	139.9	249.9	400.1	45.7	321.2	170	132.7
500	140	110	150	0	0.3	0.35	0.25	0.40	3000	200	4000	300	0.1	139.9	249.9	400.1	40.5	317.1	124	98.9
501	140	110	150	0	0.3	0.35	0.25	0.40	3000	200	4000	400	0.1	139.9	249.9	400.1	37.7	314.7	96	79.2
502	140	110	150	0	0.3	0.35	0.25	0.40	3000	200	6000	200	0.1	139.9	249.9	400.1	45.3	319.9	231	120.6
503	140	110	150	0	0.3	0.35	0.25	0.40	3000	200	6000	300	0.1	139.9	249.9	400.1	40.2	316.2	174	91.1
504	140	110	150	0	0.3	0.35	0.25	0.40	3000	200	6000	400	0.1	139.9	249.9	400.1	37.5	314.1	138	73.8
505	140	110	150	0	0.3	0.35	0.25	0.40	3000	200	8000	200	0.1	139.9	249.9	400.1	44.9	318.9	283	111.5
506	140	110	150	0	0.3	0.35	0.25	0.40	3000	200	8000	300	0.1	139.9	249.9	400.1	40.0	315.6	216	85.1
507	140	110	150	0	0.3	0.35	0.25	0.40	3000	200	8000	400	0.1	139.9	249.9	400.1	37.4	313.6	175	69.4
508	140	110	150	0	0.3	0.35	0.25	0.40	3000	200	10000	200	0.1	139.9	249.9	400.1	44.6	318.1	328	104.3
509	140	110	150	0	0.3	0.35	0.25	0.40	3000	200	10000	300	0.1	139.9	249.9	400.1	39.8	315.0	254	80.3
510	140	110	150	0	0.3	0.35	0.25	0.40	3000	200	10000	400	0.1	139.9	249.9	400.1	37.3	313.2	208	65.9
511	140	110	150	0	0.3	0.35	0.25	0.40	3000	300	2000	200	0.1	139.9	249.9	400.1	40.8	297.5	110	165.2
512	140	110	150	0	0.3	0.35	0.25	0.40	3000	300	2000	300	0.1	139.9	249.9	400.1	35.3	292.5	76	122.1
513	140	110	150	0	0.3	0.35	0.25	0.40	3000	300	2000	400	0.1	139.9	249.9	400.1	32.4	289.7	55	97.1
514	140	110	150	0	0.3	0.35	0.25	0.40	3000	300	4000	200	0.1	139.9	249.9	400.1	40.1	294.9	194	144.2
515	140	110	150	0	0.3	0.35	0.25	0.40	3000	300	4000	300	0.1	139.9	249.9	400.1	34.8	290.7	144	109.1
516	140	110	150	0	0.3	0.35	0.25	0.40	3000	300	4000	400	0.1	139.9	249.9	400.1	32.1	288.3	113	88.2
517	140	110	150	0	0.3	0.35	0.25	0.40	3000	300	6000	200	0.1	139.9	249.9	400.1	39.7	293.3	261	130.2
518	140	110	150	0	0.3	0.35	0.25	0.40	3000	300	6000	300	0.1	139.9	249.9	400.1	34.5	289.6	199	99.9
519	140	110	150	0	0.3	0.35	0.25	0.40	3000	300	6000	400	0.1	139.9	249.9	400.1	31.8	287.4	161	81.6
520	140	110	150	0	0.3	0.35	0.25	0.40	3000	300	8000	200	0.1	139.9	249.9	400.1	39.3	292.1	317	119.9
521	140	110	150	0	0.3	0.35	0.25	0.40	3000	300	8000	300	0.1	139.9	249.9	400.1	34.3	288.8	246	92.8
522	140	110	150	0	0.3	0.35	0.25	0.40	3000	300	8000	400	0.1	139.9	249.9	400.1	31.7	286.8	202	76.4
523	140	110	150	0	0.3	0.35	0.25	0.40	3000	300	10000	200	0.1	139.9	249.9	400.1	38.9	291.1	365	111.8
524	140	110	150	0	0.3	0.35	0.25	0.40	3000	300	10000	300	0.1	139.9	249.9	400.1	34.1	288.1	287	87.2
525	140	110	150	0	0.3	0.35	0.25	0.40	3000	300	10000	400	0.1	139.9	249.9	400.1	31.5	286.3	238	72.2
526	140	110	150	0	0.3	0.35	0.25	0.40	3000	400	2000	200	0.1	139.9	249.9	400.1	37.5	279.2	121	174.5
527	140	110	150	0	0.3	0.35	0.25	0.40	3000	400	2000	300	0.1	139.9	249.9	400.1	32.0	274.2	85	130.4
528	140	110	150	0	0.3	0.35	0.25	0.40	3000	400	2000	400	0.1	139.9	249.9	400.1	29.1	271.3	63	104.4
529	140	110	150	0	0.3	0.35	0.25	0.40	3000	400	4000	200	0.1	139.9	249.9	400.1	36.8	276.1	211	151.4
530	140	110	150	0	0.3	0.35	0.25	0.40	3000	400	4000	300	0.1	139.9	249.9	400.1	31.5	272.0	159	115.7
531	140	110	150	0	0.3	0.35	0.25	0.40	3000	400	4000	400	0.1	139.9	249.9	400.1	28.7	269.5	126	94.3
532	140	110	150	0	0.3	0.35	0.25	0.40	3000	400	6000	200	0.1	139.9	249.9	400.1	36.3	274.2	281	136.2
533	140	110	150	0	0.3	0.35	0.25	0.40	3000	400	6000	300	0.1	139.9	249.9	400.1	31.2	270.7	217	105.5
534	140	110	150	0	0.3	0.35	0.25	0.40	3000	400	6000	400	0.1	139.9	249.9	400.1	28.5	268.5	177	86.8
535	140	110	150	0	0.3	0.35	0.25	0.40	3000	400	8000	200	0.1	139.9	249.9	400.1	35.9	272.8	339	125.0
536	140	110	150	0	0.3	0.35	0.25	0.40	3000	400	8000	300	0.1	139.9	249.9	400.1	30.9	269.7	267	97.8
537	140	110	150	0	0.3	0.35	0.25	0.40	3000	400	8000	400	0.1	139.9	249.9	400.1	28.3	267.8	221	81.1
538	140	110	150	0	0.3	0.35	0.25	0.40	3000	400	10000	200	0.1	139.9	249.9	400.1	35.5	271.7	390	116.3
539	140	110	150	0	0.3	0.35	0.25	0.40	3000	400	10000	300	0.1	139.9	249.9	400.1	30.7	269.0	310	91.6
540	140	110	150	0	0.3	0.35	0.25	0.40	3000	400	10000	400	0.1	139.9	249.9	400.1	28.1	267.2	260	76.4

Simul.	Thickness (mm)			Poisson's Ratio				Modulus (MPa)				Point of analyses (mm)			D0 (μm)	$\mu\epsilon_t$	$\mu\epsilon$	$\mu\epsilon_v$		
	AC	Base	Subbase	Seleted Sub.	AC	Base	Subbase	Seleted Sub.	AC	Base	Subbase								Seleted Sub.	
541	140	110	160	0	0.3	0.35	0.25	0.40	3000	100	2000	200	0.1	139.9	249.9	410.1	58.8	367.0	70	121.7
542	140	110	160	0	0.3	0.35	0.25	0.40	3000	100	2000	300	0.1	139.9	249.9	410.1	53.6	362.9	46	87.0
543	140	110	160	0	0.3	0.35	0.25	0.40	3000	100	2000	400	0.1	139.9	249.9	410.1	51.0	360.7	32	67.8
544	140	110	160	0	0.3	0.35	0.25	0.40	3000	100	4000	200	0.1	139.9	249.9	410.1	58.3	365.7	132	108.3
545	140	110	160	0	0.3	0.35	0.25	0.40	3000	100	4000	300	0.1	139.9	249.9	410.1	53.3	362.1	93	79.3
546	140	110	160	0	0.3	0.35	0.25	0.40	3000	100	4000	400	0.1	139.9	249.9	410.1	50.7	360.1	71	62.8
547	140	110	160	0	0.3	0.35	0.25	0.40	3000	100	6000	200	0.1	139.9	249.9	410.1	57.9	364.8	182	99.1
548	140	110	160	0	0.3	0.35	0.25	0.40	3000	100	6000	300	0.1	139.9	249.9	410.1	53.1	361.5	133	73.6
549	140	110	160	0	0.3	0.35	0.25	0.40	3000	100	6000	400	0.1	139.9	249.9	410.1	50.6	359.7	104	58.9
550	140	110	160	0	0.3	0.35	0.25	0.40	3000	100	8000	200	0.1	139.9	249.9	410.1	57.6	364.1	225	92.1
551	140	110	160	0	0.3	0.35	0.25	0.40	3000	100	8000	300	0.1	139.9	249.9	410.1	52.9	361.1	168	69.2
552	140	110	160	0	0.3	0.35	0.25	0.40	3000	100	8000	400	0.1	139.9	249.9	410.1	50.5	359.4	134	55.8
553	140	110	160	0	0.3	0.35	0.25	0.40	3000	100	10000	200	0.1	139.9	249.9	410.1	57.4	363.5	263	86.5
554	140	110	160	0	0.3	0.35	0.25	0.40	3000	100	10000	300	0.1	139.9	249.9	410.1	52.8	360.8	199	65.5
555	140	110	160	0	0.3	0.35	0.25	0.40	3000	100	10000	400	0.1	139.9	249.9	410.1	50.4	359.1	161	53.1
556	140	110	160	0	0.3	0.35	0.25	0.40	3000	200	2000	200	0.1	139.9	249.9	410.1	46.1	322.6	94	147.3
557	140	110	160	0	0.3	0.35	0.25	0.40	3000	200	2000	300	0.1	139.9	249.9	410.1	40.7	318.0	64	107.7
558	140	110	160	0	0.3	0.35	0.25	0.40	3000	200	2000	400	0.1	139.9	249.9	410.1	37.9	315.4	46	85.0
559	140	110	160	0	0.3	0.35	0.25	0.40	3000	200	4000	200	0.1	139.9	249.9	410.1	45.5	320.5	169	128.5
560	140	110	160	0	0.3	0.35	0.25	0.40	3000	200	4000	300	0.1	139.9	249.9	410.1	40.3	316.6	124	96.3
561	140	110	160	0	0.3	0.35	0.25	0.40	3000	200	4000	400	0.1	139.9	249.9	410.1	37.6	314.3	97	77.4
562	140	110	160	0	0.3	0.35	0.25	0.40	3000	200	6000	200	0.1	139.9	249.9	410.1	45.0	319.1	228	116.0
563	140	110	160	0	0.3	0.35	0.25	0.40	3000	200	6000	300	0.1	139.9	249.9	410.1	40.0	315.7	173	88.2
564	140	110	160	0	0.3	0.35	0.25	0.40	3000	200	6000	400	0.1	139.9	249.9	410.1	37.4	313.7	138	71.6
565	140	110	160	0	0.3	0.35	0.25	0.40	3000	200	8000	200	0.1	139.9	249.9	410.1	44.6	318.1	278	106.7
566	140	110	160	0	0.3	0.35	0.25	0.40	3000	200	8000	300	0.1	139.9	249.9	410.1	39.8	315.0	214	82.0
567	140	110	160	0	0.3	0.35	0.25	0.40	3000	200	8000	400	0.1	139.9	249.9	410.1	37.3	313.2	174	67.1
568	140	110	160	0	0.3	0.35	0.25	0.40	3000	200	10000	200	0.1	139.9	249.9	410.1	44.3	317.3	321	99.5
569	140	110	160	0	0.3	0.35	0.25	0.40	3000	200	10000	300	0.1	139.9	249.9	410.1	39.6	314.5	250	77.0
570	140	110	160	0	0.3	0.35	0.25	0.40	3000	200	10000	400	0.1	139.9	249.9	410.1	37.1	312.8	206	63.4
571	140	110	160	0	0.3	0.35	0.25	0.40	3000	300	2000	200	0.1	139.9	249.9	410.1	40.6	296.8	110	161.3
572	140	110	160	0	0.3	0.35	0.25	0.40	3000	300	2000	300	0.1	139.9	249.9	410.1	35.2	292.0	76	119.6
573	140	110	160	0	0.3	0.35	0.25	0.40	3000	300	2000	400	0.1	139.9	249.9	410.1	32.3	289.3	56	95.4
574	140	110	160	0	0.3	0.35	0.25	0.40	3000	300	4000	200	0.1	139.9	249.9	410.1	39.8	294.0	192	139.3
575	140	110	160	0	0.3	0.35	0.25	0.40	3000	300	4000	300	0.1	139.9	249.9	410.1	34.7	290.1	143	105.9
576	140	110	160	0	0.3	0.35	0.25	0.40	3000	300	4000	400	0.1	139.9	249.9	410.1	31.9	287.8	113	85.9
577	140	110	160	0	0.3	0.35	0.25	0.40	3000	300	6000	200	0.1	139.9	249.9	410.1	39.3	292.3	256	124.9
578	140	110	160	0	0.3	0.35	0.25	0.40	3000	300	6000	300	0.1	139.9	249.9	410.1	34.4	289.0	197	96.3
579	140	110	160	0	0.3	0.35	0.25	0.40	3000	300	6000	400	0.1	139.9	249.9	410.1	31.7	286.9	160	79.0
580	140	110	160	0	0.3	0.35	0.25	0.40	3000	300	8000	200	0.1	139.9	249.9	410.1	38.9	291.1	309	114.4
581	140	110	160	0	0.3	0.35	0.25	0.40	3000	300	8000	300	0.1	139.9	249.9	410.1	34.1	288.1	242	89.1
582	140	110	160	0	0.3	0.35	0.25	0.40	3000	300	8000	400	0.1	139.9	249.9	410.1	31.5	286.3	200	73.6
583	140	110	160	0	0.3	0.35	0.25	0.40	3000	300	10000	200	0.1	139.9	249.9	410.1	38.6	290.1	355	106.2
584	140	110	160	0	0.3	0.35	0.25	0.40	3000	300	10000	300	0.1	139.9	249.9	410.1	33.9	287.4	282	83.3
585	140	110	160	0	0.3	0.35	0.25	0.40	3000	300	10000	400	0.1	139.9	249.9	410.1	31.4	285.8	234	69.3
586	140	110	160	0	0.3	0.35	0.25	0.40	3000	400	2000	200	0.1	139.9	249.9	410.1	37.3	278.3	120	170.0
587	140	110	160	0	0.3	0.35	0.25	0.40	3000	400	2000	300	0.1	139.9	249.9	410.1	31.9	273.6	85	127.5
588	140	110	160	0	0.3	0.35	0.25	0.40	3000	400	2000	400	0.1	139.9	249.9	410.1	29.0	270.8	64	102.4
589	140	110	160	0	0.3	0.35	0.25	0.40	3000	400	4000	200	0.1	139.9	249.9	410.1	36.5	275.1	208	146.0
590	140	110	160	0	0.3	0.35	0.25	0.40	3000	400	4000	300	0.1	139.9	249.9	410.1	31.3	271.3	157	112.1
591	140	110	160	0	0.3	0.35	0.25	0.40	3000	400	4000	400	0.1	139.9	249.9	410.1	28.6	269.0	125	91.6
592	140	110	160	0	0.3	0.35	0.25	0.40	3000	400	6000	200	0.1	139.9	249.9	410.1	35.9	273.1	275	130.4
593	140	110	160	0	0.3	0.35	0.25	0.40	3000	400	6000	300	0.1	139.9	249.9	410.1	31.0	269.9	214	101.6
594	140	110	160	0	0.3	0.35	0.25	0.40	3000	400	6000	400	0.1	139.9	249.9	410.1	28.3	267.9	175	83.9
595	140	110	160	0	0.3	0.35	0.25	0.40	3000	400	8000	200	0.1	139.9	249.9	410.1	35.5	271.7	331	119.1
596	140	110	160	0	0.3	0.35	0.25	0.40	3000	400	8000	300	0.1	139.9	249.9	410.1	30.7	269.0	262	93.6
597	140	110	160	0	0.3	0.35	0.25	0.40	3000	400	8000	400	0.1	139.9	249.9	410.1	28.1	267.2	218	77.9
598	140	110	160	0	0.3	0.35	0.25	0.40	3000	400	10000	200	0.1	139.9	249.9	410.1	35.2	270.6	378	110.3
599	140	110	160	0	0.3	0.35	0.25	0.40	3000	400	10000	300	0.1	139.9	249.9	410.1	30.5	268.2	303	87.4
600	140	110	160	0	0.3	0.35	0.25	0.40	3000	400	10000	400	0.1	139.9	249.9	410.1	28.0	266.6	254	73.1

Simul.	Thickness (mm)				Poisson's Ratio				Modulus (MPa)				Point of analyses (mm)				D0 (μm)	$\mu\epsilon_t$	$\mu\epsilon$	$\mu\epsilon_v$
	AC	Base	Subbase	Seleted Sub.	AC	Base	Subbase	Seleted Sub.	AC	Base	Subbase	Seleted Sub.								
601	140	110	170	0	0.3	0.35	0.25	0.40	3000	100	2000	200	0.1	139.9	249.9	420.1	58.7	366.6	71	119.5
602	140	110	170	0	0.3	0.35	0.25	0.40	3000	100	2000	300	0.1	139.9	249.9	420.1	53.6	362.7	47	85.8
603	140	110	170	0	0.3	0.35	0.25	0.40	3000	100	2000	400	0.1	139.9	249.9	420.1	50.9	360.5	33	67.0
604	140	110	170	0	0.3	0.35	0.25	0.40	3000	100	4000	200	0.1	139.9	249.9	420.1	58.1	365.2	132	105.4
605	140	110	170	0	0.3	0.35	0.25	0.40	3000	100	4000	300	0.1	139.9	249.9	420.1	53.2	361.8	94	77.6
606	140	110	170	0	0.3	0.35	0.25	0.40	3000	100	4000	400	0.1	139.9	249.9	420.1	50.7	359.9	72	61.6
607	140	110	170	0	0.3	0.35	0.25	0.40	3000	100	6000	200	0.1	139.9	249.9	420.1	57.7	364.3	181	95.8
608	140	110	170	0	0.3	0.35	0.25	0.40	3000	100	6000	300	0.1	139.9	249.9	420.1	53.0	361.2	134	71.6
609	140	110	170	0	0.3	0.35	0.25	0.40	3000	100	6000	400	0.1	139.9	249.9	420.1	50.5	359.4	105	57.5
610	140	110	170	0	0.3	0.35	0.25	0.40	3000	100	8000	200	0.1	139.9	249.9	420.1	57.4	363.5	223	88.6
611	140	110	170	0	0.3	0.35	0.25	0.40	3000	100	8000	300	0.1	139.9	249.9	420.1	52.8	360.7	168	66.9
612	140	110	170	0	0.3	0.35	0.25	0.40	3000	100	8000	400	0.1	139.9	249.9	420.1	50.4	359.1	134	54.2
613	140	110	170	0	0.3	0.35	0.25	0.40	3000	100	10000	200	0.1	139.9	249.9	420.1	57.1	362.9	259	82.9
614	140	110	170	0	0.3	0.35	0.25	0.40	3000	100	10000	300	0.1	139.9	249.9	420.1	52.6	360.4	198	63.2
615	140	110	170	0	0.3	0.35	0.25	0.40	3000	100	10000	400	0.1	139.9	249.9	420.1	50.3	358.9	161	51.5
616	140	110	170	0	0.3	0.35	0.25	0.40	3000	200	2000	200	0.1	139.9	249.9	420.1	45.9	322.0	95	143.9
617	140	110	170	0	0.3	0.35	0.25	0.40	3000	200	2000	300	0.1	139.9	249.9	420.1	40.6	317.6	65	105.7
618	140	110	170	0	0.3	0.35	0.25	0.40	3000	200	2000	400	0.1	139.9	249.9	420.1	37.9	315.2	47	83.7
619	140	110	170	0	0.3	0.35	0.25	0.40	3000	200	4000	200	0.1	139.9	249.9	420.1	45.2	319.8	168	124.4
620	140	110	170	0	0.3	0.35	0.25	0.40	3000	200	4000	300	0.1	139.9	249.9	420.1	40.2	316.1	124	93.6
621	140	110	170	0	0.3	0.35	0.25	0.40	3000	200	4000	400	0.1	139.9	249.9	420.1	37.5	314.0	97	75.5
622	140	110	170	0	0.3	0.35	0.25	0.40	3000	200	6000	200	0.1	139.9	249.9	420.1	44.7	318.4	225	111.5
623	140	110	170	0	0.3	0.35	0.25	0.40	3000	200	6000	300	0.1	139.9	249.9	420.1	39.9	315.2	171	85.2
624	140	110	170	0	0.3	0.35	0.25	0.40	3000	200	6000	400	0.1	139.9	249.9	420.1	37.3	313.3	138	69.5
625	140	110	170	0	0.3	0.35	0.25	0.40	3000	200	8000	200	0.1	139.9	249.9	420.1	44.3	317.3	273	102.1
626	140	110	170	0	0.3	0.35	0.25	0.40	3000	200	8000	300	0.1	139.9	249.9	420.1	39.6	314.5	211	78.9
627	140	110	170	0	0.3	0.35	0.25	0.40	3000	200	8000	400	0.1	139.9	249.9	420.1	37.1	312.8	173	64.8
628	140	110	170	0	0.3	0.35	0.25	0.40	3000	200	10000	200	0.1	139.9	249.9	420.1	44.0	316.5	314	94.8
629	140	110	170	0	0.3	0.35	0.25	0.40	3000	200	10000	300	0.1	139.9	249.9	420.1	39.4	313.9	246	73.8
630	140	110	170	0	0.3	0.35	0.25	0.40	3000	200	10000	400	0.1	139.9	249.9	420.1	37.0	312.4	204	61.1
631	140	110	170	0	0.3	0.35	0.25	0.40	3000	300	2000	200	0.1	139.9	249.9	420.1	40.4	296.0	109	157.2
632	140	110	170	0	0.3	0.35	0.25	0.40	3000	300	2000	300	0.1	139.9	249.9	420.1	35.0	291.5	76	117.1
633	140	110	170	0	0.3	0.35	0.25	0.40	3000	300	2000	400	0.1	139.9	249.9	420.1	32.2	289.0	57	93.6
634	140	110	170	0	0.3	0.35	0.25	0.40	3000	300	4000	200	0.1	139.9	249.9	420.1	39.6	293.1	190	134.5
635	140	110	170	0	0.3	0.35	0.25	0.40	3000	300	4000	300	0.1	139.9	249.9	420.1	34.5	289.5	142	102.7
636	140	110	170	0	0.3	0.35	0.25	0.40	3000	300	4000	400	0.1	139.9	249.9	420.1	31.8	287.4	113	83.6
637	140	110	170	0	0.3	0.35	0.25	0.40	3000	300	6000	200	0.1	139.9	249.9	420.1	39.0	291.4	251	119.8
638	140	110	170	0	0.3	0.35	0.25	0.40	3000	300	6000	300	0.1	139.9	249.9	420.1	34.2	288.3	194	92.8
639	140	110	170	0	0.3	0.35	0.25	0.40	3000	300	6000	400	0.1	139.9	249.9	420.1	31.6	286.5	158	76.4
640	140	110	170	0	0.3	0.35	0.25	0.40	3000	300	8000	200	0.1	139.9	249.9	420.1	38.6	290.1	302	109.2
641	140	110	170	0	0.3	0.35	0.25	0.40	3000	300	8000	300	0.1	139.9	249.9	420.1	33.9	287.5	238	85.5
642	140	110	170	0	0.3	0.35	0.25	0.40	3000	300	8000	400	0.1	139.9	249.9	420.1	31.4	285.8	197	70.9
643	140	110	170	0	0.3	0.35	0.25	0.40	3000	300	10000	200	0.1	139.9	249.9	420.1	38.2	289.2	345	101.0
644	140	110	170	0	0.3	0.35	0.25	0.40	3000	300	10000	300	0.1	139.9	249.9	420.1	33.7	286.8	275	79.7
645	140	110	170	0	0.3	0.35	0.25	0.40	3000	300	10000	400	0.1	139.9	249.9	420.1	31.2	285.3	230	66.5
646	140	110	170	0	0.3	0.35	0.25	0.40	3000	400	2000	200	0.1	139.9	249.9	420.1	37.0	277.4	120	165.5
647	140	110	170	0	0.3	0.35	0.25	0.40	3000	400	2000	300	0.1	139.9	249.9	420.1	31.7	273.0	85	124.6
648	140	110	170	0	0.3	0.35	0.25	0.40	3000	400	2000	400	0.1	139.9	249.9	420.1	28.9	270.4	64	100.3
649	140	110	170	0	0.3	0.35	0.25	0.40	3000	400	4000	200	0.1	139.9	249.9	420.1	36.2	274.1	205	140.7
650	140	110	170	0	0.3	0.35	0.25	0.40	3000	400	4000	300	0.1	139.9	249.9	420.1	31.1	270.6	156	108.6
651	140	110	170	0	0.3	0.35	0.25	0.40	3000	400	4000	400	0.1	139.9	249.9	420.1	28.5	268.5	125	89.0
652	140	110	170	0	0.3	0.35	0.25	0.40	3000	400	6000	200	0.1	139.9	249.9	420.1	35.6	272.1	269	124.9
653	140	110	170	0	0.3	0.35	0.25	0.40	3000	400	6000	300	0.1	139.9	249.9	420.1	30.8	269.2	211	97.7
654	140	110	170	0	0.3	0.35	0.25	0.40	3000	400	6000	400	0.1	139.9	249.9	420.1	28.2	267.4	173	81.0
655	140	110	170	0	0.3	0.35	0.25	0.40	3000	400	8000	200	0.1	139.9	249.9	420.1	35.2	270.7	322	113.5
656	140	110	170	0	0.3	0.35	0.25	0.40	3000	400	8000	300	0.1	139.9	249.9	420.1	30.5	268.2	256	89.7
657	140	110	170	0	0.3	0.35	0.25	0.40	3000	400	8000	400	0.1	139.9	249.9	420.1	28.0	266.6	214	74.9
658	140	110	170	0	0.3	0.35	0.25	0.40	3000	400	10000	200	0.1	139.9	249.9	420.1	34.8	269.6	367	104.7
659	140	110	170	0	0.3	0.35	0.25	0.40	3000	400	10000	300	0.1	139.9	249.9	420.1	30.2	267.5	295	83.4
660	140	110	170	0	0.3	0.35	0.25	0.40	3000	400	10000	400	0.1	139.9	249.9	420.1	27.8	266.0	249	70.0

Simul.	Thickness (mm)				Poisson's Ratio				Modulus (MPa)				Point of analyses (mm)				D0 (μm)	$\mu\epsilon_t$	$\mu\epsilon$	$\mu\epsilon_v$
	AC	Base	Subbase	Seleted Sub.	AC	Base	Subbase	Seleted Sub.	AC	Base	Subbase	Seleted Sub.								
661	140	110	180	0	0.3	0.35	0.25	0.40	3000	100	2000	200	0.1	139.9	249.9	430.1	58.5	366.2	72	117.2
662	140	110	180	0	0.3	0.35	0.25	0.40	3000	100	2000	300	0.1	139.9	249.9	430.1	53.5	362.4	48	84.5
663	140	110	180	0	0.3	0.35	0.25	0.40	3000	100	2000	400	0.1	139.9	249.9	430.1	50.9	360.4	34	66.1
664	140	110	180	0	0.3	0.35	0.25	0.40	3000	100	4000	200	0.1	139.9	249.9	430.1	57.9	364.8	132	102.5
665	140	110	180	0	0.3	0.35	0.25	0.40	3000	100	4000	300	0.1	139.9	249.9	430.1	53.1	361.5	95	75.8
666	140	110	180	0	0.3	0.35	0.25	0.40	3000	100	4000	400	0.1	139.9	249.9	430.1	50.6	359.7	73	60.4
667	140	110	180	0	0.3	0.35	0.25	0.40	3000	100	6000	200	0.1	139.9	249.9	430.1	57.5	363.7	180	92.6
668	140	110	180	0	0.3	0.35	0.25	0.40	3000	100	6000	300	0.1	139.9	249.9	430.1	52.8	360.9	133	69.6
669	140	110	180	0	0.3	0.35	0.25	0.40	3000	100	6000	400	0.1	139.9	249.9	430.1	50.4	359.2	106	56.1
670	140	110	180	0	0.3	0.35	0.25	0.40	3000	100	8000	200	0.1	139.9	249.9	430.1	57.1	363.0	220	85.2
671	140	110	180	0	0.3	0.35	0.25	0.40	3000	100	8000	300	0.1	139.9	249.9	430.1	52.6	360.4	167	64.8
672	140	110	180	0	0.3	0.35	0.25	0.40	3000	100	8000	400	0.1	139.9	249.9	430.1	50.3	358.9	134	52.6
673	140	110	180	0	0.3	0.35	0.25	0.40	3000	100	10000	200	0.1	139.9	249.9	430.1	56.8	362.3	255	79.4
674	140	110	180	0	0.3	0.35	0.25	0.40	3000	100	10000	300	0.1	139.9	249.9	430.1	52.5	360.0	196	60.9
675	140	110	180	0	0.3	0.35	0.25	0.40	3000	100	10000	400	0.1	139.9	249.9	430.1	50.1	358.6	160	49.8
676	140	110	180	0	0.3	0.35	0.25	0.40	3000	200	2000	200	0.1	139.9	249.9	430.1	45.7	321.4	95	140.6
677	140	110	180	0	0.3	0.35	0.25	0.40	3000	200	2000	300	0.1	139.9	249.9	430.1	40.5	317.2	65	103.6
678	140	110	180	0	0.3	0.35	0.25	0.40	3000	200	2000	400	0.1	139.9	249.9	430.1	37.8	314.9	48	82.2
679	140	110	180	0	0.3	0.35	0.25	0.40	3000	200	4000	200	0.1	139.9	249.9	430.1	45.0	319.1	166	120.3
680	140	110	180	0	0.3	0.35	0.25	0.40	3000	200	4000	300	0.1	139.9	249.9	430.1	40.0	315.7	123	91.0
681	140	110	180	0	0.3	0.35	0.25	0.40	3000	200	4000	400	0.1	139.9	249.9	430.1	37.4	313.7	97	73.7
682	140	110	180	0	0.3	0.35	0.25	0.40	3000	200	6000	200	0.1	139.9	249.9	430.1	44.5	317.6	221	107.2
683	140	110	180	0	0.3	0.35	0.25	0.40	3000	200	6000	300	0.1	139.9	249.9	430.1	39.7	314.7	169	82.4
684	140	110	180	0	0.3	0.35	0.25	0.40	3000	200	6000	400	0.1	139.9	249.9	430.1	37.2	312.9	137	67.4
685	140	110	180	0	0.3	0.35	0.25	0.40	3000	200	8000	200	0.1	139.9	249.9	430.1	44.0	316.5	267	97.8
686	140	110	180	0	0.3	0.35	0.25	0.40	3000	200	8000	300	0.1	139.9	249.9	430.1	39.4	314.0	208	75.9
687	140	110	180	0	0.3	0.35	0.25	0.40	3000	200	8000	400	0.1	139.9	249.9	430.1	37.0	312.4	171	62.6
688	140	110	180	0	0.3	0.35	0.25	0.40	3000	200	10000	200	0.1	139.9	249.9	430.1	43.7	315.7	306	90.4
689	140	110	180	0	0.3	0.35	0.25	0.40	3000	200	10000	300	0.1	139.9	249.9	430.1	39.2	313.4	241	70.8
690	140	110	180	0	0.3	0.35	0.25	0.40	3000	200	10000	400	0.1	139.9	249.9	430.1	36.8	312.0	201	58.8
691	140	110	180	0	0.3	0.35	0.25	0.40	3000	300	2000	200	0.1	139.9	249.9	430.1	40.1	295.3	109	153.2
692	140	110	180	0	0.3	0.35	0.25	0.40	3000	300	2000	300	0.1	139.9	249.9	430.1	34.9	291.1	77	114.5
693	140	110	180	0	0.3	0.35	0.25	0.40	3000	300	2000	400	0.1	139.9	249.9	430.1	32.1	288.6	57	91.8
694	140	110	180	0	0.3	0.35	0.25	0.40	3000	300	4000	200	0.1	139.9	249.9	430.1	39.3	292.3	187	129.8
695	140	110	180	0	0.3	0.35	0.25	0.40	3000	300	4000	300	0.1	139.9	249.9	430.1	34.3	289.0	141	99.6
696	140	110	180	0	0.3	0.35	0.25	0.40	3000	300	4000	400	0.1	139.9	249.9	430.1	31.7	287.0	112	81.3
697	140	110	180	0	0.3	0.35	0.25	0.40	3000	300	6000	200	0.1	139.9	249.9	430.1	38.7	290.5	246	114.9
698	140	110	180	0	0.3	0.35	0.25	0.40	3000	300	6000	300	0.1	139.9	249.9	430.1	34.0	287.7	191	89.5
699	140	110	180	0	0.3	0.35	0.25	0.40	3000	300	6000	400	0.1	139.9	249.9	430.1	31.4	286.0	156	73.9
700	140	110	180	0	0.3	0.35	0.25	0.40	3000	300	8000	200	0.1	139.9	249.9	430.1	38.3	289.3	294	104.2
701	140	110	180	0	0.3	0.35	0.25	0.40	3000	300	8000	300	0.1	139.9	249.9	430.1	33.7	286.9	233	82.0
702	140	110	180	0	0.3	0.35	0.25	0.40	3000	300	8000	400	0.1	139.9	249.9	430.1	31.2	285.3	194	68.3
703	140	110	180	0	0.3	0.35	0.25	0.40	3000	300	10000	200	0.1	139.9	249.9	430.1	37.9	288.3	335	96.1
704	140	110	180	0	0.3	0.35	0.25	0.40	3000	300	10000	300	0.1	139.9	249.9	430.1	33.4	286.2	269	76.2
705	140	110	180	0	0.3	0.35	0.25	0.40	3000	300	10000	400	0.1	139.9	249.9	430.1	31.1	284.8	226	63.8
706	140	110	180	0	0.3	0.35	0.25	0.40	3000	400	2000	200	0.1	139.9	249.9	430.1	36.8	276.6	119	161.0
707	140	110	180	0	0.3	0.35	0.25	0.40	3000	400	2000	300	0.1	139.9	249.9	430.1	31.6	272.5	85	121.7
708	140	110	180	0	0.3	0.35	0.25	0.40	3000	400	2000	400	0.1	139.9	249.9	430.1	28.8	270.0	64	98.1
709	140	110	180	0	0.3	0.35	0.25	0.40	3000	400	4000	200	0.1	139.9	249.9	430.1	35.9	273.2	201	135.6
710	140	110	180	0	0.3	0.35	0.25	0.40	3000	400	4000	300	0.1	139.9	249.9	430.1	31.0	270.0	154	105.1
711	140	110	180	0	0.3	0.35	0.25	0.40	3000	400	4000	400	0.1	139.9	249.9	430.1	28.3	268.0	124	86.4
712	140	110	180	0	0.3	0.35	0.25	0.40	3000	400	6000	200	0.1	139.9	249.9	430.1	35.3	271.2	263	119.6
713	140	110	180	0	0.3	0.35	0.25	0.40	3000	400	6000	300	0.1	139.9	249.9	430.1	30.6	268.6	207	94.0
714	140	110	180	0	0.3	0.35	0.25	0.40	3000	400	6000	400	0.1	139.9	249.9	430.1	28.0	266.9	170	78.2
715	140	110	180	0	0.3	0.35	0.25	0.40	3000	400	8000	200	0.1	139.9	249.9	430.1	34.8	269.8	313	108.2
716	140	110	180	0	0.3	0.35	0.25	0.40	3000	400	8000	300	0.1	139.9	249.9	430.1	30.3	267.6	250	85.9
717	140	110	180	0	0.3	0.35	0.25	0.40	3000	400	8000	400	0.1	139.9	249.9	430.1	27.8	266.1	210	72.0
718	140	110	180	0	0.3	0.35	0.25	0.40	3000	400	10000	200	0.1	139.9	249.9	430.1	34.4	268.7	355	99.5
719	140	110	180	0	0.3	0.35	0.25	0.40	3000	400	10000	300	0.1	139.9	249.9	430.1	30.0	266.8	288	79.6
720	140	110	180	0	0.3	0.35	0.25	0.40	3000	400	10000	400	0.1	139.9	249.9	430.1	27.6	265.5	243	67.1

Simul.	Thickness (mm)			Poisson's Ratio				Modulus (MPa)				Point of analyses (mm)				D0 (μm)	$\mu\epsilon_t$	$\mu\epsilon$	$\mu\epsilon_v$	
	AC	Base	Subbase	Seleted Sub.	AC	Base	Subbase	Seleted Sub.	AC	Base	Subbase	Seleted Sub.								
721	140	120	150	0	0.3	0.35	0.25	0.40	3000	100	2000	200	0.1	139.9	259.9	410.1	60.9	373.0	66	119.3
722	140	120	150	0	0.3	0.35	0.25	0.40	3000	100	2000	300	0.1	139.9	259.9	410.1	55.7	368.9	42	84.7
723	140	120	150	0	0.3	0.35	0.25	0.40	3000	100	2000	400	0.1	139.9	259.9	410.1	53.1	366.7	29	65.8
724	140	120	150	0	0.3	0.35	0.25	0.40	3000	100	4000	200	0.1	139.9	259.9	410.1	60.5	371.9	125	107.5
725	140	120	150	0	0.3	0.35	0.25	0.40	3000	100	4000	300	0.1	139.9	259.9	410.1	55.5	368.2	88	78.1
726	140	120	150	0	0.3	0.35	0.25	0.40	3000	100	4000	400	0.1	139.9	259.9	410.1	52.9	366.1	66	61.5
727	140	120	150	0	0.3	0.35	0.25	0.40	3000	100	6000	200	0.1	139.9	259.9	410.1	60.2	371.1	175	99.2
728	140	120	150	0	0.3	0.35	0.25	0.40	3000	100	6000	300	0.1	139.9	259.9	410.1	55.3	367.7	127	73.1
729	140	120	150	0	0.3	0.35	0.25	0.40	3000	100	6000	400	0.1	139.9	259.9	410.1	52.7	365.8	99	58.1
730	140	120	150	0	0.3	0.35	0.25	0.40	3000	100	8000	200	0.1	139.9	259.9	410.1	59.9	370.5	218	92.8
731	140	120	150	0	0.3	0.35	0.25	0.40	3000	100	8000	300	0.1	139.9	259.9	410.1	55.1	367.4	161	69.1
732	140	120	150	0	0.3	0.35	0.25	0.40	3000	100	8000	400	0.1	139.9	259.9	410.1	52.6	365.6	128	55.4
733	140	120	150	0	0.3	0.35	0.25	0.40	3000	100	10000	200	0.1	139.9	259.9	410.1	59.7	370.0	256	87.7
734	140	120	150	0	0.3	0.35	0.25	0.40	3000	100	10000	300	0.1	139.9	259.9	410.1	55.0	367.0	192	65.8
735	140	120	150	0	0.3	0.35	0.25	0.40	3000	100	10000	400	0.1	139.9	259.9	410.1	52.6	365.4	154	53.0
736	140	120	150	0	0.3	0.35	0.25	0.40	3000	200	2000	200	0.1	139.9	259.9	410.1	47.6	328.3	90	145.3
737	140	120	150	0	0.3	0.35	0.25	0.40	3000	200	2000	300	0.1	139.9	259.9	410.1	42.2	323.6	60	105.6
738	140	120	150	0	0.3	0.35	0.25	0.40	3000	200	2000	400	0.1	139.9	259.9	410.1	39.4	321.1	43	83.0
739	140	120	150	0	0.3	0.35	0.25	0.40	3000	200	4000	200	0.1	139.9	259.9	410.1	47.0	326.5	163	128.5
740	140	120	150	0	0.3	0.35	0.25	0.40	3000	200	4000	300	0.1	139.9	259.9	410.1	41.8	322.4	118	95.5
741	140	120	150	0	0.3	0.35	0.25	0.40	3000	200	4000	400	0.1	139.9	259.9	410.1	39.1	320.1	91	76.3
742	140	120	150	0	0.3	0.35	0.25	0.40	3000	200	6000	200	0.1	139.9	259.9	410.1	46.6	325.3	222	117.0
743	140	120	150	0	0.3	0.35	0.25	0.40	3000	200	6000	300	0.1	139.9	259.9	410.1	41.6	321.7	166	88.2
744	140	120	150	0	0.3	0.35	0.25	0.40	3000	200	6000	400	0.1	139.9	259.9	410.1	38.9	319.6	132	71.2
745	140	120	150	0	0.3	0.35	0.25	0.40	3000	200	8000	200	0.1	139.9	259.9	410.1	46.3	324.4	272	108.4
746	140	120	150	0	0.3	0.35	0.25	0.40	3000	200	8000	300	0.1	139.9	259.9	410.1	41.4	321.1	208	82.5
747	140	120	150	0	0.3	0.35	0.25	0.40	3000	200	8000	400	0.1	139.9	259.9	410.1	38.8	319.2	168	67.1
748	140	120	150	0	0.3	0.35	0.25	0.40	3000	200	10000	200	0.1	139.9	259.9	410.1	46.0	323.6	316	101.5
749	140	120	150	0	0.3	0.35	0.25	0.40	3000	200	10000	300	0.1	139.9	259.9	410.1	41.2	320.6	244	77.9
750	140	120	150	0	0.3	0.35	0.25	0.40	3000	200	10000	400	0.1	139.9	259.9	410.1	38.7	318.8	200	63.7
751	140	120	150	0	0.3	0.35	0.25	0.40	3000	300	2000	200	0.1	139.9	259.9	410.1	41.8	302.3	105	159.8
752	140	120	150	0	0.3	0.35	0.25	0.40	3000	300	2000	300	0.1	139.9	259.9	410.1	36.3	297.5	72	117.8
753	140	120	150	0	0.3	0.35	0.25	0.40	3000	300	2000	400	0.1	139.9	259.9	410.1	33.5	294.8	53	93.5
754	140	120	150	0	0.3	0.35	0.25	0.40	3000	300	4000	200	0.1	139.9	259.9	410.1	41.1	300.0	187	139.8
755	140	120	150	0	0.3	0.35	0.25	0.40	3000	300	4000	300	0.1	139.9	259.9	410.1	35.9	295.9	138	105.4
756	140	120	150	0	0.3	0.35	0.25	0.40	3000	300	4000	400	0.1	139.9	259.9	410.1	33.1	293.5	108	85.1
757	140	120	150	0	0.3	0.35	0.25	0.40	3000	300	6000	200	0.1	139.9	259.9	410.1	40.7	298.4	251	126.5
758	140	120	150	0	0.3	0.35	0.25	0.40	3000	300	6000	300	0.1	139.9	259.9	410.1	35.6	294.9	191	96.7
759	140	120	150	0	0.3	0.35	0.25	0.40	3000	300	6000	400	0.1	139.9	259.9	410.1	32.9	292.8	154	78.9
760	140	120	150	0	0.3	0.35	0.25	0.40	3000	300	8000	200	0.1	139.9	259.9	410.1	40.3	297.3	305	116.6
761	140	120	150	0	0.3	0.35	0.25	0.40	3000	300	8000	300	0.1	139.9	259.9	410.1	35.4	294.1	237	90.0
762	140	120	150	0	0.3	0.35	0.25	0.40	3000	300	8000	400	0.1	139.9	259.9	410.1	32.8	292.2	194	74.0
763	140	120	150	0	0.3	0.35	0.25	0.40	3000	300	10000	200	0.1	139.9	259.9	410.1	40.0	296.4	352	108.9
764	140	120	150	0	0.3	0.35	0.25	0.40	3000	300	10000	300	0.1	139.9	259.9	410.1	35.2	293.5	277	84.7
765	140	120	150	0	0.3	0.35	0.25	0.40	3000	300	10000	400	0.1	139.9	259.9	410.1	32.6	291.8	229	69.9
766	140	120	150	0	0.3	0.35	0.25	0.40	3000	400	2000	200	0.1	139.9	259.9	410.1	38.3	283.8	116	169.0
767	140	120	150	0	0.3	0.35	0.25	0.40	3000	400	2000	300	0.1	139.9	259.9	410.1	32.9	279.0	81	125.9
768	140	120	150	0	0.3	0.35	0.25	0.40	3000	400	2000	400	0.1	139.9	259.9	410.1	30.0	276.2	60	100.6
769	140	120	150	0	0.3	0.35	0.25	0.40	3000	400	4000	200	0.1	139.9	259.9	410.1	37.6	280.9	203	146.9
770	140	120	150	0	0.3	0.35	0.25	0.40	3000	400	4000	300	0.1	139.9	259.9	410.1	32.4	277.0	152	112.0
771	140	120	150	0	0.3	0.35	0.25	0.40	3000	400	4000	400	0.1	139.9	259.9	410.1	29.6	274.6	120	91.0
772	140	120	150	0	0.3	0.35	0.25	0.40	3000	400	6000	200	0.1	139.9	259.9	410.1	37.1	279.2	271	132.4
773	140	120	150	0	0.3	0.35	0.25	0.40	3000	400	6000	300	0.1	139.9	259.9	410.1	32.1	275.8	209	102.3
774	140	120	150	0	0.3	0.35	0.25	0.40	3000	400	6000	400	0.1	139.9	259.9	410.1	29.4	273.7	170	84.0
775	140	120	150	0	0.3	0.35	0.25	0.40	3000	400	8000	200	0.1	139.9	259.9	410.1	36.8	277.9	328	121.7
776	140	120	150	0	0.3	0.35	0.25	0.40	3000	400	8000	300	0.1	139.9	259.9	410.1	31.8	274.9	257	94.9
777	140	120	150	0	0.3	0.35	0.25	0.40	3000	400	8000	400	0.1	139.9	259.9	410.1	29.2	273.0	212	78.5
778	140	120	150	0	0.3	0.35	0.25	0.40	3000	400	10000	200	0.1	139.9	259.9	410.1	36.4	276.9	377	113.4
779	140	120	150	0	0.3	0.35	0.25	0.40	3000	400	10000	300	0.1	139.9	259.9	410.1	31.6	274.2	299	89.0
780	140	120	150	0	0.3	0.35	0.25	0.40	3000	400	10000	400	0.1	139.9	259.9	410.1	29.1	272.5	249	74.1

Simul.	Thickness (mm)			Poisson's Ratio				Modulus (MPa)				Point of analyses (mm)				D0 (μm)	$\mu\epsilon_t$	$\mu\epsilon$	$\mu\epsilon_v$	
	AC	Base	Subbase	Seleted Sub.	AC	Base	Subbase	Seleted Sub.	AC	Base	Subbase	Seleted Sub.								
781	140	120	160	0	0.3	0.35	0.25	0.40	3000	100	2000	200	0.1	139.9	259.9	420.1	60.8	372.6	67	117.3
782	140	120	160	0	0.3	0.35	0.25	0.40	3000	100	2000	300	0.1	139.9	259.9	420.1	55.7	368.6	43	83.7
783	140	120	160	0	0.3	0.35	0.25	0.40	3000	100	2000	400	0.1	139.9	259.9	420.1	53.0	366.5	30	65.1
784	140	120	160	0	0.3	0.35	0.25	0.40	3000	100	4000	200	0.1	139.9	259.9	420.1	60.3	371.4	126	104.8
785	140	120	160	0	0.3	0.35	0.25	0.40	3000	100	4000	300	0.1	139.9	259.9	420.1	55.4	367.9	89	76.5
786	140	120	160	0	0.3	0.35	0.25	0.40	3000	100	4000	400	0.1	139.9	259.9	420.1	52.8	366.0	68	60.5
787	140	120	160	0	0.3	0.35	0.25	0.40	3000	100	6000	200	0.1	139.9	259.9	420.1	59.9	370.6	175	96.1
788	140	120	160	0	0.3	0.35	0.25	0.40	3000	100	6000	300	0.1	139.9	259.9	420.1	55.2	367.4	128	71.2
789	140	120	160	0	0.3	0.35	0.25	0.40	3000	100	6000	400	0.1	139.9	259.9	420.1	52.7	365.6	100	56.8
790	140	120	160	0	0.3	0.35	0.25	0.40	3000	100	8000	200	0.1	139.9	259.9	420.1	59.6	369.9	217	89.5
791	140	120	160	0	0.3	0.35	0.25	0.40	3000	100	8000	300	0.1	139.9	259.9	420.1	55.0	367.0	161	67.0
792	140	120	160	0	0.3	0.35	0.25	0.40	3000	100	8000	400	0.1	139.9	259.9	420.1	52.5	365.3	128	53.9
793	140	120	160	0	0.3	0.35	0.25	0.40	3000	100	10000	200	0.1	139.9	259.9	420.1	59.4	369.4	253	84.1
794	140	120	160	0	0.3	0.35	0.25	0.40	3000	100	10000	300	0.1	139.9	259.9	420.1	54.8	366.7	192	63.5
795	140	120	160	0	0.3	0.35	0.25	0.40	3000	100	10000	400	0.1	139.9	259.9	420.1	52.4	365.1	154	51.4
796	140	120	160	0	0.3	0.35	0.25	0.40	3000	200	2000	200	0.1	139.9	259.9	420.1	47.4	327.7	90	142.3
797	140	120	160	0	0.3	0.35	0.25	0.40	3000	200	2000	300	0.1	139.9	259.9	420.1	42.1	323.3	61	103.7
798	140	120	160	0	0.3	0.35	0.25	0.40	3000	200	2000	400	0.1	139.9	259.9	420.1	39.3	320.8	44	81.8
799	140	120	160	0	0.3	0.35	0.25	0.40	3000	200	4000	200	0.1	139.9	259.9	420.1	46.8	325.8	163	124.5
800	140	120	160	0	0.3	0.35	0.25	0.40	3000	200	4000	300	0.1	139.9	259.9	420.1	41.7	322.0	119	93.0
801	140	120	160	0	0.3	0.35	0.25	0.40	3000	200	4000	400	0.1	139.9	259.9	420.1	39.0	319.8	92	74.6
802	140	120	160	0	0.3	0.35	0.25	0.40	3000	200	6000	200	0.1	139.9	259.9	420.1	46.3	324.5	220	112.6
803	140	120	160	0	0.3	0.35	0.25	0.40	3000	200	6000	300	0.1	139.9	259.9	420.1	41.4	321.2	165	85.3
804	140	120	160	0	0.3	0.35	0.25	0.40	3000	200	6000	400	0.1	139.9	259.9	420.1	38.8	319.2	132	69.2
805	140	120	160	0	0.3	0.35	0.25	0.40	3000	200	8000	200	0.1	139.9	259.9	420.1	46.0	323.6	268	103.8
806	140	120	160	0	0.3	0.35	0.25	0.40	3000	200	8000	300	0.1	139.9	259.9	420.1	41.2	320.6	206	79.5
807	140	120	160	0	0.3	0.35	0.25	0.40	3000	200	8000	400	0.1	139.9	259.9	420.1	38.7	318.8	167	64.9
808	140	120	160	0	0.3	0.35	0.25	0.40	3000	200	10000	200	0.1	139.9	259.9	420.1	45.7	322.8	310	96.9
809	140	120	160	0	0.3	0.35	0.25	0.40	3000	200	10000	300	0.1	139.9	259.9	420.1	41.0	320.1	241	74.8
810	140	120	160	0	0.3	0.35	0.25	0.40	3000	200	10000	400	0.1	139.9	259.9	420.1	38.5	318.4	198	61.4
811	140	120	160	0	0.3	0.35	0.25	0.40	3000	300	2000	200	0.1	139.9	259.9	420.1	41.6	301.6	105	156.0
812	140	120	160	0	0.3	0.35	0.25	0.40	3000	300	2000	300	0.1	139.9	259.9	420.1	36.2	297.1	73	115.4
813	140	120	160	0	0.3	0.35	0.25	0.40	3000	300	2000	400	0.1	139.9	259.9	420.1	33.4	294.5	54	91.9
814	140	120	160	0	0.3	0.35	0.25	0.40	3000	300	4000	200	0.1	139.9	259.9	420.1	40.9	299.1	185	135.2
815	140	120	160	0	0.3	0.35	0.25	0.40	3000	300	4000	300	0.1	139.9	259.9	420.1	35.7	295.3	137	102.4
816	140	120	160	0	0.3	0.35	0.25	0.40	3000	300	4000	400	0.1	139.9	259.9	420.1	33.0	293.1	108	82.9
817	140	120	160	0	0.3	0.35	0.25	0.40	3000	300	6000	200	0.1	139.9	259.9	420.1	40.4	297.5	247	121.5
818	140	120	160	0	0.3	0.35	0.25	0.40	3000	300	6000	300	0.1	139.9	259.9	420.1	35.4	294.3	189	93.4
819	140	120	160	0	0.3	0.35	0.25	0.40	3000	300	6000	400	0.1	139.9	259.9	420.1	32.8	292.3	153	76.4
820	140	120	160	0	0.3	0.35	0.25	0.40	3000	300	8000	200	0.1	139.9	259.9	420.1	40.0	296.4	299	111.4
821	140	120	160	0	0.3	0.35	0.25	0.40	3000	300	8000	300	0.1	139.9	259.9	420.1	35.2	293.5	233	86.5
822	140	120	160	0	0.3	0.35	0.25	0.40	3000	300	8000	400	0.1	139.9	259.9	420.1	32.6	291.7	192	71.3
823	140	120	160	0	0.3	0.35	0.25	0.40	3000	300	10000	200	0.1	139.9	259.9	420.1	39.7	295.5	343	103.6
824	140	120	160	0	0.3	0.35	0.25	0.40	3000	300	10000	300	0.1	139.9	259.9	420.1	35.0	292.9	271	81.0
825	140	120	160	0	0.3	0.35	0.25	0.40	3000	300	10000	400	0.1	139.9	259.9	420.1	32.5	291.3	225	67.2
826	140	120	160	0	0.3	0.35	0.25	0.40	3000	400	2000	200	0.1	139.9	259.9	420.1	38.1	282.9	116	164.7
827	140	120	160	0	0.3	0.35	0.25	0.40	3000	400	2000	300	0.1	139.9	259.9	420.1	32.7	278.4	81	123.2
828	140	120	160	0	0.3	0.35	0.25	0.40	3000	400	2000	400	0.1	139.9	259.9	420.1	29.9	275.8	61	98.7
829	140	120	160	0	0.3	0.35	0.25	0.40	3000	400	4000	200	0.1	139.9	259.9	420.1	37.3	280.0	200	141.8
830	140	120	160	0	0.3	0.35	0.25	0.40	3000	400	4000	300	0.1	139.9	259.9	420.1	32.2	276.3	151	108.6
831	140	120	160	0	0.3	0.35	0.25	0.40	3000	400	4000	400	0.1	139.9	259.9	420.1	29.5	274.1	120	88.6
832	140	120	160	0	0.3	0.35	0.25	0.40	3000	400	6000	200	0.1	139.9	259.9	420.1	36.8	278.2	266	126.9
833	140	120	160	0	0.3	0.35	0.25	0.40	3000	400	6000	300	0.1	139.9	259.9	420.1	31.9	275.1	206	98.6
834	140	120	160	0	0.3	0.35	0.25	0.40	3000	400	6000	400	0.1	139.9	259.9	420.1	29.3	273.1	168	81.2
835	140	120	160	0	0.3	0.35	0.25	0.40	3000	400	8000	200	0.1	139.9	259.9	420.1	36.4	276.9	320	116.1
836	140	120	160	0	0.3	0.35	0.25	0.40	3000	400	8000	300	0.1	139.9	259.9	420.1	31.6	274.2	252	91.0
837	140	120	160	0	0.3	0.35	0.25	0.40	3000	400	8000	400	0.1	139.9	259.9	420.1	29.1	272.5	209	75.6
838	140	120	160	0	0.3	0.35	0.25	0.40	3000	400	10000	200	0.1	139.9	259.9	420.1	36.1	275.9	366	107.7
839	140	120	160	0	0.3	0.35	0.25	0.40	3000	400	10000	300	0.1	139.9	259.9	420.1	31.4	273.5	292	85.0
840	140	120	160	0	0.3	0.35	0.25	0.40	3000	400	10000	400	0.1	139.9	259.9	420.1	28.9	271.9	245	71.0

Simul.	Thickness (mm)			Poisson's Ratio				Modulus (MPa)				Point of analyses (mm)				D0 (μm)	$\mu\epsilon_t$	$\mu\epsilon$	$\mu\epsilon_v$	
	AC	Base	Subbase	Seleted Sub.	AC	Base	Subbase	Seleted Sub.	AC	Base	Subbase	Seleted Sub.								
841	140	120	170	0	0.3	0.35	0.25	0.40	3000	100	2000	200	0.1	139.9	259.9	430.1	60.6	372.2	68	115.3
842	140	120	170	0	0.3	0.35	0.25	0.40	3000	100	2000	300	0.1	139.9	259.9	430.1	55.6	368.4	44	82.5
843	140	120	170	0	0.3	0.35	0.25	0.40	3000	100	2000	400	0.1	139.9	259.9	430.1	53.0	366.4	31	64.4
844	140	120	170	0	0.3	0.35	0.25	0.40	3000	100	4000	200	0.1	139.9	259.9	430.1	60.1	371.0	127	102.0
845	140	120	170	0	0.3	0.35	0.25	0.40	3000	100	4000	300	0.1	139.9	259.9	430.1	55.3	367.6	90	74.9
846	140	120	170	0	0.3	0.35	0.25	0.40	3000	100	4000	400	0.1	139.9	259.9	430.1	52.7	365.8	69	59.4
847	140	120	170	0	0.3	0.35	0.25	0.40	3000	100	6000	200	0.1	139.9	259.9	430.1	59.7	370.1	174	93.0
848	140	120	170	0	0.3	0.35	0.25	0.40	3000	100	6000	300	0.1	139.9	259.9	430.1	55.0	367.1	128	69.3
849	140	120	170	0	0.3	0.35	0.25	0.40	3000	100	6000	400	0.1	139.9	259.9	430.1	52.6	365.4	101	55.5
850	140	120	170	0	0.3	0.35	0.25	0.40	3000	100	8000	200	0.1	139.9	259.9	430.1	59.4	369.4	215	86.2
851	140	120	170	0	0.3	0.35	0.25	0.40	3000	100	8000	300	0.1	139.9	259.9	430.1	54.8	366.7	161	64.9
852	140	120	170	0	0.3	0.35	0.25	0.40	3000	100	8000	400	0.1	139.9	259.9	430.1	52.4	365.1	129	52.4
853	140	120	170	0	0.3	0.35	0.25	0.40	3000	100	10000	200	0.1	139.9	259.9	430.1	59.1	368.8	250	80.7
854	140	120	170	0	0.3	0.35	0.25	0.40	3000	100	10000	300	0.1	139.9	259.9	430.1	54.7	366.3	191	61.3
855	140	120	170	0	0.3	0.35	0.25	0.40	3000	100	10000	400	0.1	139.9	259.9	430.1	52.3	364.9	154	49.9
856	140	120	170	0	0.3	0.35	0.25	0.40	3000	200	2000	200	0.1	139.9	259.9	430.1	47.2	327.2	91	139.1
857	140	120	170	0	0.3	0.35	0.25	0.40	3000	200	2000	300	0.1	139.9	259.9	430.1	42.0	322.9	62	101.9
858	140	120	170	0	0.3	0.35	0.25	0.40	3000	200	2000	400	0.1	139.9	259.9	430.1	39.2	320.6	45	80.5
859	140	120	170	0	0.3	0.35	0.25	0.40	3000	200	4000	200	0.1	139.9	259.9	430.1	46.5	325.1	161	120.6
860	140	120	170	0	0.3	0.35	0.25	0.40	3000	200	4000	300	0.1	139.9	259.9	430.1	41.5	321.6	118	90.5
861	140	120	170	0	0.3	0.35	0.25	0.40	3000	200	4000	400	0.1	139.9	259.9	430.1	38.9	319.5	93	72.9
862	140	120	170	0	0.3	0.35	0.25	0.40	3000	200	6000	200	0.1	139.9	259.9	430.1	46.1	323.8	217	108.4
863	140	120	170	0	0.3	0.35	0.25	0.40	3000	200	6000	300	0.1	139.9	259.9	430.1	41.2	320.7	164	82.6
864	140	120	170	0	0.3	0.35	0.25	0.40	3000	200	6000	400	0.1	139.9	259.9	430.1	38.7	318.9	132	67.2
865	140	120	170	0	0.3	0.35	0.25	0.40	3000	200	8000	200	0.1	139.9	259.9	430.1	45.7	322.8	263	99.4
866	140	120	170	0	0.3	0.35	0.25	0.40	3000	200	8000	300	0.1	139.9	259.9	430.1	41.0	320.1	203	76.6
867	140	120	170	0	0.3	0.35	0.25	0.40	3000	200	8000	400	0.1	139.9	259.9	430.1	38.5	318.4	166	62.8
868	140	120	170	0	0.3	0.35	0.25	0.40	3000	200	10000	200	0.1	139.9	259.9	430.1	45.4	322.1	303	92.5
869	140	120	170	0	0.3	0.35	0.25	0.40	3000	200	10000	300	0.1	139.9	259.9	430.1	40.8	319.6	237	71.8
870	140	120	170	0	0.3	0.35	0.25	0.40	3000	200	10000	400	0.1	139.9	259.9	430.1	38.4	318.1	196	59.2
871	140	120	170	0	0.3	0.35	0.25	0.40	3000	300	2000	200	0.1	139.9	259.9	430.1	41.4	300.9	105	152.2
872	140	120	170	0	0.3	0.35	0.25	0.40	3000	300	2000	300	0.1	139.9	259.9	430.1	36.1	296.6	73	113.1
873	140	120	170	0	0.3	0.35	0.25	0.40	3000	300	2000	400	0.1	139.9	259.9	430.1	33.3	294.2	54	90.2
874	140	120	170	0	0.3	0.35	0.25	0.40	3000	300	4000	200	0.1	139.9	259.9	430.1	40.6	298.3	183	130.6
875	140	120	170	0	0.3	0.35	0.25	0.40	3000	300	4000	300	0.1	139.9	259.9	430.1	35.6	294.8	137	99.4
876	140	120	170	0	0.3	0.35	0.25	0.40	3000	300	4000	400	0.1	139.9	259.9	430.1	32.9	292.7	108	80.8
877	140	120	170	0	0.3	0.35	0.25	0.40	3000	300	6000	200	0.1	139.9	259.9	430.1	40.1	296.7	242	116.6
878	140	120	170	0	0.3	0.35	0.25	0.40	3000	300	6000	300	0.1	139.9	259.9	430.1	35.3	293.7	187	90.1
879	140	120	170	0	0.3	0.35	0.25	0.40	3000	300	6000	400	0.1	139.9	259.9	430.1	32.7	291.9	152	74.0
880	140	120	170	0	0.3	0.35	0.25	0.40	3000	300	8000	200	0.1	139.9	259.9	430.1	39.7	295.5	292	106.4
881	140	120	170	0	0.3	0.35	0.25	0.40	3000	300	8000	300	0.1	139.9	259.9	430.1	35.0	292.9	229	83.0
882	140	120	170	0	0.3	0.35	0.25	0.40	3000	300	8000	400	0.1	139.9	259.9	430.1	32.5	291.3	189	68.8
883	140	120	170	0	0.3	0.35	0.25	0.40	3000	300	10000	200	0.1	139.9	259.9	430.1	39.3	294.6	334	98.6
884	140	120	170	0	0.3	0.35	0.25	0.40	3000	300	10000	300	0.1	139.9	259.9	430.1	34.8	292.3	266	77.5
885	140	120	170	0	0.3	0.35	0.25	0.40	3000	300	10000	400	0.1	139.9	259.9	430.1	32.3	290.8	222	64.5
886	140	120	170	0	0.3	0.35	0.25	0.40	3000	400	2000	200	0.1	139.9	259.9	430.1	37.9	282.1	115	160.4
887	140	120	170	0	0.3	0.35	0.25	0.40	3000	400	2000	300	0.1	139.9	259.9	430.1	32.6	277.9	81	120.5
888	140	120	170	0	0.3	0.35	0.25	0.40	3000	400	2000	400	0.1	139.9	259.9	430.1	29.8	275.4	61	96.8
889	140	120	170	0	0.3	0.35	0.25	0.40	3000	400	4000	200	0.1	139.9	259.9	430.1	37.1	279.1	197	136.7
890	140	120	170	0	0.3	0.35	0.25	0.40	3000	400	4000	300	0.1	139.9	259.9	430.1	32.0	275.7	149	105.2
891	140	120	170	0	0.3	0.35	0.25	0.40	3000	400	4000	400	0.1	139.9	259.9	430.1	29.4	273.6	119	86.1
892	140	120	170	0	0.3	0.35	0.25	0.40	3000	400	6000	200	0.1	139.9	259.9	430.1	36.5	277.2	260	121.6
893	140	120	170	0	0.3	0.35	0.25	0.40	3000	400	6000	300	0.1	139.9	259.9	430.1	31.7	274.4	203	94.9
894	140	120	170	0	0.3	0.35	0.25	0.40	3000	400	6000	400	0.1	139.9	259.9	430.1	29.1	272.6	166	78.5
895	140	120	170	0	0.3	0.35	0.25	0.40	3000	400	8000	200	0.1	139.9	259.9	430.1	36.1	275.9	311	110.7
896	140	120	170	0	0.3	0.35	0.25	0.40	3000	400	8000	300	0.1	139.9	259.9	430.1	31.4	273.5	247	87.2
897	140	120	170	0	0.3	0.35	0.25	0.40	3000	400	8000	400	0.1	139.9	259.9	430.1	28.9	271.9	206	72.7
898	140	120	170	0	0.3	0.35	0.25	0.40	3000	400	10000	200	0.1	139.9	259.9	430.1	35.7	274.9	355	102.3
899	140	120	170	0	0.3	0.35	0.25	0.40	3000	400	10000	300	0.1	139.9	259.9	430.1	31.2	272.8	285	81.2
900	140	120	170	0	0.3	0.35	0.25	0.40	3000	400	10000	400	0.1	139.9	259.9	430.1	28.7	271.4	240	68.1

Simul.	Thickness (mm)				Poisson's Ratio				Modulus (MPa)				Point of analyses (mm)			D0 (μm)	$\mu\epsilon_t$	$\mu\epsilon$	$\mu\epsilon_v$	
	AC	Base	Subbase	Seleted Sub.	AC	Base	Subbase	Seleted Sub.	AC	Base	Subbase	Seleted Sub.								
901	140	120	180	0	0.3	0.35	0.25	0.40	3000	100	2000	200	0.1	139.9	259.9	440.1	60.5	371.9	69	113.2
902	140	120	180	0	0.3	0.35	0.25	0.40	3000	100	2000	300	0.1	139.9	259.9	440.1	55.5	368.2	45	81.3
903	140	120	180	0	0.3	0.35	0.25	0.40	3000	100	2000	400	0.1	139.9	259.9	440.1	52.9	366.2	32	63.6
904	140	120	180	0	0.3	0.35	0.25	0.40	3000	100	4000	200	0.1	139.9	259.9	440.1	59.9	370.5	127	99.3
905	140	120	180	0	0.3	0.35	0.25	0.40	3000	100	4000	300	0.1	139.9	259.9	440.1	55.1	367.4	91	73.2
906	140	120	180	0	0.3	0.35	0.25	0.40	3000	100	4000	400	0.1	139.9	259.9	440.1	52.7	365.6	69	58.3
907	140	120	180	0	0.3	0.35	0.25	0.40	3000	100	6000	200	0.1	139.9	259.9	440.1	59.5	369.6	173	89.9
908	140	120	180	0	0.3	0.35	0.25	0.40	3000	100	6000	300	0.1	139.9	259.9	440.1	54.9	366.8	128	67.4
909	140	120	180	0	0.3	0.35	0.25	0.40	3000	100	6000	400	0.1	139.9	259.9	440.1	52.5	365.2	101	54.2
910	140	120	180	0	0.3	0.35	0.25	0.40	3000	100	8000	200	0.1	139.9	259.9	440.1	59.2	368.9	212	83.0
911	140	120	180	0	0.3	0.35	0.25	0.40	3000	100	8000	300	0.1	139.9	259.9	440.1	54.7	366.3	160	62.8
912	140	120	180	0	0.3	0.35	0.25	0.40	3000	100	8000	400	0.1	139.9	259.9	440.1	52.3	364.9	129	51.0
913	140	120	180	0	0.3	0.35	0.25	0.40	3000	100	10000	200	0.1	139.9	259.9	440.1	58.9	368.2	246	77.4
914	140	120	180	0	0.3	0.35	0.25	0.40	3000	100	10000	300	0.1	139.9	259.9	440.1	54.5	366.0	189	59.2
915	140	120	180	0	0.3	0.35	0.25	0.40	3000	100	10000	400	0.1	139.9	259.9	440.1	52.2	364.6	154	48.3
916	140	120	180	0	0.3	0.35	0.25	0.40	3000	200	2000	200	0.1	139.9	259.9	440.1	47.0	326.6	91	136.0
917	140	120	180	0	0.3	0.35	0.25	0.40	3000	200	2000	300	0.1	139.9	259.9	440.1	41.9	322.6	62	99.9
918	140	120	180	0	0.3	0.35	0.25	0.40	3000	200	2000	400	0.1	139.9	259.9	440.1	39.2	320.3	46	79.2
919	140	120	180	0	0.3	0.35	0.25	0.40	3000	200	4000	200	0.1	139.9	259.9	440.1	46.3	324.5	160	116.8
920	140	120	180	0	0.3	0.35	0.25	0.40	3000	200	4000	300	0.1	139.9	259.9	440.1	41.4	321.2	118	88.1
921	140	120	180	0	0.3	0.35	0.25	0.40	3000	200	4000	400	0.1	139.9	259.9	440.1	38.8	319.2	93	71.1
922	140	120	180	0	0.3	0.35	0.25	0.40	3000	200	6000	200	0.1	139.9	259.9	440.1	45.8	323.1	214	104.3
923	140	120	180	0	0.3	0.35	0.25	0.40	3000	200	6000	300	0.1	139.9	259.9	440.1	41.1	320.3	163	79.9
924	140	120	180	0	0.3	0.35	0.25	0.40	3000	200	6000	400	0.1	139.9	259.9	440.1	38.6	318.6	131	65.2
925	140	120	180	0	0.3	0.35	0.25	0.40	3000	200	8000	200	0.1	139.9	259.9	440.1	45.4	322.1	258	95.3
926	140	120	180	0	0.3	0.35	0.25	0.40	3000	200	8000	300	0.1	139.9	259.9	440.1	40.8	319.6	200	73.7
927	140	120	180	0	0.3	0.35	0.25	0.40	3000	200	8000	400	0.1	139.9	259.9	440.1	38.4	318.1	164	60.7
928	140	120	180	0	0.3	0.35	0.25	0.40	3000	200	10000	200	0.1	139.9	259.9	440.1	45.1	321.3	296	88.2
929	140	120	180	0	0.3	0.35	0.25	0.40	3000	200	10000	300	0.1	139.9	259.9	440.1	40.6	319.1	233	68.9
930	140	120	180	0	0.3	0.35	0.25	0.40	3000	200	10000	400	0.1	139.9	259.9	440.1	38.3	317.7	193	57.0
931	140	120	180	0	0.3	0.35	0.25	0.40	3000	300	2000	200	0.1	139.9	259.9	440.1	41.2	300.2	104	148.4
932	140	120	180	0	0.3	0.35	0.25	0.40	3000	300	2000	300	0.1	139.9	259.9	440.1	36.0	296.2	73	110.6
933	140	120	180	0	0.3	0.35	0.25	0.40	3000	300	2000	400	0.1	139.9	259.9	440.1	33.2	293.8	55	88.5
934	140	120	180	0	0.3	0.35	0.25	0.40	3000	300	4000	200	0.1	139.9	259.9	440.1	40.3	297.5	180	126.1
935	140	120	180	0	0.3	0.35	0.25	0.40	3000	300	4000	300	0.1	139.9	259.9	440.1	35.4	294.3	135	96.5
936	140	120	180	0	0.3	0.35	0.25	0.40	3000	300	4000	400	0.1	139.9	259.9	440.1	32.8	292.3	108	78.6
937	140	120	180	0	0.3	0.35	0.25	0.40	3000	300	6000	200	0.1	139.9	259.9	440.1	39.8	295.9	238	111.9
938	140	120	180	0	0.3	0.35	0.25	0.40	3000	300	6000	300	0.1	139.9	259.9	440.1	35.1	293.1	184	86.9
939	140	120	180	0	0.3	0.35	0.25	0.40	3000	300	6000	400	0.1	139.9	259.9	440.1	32.6	291.5	150	71.6
940	140	120	180	0	0.3	0.35	0.25	0.40	3000	300	8000	200	0.1	139.9	259.9	440.1	39.4	294.7	285	101.7
941	140	120	180	0	0.3	0.35	0.25	0.40	3000	300	8000	300	0.1	139.9	259.9	440.1	34.8	292.3	225	79.7
942	140	120	180	0	0.3	0.35	0.25	0.40	3000	300	8000	400	0.1	139.9	259.9	440.1	32.4	290.9	186	66.3
943	140	120	180	0	0.3	0.35	0.25	0.40	3000	300	10000	200	0.1	139.9	259.9	440.1	39.0	293.8	325	93.8
944	140	120	180	0	0.3	0.35	0.25	0.40	3000	300	10000	300	0.1	139.9	259.9	440.1	34.6	291.7	260	74.2
945	140	120	180	0	0.3	0.35	0.25	0.40	3000	300	10000	400	0.1	139.9	259.9	440.1	32.2	290.4	217	62.0
946	140	120	180	0	0.3	0.35	0.25	0.40	3000	400	2000	200	0.1	139.9	259.9	440.1	37.6	281.3	114	156.2
947	140	120	180	0	0.3	0.35	0.25	0.40	3000	400	2000	300	0.1	139.9	259.9	440.1	32.5	277.4	81	117.7
948	140	120	180	0	0.3	0.35	0.25	0.40	3000	400	2000	400	0.1	139.9	259.9	440.1	29.7	275.0	61	94.8
949	140	120	180	0	0.3	0.35	0.25	0.40	3000	400	4000	200	0.1	139.9	259.9	440.1	36.8	278.2	194	131.8
950	140	120	180	0	0.3	0.35	0.25	0.40	3000	400	4000	300	0.1	139.9	259.9	440.1	31.9	275.1	148	101.9
951	140	120	180	0	0.3	0.35	0.25	0.40	3000	400	4000	400	0.1	139.9	259.9	440.1	29.3	273.2	118	83.6
952	140	120	180	0	0.3	0.35	0.25	0.40	3000	400	6000	200	0.1	139.9	259.9	440.1	36.2	276.3	254	116.5
953	140	120	180	0	0.3	0.35	0.25	0.40	3000	400	6000	300	0.1	139.9	259.9	440.1	31.5	273.8	199	91.4
954	140	120	180	0	0.3	0.35	0.25	0.40	3000	400	6000	400	0.1	139.9	259.9	440.1	29.0	272.2	164	75.8
955	140	120	180	0	0.3	0.35	0.25	0.40	3000	400	8000	200	0.1	139.9	259.9	440.1	35.8	275.0	303	105.6
956	140	120	180	0	0.3	0.35	0.25	0.40	3000	400	8000	300	0.1	139.9	259.9	440.1	31.2	272.9	241	83.6
957	140	120	180	0	0.3	0.35	0.25	0.40	3000	400	8000	400	0.1	139.9	259.9	440.1	28.8	271.5	202	69.9
958	140	120	180	0	0.3	0.35	0.25	0.40	3000	400	10000	200	0.1	139.9	259.9	440.1	35.4	274.0	344	97.2
959	140	120	180	0	0.3	0.35	0.25	0.40	3000	400	10000	300	0.1	139.9	259.9	440.1	31.0	272.1	278	77.5
960	140	120	180	0	0.3	0.35	0.25	0.40	3000	400	10000	400	0.1	139.9	259.9	440.1	28.6	270.9	235	65.2